



University
of Glasgow

Elsberger, Beatrix (2010) *The role of Src kinase and Src kinase family members in breast cancer*. PhD thesis.

<http://theses.gla.ac.uk/2291/>

Copyright and moral rights for this thesis are retained by the author

A copy can be downloaded for personal non-commercial research or study, without prior permission or charge

This thesis cannot be reproduced or quoted extensively from without first obtaining permission in writing from the Author

The content must not be changed in any way or sold commercially in any format or medium without the formal permission of the Author

When referring to this work, full bibliographic details including the author, title, awarding institution and date of the thesis must be given

**THE ROLE OF SRC KINASE
AND SRC KINASE FAMILY MEMBERS
IN BREAST CANCER**

Miss Beatrix Elsberger
MBChB, MRCSEd, MD

Section of Surgical Sciences and Translational Research
Division of Cancer Sciences and Molecular Pathology

Submitted to the University of Glasgow for the
degree of Doctor of Philosophy

December 2010

Acknowledgements

I would like to thank Prof Donny McMillan and Dr Val Brunton for all their support and encouragement during the period of my research.

I also must thank Pamela McCall, Dr Liane McGlynn, Alan McIntyre and Fiona Jordan for their patience, helping me in developing my laboratory techniques and skills.

Additional thanks must go to Claire Orange, who patiently scanned literally hundreds of slides into Slidepath for me to analyse.

I would like to thank the Royal College of Surgeons of Edinburgh, the Royal College of Physicians and Surgeons of Glasgow and the Glasgow Royal Endowment Grant for their financial support.

I also would like to thank the late Professor Tim Cooke, who believed in me right from the beginning of my research time in Glasgow.

Last, but not least I would like to thank my supervisor Dr Joanne Edwards for giving me the chance to embark on a project which was exciting, challenging, successful and timely. Dr Edwards gave me the opportunity to pursue my interest in breast cancer, wakened my curiosity in translational research and let me develop essential research skills.

Finally I would like to thank my husband for his everlasting support and tolerance and would like to dedicate this work to my family; Ian, Anna and Ellie.

Abstract

This project highlighted that Src and Src kinase family (SFK) members play a definitive role in breast cancer. Due to the paucity of translational studies, we investigated if SFK members are expressed in human breast tissue. Eight SFK members were present with distinct mRNA expression patterns in normal, non-malignant and malignant breast tissue. Immunohistochemistry was employed to investigate protein expression and activation of Src and SFK members. Survival analysis revealed that c-Src and activated Y419Src were associated with worse patient outcome, confirming current *in vitro* literature, whereas a different phosphorylation site of Src (Y215) and expression of Lck was associated with improved clinical outcome. Dasatinib was employed in different breast cancer cell lines to establish its effect on those phosphorylation sites. Decreased expression of c-Src and Y419Src was observed, whilst Y215Src expression stayed unchanged, providing a rationale for using this Src kinase inhibitor in clinical trials.

Table of Contents

| | |
|--|----|
| Acknowledgements | 2 |
| Abstract | 3 |
| Table of Contents | 4 |
| List of Tables | 8 |
| List of Figures | 11 |
| List of Pictures | 15 |
| List of Appendices..... | 16 |
| List of Publications | 17 |
| List of Abbreviations..... | 18 |
| Summary | 22 |
| Chapter 1 Introduction | 26 |
| 1.1 Breast cancer | 27 |
| 1.1.1 Incidence and survival rates | 27 |
| 1.1.2 Risk factors | 29 |
| 1.1.3 Symptoms and detection of breast cancer | 32 |
| 1.1.4 Malignant invasive neoplasms of the breast | 33 |
| 1.1.5 In situ carcinoma | 46 |
| 1.1.6 Early breast cancer | 46 |
| 1.1.7 Advanced breast cancer..... | 48 |
| 1.2 Src kinase family members | 49 |
| 1.2.1 c-Src | 49 |
| 1.2.2 Structure of Src | 49 |
| 1.2.3 Activation of Src | 50 |
| 1.2.4 Src and its role in oncogenesis | 53 |

| | | |
|---|--|-----|
| 1.2.5 | Src in breast cancer | 60 |
| 1.2.6 | Lyn | 62 |
| 1.2.7 | Lck..... | 64 |
| 1.3 | Src kinase inhibitors | 67 |
| 1.3.1 | SH2/SH3 inhibitors | 67 |
| 1.3.2 | ATP-competitive Src kinase inhibitors..... | 69 |
| 1.4 | Hypothesis and statement of aims..... | 75 |
| Chapter 2 mRNA expression of Src kinase family members in breast tissue..... | | 77 |
| 2.1 | Introduction | 78 |
| 2.2 | Methods..... | 78 |
| 2.2.1 | Patient cohort | 78 |
| 2.2.2 | Quantitative reverse transcriptase polymerase chain reaction | 79 |
| 2.2.3 | Statistical analysis | 83 |
| 2.3 | Results..... | 85 |
| 2.3.1 | Clinico-pathological details of cohort..... | 85 |
| 2.3.2 | mRNA expression levels in human breast tissue | 88 |
| 2.3.3 | Src kinase family member expression in breast cancer specimen | 89 |
| 2.3.4 | Src kinase family member expression in non-malignant breast tissue | 95 |
| 2.3.5 | SFK member expression in normal/ breast reduction tissue..... | 98 |
| 2.4 | Discussion | 101 |
| Chapter 3 Protein expression of Src kinase family members and their association with clinical outcome of breast cancer patients | | 105 |
| 3.1 | Introduction | 106 |
| 3.2 | Methods..... | 107 |
| 3.2.1 | Tissue microarray construction | 107 |
| 3.2.2 | Patient cohort | 108 |

| | | |
|--|--|-----|
| 3.2.3 | Western blotting | 109 |
| 3.2.4 | Immunohistochemistry..... | 117 |
| 3.2.5 | Immunohistochemistry scoring..... | 123 |
| 3.2.6 | Statistical analysis of all immunohistochemistry studies..... | 133 |
| 3.3 | Results..... | 135 |
| 3.3.1 | Clinico-pathological details of patient cohort..... | 135 |
| 3.3.2 | c-Src kinase protein expression in invasive breast cancers..... | 136 |
| 3.3.3 | Src kinase family member expression in invasive breast cancer..... | 145 |
| 3.3.4 | Protein expression of various activation sites of Src kinase in breast cancer specimens..... | 160 |
| 3.3.5 | Ki67 expression and its association with Src kinase expression..... | 203 |
| 3.4 | Discussion..... | 207 |
| Chapter 4 Effects of Src inhibitor Dasatinib on Src kinase family member expression and phosphorylation status in breast cancer cell lines | | 222 |
| 4.1 | Introduction..... | 223 |
| 4.2 | Methods..... | 224 |
| 4.2.1 | In-vitro studies | 224 |
| 4.2.2 | Effect of steroid exposure and withdrawal on total Src kinase..... | 227 |
| 4.2.3 | Quantification of <i>SRC</i> mRNA expression in cell lines | 228 |
| 4.2.4 | Stimulation and inhibition of Src kinase, activated Src kinase, SFK members and downstream substrate Y861FAK | 230 |
| 4.3 | Results..... | 239 |
| 4.3.1 | Expression of Src kinase after steroid exposure and withdrawal in the breast cancer cell lines | 239 |
| 4.3.2 | Drug stimulation and inhibition experiments in breast cancer cell lines | 241 |
| 4.4 | Discussion | 282 |

| | |
|--|-----|
| Chapter 5 Discussion/ Conclusion | 289 |
| List of References | 295 |
| Appendices | 322 |

List of Tables

| | |
|--|-----|
| Table 1.1: Rare familial cancer syndromes associated with breast cancer | 32 |
| Table 1.2: TNM classification of invasive breast cancer | 35 |
| Table 1.3: Nottingham Prognostic Index | 37 |
| Table 1.4: Distribution of ER and PgR receptor status in breast cancer | 40 |
| Table 1.5: HER2 classification | 42 |
| Table 1.6: Different surgical treatment options | 45 |
| Table 2.1: Details of SKF member genes | 82 |
| Table 2.2: Overview of clinico-pathological features of mRNA cohorts | 86 |
| Table 2.3: Expression levels of SKF members in different breast tissue types | 88 |
| Table 2.4: Non-parametric correlations between each SKF member | 93 |
| Table 2.5: Correlations between <i>SRC</i> and other SKF members in the N cohort | 99 |
| Table 3.1: Immunohistochemistry antibody information..... | 120 |
| Table 3.2: ICC scores for each protein expression analysis | 124 |
| Table 3.3: Overview of IHC patient characteristics..... | 135 |
| Table 3.4: Descriptive statistics of c-Src histoscores..... | 139 |
| Table 3.5: c-Src expression in patient subgroups..... | 139 |
| Table 3.6: The interrelationships between c-Src expression and the clinico-pathological characteristics of patients | 141 |
| Table 3.7: Impact of clinico-pathological factors and c-Src expression on patient survival | 144 |
| Table 3.8: Descriptive statistics of Lyn histoscores..... | 149 |
| Table 3.9: Lyn expression in patient subgroups..... | 149 |
| Table 3.10: Interrelationship between clinicopathological characteristics and Lyn expression of breast cancer patients | 150 |

| | |
|---|-----|
| Table 3.11: Impact of clinico-pathological factors and Lyn expression on patient survival | 151 |
| Table 3.12: Descriptive statistics for Lck histoscores..... | 153 |
| Table 3.13: Lck expression in different patient subgroups | 153 |
| Table 3.14: Correlations between SFK member and clinico-pathological characteristics of breast cancer patients | 156 |
| Table 3.15: Impact of Lck expression on breast cancer patient survival..... | 159 |
| Table 3.16: Descriptive statistics for anti-Clone 28 histoscores | 164 |
| Table 3.17: anti-Clone 28 expression in patient groups..... | 164 |
| Table 3.18: Interrelationship between clinico-pathological features of the cohort, c-Src and anti-Clone 28 expression..... | 165 |
| Table 3.19: Impact of AC28 protein expression on patient survival | 167 |
| Table 3.20: Descriptive statistics for Clone 28 histoscores | 171 |
| Table 3.21: Clone 28 expression in patient subgroups | 171 |
| Table 3.22: Correlations between clinico-pathological features of the cohort, c-Src, AC28 and Clone 28 expression | 172 |
| Table 3.23: Impact of Clone 28 protein expression on patient survival. | 174 |
| Table 3.24: Y419Src expression in patient subgroups..... | 176 |
| Table 3.25: Descriptive statistics for Y419Src histoscores..... | 176 |
| Table 3.26: Interrelationship between clinico-pathological features of the cohort, c-Src and Y419Src expression | 179 |
| Table 3.27: Impact of Y419Src expression on patient survival..... | 181 |
| Table 3.28: Descriptive statistics for Y215Src histoscores..... | 184 |
| Table 3.29: Y215Src expression in patient subgroups | 184 |
| Table 3.30: Correlations between pathological features of cohort and Y215Src expression | 187 |

| | |
|--|-----|
| Table 3.31: The interrelationships between c-Src and all activation sites | 189 |
| Table 3.32: Impact of Y215Src expression on patient survival | 193 |
| Table 3.33: Survival analysis in ER negative patient cohort with all Src and SFK members | 195 |
| Table 3.34: Survival analysis in ER positive patient cohort with all Src and SFK members | 198 |
| Table 3.35: Overview of the ER/HER2 negative patient and ER/PgR/HER2 negative patient subgroup and their survival analysis with Y215Src expression..... | 201 |
| Table 3.36: Descriptive statistics for Ki67 expression in patient cohort | 203 |
| Table 3.37: Distribution of patients in each Ki67 subgroup | 203 |
| Table 3.38: Correlations between Ki67, clinico-pathological features of the cohort and all Src and SFK expressions..... | 206 |
| Table 4.1: Breast cancer cell lines and their ER/HER2 status | 225 |
| Table 4.2: Overview of different drug treatments, exposure time and concentration..... | 231 |
| Table 4.3: Overview of contents of each flasks | 232 |
| Table 4.4: Overview of the primary antibodies used for cell pellet IHC staining | 234 |
| Table 4.5: ICCC scores for nuclear, cytoplasmic and membrane expression..... | 235 |
| Table 4.6: Statistical overview of expression differences with Y215Src antibody | 246 |
| Table 4.7: Statistical overview of basal expression of Lck in untreated cell lines | 252 |
| Table 4.8: Statistical analysis of drug treatment Y215Src expression differences | 257 |
| Table 4.9: Overview of statistical correlation between Y215Src expression and difference drug treatments..... | 265 |
| Table 4.10: Statistical analysis of Y215Src expression changes after drug treatments | 272 |
| Table 4.11: Statistical overview of nuclear, cytoplasmic and membrane Lck expression on cell line cell pellets after drug treatments | 279 |

List of Figures

| | |
|---|----|
| Figure 1.1: Breast cancer incidence and mortality | 28 |
| Figure 1.2: Survival rates for selected cancers..... | 28 |
| Figure 1.3: Schematic overview of Oestrogen-Receptor–Signalling Pathways | 39 |
| Figure 1.4: Basic structure of Src..... | 50 |
| Figure 1.5: Configuration change of Src..... | 51 |
| Figure 1.6: Open configuration of Src after phosphorylation at Tyr 215 | 52 |
| Figure 1.7: Mechanisms on tumour cell behaviour mediated by Src..... | 58 |
| Figure 1.8: Molecular structures of SH2/SH3 inhibitors | 67 |
| Figure 1.9: Molecular structure of ATP-competitive Src kinase inhibitors..... | 69 |
| Figure 2.1: Agarose gel electrophoresis for RNA quality control | 80 |
| Figure 2.2: Agarose gel electrophoresis for quality control for cDNA..... | 81 |
| Figure 2.3: <i>SRC</i> mRNA expression levels in normal, non-malignant and malignant breast specimens | 89 |
| Figure 2.4: Overview of all SFK member expression in malignant breast tissue..... | 90 |
| Figure 2.5: <i>LCK</i> mRNA expression in N, NM and M breast tissue | 90 |
| Figure 2.6: <i>LCK</i> expression in ER negative compared to ER positive patients..... | 91 |
| Figure 2.7: Correlation between <i>SRC</i> and <i>LYN</i> mRNA expression in the M cohort | 92 |
| Figure 2.8: Correlation between <i>SRC</i> and <i>YES</i> mRNA expression in the M cohort..... | 92 |
| Figure 2.9: Kaplan Meier survival graph for mRNA expression <i>SRC</i> in ER positive patients. | 94 |
| Figure 2.10: Overview of SFK member expression in non-malignant breast tissue | 95 |
| Figure 2.11: <i>YES</i> mRNA expression levels in N, NM and M breast specimens | 96 |
| Figure 2.12: Correlations between <i>SRC</i> and <i>LYN</i> expression in the NM cohort | 97 |
| Figure 2.13: Correlations between <i>SRC</i> and <i>YES</i> expression in the NM cohort..... | 97 |

| | |
|---|-----|
| Figure 2.14: Overview of SFK member expression in normal breast tissue | 98 |
| Figure 2.15: Correlation between <i>SRC</i> and <i>LCK</i> expression in the N cohort | 99 |
| Figure 2.16: Correlation between <i>SRC</i> and <i>LYN</i> expression in the N cohort | 100 |
| Figure 2.17: Correlation between <i>SRC</i> and <i>FYN</i> expression in the N cohort | 100 |
| Figure 3.1: Western blot transfer sandwich | 114 |
| Figure 3.2: Indirect immunohistochemistry method | 118 |
| Figure 3.3: Scattered Plots and Bland-Altman Plots for all antibodies | 125 |
| Figure 3.4: Scattered Plot and Bland-Altman Plot for Ki67 | 132 |
| Figure 3.5: Western Blotting for specificity of c-Src antibody..... | 136 |
| Figure 3.6: Histograms for c-Src..... | 137 |
| Figure 3.7: Kaplan Meier survival curve for cytoplasmic c-Src expression..... | 143 |
| Figure 3.8: Western Blotting for specificity of Lyn antibody..... | 146 |
| Figure 3.9: Histograms for Lyn expression..... | 147 |
| Figure 3.10: Western Blotting for specificity of Lck antibody | 152 |
| Figure 3.11: Histograms for Lck expression..... | 154 |
| Figure 3.12: Kaplan Meier survival curve for membrane Lck expression | 158 |
| Figure 3.13: Western Blotting for specificity of anti-Clone 28 antibody | 161 |
| Figure 3.14: Histograms for anti-Clone 28 expression in invasive breast carcinoma | 162 |
| Figure 3.15: Western Blotting for specificity of Clone 28 antibody..... | 168 |
| Figure 3.16: Histograms for Clone 28 expression | 169 |
| Figure 3.17: Western Blotting for specificity of Y416Src antibody | 175 |
| Figure 3.18: Histograms for Y419Src expression..... | 177 |
| Figure 3.19: Kaplan Meier survival curve for membrane Y419Src expression | 182 |
| Figure 3.20: Western Blotting for specificity of Y216Src antibody..... | 183 |
| Figure 3.21: Histograms for Y215Src expression in invasive breast carcinoma..... | 185 |

| | |
|---|-----|
| Figure 3.22: Kaplan Meier survival curve for nuclear and cytoplasmic Y215Src expression | 192 |
| Figure 3.23: Kaplan Meier Survival Curve for cytoplasmic Y215Src in ER negative patients compared to ER positive patients | 194 |
| Figure 3.24: Kaplan Meier Survival Curve for cytoplasmic Y215Src in ER negative patients compared to ER positive patients | 197 |
| Figure 3.25: Kaplan Meier Survival Curve for cytoplasmic Y215Src in ER/HER2 negative patients. | 200 |
| Figure 3.26: Histogram for Ki67 histoscores | 204 |
| Figure 3.27: Kaplan Meier survival curves for all three Ki67 subgroups..... | 205 |
| Figure 4.1: Upregulated HER2 receptor in MCF7 cell line | 224 |
| Figure 4.2: Neubauer haemocytometer | 226 |
| Figure 4.3: Scattered Plots and Bland-Altman Plots for cell pellet double-scores | 237 |
| Figure 4.4: Western Blots for c-Src expression after steroid exposure and withdrawal.... | 240 |
| Figure 4.5: <i>SRC</i> mRNA expression in different cell lines | 240 |
| Figure 4.6: Differences in basal nuclear, cytoplasmic and membrane c-Src expression...242 | |
| Figure 4.7: Differences in basal cytoplasmic and membrane Y419Src expression.....244 | |
| Figure 4.8: Basal Y215Src expression difference in cell line cell pellets.....247 | |
| Figure 4.9: Differences in basal expression of nuclear, cytoplasmic and membrane Y861FAK on cell pellets.....250 | |
| Figure 4.10: Nuclear, cytoplasmic and membrane basal Lck expression in cell lines | 253 |
| Figure 4.11: Changes of c-Src expression in MDAMB231 after drug treatments | 259 |
| Figure 4.12: Changes of Y419Src expression in MDAMB231 after drug treatments.....259 | |
| Figure 4.13: Changes of Y215Src expression in MDAMB231 after drug treatments.....260 | |
| Figure 4.14: Changes of Y861FAK expression in MDAMB231 after drug treatments260 | |
| Figure 4.15: c-Src expression in MCF7 cell line after drug treatments | 267 |

| | |
|--|-----|
| Figure 4.16: Y419Src expression in MCF7cell line after drug treatments | 267 |
| Figure 4.17: Y215Src expression in MCF7cell line after drug treatments | 268 |
| Figure 4.18: Y861FAK expression in MCF7cell line after drug treatments..... | 268 |
| Figure 4.19: c-Src expression in MCF7HER2 after drug treatments..... | 275 |
| Figure 4.20: Y419Src expression in MCF7HER2 after drug treatments..... | 275 |
| Figure 4.21: Y215Src expression in MCF7HER2 after drug treatments..... | 276 |
| Figure 4.22: Y861FAK expression in MCF7HER2 after drug treatments | 276 |
| Figure 4.23: Expression differences of Lck in cell pellets after drug treatments | 280 |

List of Pictures

| | |
|--|-----|
| Picture 1.1: HE-staining of invasive ductal carcinoma..... | 34 |
| Picture 1.2: HER2-positive breast carcinoma | 42 |
| Picture 3.1: Immunohistochemistry staining with c-Src antibody | 138 |
| Picture 3.2: IHC staining with Lyn antibody | 148 |
| Picture 3.3: IHC staining with Lck antibody | 155 |
| Picture 3.4: IHC staining with AC28 antibody | 163 |
| Picture 3.5: IHC staining with Clone 28 antibody | 170 |
| Picture 3.6: IHC staining with Y416Src antibody | 178 |
| Picture 3.7: IHC staining with Y215Src | 186 |
| Picture 3.8: IHC staining with Ki67..... | 204 |
| Picture 4.1: IHC staining with c-Src on untreated cell line cell pellets | 243 |
| Picture 4.2: IHC staining with Y416Src on untreated cell line cell pellets..... | 245 |
| Picture 4.3: IHC staining with Y216Src antibody on untreated cell line cell pellets..... | 248 |
| Picture 4.4: IHC staining with Y861FAK on untreated cell line cell pellets..... | 251 |
| Picture 4.5: IHC staining with Lck antibody on untreated cell line cell pellets..... | 254 |
| Picture 4.6: Change of Y419Src staining after drug treatments..... | 262 |
| Picture 4.7: Changes in c-Src expression in MCF7 cell pellets after drug treatments..... | 270 |
| Picture 4.8: IHC staining with Y861FAK on cell line cell pellets..... | 278 |
| Picture 4.9: IHC staining with Lck antibody on cell pellets | 281 |

List of Appendices

| | |
|--|-----|
| Appendix 1: Materials for mRNA expression of SKF members | 322 |
| Appendix 2: Materials for protein expression of SKF members | 325 |
| Appendix 3: Materials for Dasatinib and cell line experiments..... | 336 |

List of Publications

Is the biology of breast cancer changing? A study of hormone receptor status 1984-86 and 1996-1997.

Brown SBF, Mallon EA, Edwards J, Campbell FM, McGlynn LM, Elsberger B and Cooke TG. **Br J Cancer** (2009);100(5):807-10. PMID: 19223901

Expressions of total and activated c-Src correlate differently with patient survival in ER and HER2 negative breast cancer patients. Implication for use of Src kinase inhibitors in triple negative patients?

Elsberger B, Tan BA, Brown S, Mallon E, Tovey, S, Cooke TC, Brunton VG, Edwards J. **Am J Path** (2009);175(4):1389-97. PMID: 19762712

Is Src a viable target for treating solid tumours? (review)

Elsberger B, Stewart B, Tartarov O and Edwards J. **CCDT** (2010);10(6) [Epub ahead of print] PMID: 20578988.

Breast cancer patients' clinical outcome measures are associated with Src kinase family member expression.

Elsberger B, Fullerton R, Zino R, Jordan F, Mitchell TJ, Brunton VG, Mallon EA, Shiels PG, Edwards J- **Br J Cancer** (2010);103(6):899-909. PMID: 20717116

Src family in tamoxifen resistance: A translational study. Tovey SM, Tan BA, Murphy D, Elsberger B, Edwards JE- re-submitted to **Br J Cancer** after corrections.

Inactive or even partially active Src kinase does not influence breast cancer patients' survival outcome.

Elsberger B, Tan BA, Mallon EA, Brunton VG, Edwards J. **Br J Cancer** (2010); [Epub ahead of print] PMID: 21063412

List of Abbreviations

| | |
|------------------------|--|
| AC28 | anti-Clone 28 |
| AF-1 | Activation function 1 |
| AI | Aromatase Inhibitor |
| AKT | protein kinase B family |
| ANC | Axillary Node Clearance |
| ANS..... | Axillary Node Sample |
| AP-1 | Activator protein 1= transcription factor |
| ATP | Adenosine-5'-triphosphate |
| ATM..... | Ataxia Telangiectasia Mutated gene |
| BE..... | Beatrix Elsberger |
| BMI..... | Body Mass Index |
| bp..... | base pair |
| BRCA..... | Breast Cancer gene/ tumour suppressor gene |
| BSA..... | Bovine serum albumin |
| Ca | Carcinoma |
| CD | Cluster of differentiation |
| CI..... | Confidence Interval |
| CMF | Chemotherapy combination: Cyclophosphamide, methotrexate and fluorouracil 5FU |
| CoA..... | Coenzyme A |
| Conc | Concentration |
| CML..... | Chronic myeloid leukaemia |
| CREB | Transcription factor |
| c-Src | total Src kinase |
| CXCR..... | Chemokine receptor |
| DASA..... | Dasatinib |
| dH ₂ O..... | Distilled water |
| DCIS..... | Ductal carcinoma in situ |
| DIEP..... | Deep Inferior Epigastric Artery |
| DMEM | Dulbecco's Modified Eagle Media |
| DNA/DNS..... | Desoxyribonucleic acid |
| DPX | Dibutyl Phtalate containing Xylene |

| | |
|-------------------------------------|--|
| DSS | Disease specific survival |
| E2 | Oestradiol |
| E. coli | Escherichia coli bacterium |
| ECM | Extracellular matrix |
| e.g. | for example |
| ED | Combination therapy of EGF and Dasatinib |
| EDTA | Ethylenediaminetetraacetic acid |
| EGF | Epidermal growth factor |
| EGFR | Epidermal growth factor receptor (=HER1) |
| EIA | Enzyme Immunoassay |
| ELISA | Enzyme Linked Immunosorbent Assay |
| ER..... | Oestrogen receptor |
| ErbB-2..... | Erythroblastosis oncogene B-2 |
| ERK1/2..... | Extracellular signal-regulated kinase 1/2 = MAPK 1/2 |
| FAK..... | Focal adhesion kinase |
| FISH | Fluorescence in situ hybridization |
| FGFR..... | Fibroblast growth factor receptor |
| g..... | Gravity ($1g = 9,81 \text{ m/s}^2$) |
| GAPDH..... | Glyceraldehyde-3-phosphate dehydrogenase |
| GRIP1..... | Glucocorticoid receptor interacting protein 1 |
| HBBS | Hank's Buffered Saline Solution |
| HCL..... | Hydrochloric Acid |
| HD | Combination therapy of Heregulin and Dasatinib |
| HE | Haematoxylin Eosin |
| HER2..... | Human Epidermal Growth Factor Receptor 2 |
| HOAc | Acetaldehyde |
| H ₂ O ₂ | Hydrogen peroxide |
| HPRT | Hypoxanthine-guanine phosphoribosyl-transferase |
| HR | Hazard ratio |
| HRG | Heregulin |
| HRP..... | Horseradish Peroxidase |
| HRT..... | Hormone Replacement Therapy |
| ICCC | Interclass correlation coefficient |
| JE..... | Joanne Edwards |

| | |
|--------------------------|---|
| IGF-1R | Insulin-like growth factor 1 receptor |
| IgG | Immunoglobulin G |
| IHC | Immunohistochemistry |
| IL | Interleukin |
| IQR | Interquartile range |
| kDa | Kilo Daltons |
| LPS | Lipopolysaccharide |
| LCIS | Lobular Carcinoma In Situ |
| LD | Latissimus Dorsi (Muscle) |
| LHRH | Luteinizing-Hormone-Releasing Hormone |
| LQ | Lower quartile |
| LKB1 | (Gene) |
| M | Molar |
| MAPK | Mitogen-activated protein kinase |
| mA | Milliampere |
| ml | Millilitre |
| mm | Millimeter |
| MNAR | Modulator of nongenomic action of the oestrogen receptor |
| mRNA | messenger ribonucleic acid |
| μl | Microlitre |
| NaOH | Sodium |
| NHS | National Health Service |
| NPI | Nottingham Prognostic Index |
| Nm | Nanometer |
| O.D ₅₉₅ | Optical Density at 595 nm |
| PAGE | Poly Acrylamide Gel Electrophoresis |
| PCR | Polymerase chain reaction |
| PDGFR | Platelet-derived growth factor receptor |
| PgR | Progesterone Receptor |
| PI3-K | Phosphatidylinositol 3-kinase |
| PTEN | Phosphatase and Tensin homolog (gene) |
| PVDF | Polyvinylidenedifluoride |
| ROM | Reactive Oxygen-Metabolites |

| | |
|---------------------|--|
| rpm | Rounds per minute |
| RT-PCR..... | Reverse transcriptase polymerase chain reaction |
| SCLC..... | Small cell lung cancer |
| SDS | Sodium Dodecyl Sulphate |
| SFK | Src kinase family |
| SH-domains..... | Conserved protein domains |
| SHBG | Sex Hormone Binding Globulin |
| SIEA..... | Superficial Inferior Epigastric Artery |
| SIGN | Scottish Intercollegiate Guidelines Network |
| SLNB | Sentinel Lymph Node Biopsy |
| STAT..... | Signal transducer and activator of transcription |
| STK11 | Serine/Threonine Kinase 11/ tumour suppressor gene |
| S.T.W.S. | Scott's Tap Water Substitute |
| spp. | Species |
| TCR..... | T-cell receptor |
| TBS | Wash buffer for IHC and Western Blotting |
| TEMED..... | Tetramethylethylenediamine |
| Temp | Temperature (°C) |
| TGF- α | Transforming growth factor <i>alpha</i> |
| TMA..... | Tissue Microarray |
| TRAM..... | Transverse Rectus Abdominis Muscle |
| TTBS..... | Wash buffer for Western Blotting |
| TP53 | Tumour protein 53/ tumour suppressor gene |
| Tyr..... | Tyrosine |
| u-PAR..... | urokinase plasminogen activator receptor |
| UQ..... | Upper quartile |
| UK..... | United Kingdom |
| V | Volt |
| VEGFR..... | Vascular endothelial growth factor receptor |
| w/v..... | weight/volume |
| XR | X-rays |
| Y861FAK..... | Focal adhesion kinase phosphorylated at tyrosine 861 |
| Y215Src | Src kinase phosphorylated at tyrosine site 215 |
| Y419Src | Src kinase phosphorylated at tyrosine site 419 |

Summary

There is a paucity of translational clinical studies, to support *in vitro* evidence indicating a role for Src kinase and Src kinase family members in breast cancer.

In vitro studies demonstrated that Src plays an important role as a regulator of cell proliferation and survival. Evidence from those studies also suggests that elevated c-Src activity promotes cellular invasion and motility in Tamoxifen resistant breast cancer cells providing a link between the HER family and steroid receptors. Other reports propose that c-Src may be implicated in aggressive 'triple negative' breast cancer.

There are at least eight other members of the Src kinase family present throughout mammalian cells with different expression patterns. Again there is little published data on the role of other Src kinase family members in breast cancer. Microarray studies have demonstrated that Lyn is upregulated in models of endocrine resistance and Lck is implicated in hypoxia induced breast cancer progression.

Activation of Src is complicated and can occur in different ways. It either involves dephosphorylation of a negative regulatory domain as well as phosphorylation of an activation loop (classical activation pathway) and/or activation by protein interactions or more recently discovered by direct phosphorylation of Y215Src increasing activation by 50fold.

Several Src kinase inhibitors have enrolled in phase I, II even phase III clinical trials in breast cancer. The rationale for those trials in patients with advance breast cancer was mainly based on cell line studies strongly supporting the role of Src and SFK members in breast cancer progression and metastasis, but with very limited proof of translational studies indicating clinical significance of abnormal SFK expression and activation in breast cancer.

In the current study we therefore aimed to assess expression and activation of Src and SFK members in large patient cohorts, with full clinical data and follow-up as well as investigating effects of the clinically trialled Src kinase inhibitor Dasatinib on Src and its various activation sites, utilising fresh frozen tissue and tissue micro arrays, in conjunction with *in vitro* functional studies.

Using RT-PCR we determined mRNA expression levels for all SFK members in human breast tissue specimens. Src and other SFK members were expressed at different levels in normal, non-malignant and malignant breast tissue. Src and Lyn were the most highly expressed SFK member in non-malignant and malignant tissue. Lck was higher expressed in ER negative, compared to ER positive tumours.

This varied significantly from the expression profile of normal breast tissue specimens, where Fyn was the most highly expressed SFK member followed by Src and Lyn.

Having identified which Src kinase family members were the most noteworthy in breast tumours, the role of Src kinase, Lyn and Lck protein expression was investigated by immunohistochemistry in an expanded cohort of clinical breast cancer specimens. Four separated Src phosphorylation sites were also incorporated in this study to explore their clinical relevance and impact on patient outcome. Additionally, Ki67 expression was examined to determine if high tumour proliferation was linked to SFK members' expression and activation.

Increased cytoplasmic c-Src kinase expression was significantly associated with decreased disease specific survival. These results are in keeping with cell line studies, demonstrating that c-Src is associated with more aggressive growth and poor clinical outcome. c-Src expression also correlated with increased tumor grade, ER negativity and HER2 positivity. No significant associations with survival were detected with Lyn at any cellular location. However, membrane Lck expression was significantly associated with longer survival of

breast cancer patients. Even so, none of the patients expressing Lck at the cellular membrane died of breast cancer related causes.

When Src kinase was activated at the classical site Y419 and located in the cellular membrane, it was associated with shorter disease specific survival, increasing grade, tumour size, ER negativity and HER2 positivity. While our results with Y419 support the role of Src kinase activation currently described in the literature, we found contradictory results with the alternative activation site Y215. Phosphorylation at this site was strongly associated with improved survival and was demonstrated to be independent of other known clinical parameters on multivariate analysis. It remains unclear why Y419Src and Y215Src are associated with different outcome measures. These contrasting roles may be due to phosphorylation at Y215 and Y419 residing in different SH protein domains. Phosphorylation in different domains may result in varying protein configurations, which might enable activation of other downstream signalling pathways. An alternative explanation of these results may be that the antibodies detect phosphorylation of other Src kinase family members (e.g. Lyn, Fyn, Yes) in addition or in preference to c-Src, as the phosphorylated regions are highly conserved. However we could not establish a link with SFK member Lck, which also showed improved patient outcome.

Examining ER, PgR and HER2 negative breast tumours as a representation of the triple negative group of breast tumours, we found that high cytoplasmic Y215 Src kinase expression resulted again in a significant survival advantage.

Based on our findings in clinical specimens we moved our attention to cell line studies. Four breast cancer cell lines, each representing one of the breast cancer subgroups, were studied to observe effects of Src kinase inhibitor Dasatinib on the various Src phosphorylation sites, SFK member Lck and downstream substrate Y861FAK. Membrane expression of phosphorylation site Y419Src, which was associated with decreased survival in the IHC study, was significantly reduced in all cell lines, yet almost abolished in the

triple negative cell line. Expression of downstream substrate Y861FAK, in this study functioning as a biomarker for Src activation and inhibition, was also diminished, whereas expression of activation site Y215, associated with improved clinical outcome of breast cancer patients, remained unchanged in all cellular compartments.

This comprehensive study on expression and activation of Src and SFK members and their response to Src kinase inhibitor Dasatinib fills a gap in current literature. It strengthens the role of Src in breast cancer, potentially provides a diagnostic method for identification of patients that would respond to Src inhibitors and justifies the use of Src inhibitors in the clinical setting.

CHAPTER 1

INTRODUCTION

1.1 Breast Cancer

1.1.1 Incidence and Survival Rates

Breast cancer is the most common female malignancy worldwide and accounts for over 32% of all cancer cases among women in England (1). Between 1981 and 2005, breast cancer incidence increased by a substantial 57% (1), with 45500 women and 300 men being newly diagnosed with the disease in 2005 in England (figure 1.1) and 4030 women and 20 men in Scotland (2). Although the incidence rates continue to increase, mortality has in fact decreased by almost a fifth in the last ten years. This is most likely due to earlier detection, minimization of risk factors and improved treatment. Survival rates in England have improved over the period 1999-2003. Breast cancer survival at five years was 81% (1) (figure 1.2). Survival from breast cancer is higher than that for cervical cancer and much higher than that for the other major cancers in women- lung, colorectal and ovarian. For women diagnosed in 2001-03, 72% are likely to survive for at least ten years. However, survival is still decreasing more than ten years after diagnosis, and only 64% are likely to survive for at least 20 years (3).

Figure 1.1: Breast cancer incidence and mortality

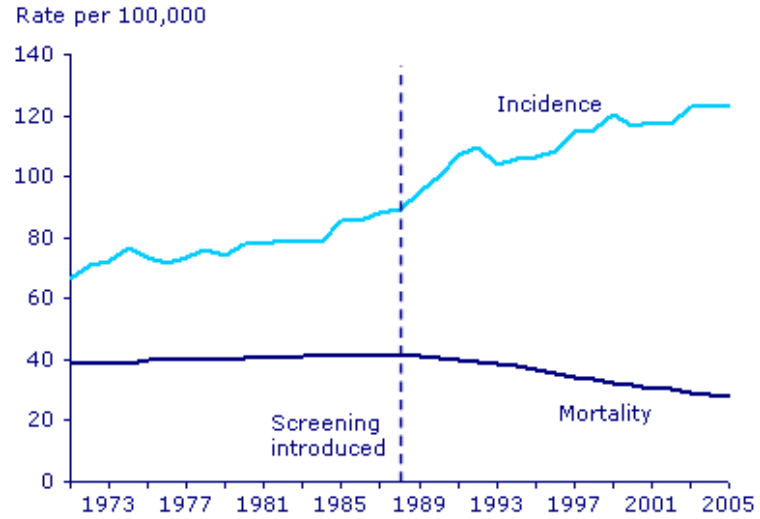


Figure 1.1: Diagram showing female breast cancer incidence and mortality between 1971-2005 in England (1).

Figure 1.2: Survival rates for selected cancers

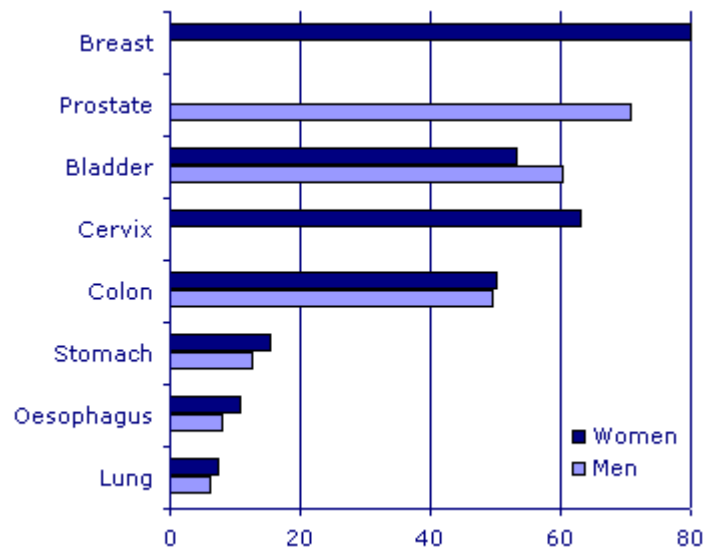


Figure 1.2: Five year relative survival rates for selected cancers for adults diagnosed during 1999-2003, England (1)

1.1.2 Risk Factors

The risk of developing breast cancer is strongly linked to age – nearly three-quarters of cases occur in women over 65 (3).

Many of the established risk factors are linked to oestrogen. The risk is increased by early menarche, late menopause, and obesity in postmenopausal women. Early pregnancy and breast feeding seems to have a protective effect (4). HRT increases the risk of breast cancer and reduces the sensitivity of mammography (5-8). The risk of breast cancer for current users of HRT is 66% higher than for never-users. The effect is substantially greater for oestrogen-progestagen combinations than for oestrogen only HRT. Risk also increases with duration of use: the risk for current users of oestrogen-progestagen combinations for 10 or more years was 2.31 (CI: 2.08-2.56) compared to 1.74 (CI: 1.60-1.89) for one to four years of use. Risk decreases with cessation of use. In the UK over the past ten years, it is estimated that 20,000 extra breast cancer cases have occurred among women aged 50-64 as a result of HRT use and three quarters (15,000) of these additional breast cancers are due to the use of oestrogen-progestagen HRT (8).

About 8% of breast cancer cases in the UK may be attributable to overweight and obesity (9). In one pooled analysis the risk of developing breast cancer was increased by around 30% in postmenopausal women with a BMI $>28\text{kg/m}^2$ compared to a BMI of less than 21kg/m^2 (10). After the menopause, when the ovaries stop producing oestrogen, adipose tissue is the primary source of endogenous oestrogen so obese and overweight women are exposed to higher levels of oestrogen. Obesity is also associated with lower levels of sex hormone binding globulin (SHBG), which increases the amount of bio available oestradiol (11). In premenopausal women, some but not all studies have observed that a higher BMI is associated with a slightly lower risk of breast cancer – possibly because it results in decreased exposure to endogenous oestrogens through increased anovulatory cycles.

A recent report from the International Agency for Research on Cancer concluded that physical activity has a preventive effect on breast cancer (12). This may be an indirect effect with exercise lowering BMI, or a direct effect on hormonal and growth factor levels. The magnitude of this effect varies between studies; a typical result is a 30-40% reduction in the risk of breast cancer with a few hours per week of vigorous activity versus none (4). A significant association between alcohol intake and breast cancer has been found, with an increase of risk of 7% for each alcoholic drink consumed on a daily basis (13). Around 4% of breast cancers in women in developed countries may be attributable to alcohol. Although alcohol and tobacco smoking are closely related social habits, there is no direct association between tobacco and breast cancer.

Ionising radiation is an established risk factor for breast cancer and excessive exposure to radiation should be avoided. The effect of radiation on the breast is strongly related to age at exposure i.e. the younger the woman is exposed the greater the excess risk. A recent study estimated that exposure to diagnostic x-rays may be responsible for 29 cases per year of female breast cancer before the age of 75 in the UK, an attributable risk of 0.1%. Overall 0.6% of the cumulative risk of cancer to age 75 might be radiation-induced in the UK— approximately 700 cases of cancer each year. This was low compared to the other developed countries studied (14). Another group at increased risk are women treated for Hodgkin's disease by mantle irradiation where there is an approximate doubling of lifetime risk. Women treated in this way before age 35 are being recalled nationally and offered special surveillance.

Breast cancer is one of the few cancers to have a higher incidence in the more affluent social classes (15). The age standardised incidence rate is 115.1 per 100,000 women in the least deprived quintile compared to 97.3 in the most deprived quintile. This is probably a reflection of other factors including reproductive history and early nutrition.

Benign breast disease is a generic term describing all non-malignant breast conditions. As such it encompasses diseases associated with an increased risk of breast cancer and others that do not have a raised risk. The commonest breast lump in young women is a fibroadenoma, which is not associated with an increased risk of breast cancer. Women in their 30s and 40s may develop cysts and those that suffer multiple cysts are at slightly increased risk of breast cancer. Women who have had biopsies that showed proliferative breast disease without atypia have a two-fold increased risk, while women with atypical hyperplasia have a two to five-fold increased risk (16-18).

If a woman has had breast cancer, her risk of developing a second primary breast cancer is two to six times the risk seen in the general population of developing a primary breast cancer (19).

A woman with one affected first degree relative (mother or sister) has approximately double the risk of breast cancer of a woman with no family history of the disease; if two (or more) relatives are affected, her risk increases even further (20).

However, over 85% of women who have a close relative with breast cancer will never develop the disease and 85% of women with breast cancer have no family history of it (21). In developed countries it is estimated that hereditary factors contribute around a quarter of inter-individual differences in susceptibility to breast cancer, while environmental and lifestyle factors contribute the remaining three-quarters (4). A small proportion of women have a particularly strong family history of breast cancer. Mutations in the breast cancer susceptibility genes BRCA1 and BRCA2 account for the majority of families with four or more members affected (2-5% of all breast cancers) (22). Women carrying such a mutation have a 50-80% chance of developing the disease.

Genetic testing for faulty BRCA genes is available on the NHS for women with a very strong family history. Increased susceptibility to breast cancer is also a feature of several rare, familial cancer syndromes (table 1.1).

Table 1.1: Rare familial cancer syndromes associated with breast cancer

| Gene | Cancer Syndrome | Associated Tumours |
|-------------------|-------------------------------|--|
| BRCA1 | Breast/Ovarian Predisposition | Breast/Ovarian/Bowel/Prostate |
| BRCA2 | Breast/Ovarian Predisposition | Breast (incl.male)/Ovarian/ Prostate/ Pancreatic |
| TP53 | Li Fraumeni Syndrome | Childhood Sarcoma/ Leukaemia/ Brain/ Early Onset Breast |
| PTEN | Cowden's Syndrome | Breast/GI/ Thyroid (benign & malignant) |
| STK11/LKB1 | Peutz-Jeughers Syndrome | Breast/GI/Pancreatic/Ovarian |
| ATM | Ataxia telegiectasia | Non-Hodgkin Lymphoma/ Ovarian/ Breast |

Table 1.1 listing up different genetic mutations of rare familial cancer syndromes associated with breast cancer

Since breast cancer affects one woman in nine there will be many women who have a mother or sister with the disease. But only if there are several family members with early onset breast cancer is there a likelihood of a significant inherited predisposition to the disease (23).

1.1.3 Symptoms and Detection of breast cancer

The breast screening programme was introduced in 1988 with the aim of reducing the number of women dying from breast cancer. Initially breast screening was offered every three years to all women aged between 50 and 64. Mammography detects a large percentage of breast cancers early before any symptoms are noticed. By 1998, mortality was around 20% lower than it would have been without screening. The decrease of

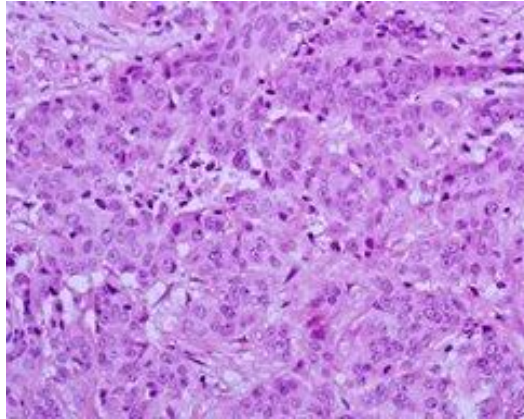
mortality occurred in all age groups, but was greatest in women aged 55 to 69. The age range was stepwise extended over the years. Since 2008 proposals are in place to invite women between age 47 and 73 every three years (1) for breast screening. Scotland currently screens women between the age of 50 and 70.

Generally women should be “breast-aware”. If a change in the breast has been noticed on regular self-examination a referral to a specialist breast clinic is necessary. Symptomatic patients can present with clinical signs like breast lumps, change in size or shape of the breast, dimpling of breast skin, nipple inversion, change in the nipple, swelling or lump in the axilla a blood-stained discharge from the nipple and/or rash around the nipple (Paget’s disease).

1.1.4 Malignant invasive neoplasms of the breast

Breast cancer derives from epithelial cells, found in the terminal duct or lobular unit. Main pathological characteristic is breaching the basement membrane of the duct or lobules and dissemination of cancer cells into the surrounding adjacent normal tissue. Almost 80% of all breast cancers are invasive ductal carcinomas (picture 1.1). This common type of cancer originates from breast ducts, invades fatty breast tissue, local neural tissue and vascular structures.

Approximately 10% of diagnosed invasive breast cancers are lobular. Some other tumours show distinct pattern of growth and cellular morphology and therefore can be identified as certain types of breast cancer. Less common, variants of invasive breast cancer are tubular, mucinous, micropapillary, cribriform and medullary carcinoma.

Picture 1.1: HE-staining of invasive ductal carcinoma

Picture 1.1: This picture shows a Grade 3 invasive ductal breast carcinoma with HE-staining (haematoxylin and eosin staining); original magnification $\times 200$.

1.1.4.1 Predictive and Prognostic Markers***Tumour differentiation***

The grade of tumour depends on its histological appearance and reflects tissue differentiation associated with neoplasia. Grading of breast tumours is based on tubule formation (% of cancer cells composed of tubular structures), nuclear pleomorphism (changes in cell size and uniformity) and mitotic count (rate of cell division).

Each of these is scored from 1 to 3. All three scores are added up to a final score, ranging between 3 and 9. Tumours with scores of 3-5 are considered as Grade 1, well differentiated tumours. Grade 2 tumours (final score 6-7) are moderately differentiated, whilst Grade 3 poorly differentiated tumours score final count of 8-9. Patients with Grade 1 tumours have a better prognosis than Grade 3 tumours (24).

Tumour stage

Stage incorporates the tumour size and the extent of the disease spread. TNM staging is commonly used to classify breast cancer (table 1.2).

T represents tumour size of the primary, N relates to lymph node involvement and M correlates whether or not the disease has metastasised to other organs. Patients with stage I breast cancer have a better prognosis than patients with stage IV (25).

Table 1.2: TNM classification of invasive breast cancer

| Stage | Size of TU | LN involvement | Metastases |
|-------------|---|--|------------------------------|
| I | T1 < 2 cm | N0 no LN involved | M0 no metastases |
| IIa | T0 no evidence of primary | N1 <4 LN involved | M0 |
| | T1 | N1 | M0 |
| | T2 2-5 cm | N0 | M0 |
| IIb | T2 | N1 | M0 |
| | T3 > 5 cm | N0 | M0 |
| IIIa | T0–T3 | N2 >4 LN involved and fixed to other structures | M0 |
| IIIb | T0-4 | N2 | M0 |
| IIIc | T0-4 | N3 incl. IM and SC LNs | M0 |
| IV | T4 any size and/or involving skin, chestwall | N1-3 | M1 distant metastases |

Table 1.2: Staging of breast cancer depends on tumour size, lymph node involvement (axillary, internal mammary (IM) and supraclavicular (SC)) and metastasis. It ranges from stage I to IV. Inflammatory breast cancer is considered as at least a stage IIIb.

Nottingham prognostic index

In 1982, a retrospective analysis was performed investigating prognostic potential of nine aspects in primary operable invasive breast cancer: age, menopausal state, tumour size and grade, lymph node status, cellular reaction, sinus histiocytosis and oestrogen receptor expression (26). Via multivariate analysis three factors remained significant. These independent prognostic markers (histological tumour grade, lymph node status and size) were combined to a formula (see below), which is known to establish the Nottingham Prognostic Index (NPI).

$NPI = \text{histological grade} + \text{lymphnode status} + (0.02 \times \text{tumours size (mm)})$

Grade 1= 1 point No lymph node involvement= 1 point

Grade 2= 2 points <4 lymph nodes= 2 points

Grade 3= 3 points >4 lymph nodes= 3 points

The NPI score is a guidance to select appropriate adjuvant therapy for each individual patient (table 1.3); higher the score, the worse the prognosis of the patient (24;26).

Table 1.3: Nottingham Prognostic Index

| NPI score | Annual Mortality | 15 year survival | Adjuvant therapy |
|----------------------------|-------------------------|-------------------------|---|
| < 3.4 Low risk | 3% | 80% | Dependant on ER/PgR status, menopausal status: tamoxifen for 5 years |
| 3.4 – 5.4 Moderate risk | 7% | 42% | Dependant on ER/PgR status, menopausal status: Switch therapy tamoxifen- AI or AI for 5 years |
| >5.4 High risk | 30% | 13% | Hormonal therapy plus chemotherapy; depending on age and comorbidities |

Table 1.3: NPI scores are calculated using tumour grade, size and lymph node status. These scores group patients into low risk, moderate and high risk and determine their most appropriate adjuvant treatment regime.

Steroid hormone receptors

Oestrogen plays an important role in the development of breast cancer (27). The oestrogen signal is mediated by the estrogen receptor, which is a transcription factor belonging to the steroid hormone receptor family.

The mechanisms through which oestrogens contribute to each phase of the carcinogenic process (initiation, promotion, and progression) are multifaceted.

The classic mechanism of direct action of oestrogen on nuclear DNA involves the binding of the hormone to nuclear oestrogen receptors, which then binds as dimers to oestrogen-response elements in the regulatory regions of oestrogen-responsive genes and associate with basal transcription factors, co-activators and co-repressors to alter gene expression (28).

Since the initial discovery and characterization of the oestrogen receptor α (ER α) in the 1960s, research on mechanisms of oestrogen-receptor signalling has revealed its complexity, as represented by the discovery of oestrogen receptor β (ER β) in 1996 and of signalling pathways mediated by oestrogen receptors that become associated with mitochondria and the plasma membrane (29;30).

ER α and ER β have only 53 percent homology in their ligand-binding domains; which accounts for different responses of the two receptors to various ligands. For example, tamoxifen has been reported to be both an agonist and an antagonist for ER α , but only an antagonist for ER β .

The receptors also vary in their activation domains, suggesting that they may recruit different proteins to the transcription complexes, thereby altering the specificity of their genomic transcriptional effects.

Furthermore, oestrogen receptors interact with co-activator proteins (e.g. AP-1) to stimulate the activity of other transcription factors (figure 1.3).

Finally, various tyrosine kinase growth-factor receptors can activate oestrogen receptors by phosphorylation in the absence of a ligand (figure 1.3).

Non-transcriptional effects involve a membrane-bound form of ER α , ER β , or both to facilitate cross-talk between the membrane oestrogen-receptor–signalling process and other signal-transduction pathways, such as the epidermal growth factor receptor (EGFR) and insulin-like growth factor 1 receptor (IGF1)–signalling pathways, suggesting oestrogenic control of cell proliferation and inhibition of apoptosis and possible implications for therapy (figure 1.3) (28;29;31).

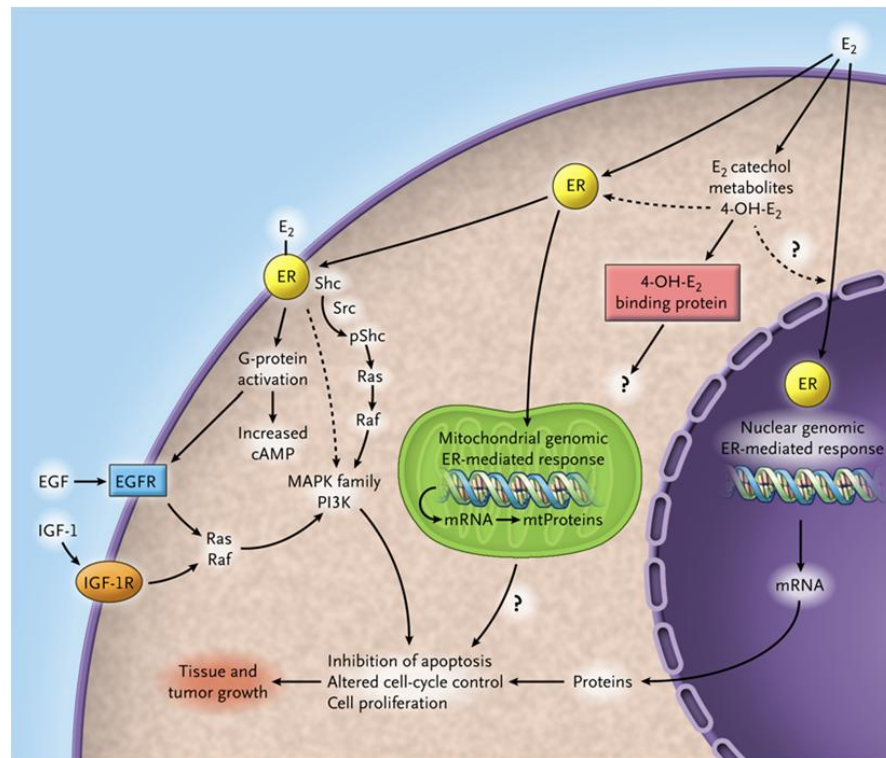
Figure 1.3: Schematic overview of Oestrogen-Receptor–Signalling Pathways

Figure 1.3: Schematic overview of Oestrogen-Receptor–Signalling Pathways (27). *cAMP*= cyclic AMP, *E₂*= oestradiol, *4-OH-E₂*, *4-hydroxyestradiol*, *ER*= oestrogen receptor, *EGF*= epidermal growth factor, *EGFR*= epidermal growth factor receptor, *IGF-1*= insulin-like growth factor 1, *IGF-1R* insulin-like growth factor 1 receptor, *MAPK*= mitogen-activated protein kinase, *mRNA*= messenger RNA, *PI3K*= phosphoinositide 3 kinase, *mtProteins*= mitochondrial proteins, and *pShc* phosphorylated *Shc* protein.

The strongest evidence for the role of oestrogen in breast cancer has emerged from the experience with the selective oestrogen receptor modulator tamoxifen for the treatment and prevention of breast cancer. Individual trials and a meta-analysis of randomized clinical trials have shown that tamoxifen reduces the risk of recurrence for women of any age with invasive or in situ breast cancer that expresses ER α , the progesterone receptor, or both (32).

Approximately 22% of all breast cancers are oestrogen and progesterone receptor positive at the time of diagnosis (table 1.4).

Table 1.4: Distribution of ER and PgR receptor status in breast cancer

| Breast Cancer Types | | Frequency |
|---------------------|--------------|-----------|
| ER positive | PgR negative | 55% |
| ER positive | PgR positive | 22% |
| ER negative | PgR negative | 20% |
| ER negative | PgR positive | 3% |

Table 1.4 displays the frequency of the oestrogen receptor and progesterone receptor in different phenotypes of breast cancer (33).

ER positive breast cancer patients respond and benefit from adjuvant hormonal therapy, which is tailored to the patient's risk of early relapse and menopausal status. The aim of endocrine therapy is to reduce the level of oestrogen; either through antagonising with oestrogen on the receptor (tamoxifen), downregulation of receptor (fulvestrant) or through inhibition of oestrogen synthesis (aromatase inhibitors).

Most tumours initially respond to endocrine therapy, but many will eventually develop resistance (acquired hormone resistance). However, some tumours fail to respond to endocrine treatment from the beginning (constitutive resistance) despite expressing hormone receptors (32).

Progesterone receptor exists as two isoforms, PRA and PRB, which are transcribed from a single gene under the control of distinct promoters (34). Both isoforms bind progestins and directly activate the expression of genes that contain progesterone response elements in their promoters. Alternatively, the PgRs can cooperate with other transcription factors to induce gene transcription.

PgR expression has been shown to be associated with increased benefit from adjuvant tamoxifen (35). In particular, ER-positive/PgR-positive patients showed a significantly higher reduction of relative risk of recurrence and death compared with ER-positive/PgR-negative patients. Interestingly, analysis of data from adjuvant treatment of postmenopausal breast cancer patients also shows that aromatase inhibitors are impressively more effective than tamoxifen in ER-positive/PgR-negative patients (36). In this respect, it has been hypothesized that loss of PgR expression might reflect a sustained activation of growth factor signalling pathways (37). In fact, it has been demonstrated that activation of the PI3K/AKT pathway — which might be determined by either IGF-1R or EGFR/ErbB-2 tyrosine kinases in breast cancer cells — downregulates the transcription of the PgR gene (38).

Human Epidermal Growth Factor Receptor

HER2, initially discovered in 1985 by two independent laboratories (39;40), is a 185-kDa transmembrane receptor in the HER family of receptor tyrosine kinases, which also includes EGFR (HER1), HER3 and HER4. Each of these receptors consists of an extracellular binding domain, a transmembrane lipophilic segment, and (except for HER3) a functional intracellular tyrosine kinase domain. The tyrosine kinase domains can be activated by both homodimerization and heterodimerization, generally induced by specific ligands. Unlike the extracellular domains of the three other HER receptors, HER2 can adopt a fixed conformation resembling a ligand-activated state, permitting it to dimerize in the absence of a ligand (41) and, once activated, able to induce signalling that promotes proliferation and survival.

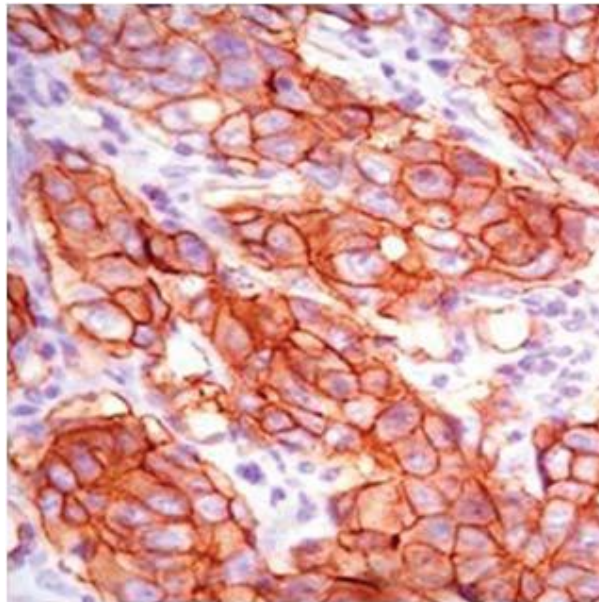
The advent of standardized FDA-approved tests for protein overexpression is based on immunohistochemistry combined with gene amplification based on fluorescence in situ hybridization. This has led to an overall improvement in HER2 status assessment (table 1.5).

Table 1.5: HER2 classification

| HER2 status | IHC (HercepTest) | FISH |
|-------------|------------------|----------|
| Negative | 1+ | |
| Negative | 2+ | Negative |
| Positive | 2+ | Positive |
| Positive | 3+ | |

Table 1.5 demonstrates when HER2 is classed as positive. All IHC HercepTest HER2 2+ tumours should undergo FISH to assess its gene amplification.

The biological characteristics of HER2 3+ tumours probably reflect the amplification of HER2 as a driving event that conditions other pathological and biological features, such as high vascular invasion and high proliferation rates (picture 1.2).

Picture 1.2: HER2-positive breast carcinoma

Picture 1.2: Immunohistochemistry (IHC) performed by HercepTest on formalin-fixed paraffin-embedded section of HER2-positive breast carcinoma (HER2 3+).

HER2 amplification/overexpression is an early event in breast carcinogenesis. 50-60% of ductal carcinomas in situ are overexpressing HER2 (42) compared to only about 25% of invasive carcinomas. This might indicate that this alteration is relevant, but not sufficient to induce oncogenic transformation. p53 status greatly influences the final effect of HER2 overexpression in tumour cells in promoting proliferation versus apoptosis and in blocking of proliferation. HER2 overexpression was found to be associated with proliferation when induced in tumour cells with mutated p53. In contrast HER2-transfected cells bearing wild-type p53 became apoptotic shortly after transfection. Additionally, stabilization of apoptosis-resistant cells showed decreased proliferation (43).

Various clinical studies have evaluated the relationship between HER2 and breast cancer outcome, and most have shown that women with HER2-positive tumours have a poorer prognosis than those with HER2-negative tumours (44;45).

HER2-positivity has also been related to endocrine therapy unresponsiveness, even in hormone-receptor positive patients (46;47). The main mechanism of resistance of breast cancer cells to endocrine therapy is loss of expression of ER. In this regard, the levels of expression of EGFR, ErbB-2 and TGF α are generally higher in ER negative breast cancer as compared with ER-positive tumours (48). Heregulin, which can activate both EGFR (HER1) and HER2 through formation of heterodimers with either HER3 or HER4, has been shown to depress ER α or its transcriptional activity (49;50). Tamoxifen as well as oestrogen induces activation of EGFR/HER2 signalling, which leads to activation of both MAPK and AKT signal transduction pathways.

Two major types of receptor inhibitors have been developed for therapy:

humanized monoclonal antibodies directed against the HER2 extracellular domain, e.g. trastuzumab (Herceptin); and

small-molecule tyrosine kinase inhibitors, which compete with ATP in the kinase domain of this receptor to impair the transmission of proliferation signal, e.g. lapatinib (Tykerb).

Proven survival benefit of anti-HER2 driven therapies demonstrated in clinical trials indicates that HER2 is one of the most promising molecules for targeted therapy (51). Trastuzumab, the recombinant humanized monoclonal antibody, is approved for the management of all metastatic and some early breast cancers with HER2 overexpression. Patients with advanced breast cancer, on trastuzumab treatment, can show tumour shrinkage. Even progressing patients can benefit from trastuzumab continuation therapy, most likely through the blockage of alternative HER proliferation pathways, leading to improved survival. However, this HER2 blockade of tumour cell growth can be circumvented through alternative growth signalling pathways. If trastuzumab controls disease progression primarily through cytostatic activity (blockade of HER2-driven proliferation), a combination of trastuzumab and cytotoxic agents represents future targeted systemic therapy for HER2 positive patients.

1.1.4.2 Treatment Options

National treatment guidelines (SIGN) have been published to improve and standardise the treatment of breast cancer in the UK.

Surgery and radiotherapy are used to control local disease, and systemic treatments (chemotherapy and/or hormonal therapy) to combat frank or occult metastatic disease.

Systemic treatments may also be administered as neoadjuvant treatment to shrink the size of the tumor prior to surgery.

Nearly all patients, depending on their comorbidities and stage of their disease, have some form of surgery (table 1.6). The objective of surgery is to remove the disease and identify the extent of disease. This can be either done by either a wide local excision, removing only the breast lump and marginal areas of normal breast tissue, or a simple mastectomy, removing the entire breast. An assessment of the regional axillary lymph node is needed to determine the disease spread beyond the breast. Standard of surgical treatment of a small

invasive breast cancer is an axillary sentinel lymph node biopsy (SLNB). If this lymph node is positive, the surgeon proceeds to an axillary clearance (ANC), removing all of the axillary lymph nodes. Staging tests, ranging from simple blood tests to MRI scans, can be carried out to assess the extent of the disease.

Table 1.6: Different surgical treatment options

| Breast | Axilla | Breast Reconstruction | |
|---|--|-------------------------|-------------------------|
| Mastectomy | +/- SLNB | +/- LD flap | |
|  | +/- ANS | +/- TRAM flap | |
| | +/- ANC | +/- DIEP reconstruction | |
| |  | | +/- SIEA reconstruction |
| | | | +/- Breast Implants |
| | | | +/- Breast Prothesis |
| Wide Local Excision | +/- SLNB | | |
|  | +/- ANS | | |
| | +/- ANC | | |

Table 1.6 showing various surgical treatment options for operable breast cancer comprising breast and axillary area plus reconstruction options offered after mastectomy

In today’s clinical practice every patient's treatment will be discussed and decided on at a multidisciplinary meeting integrating the stage and grade of their tumour, lymph node steroid hormones and HER2 receptor status, menopausal status and general health. Less aggressive treatment, e.g. systemic hormonal therapy for oestrogen positive breast cancer, may be appropriate for frail, elderly patients, avoiding mastectomy and irradiation.

1.1.5 In situ carcinoma

In situ carcinoma (Roman: meaning "in the natural or normal place") is known as a precancerous/ pre-invasive stage of a cancer. Histopathology defines it as lesions composed of malignant cells that are confined to their natural basement membrane boundaries (52), meaning the tumour cells are still constrained to the site where they originated and they have neither invaded neighbouring tissues nor giving away micro-metastasis. Two different types of carcinoma in situ can arise in the breast; lobular carcinoma in situ (LCIS) or ductal carcinoma in situ (DCIS). The treatment of lobular carcinoma in situ is mainly surveillance, whereas ductal carcinoma in situ is often treated by complete local excision as there is a strong possibility that it will progress to invasive carcinoma (53).

The UK/ANZ DCIS trial reported on the benefit of radiotherapy over tamoxifen for women with completely excised ductal carcinoma in situ (54).

1.1.6 Early breast cancer

Early breast cancer is potentially curable. Surgery is carried out to remove the tumour with an increasing trend towards more conservative surgery and reconstruction of the breast. During surgery, axillary lymph nodes are checked to see whether cancer has spread beyond the breast. New techniques like axillary lymph node sampling (ANS) and/ or sentinel lymph node biopsy help to reduce the significant disability of lymphoedema of the arm.

A short course of radiotherapy is given to patients who have had conservative surgery (wide local excision) or considered at high risk of local recurrence. High-energy radiation kills cancer cells. A review of clinical trials involving radiotherapy over the last 40 years showed a significant reduction in the number of patients relapsing following radiotherapy (55). Around 2% of women treated with breast conserving surgery and radiotherapy have

local recurrence, and if this is within the first two years they appear to have a worse prognosis than those with longer disease-free survival.

Adjuvant chemotherapy is standard treatment for women with lymph node positive disease and for lymph node negative women with high grade, ER negative/HER2 positive tumours. An overview of clinical trials of adjuvant multi-agent chemotherapy in early stage breast cancer patients, under the age of 50, showed a 35% recurrence risk and a 27% death risk reduction (56). Some patients, for example young patients with large tumours with regional lymph node spread, may receive neo-adjuvant chemotherapy to shrink the tumour, allowing more conservative surgery. Chemotherapy is recommended to patients with moderate and poorly differentiated tumours and commonly given to women who have ER negative tumours. Standard treatment of the past was a CMF combination; cyclophosphamide, methotrexate and 5-fluorouracil. There is increasing evidence to that an anthracycline e.g. Epirubicin or Doxorubicin (57) should be added to the regime. Recent results from TACT trial showed an equivalent benefit from taxanes e.g. docetaxel for early stage breast cancers (58). Clinical trials are ongoing to establish the best chemotherapy regimens.

Women, who have oestrogen sensitive (ER positive) tumours, can receive hormonal therapy to block the cancer-promoting effect of oestrogen (59). Over the past 30 years tamoxifen has been the gold standard and its use significantly reduced the risk of recurrence and increase ten year survival in women with ER positive and ER unknown status tumours (60);(61). Trials are ongoing to establish even more effective drugs and regimens for pre- and postmenopausal patients, taking into account side-effects, disease free and overall survival times. Results from the ATAC trial, comparing an aromatase inhibitor (anastrozole) alone, anastrozole plus tamoxifen, and tamoxifen alone for postmenopausal women, have shown benefits of anastrozole over tamoxifen in disease-free survival in early breast cancer (62). Most postmenopausal women receive tamoxifen for

five years. New switch therapies (3 years tamoxifen followed by an aromatase inhibitor) have been developed and trialed for women with a moderate to high Nottingham Prognostic Index. In premenopausal women oestrogen production may be stopped by surgery (bilateral oophorectomy), radiotherapy or drugs that reversibly suppress the ovaries (LHRH analogues such as Goserelin).

1.1.7 Advanced breast cancer

Minority of patients present with advanced breast cancer. Surgery and radiotherapy is useful in controlling local disease. Systemic treatment (e.g. Chemotherapy and/ or endocrine therapy) is considered to control the cancer and improve quality of life.

High levels of HER2 are associated with ER and PR negativity and poorer prognosis. A monoclonal antibody treatment (Herceptin) has been shown to provide clinical benefit to patients with high levels of HER2 receptor (63). When Herceptin is combined with chemotherapy survival is significantly improved (64). Primary treatment in elderly frail ER positive breast cancer patients should be hormonal therapies including tamoxifen and aromatase inhibitors.

1.2 Src kinase family members

The Src kinase family is a family of non-receptor tyrosine kinases. Src, most widely known and investigated, is the prototypical member of this eight-strong group of structurally related proteins, expressed in mammalian cells. Src family kinases are regulatory proteins, playing key roles in cell differentiation, motility, proliferation and cell survival (65). The Src family comprises Blk, Fgr, Fyn, Hck, Lck, Lyn, Src, and Yes (alphabetically listed) (66). Each SFK member has a different distribution in normal tissues. Src is expressed ubiquitously. It is found in a range of foetal and adult tissues. However neurons, osteoclasts, and platelets express a 5- to 20-fold higher protein level than most other cells (67). Blk, Hck, and Fgr are found solely within blood cells; Lck and Lyn are found in blood cells and brain; Yes, Fyn and Src are ubiquitously expressed (68).

1.2.1 c-Src

In 1911, research into chicken sarcomas led to the identification of a transmissible noncellular agent that could give rise to new sarcomas (69). It was a further 60 years until the agent responsible for this transformation process was identified as the viral *SRC* gene (*v-SRC*) (70). Subsequent research found that normal avian DNA contained a gene that was closely related to *v-Src*, termed cellular *Src* (*c-SRC*), which was the first human proto-oncogene to be identified (71).

1.2.2 Structure of Src

The three dimensional structure of c-Src is well understood. The Src protein is a 60kDa tyrosine kinase. It has a N-terminal 14-carbon myristoyl sequence, a SH4 domain, an unique segment, a SH3 and SH2 domain, a protein-tyrosine kinase domain and a short C-terminal regulatory tail (figure 1.4). The N-terminal myristylation of Src is required to join

cellular membranes and is crucial for the transformation of oncogenic Src mutants (72). In fibroblasts Src is bound to endosomes, perinuclear membranes, secretory vesicles and the cytoplasmic face of the plasma membrane by its N-terminal myristoyl group (67), where it can interact with a variety of growth factors and integrin receptors (73). The unique amino-terminal domain varies between Src kinase family members. The four distinct Src-homology (SH1-4) domains are involved in autoregulating Src kinase activity and interacting with substrates to form intracellular signalling complexes (73). Src activation is dependent on the interaction of different SH domains with each other and a carboxy-terminal (C-terminal) domain.

Figure 1.4: Basic structure of Src

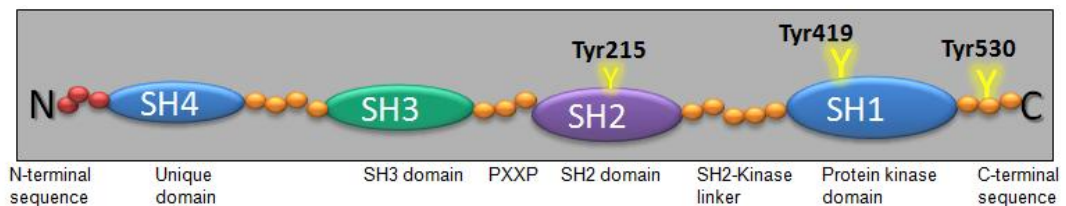


Figure 1.4 displays a one dimensional schematic overview of the basic structure of Src. Src kinase family members are 52-62kDa proteins composed of distinct functional regions.

1.2.3 Activation of Src

The interaction of these SH domains is highly dependent upon the phosphorylation state of various tyrosine residues within the protein. In the inactive state, Src kinase is phosphorylated at the tyrosine 530 site by the tyrosine kinases; C-terminal Src kinase (Csk) and Csk homology kinase (Chk). This is a highly conserved site among all Src kinase family members located in the C-terminal tail of the protein. In activated mutants of the Src kinase protein the C-terminal tyrosine is often missing or hypophosphorylated, producing a constitutively active protein, as is also the case with the v-Src protein.

Phosphorylation of the tyrosine 530 site results in a folded, inactive configuration of the Src kinase protein by promoting intramolecular binding of the C-terminus to the SH2 domain (73). It is also possible that in this phosphorylated state the SH3 domain may bind to the SH1 domain to further fold and inactivate the protein (74). Subsequent dephosphorylation of the tyrosine 530 site by tyrosine phosphatases and intermolecular autophosphorylation of the activation loop tyrosine 419 promotes activation of Src kinase activity (75). It is possible that phosphorylation of the tyrosine 419 site may stabilise the catalytic domain in an active conformation or may facilitate substrate access to the active site of the kinase (70). This describes the well established classical activation pattern of Src kinase – dephosphorylation of tyrosine 530 and phosphorylation of tyrosine 419 to induce a conformational ‘unfolding’ of the protein, permitting substrate access to the protein kinase domain (figure 1.5).

Figure 1.5: Configuration change of Src

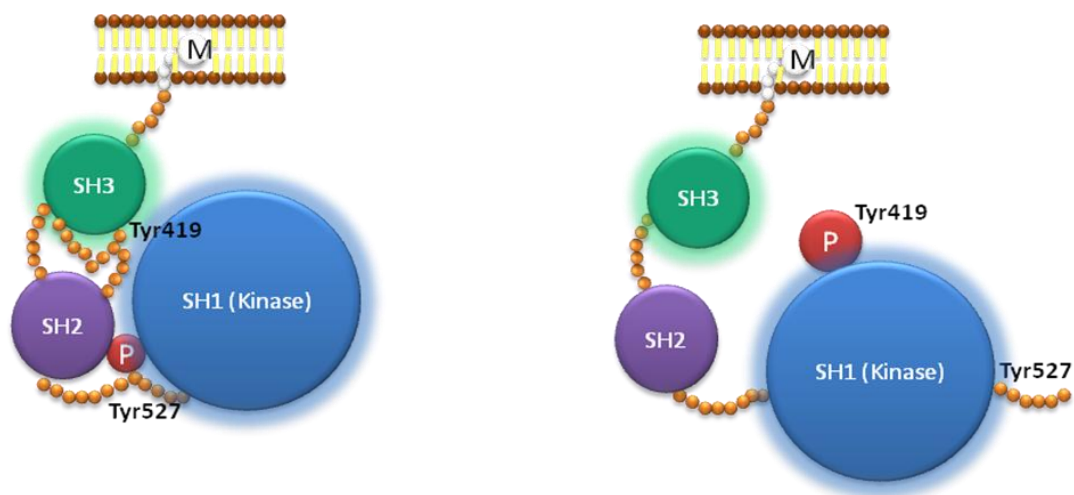


Figure 1.5: Src configuration changes when activated via dephosphorylation of Tyr527 and phosphorylation of Tyr419 (classical activation sites).

There are further tyrosine phosphorylation sites within Src kinase; however, their roles have not been fully defined. *In vitro* studies have shown that the activated platelet-derived

growth factor receptor (PDGFR) will phosphorylate the tyrosine 215 site within the SH2 domain overriding the inhibitory phosphorylated state of tyrosine 530. The suggested mechanism for this is a decrease in the intramolecular interaction of the SH2 domain with the tyrosine 530 phosphorylated C-terminal tail, thus opening the protein to its active conformation (figure 1.6). PDGF or HER2 driven phosphorylation of c-Src at Y215 on SH2 has been shown to block binding to the c-terminal regulatory sequence and result in a 50-fold activation of Src (76).

Figure 1.6: Open configuration of Src after phosphorylation at Tyr 215

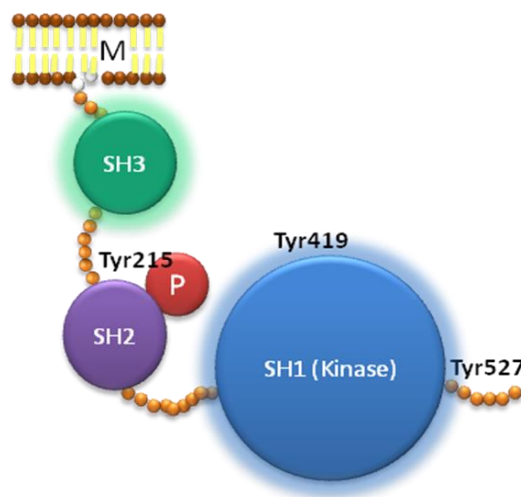


Figure 1.6: Open configuration of Src when activated at Tyr215 (alternative activation site).

In addition to this, the activated PDGFR has been shown to phosphorylate the tyrosine 138 site within the SH3 domain, although the consequences are less clear. Phosphorylation at the tyrosine 138 site has not been shown to be required for Src kinase activation, but may be involved in SH3 domain interactions.

Although Src SH3 interactions remain to be fully elucidated, the SH3 domain of the protein has been shown to bind to substrates containing proline-rich regions (77). The SH2 and SH3 domains can bind to growth factor receptors that contain their own tyrosine

kinase activities, including EGFR, HER2, PDGFR, VEGFR and FGFR. The SH2 and SH3 domains can also bind to and activate cytoskeletal proteins such as FAK and p130^{CAS} (66). This direct interaction with substrates that contain their own tyrosine kinase domains can activate the intrinsic tyrosine kinase activity of Src, potentially altering localisation of Src to sites of action (78).

SFKs can be found at different subcellular locations. They are most abundantly localised in the cell cytoplasm, but are re-localised to the membrane when activated. Subcellular localisation has also been suggested to regulate Src activity (79). In studies examining the role of the SH3 domain in assembly of focal adhesions, the inactive form of Src was localised to the perinuclear region of cells in association with microtubules. Upon activation, the SH3 domain associated with actin filaments and Src was transported to the plasma membrane where it is recruited to focal adhesions (80).

1.2.4 Src and its role in oncogenesis

In normal tissue, Src acts as a signal-transduction hub, co-ordinating intracellular responses to extracellular stimuli. Src has a prominent role in multiple cellular processes, including proliferation, adhesion, and motility (65). These processes also play important roles in oncogenesis and cancer progression, suggesting that during oncogenesis, tumour cells may hijack these normal cellular processes through aberrant Src activation or dysregulation of Src expression (66). *In vitro* and *in vivo* studies verified this hypothesis by showing that overexpression or activation of Src transforms cells and induces tumorigenesis. c-Src overexpression in mouse fibroblasts induced transformation and anchorage-independent growth through an unidentified mechanism (81).

Tumour progression from early disease to advanced or metastatic disease typically involves both tumour growth (cellular proliferation) and metastasis to distant sites (cellular migration). Metastasis is a complex multistep process involving loss of cellular adhesion,

increased motility, intravasation, invasion, extravasation, resistance to anoikis, colonisation of a site distant to the primary tumour, and angiogenesis (82). Each of these processes is regulated to some extent by Src (66), suggesting that Src plays a role in the advancement and metastasis of solid tumours.

The involvement of Src in the metastatic process is supported by several studies. Src activity in the NBT-II rat carcinoma cell line promotes cell scattering *in vitro*. Injection of these cells into nude mice produced poorly differentiated primary tumours that gave rise to micrometastases with elevated Src expression. This suggests that Src activity correlates with decreased tissue organisation and increased metastatic potential compared with the parent line (83). Overexpression of Csk, a negative regulator of SFK activity, in a highly metastatic mouse colon carcinoma cell line, significantly decreased *in vivo* metastasis and *in vitro* invasiveness (84). The role of Src in metastasis is also supported by decreased occurrence of metastases in the presence of Src inhibitors (85). In addition, metastatic cancer models using MDA-MB-231 cells transfected with a kinase-dead Src showed a decrease in development of bone metastases and increased survival in female nude mice (86).

The potential roles of Src in tumour proliferation and each of the various stages of metastasis are discussed below.

1.2.4.1 Proliferation

Studies using SFK inhibitors in cellular models of solid tumours have demonstrated that blocking Src activity inhibits proliferation by inducing cell cycle arrest (87). Activation of integrins or growth factor receptors also appears to involve Src-mediated phosphorylation of FAK at cell-matrix adhesions. Proliferation is stimulated through the Ras/Raf/MEK/ERK pathway (88).

In prostate cancer, it is well established that proliferation in primary tumours is driven by androgens. However, in castration resistant tumours, proliferation is dependent on growth factors stimulating oncogenic signals via signal transduction cascades (89). Tatarov *et al.* have recently demonstrated that Src kinase inhibitors only inhibit proliferation in castration resistant cells and not androgen sensitive cells. These results suggest that Src kinase only controls proliferation once the tumour has progressed to the more aggressive phenotype. This effect was not due to absence of androgens, as exposure of tumour cells to androgen containing medium did not rescue cells from Src kinase inhibitor induced suppression of proliferation (90).

1.2.4.2 Loss of Adhesion

Tumour cell invasion and metastasis requires a controlled disruption of interactions with neighbouring cells and the extracellular matrix (ECM). Src has a well-documented negative role in regulating cell–cell adherens junctions and cell–matrix focal adhesions. Activated Src destabilises focal adhesions by promoting redistribution of component proteins including FAK, cadherins, and catenins (91). Src also suppresses localisation of E-cadherin to focal adhesions, further decreasing cellular adhesion (92). A recent study has shown that *in vivo* Src inhibitor treatment blocked mobilisation of E-cadherin, stabilising it at adherens junctions. This result supports the potential use of Src-targeted agents as anti-invasive drugs to stabilise cell–cell adhesion (93).

1.2.4.3 Motility and Migration

Cell motility can be thought of as a series of well-co-ordinated detachment and reattachment events. During metastasis, both cell–cell and cell–matrix contacts undergo major changes to permit migration, which is Src signalling dependent (94). Src also regulates cortactin, a putative regulator of cell motility that was originally identified in Src-

transformed cells. Cortactin is a substrate of Src that appears to play a role in reorganising actin filaments within the cytoskeleton at the leading edge of migrating cells (95;96).

1.2.4.4 Invasion

The process of invasion is dependent on two major processes: increased motility and/or migration, as described above and increased degradation of the ECM. *In vitro*, cancer cell invasion is associated with the formation of actin-rich membrane protrusions termed invadopodia, which degrade the ECM. Src interacts with FAK to regulate invadopodia formation by phosphorylating cortactin and altering actin assembly. Src inhibition decreases the formation (87;97) and inhibition of invadopodia (90). Src has also been shown to promote expression of both membrane-bound and secreted matrix metalloproteases in cancer cell lines that are important in degrading basement membrane and ECM during invasion (98;99).

1.2.4.5 Intravasation and Extravasation

Mechanisms regulating intravasation, i.e. penetration of tumour cells into blood vessels, remain relatively uncharacterised. However, preclinical studies in gastric and colorectal cancer have shown that Src signalling occurs during *in vitro* models of intravasation in association with upregulated expression of chemokine receptors (CXCR1 and CXCR2) and the urokinase plasminogen activator receptor (u-PAR). u-PAR expression is associated with poor patient survival, promotion of invasion via a Src-dependent mechanism, and promotion of metastasis. In a chorioallantoic membrane model, treatment with Src inhibitors significantly decreased invasion and intravasation (100).

Src has also been implicated in extravasation, i.e. passage of cells from the circulation across the vascular walls to the target tissue stroma. The mechanism involved is distinct from intravasation and appears to be dependent on VEGF, a regulator of angiogenesis and vascular permeability. Activation of VEGFR transiently activates Src signalling in vascular

endothelial cells leading to disruption of cell–cell junctions and increased vascular permeability, allowing tumour cells to extravasate (101;102). Therefore, disrupting Src signalling and Src-regulated VEGF expression may protect against VEGF-induced increases in vascular permeability, preventing establishment of a metastatic colony of cancer cells in tissues distant to the primary tumour.

1.2.4.6 Cell Survival

Detachment of adherent cells from the ECM and loss of cell–cell adherens junctions typically results in a form of programmed cell death termed anoikis (103). Resistance to anoikis appears to occur commonly in metastatic disease and is conferred by activation of prosurvival pathways that allow anchorage-independent growth and survival, metastasis and colonisation of distant organs. Src protects from apoptosis by activating two antiapoptotic kinases: PI3-K and extracellular signal-regulated kinase 1 or 2 (ERK1/2) (104). Research in metastatic prostate cancer cells has shown that anoikis resistance is related to sustained ligand-independent activation and phosphorylation of EGFR caused by oxidation and activation of Src. This activates prosurvival signals and degrades the proapoptotic protein Bim, conferring increased cell survival and decreased apoptosis (105). The role of Src in anoikis resistance suggests that Src-targeting therapies may promote anoikis, decreasing the likelihood of a viable metastatic cell reaching a suitable site for colonisation.

1.2.4.7 Angiogenesis

Development of a blood supply is critical for the growth of tumours. Src activity increases in response to hypoxia in the inner hypoxic regions of solid tumours, inducing expression of VEGF to promote angiogenesis (106). Src plays a key role in regulating VEGF expression with Src-dependent phosphorylation of signal transducer and activator of transcription-3 (STAT3) being required for expression of VEGF (105). The importance of

Src in VEGF expression is highlighted by the finding, that Src inhibition reduces VEGF expression in human solid tumour cell lines, decreasing *in vitro* proangiogenic activity (107).

Yeatman *et al.* is illustrating a selection of mechanisms and effects of c-Src on tumour cell behaviours (figure 1.7, (66))

Figure 1.7: Mechanisms on tumour cell behaviour mediated by Src

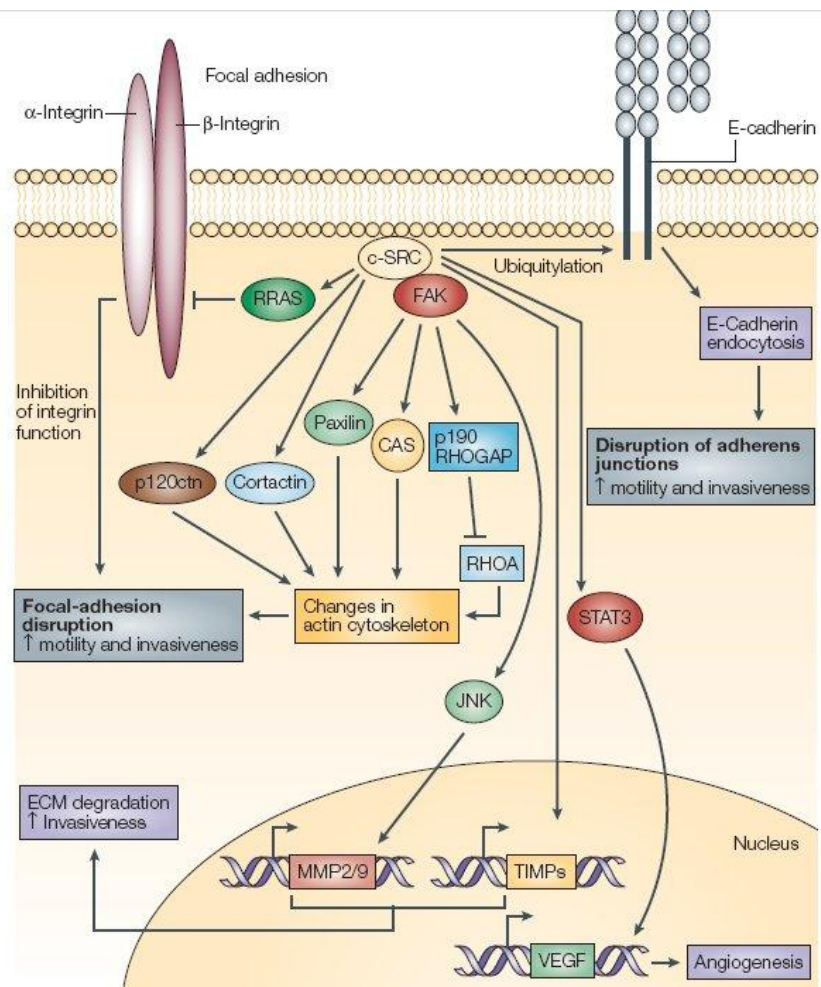


Figure 1.7 displays a range of mechanism on tumour cell behaviour mediated by interactions with various substrates and binding partners. Turnover of focal adhesions is required for motility and invasiveness via loss of cell-cell adhesion mediated by E-Cadherin or by binding and activation of FAK, which leads to phosphorylation of other substrates such as paxillin, CAS and p190RhoGAP causing focal adhesion disruption. Activation of FAK stimulates the JNK signalling pathway resulting in increased

expression of matrix metalloproteinases (MMP2 and MMP9). c-Src also induces expression of various tissue inhibitors of metalloproteinases (TIMPs). MMPs promote breakdown of extracellular matrix (ECM), which is required for tumour invasion of surrounding tissue. STAT3 (Signal transducer and activator of transcription 3) activation leads to increased expression of VEGF (vascular endothelial growth factor), a signalling molecule that promotes tumour angiogenesis (66).

1.2.4.8 Bone Metastases

Bone is a common site for metastasis, particularly from breast or prostate primaries, and is associated with high morbidity and essentially an incurable state. In addition to its roles in oncogenesis and metastasis to visceral tissues, Src is essential for regulating the bone resorptive activity of osteoclasts in bone metastases (108). In their physiological state, activated osteoclasts attach to bone in an integrin-dependent manner, activating Src and forming a membrane structure termed the ruffled border. Osteoclasts then release hydrogen ions into the osteoclast–bone interface to dissolve the bone matrix (109). Src-deficient osteoclasts show impaired migration and ruffled border formation, and in animals with targeted disruption of the *SRC* gene, defects in bone resorption are seen, causing osteopetrosis (110).

In bone metastases, Src-mediated crosstalk between tumour cells and osteoclasts can initiate a cycle of bone destruction, during which tumour cells activate osteoclasts by secretion of paracrine factors, such as parathyroid hormone-related peptide. The ensuing bone resorption releases matrix-bound growth factors such as transforming growth factor β , IGF I and II, FGFs, and PDGFs, which in turn promote growth of tumour cells (111).

Src kinase has now been suggested to have a role in clinically dormant breast cancer micrometastases, where a Src activity gene expression signature was shown on multivariate analysis to be an independent predictor of late-onset breast cancer bone metastases (112).

1.2.5 Src in breast cancer

A number of mainly *in vitro* studies have suggested a role for Src in breast cancer. But there has been a limited amount of *in vivo* studies over the past 20 years, which reported elevated levels of Src kinase in breast cancer tissue compared to normal tissue (113); (114). Translational studies investigating SFK member expression in human breast tumour and correlating expression and activation to clinical parameters are surprisingly limited. Only recently a study demonstrated an association between activated c-Src and reduced recurrence-free survival in DCIS (115). A larger study linked expression of activated c-Src in invasive breast cancer with lower proliferation indices, smaller tumour size and lower grade, but patient survival information was not available for this cohort (116). Further research on expression and activation of Src and Src family members in large patient cohorts with full clinical data and follow-up is needed to bridge the gap between *in-vitro* studies and clinical setting.

1.2.5.1 Interaction with steroid hormone receptors

It's well established that the oestrogenic signalling plays a critical role in promoting breast cancer cell growth. Characteristically, a ligand-induced activation of oestrogen receptors results in gene transcription. Src is able to potentiate the AF-1 (activation function 1) dependent gene transcription function of the oestrogen receptor by either indirect phosphorylation of nuclear ER via ERK1/2 (MAPK pathway) (117) and Akt (118) or through regulation of FAK-p130CAS-JNK pathway activity with its subsequent activation of co-activator molecules including CBP (CREB/EGFR binding protein) and GRIP1 (glucocorticoid receptor interacting protein 1), which further facilitate AF-1 gene transcription (117). This effect can occur in the absence or presence of liganded oestrogen receptor. Interestingly, this ligand can be oestrogen, but also tamoxifen.

Regulation of numerous cellular processes such as proliferation, differentiation and apoptosis can be activated via the oestrogen receptor by distinct cytoplasmic protein cascades, initiated in the cytosolic/ membrane compartment (119). Ligand binding on the oestrogen receptor leads to rapid activation of the ERK and Akt pathways in a Src dependent manner. This can happen in ER positive breast cancer cells and in cells temporarily expressing oestradiol (120;121).

Actual interaction between Src and the oestrogen receptor enhances oestrogen-mediated gene transcription. This may be facilitated by intermediate adapter-molecules such as the MNAR protein (122).

1.2.5.2 Interaction with receptors of the HER family

In human mammary carcinomas HER family members are involved in regulating cell growth, survival, migration and metastasis. EGFR (HER1) and HER2 are over-expressed in certain breast cancers and often associated with Src over-expression (123);(124). Synergism between Src and EGFR enhances neoplastic growth of breast epithelial cells (124). This occurs via Src-mediated phosphorylation of EGFR at tyrosine site 845. Src is also involved with the HER2 pathway signalling resulting in a more aggressive disease phenotype. HER2 signalling up-regulates Src kinase activity by enhancing its phosphorylation on tyrosine site 215 (125). This is associated with increased activity of FAK (126), promoting cell migration. Interestingly, HER2 over-expressing tumours also showed increased levels of phosphorylated Y215Src kinase. Cell signalling through HER2 has also been demonstrated to boost Src expression and stability resulting in cancer dissemination (127). The association of Src and HER3- and HER4- mediated signalling pathways is less clear. Ishzawar et al. have shown that Src is able to enhance HER2/HER3 signalling and their biological functions by promoting HER2/HER3 heterodimerisation (128).

1.2.5.3 Regulated crosstalk between steroid receptors and growth factor receptors by Src

Many of the signalling molecules are found within both the growth factor- and steroid hormone activated pathways. Dysregulation of one of those signalling molecules could end in abnormal activation of both pathways, leading to uncontrolled cell proliferation and survival (129). Furthermore, EGFR/HER2 activation can potentiate ER signalling, prompting ligand-independent gene transcription and cellular proliferation. On the other hand the oestrogen receptor can utilise membrane-bound EGFR to signal through various kinase cascades influencing genomic and non-genomic actions of oestrogen in breast cancer cells (31). This complex crosstalk between growth factor receptors and steroid hormone receptors has been linked to acquisition of endocrine resistance and cancer progression (130). Src can play a part as a mediator of this crosstalk suggesting a role for Src in breast cancer. Varricchio's study showed that disruption of the ER-Src complex prevents prostate and breast cancer cell growth, suggesting that inhibition of association of steroid receptors with Src or inhibition of Src activity may have therapeutic applications for patients with ER positive tumours (131).

1.2.6 Lyn

Lyn is one of the members of the Src kinase family of non-receptor protein tyrosine kinases. It is predominately expressed in haematopoietic cells (erythroid/myeloid and B lymphoid origin) (132), but has been also detected in neurons, prostate and colon cells (133;134). Lyn's function has primarily been studied in hematopoietic cells where is involved in the transmission of signals from a number of receptors such as Epo, c-Kit, B cell antigen, and c-Mpl receptors (135;136). It is associated with the high-affinity IgE receptor in basophils and with p120 Ras-GAP in thrombin-stimulated platelets (137). This association corresponds to an increase in Lyn kinase activity.

It has also been implicated in the regulation of cell signalling mechanisms through phosphorylation of a number of signalling molecules including PI3Kinase, STAT5 and ERK1/2 (138).

It was first identified in 1987 as a gene with high homology to other members of the Src kinase family. This gene is localised on the human chromosome 8q13.

1.2.6.1 Lyn's protein structure

Lyn exists as two distinct isoforms, designated p56, containing 512 amino acids, and p53 with 491 amino acids. As already mentioned its structure is very similar to other Src kinase family members. Its amino (N) terminal ending contains a sequence for attachment of the fatty acid myristate. During translation, the amino-terminal methionine is removed and myristate is attached covalently to the adjacent glycine. This modification is required for association of Lyn with the plasma membrane.

Whilst this N terminus of each member is unique, the Src family shares significant homology in the kinase domain, as well as the SH2/SH3 protein interaction domains. Tyrosine phosphorylation controls the activity of Lyn in two opposing ways (139).

Phosphorylation of the C-terminal tail at tyrosine site 508 inhibits Lyn activity through promoting its association with the kinase's own SH2 domain. This is equivalent to tyrosine site 530 of c-Src. In contrast, phosphorylation of a residue within the activation loop (tyrosine site 397= tyrosine site 419 of c-Src) results in activation of Lyn (139). Lyn activity is also regulated partly by Csk (136).

1.2.6.2 Lyn and its clinical manifesto

Lyn plays an important role in leukaemia. This has been suggested by several studies (140-142). Elevated Lyn kinase activity was found in primary acute myeloid leukaemia (AML) cells (140). Whilst in chronic myeloid leukaemia (CML) the BCR-Abl fusion protein is

the initiating molecule, Lyn plays a crucial downstream role in BCR-Abl-induced leukaemogenesis (141;142).

Lyn is also involved in the development of certain solid tumours. Colon carcinoma cells utilize Lyn in the activation of the Akt (anti-apoptotic) pathway, and chemo-resistant colonic cancer cells displayed elevated Lyn kinase activity (134). Via signalling mechanisms, Lyn regulates prostate cancer cells (143). Inhibition of Lyn in prostate cancer cell lines resulted in reduced proliferation *in vitro* and in prostatic cancer xenograft models (133).

Members of the Src kinase family are important targets for therapeutic intervention. Several small molecule inhibitors have been developed; Most of them act as ATP competitive inhibitors (e.g. Dasatinib). This was possible because of identification of crystal protein structures enabling detailed investigations of how Src family kinases are regulated and how small molecule inhibitors can inactivate these enzymes.

1.2.7 Lck

Lck (leukocyte-specific tyrosine kinase) is a 56 kDa protein found mainly in haematopoietic cells. It is most commonly expressed on the cell membrane of T-cells and at a constant level throughout T-cell development. Activation of Lck is a required step in T cell activation. T-cell activation is a critical step in cell mediated immunity. Following binding of an antigen to the cell antigen receptor (TCR), a signalling cascade is activated that results in cytokine release, cell proliferation and cell survival (144).

Immunofluorescence has shown that 50 – 90% of cellular Lck is known to be bound to CD4 in CD4+ cells and 10-25% to CD8 in CD8+ cells (145). A small amount is also known to be attached to the IL2 receptor and play a role in IL2 signalling (146). In cells, where none of these receptors are present, a fraction is seen to locate at the plasma membrane and the rest is present in peri-centrisomal vesicles (145;147). Lck's protein

structure is very similar to other SFK members apart from its unique terminal SH4 chain (figure 1.4). At the N-terminus is a short sequence for lipid attachment, which is involved in the localisation of kinases to the membrane. This attachment is mediated by either myristoylation (e.g. Lyn) or in case of Lck and Fyn by palmitoylation (148).

The inactive, closed conformation of Lck is stabilised by phosphorylation of the C-terminal 505 tyrosine residue, which could be seen as equivalent to Tyrosine site 530 in Src. The active conformation is promoted by phosphorylation of the activation loop on tyrosine site 394 (equivalent of Tyr419 in Src). This is known to increase Lck's catalytic activity 2 – 4 fold (149).

As well as being implicated in T-cell receptor (TCR) signal transduction (149;150), Lck is known to engage in thymocyte formation. Increasing Lck activity seems to promote CD4 commitment, whereas decreasing activity promotes CD8 commitment (151). Lck is also involved in TCR-dependent homeostatic proliferation, occurring in times of lymphopenia (149).

Lck may also play a role in mitochondrial apoptosis independent of its principle function in TCR signalling (151). Cell line experiments showed that a Lck deficiency resulted in resistance to apoptosis induced by anticancer drugs.

1.2.7.1 Lck expression in cancer

Despite Lck's predominance in T-cells, Lck mRNA has been observed in B-cell chronic leukaemia (B-CLL) (152). Lck expression is a feature of CD5⁽⁺⁾ B1 cells. These cells are the normal counterpart of CLL cells undergoing oncogenic transformation (153). Furthermore CD5⁽⁻⁾ B2 cells are thought to acquire the capacity to express Lck ectopically upon transformation by EBV (153).

Elevated Lck activity was seen in small cell lung cancer (SCLC), downstream of stem cell factor mediated Kit stimulation (150). Another study showed that high levels of Lck activity can cause thymic lymphomas (154).

Studies, investigating tumour infiltrating lymphocytes, have shown that Lck expression is significantly decreased in breast carcinoma, renal cell carcinoma and tumour involved lymph nodes of patients with melanoma (155-157). For almost 20 years, it has been known that Lck is expressed in human breast cancer tissue. 25-30% of the tumours analyzed in this proto-oncogene screening study, showed significant expression of either erbB, Src, Raf1, Lck or H-Ras (158). Increased expression of Lck was seen in higher grade breast tumours (159).

Lck interacts with Syk, another member of the family of non-receptor tyrosine kinases, via a cross-talk mechanism in hypoxia induced breast cancer progression (159). Syk acts as a negative regulator and Lck a positive regulator. Lck, activated by hypoxia/ reoxygenation, inhibits MeI CAM, a tumour suppressor in breast carcinoma (159), which promotes breast cancer progression.

The high homology that exists between members of this family complicates the design of inhibitors specific to a single isoform.

Inhibitors with modified pyrimidine cores represent the most intensely studied group of compounds that inhibit SFKs. The earliest members of this family were the pyrazolopyrimidine inhibitors PP1 and PP2. Unfortunately these inhibitors lack specificity within the Src kinase family.

1.3 Src kinase inhibitors

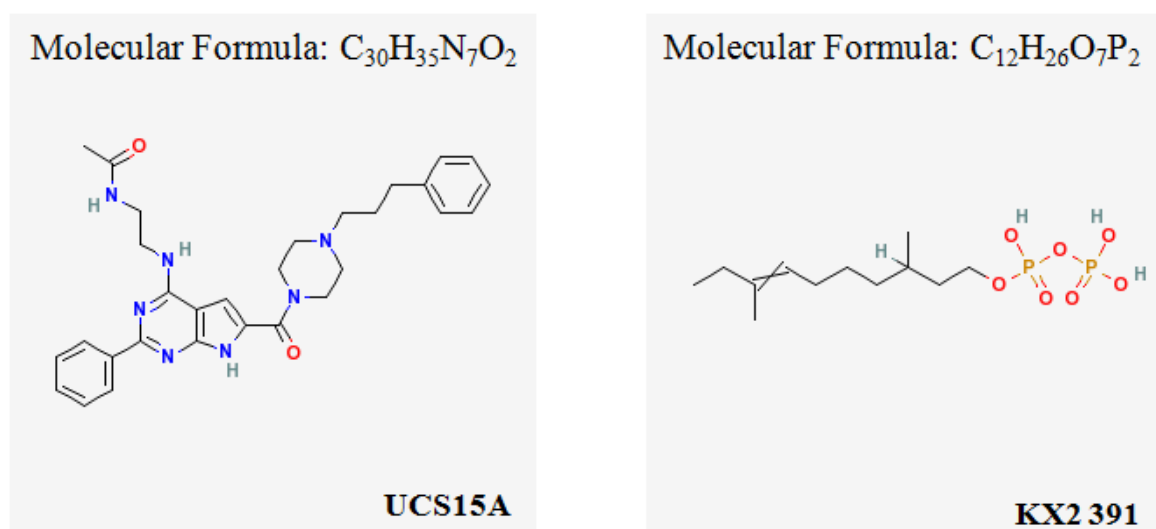
Src has many roles in regulating signal transduction during tumour cell proliferation and metastasis. Increasing evidence from cancer cell lines and human tumour tissue highlights Src as an important target for drug therapies aimed at preventing progression of disease or metastatic spread.

There are two main categories of Src inhibitors currently being developed: agents that block substrate binding to SH2 or SH3 domains and ATP-competitive kinase inhibitors.

1.3.1 SH2/SH3 inhibitors

SH2/SH3 inhibitors are a class of Src inhibitors that were designed to prevent Src binding to and activating downstream signalling substrates. Three SH2/SH3 inhibitors are undergoing either preclinical or early clinical trials: **UCS15A**, **AP22408**, and **KX2 391** (figure 1.8).

Figure 1.8: Molecular structures of SH2/SH3 inhibitors



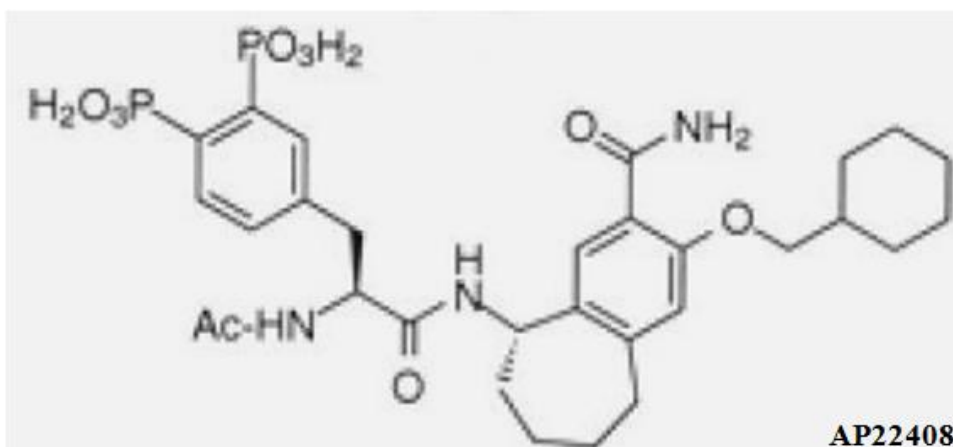


Figure 1.8: Simplified compound 2D structure of the three above mentioned SH2/SH3 inhibitors UCS15A, KX2 391 and AP22408

UCS15A is a proline-rich agent that interacts with proline-rich regions of the SH3 domain. In preclinical studies, UCS15A inhibited SH3-mediated protein–protein interactions in colon cancer cells (160) and *in vitro* bone resorption by osteoclast-like cells (161).

KX2 391, formerly KX 01 (Kinex Pharmaceuticals) is an orally available, non-ATP–competitive Src inhibitor designed to target the substrate-binding pocket of Src. KX2 391 is currently in early clinical studies in patients with solid tumours. A preclinical study in four liver cancer cell lines showed that KX2 391 had potent anti-proliferative activity (162).

AP22408 is a nonpeptide phosphotyrosine mimic with osteoclast-targeting properties, with the potential to specifically target bone metastases while avoiding unwanted inhibition of Src-dependent activities in other cells types. AP22408 has shown anti-resorptive activity in models of osteoclast bone resorption (163).

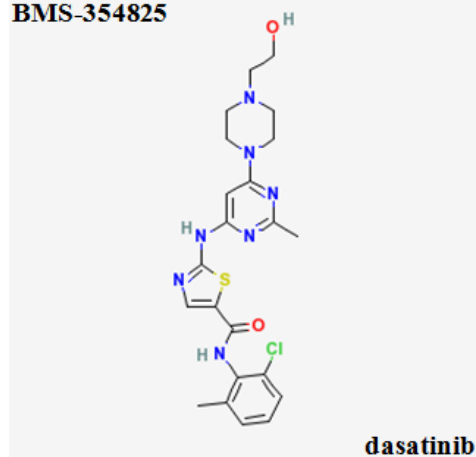
1.3.2 ATP-competitive Src kinase inhibitors

Each of the following three agents is an orally active small molecule, which inhibits the kinase activity of the SH1 domain of Src. These ATP-competitive Src kinase inhibitors have reached clinical application to date: **dasatinib** (SPRYCEL[®], Bristol-Myers Squibb), **saracatinib** (AZD0530, AstraZeneca), and **bosutinib** (SKI-606, Wyeth) (figure 1.9).

Figure 1.9: Molecular structure of ATP-competitive Src kinase inhibitors

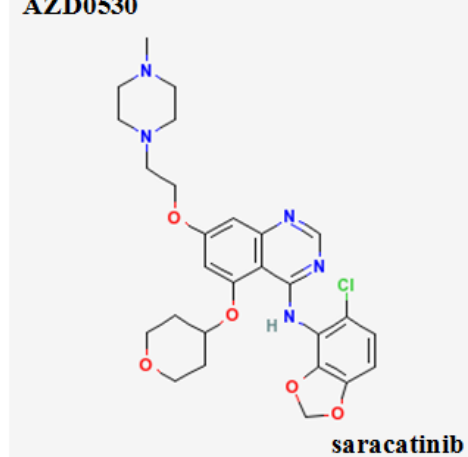
Molecular Formula: $C_{22}H_{26}ClN_7O_2S$

BMS-354825



Molecular Formula: $C_{27}H_{32}ClN_5O_5$

AZD0530



Molecular Formula: $C_{26}H_{29}Cl_2N_5O_3$

SKI-606

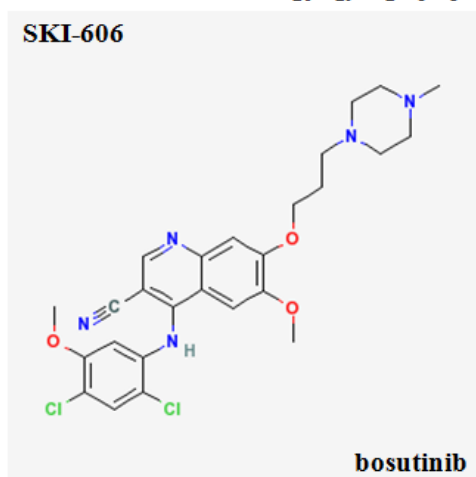


Figure 1.9: Simplified compound 2D structure of the three ATP-competitive inhibitors dasatinib, saracatinib and bosutinib, which have already reached clinical trial stage.

Dasatinib is a tyrosine kinase inhibitor of Abl, Src and SFKs (164;165). It is currently approved for the treatment of patients with certain types of leukaemia based on its potent inhibition of Bcr-Abl (166). Preclinical *in vitro* and *in vivo* studies have demonstrated that dasatinib inhibits FAK and p130^{CAS} signalling downstream of Src, cell adhesion, and migration in prostate cancer cell lines (167), and integrin-dependent adhesion and migration in colon cancer cell lines (168). Different subtypes of breast cancer cell lines have exhibited different sensitivities to dasatinib *in vitro*. Triple-negative breast cancer cell lines, which are considered to be equivalent to basal breast cell lines, and those representative of post-epithelial/mesenchymal transition cells were more sensitive to dasatinib-induced growth inhibition than luminal cell lines (169;170). In cells that overexpressed EGFR or members of the HER family, dasatinib induced cell-cycle arrest and caspase-mediated apoptosis and attenuated cell migration and invasion (171). Dasatinib also showed activity in preclinical models of EGFR-dependent sarcomas and lung cancers, inducing apoptosis and inhibiting downstream signalling, migration, and invasion (172;173).

In vivo models of metastatic prostate cancer showed decreased growth and metastasis to lymph nodes following dasatinib treatment in both androgen-sensitive and -insensitive disease. Dasatinib was not only effective at arresting the cell cycle and preventing metastatic spread, but also able to inhibit formation of bone metastases. In bone metastasis models, dasatinib inhibited the growth of prostate tumour cells in bone (174;175).

Saracatinib is an inhibitor of SFKs, EGFR, c-Kit, EphA2 and the Src-regulator Csk (176).

In vitro studies of saracatinib have shown anti-proliferative, anti-migratory, and anti-invasive activity in several cancer cell lines, including breast, prostate, colon, and non-small cell lung cancer (NSCLC) (176-178). However, *in vivo* findings have been less consistent. In one study, saracatinib inhibited growth and metastasis of an androgen-independent prostate cancer cell line xenograft (179), whereas other studies showed

moderate growth delay in four out of 10 xenografts of various types (176), and inhibition of *in vivo* tumour growth three out of 16 pancreatic tumour xenografts (180). An *in vitro* study demonstrated reversible inhibition of migration of osteoclast precursors, osteoclastogenesis and osteoclast-mediated bone resorption suggesting that saracatinib may have some activity against bone metastases (181).

Bosutinib (formerly SKI-606) has demonstrated activity as an inhibitor of Src, SFKs and Bcr-Abl in leukaemia and lymphoma cell lines (182). Preclinical studies on solid tumour cell lines showed that bosutinib inhibited *in vitro* growth and motility of colorectal carcinoma cells (183). In NSCLC cell lines, bosutinib inhibited phosphorylation of downstream Src substrates and enhanced gefitinib-induced apoptosis (184). *In vitro* studies using the MDA-MB-231 metastatic breast cancer cell line showed that bosutinib inhibited proliferation, invasion and migration *in vitro*. Analogous results were observed in xenograft studies including a decrease in tumour size compared with control animals, in addition to inhibition of angiogenesis, growth factor expression and Src signalling (85). Other xenograft studies found that bosutinib inhibited Src phosphorylation and growth of subcutaneous colorectal tumour xenografts (185).

Given the roles of Src in solid tumours discussed above, it is expected that Src inhibitors would arrest tumour growth and prevent metastasis, rather than having a cytotoxic effect. To fully assess the potential clinical benefits of Src inhibitors, trials need to be performed in patients with various stages of disease, including patients without metastases to assess any activity in preventing disease progression. With the aim to further improve the outcome of patients treated with Src-targeting agents, work is ongoing to identify gene signatures or pharmacodynamic markers that could predict sensitivity to Src inhibition in individual patients (180;186;187). The goal of this approach is to enrich study populations

with patients who might have an increased likelihood of response to a Src inhibitor, thereby providing a more definitive assessment of this class of agents.

The potential effect of dasatinib in solid tumours may be multiple as effects on migration and invasion have been reported as well as inhibition of proliferation (164;167;188). It remains unclear, which of these mechanisms will become more relevant in the clinical application of dasatinib in solid tumours of epithelial origin. The introduction of molecularly targeted agent into the clinic has led to a re-evaluation of clinical trial design as many of these agents are not cytotoxic, and conventional measures of reduction in tumour bulk and the use of maximum tolerated dose based on toxicity do not apply.

Phospho-specific antibodies have provided useful reagents for analysis of signalling pathways in clinical samples. Serrels *et al.* have identified autophosphorylation of Src on Tyrosine site 419 and phosphorylation of paxillin on Tyr118 as potential biomarkers of dasatinib activity in colon cancers.

A large number of phase I and phase II clinical trials are underway with Src inhibitors against a range of different tumour types, both as single agent or in combination with other therapeutics, to determine the objective response rate of patients with advanced metastatic disease (189).

One major problem still remains: how to assess which tumours will respond to Src inhibitors, so patient can be selected who will probably benefit most from the treatment. Applicability of microarray gene analysis in the clinical setting is now being tested after identifying a gene signature that was able to predict response to dasatinib in cell lines (170). Response rate with molecular target therapy in unselected patient groups have been so far very modest and this is most likely indicate that in most solid tumours no single molecular event drives tumourigenesis.

As we know Src associates with EGFR and that inhibition of Src activity in tumours overexpressing EGFR induces apoptosis, even in tumours resistant to EGFR therapies

(190). A number of clinical trials are in progress looking at combining dasatinib with EGFR inhibitors. Other promising preclinical data have prompted clinical evaluation with cytotoxic agents such as gemtamine and paclitaxel (191).

Inhibition of Src may have a potent anti-invasive effect, which may prevent tumour dissemination rather reduces tumour bulk. Again remains difficult to assess efficacy of the drugs in the clinical setting. These agents are more likely effective in patients with pre-invasive disease or patients with surgically resectable cancers with a high risk of recurrent disease due to presence of micrometastases. It is absolutely crucial to identify validated biomarkers to assess and monitor both target inhibition and anti-invasive efficacy to conduct clinical trials judiciously.

Summary

Almost 42,000 women die annually in the UK of breast cancer. Worldwide high-profile public screening efforts detect breast cancer now at an early stage. These patients are generally treated by surgery with adjuvant endocrine therapy and radiotherapy. A variety of host and tumour characteristics are used to aid decision-making in this setting including tumour size and grade, involvement of axillary lymph nodes, hormone receptor status and the presence or absence of HER2 over-expression. If breast cancer reaches advanced to metastatic stages further adjuvant oncological systemic treatments are available. However, adjuvant treatments have significant potential toxicities in addition to considerable economic cost. The aim of adjuvant treatment is to reduce the risk of distant recurrences of cancer but accurate identification of those women at most risk of is difficult. There is therefore an urgent need for novel prognostic indicators in breast cancer therapy. Molecular techniques and gene expression profiles have shown some value in more accurate identification of patients at risk.

Src has a well-characterised role in normal cellular functions, such as proliferation, adhesion and motility. These functions are also elemental for tumour growth and metastasis. Preclinical studies suggest that targeting Src has the potential to block multiple steps in the oncogenic process. Existing and emerging data in human tissues confirm that Src expression and/or activation are elevated in tumours compared with normal tissue, and levels appear to be highest in metastatic tissue.

Nevertheless, it is also apparent that Src activity and expression varies between patients and tumour types, and that the subcellular localisation of Src and phosphorylation of different tyrosine residues might have clinical significance. This aspect of Src biology is being actively researched and could guide future clinical investigations.

Preclinical and early-phase clinical studies suggest that Src inhibitors have cytostatic effects against tumours. Trials are ongoing to identify patient populations who might derive a clinical benefit from this class of drug therapy, including studies of combination therapy. Following encouraging early data, the potential activity of Src inhibitors in patients with bone metastases is also being evaluated. Parallel clinical and laboratory studies with a strong translational research component are needed to fully define the role of Src in cancer and the therapeutic potential of Src inhibitors.

1.4 Hypothesis and statement of aims

It is established that Src family kinases play an important part in the development and progression of cancer. Numerous *in vitro* studies have shown that elevated Src activity promotes cellular invasion and increases cell migration. They are also suggesting a link between HER and steroid receptors (ER/PgR) with Src kinase family members in breast cancer. Despite this, there is a paucity of translational clinical studies, to support *in vitro* evidence demonstrating a role for c-Src in breast cancer. Src kinase inhibitors have already entered phase II clinical trials for advanced and metastatic breast cancer without identification of adequate biomarkers and detailed knowledge of their effect on individual kinases in human breast tissue.

We hypothesise that with this study we will not only advance the understanding of the role of Src in human breast cancer but also potentially provide the prospect of identification of a biomarker for patients that would respond and benefit from Src inhibitors.

Aim of this project is to perform a comprehensive investigation into the clinical significance of Src kinase family expression and activation in human breast tumours, carefully noting cellular location and expression profiles of Src family members using already constructed tissue microarray in conjunction with *in vitro* cell line studies.

Project aims

1. To identify which Src kinase family members are expressed in human breast tissue and establish if mRNA expression profiles vary between normal, non-malignant breast tissue and invasive breast cancer.
2. To select and optimise antibodies for the detection of Src kinase family members and their activation sites in human breast cancer specimens, using paraffin-embedded tissue micro arrays.
3. To link expression of Src kinase family members with clinical parameters in order to establish association to patients' outcome.
4. To examine the effect and relevance of Src kinase inhibitor Dasatinib on expression and activation of Src and SFK members regards their staining intensity and cellular location within breast cancer cell lines representing the four different subgroups of breast cancer patients.
5. To investigate the effect of Dasatinib a non-selective, clinically trialled Src kinase inhibitor on the expression of different Src phosphorylation sites in breast cancer cell lines.

CHAPTER 2

mRNA EXPRESSION OF SRC KINASE FAMILY MEMBERS IN BREAST TISSUE

2.1 Introduction

Src kinase is implicated as a regulator of cell proliferation and survival and has a complex role in cell adhesion, proliferation and motility (65). *In vitro* studies show convincing evidence for a role for Src in breast cancer, but this is currently not supported by translational clinical studies. Additionally, there is little published evidence on the role of other Src family members in breast cancer. The aim of this study was to determine, via real time PCR, if Src and other Src kinase family (SKF) member were at all expressed in human breast tissue specimens, to verify if mRNA expression levels were different in normal, non-malignant and invasive breast cancer tissue and to investigate if these expression levels were associated with clinical parameters and patient outcome.

2.2 Methods

Materials used within this chapter are listed in appendix 1.

2.2.1 Patient Cohort

This cohort contained 139 patients in total and was subdivided into:

Patient group 1 (M) consisted of malignant tissue samples, taken from 81 breast cancer patients at time of primary tumour resection. All patients were diagnosed with operable invasive breast carcinoma between 1987 and 2005 in the Greater Glasgow area.

Patient group 2 (NM) included non-malignant tissue samples from 48 breast cancer patients taken from disease free areas of mastectomy resection specimens.

Patient group 3 (N) comprised of 10 normal breast tissue specimens obtained from reduction mammoplasties.

All samples were taken at time of surgical resection, assessed and confirmed by a pathologist, then snap frozen and stored in liquid nitrogen. ER and PgR status was determined as a routine diagnostic measure in the local pathology department.

Clinical and pathological characteristics, including age, tumour grade, size and histology, lymph node involvement, steroid receptor status and HER2 status are shown in table 2.2, result section of this chapter.

2.2.2 Quantitative Reverse Transcriptase Polymerase Chain Reaction

2.2.2.1 Tissue processing

Following the resection of the primary tumour, representative parts of malignant (M) and non-malignant (NM) breast tissue were identified by a pathologist, frozen and stored in liquid nitrogen. Normal (N) breast tissue was selected and taken from different sites of breast reduction specimens. ER and PgR receptor status were determined by immunohistochemistry as routine diagnostic measures in the Glasgow Royal Infirmary Pathology Department for malignant and non-malignant breast tissue. ER and PgR were scored as negative when histoscore was less than 10. PgR and HER2 receptor status were infrequently measured on patients' specimen before the year 2000. Breast tumours were deemed as HER2 positive if scored 3+ by HERCEPT test or if 2+ by HERCEPT test and amplified by Fluorescent in situ hybridization (FISH) using the Pathvision test (Vysis Ltd, USA).

2.2.2.2 RNA isolation

50 – 75 mg of breast tissue was ground in a mortar and pestle in liquid nitrogen. Total mRNA was extracted using the TRIZOL[®] method according to manufacturer's protocol. RNA quantity and quality was assessed by UV spectrometry (GeneQuant machine) and by examination of rRNA bands after agarose gel electrophoresis.

Only samples, which showed both 18S band and a stronger expressed 28S band, were included in this study (figure 2.1).

Figure 2.1: Agarose gel electrophoresis for RNA quality control

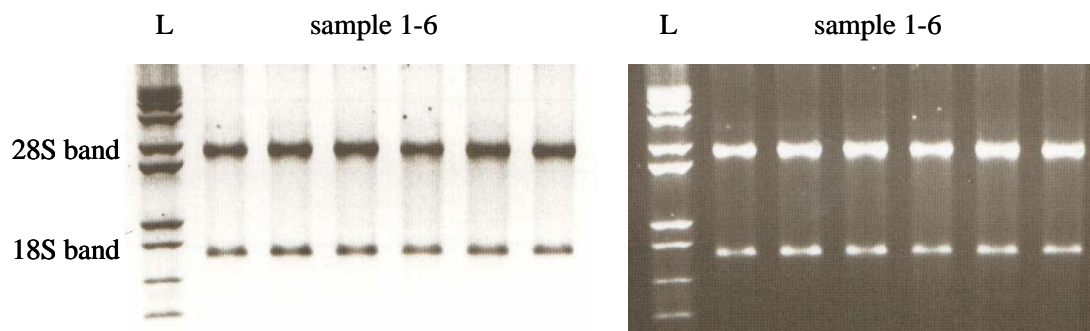


Figure 2.1 shows an agarose gel with six invasive breast cancer rRNA samples with appropriate expression at 18S and 28S. After this quality control step samples were utilised for cDNA synthesis. L= Ladder; sample 1-6= invasive breast cancer sample 1-6

2.2.2.3 cDNA synthesis

To guarantee no other DNA was present, DNA-free DNase treatment and removal reagent kit was added. Samples were incubated for 30 min at 37°C. To ensure the same amount of cDNA being used for quantification of mRNA, a starting concentration of 1000ng of tRNA was applied for each sample. Random hexamer primers (50ng) were used for First Strand cDNA Synthesis using SuperScript™ II RT according to manufacturer's instructions. Before using cDNA for PCR amplification, 2 units of RNase H were added to samples and incubated for 20 minutes at 37°C. Quality of cDNA was assessed by using a PCR control run with human β -actin.

Product bands were assessed by examination of agarose gel electrophoresis. Only samples, which showed equal product bands at 330 bp, were utilised (figure 2.2).

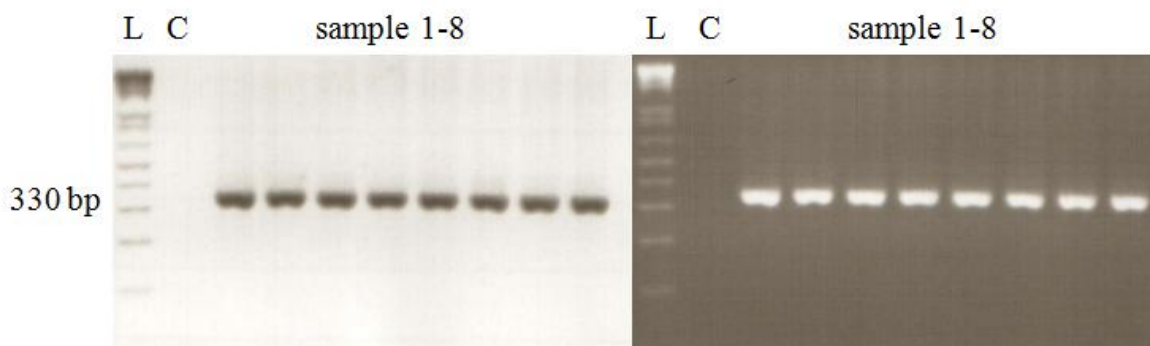
Figure 2.2: Agarose gel electrophoresis for quality control for cDNA

Figure 2.2 demonstrates a PCR control run with human β -actin to assess quality of cDNA. An equal band of each sample, at 330 bp on agarose gel electrophoresis, was essential for the cDNA to be used for mRNA quantification. L= Ladder, C= negative control, sample 1-8= invasive breast cancer sample 1-8

2.2.2.4 Quantification of mRNA

Real-time quantitative PCR was performed using an ABI Prism 7900 Sequence Detection System (Applied Biosystems, UK) and TaqMan® Gene Expression Assays (table 2.1). For the TaqMan® Gene Expression Assays the manufacturer's protocol with recommended 40 rounds of amplification was applied. Thermal cycler conditions were 50°C for 2 min, 95°C for 10 min followed by 40x 95°C for 15 sec and 60°C for 1 min. Product melting curve analysis and gel electrophoresis experiments were used to ensure that only one product of the expected size was amplified.

Table 2.1: Demographic details of SKF member genes

| Gene | Gene Expression Assay ID | Exon boundary spanned according to product insert | Amplicon Length | Threshold value (Ct) |
|--------------|-----------------------------|--|--------------------|-------------------------|
| <i>SRC</i> | Hs00178494_m1 | 7-8 | 70 | 0.28263707 |
| <i>LCK</i> | Hs00178427_m1 | 9-10 | 104 | 0.26297827 |
| <i>LYN</i> | Hs00176719_m1 | 12-13 | 70 | 0.34538345 |
| <i>YES</i> | Hs00736972_m1 | 2-3 | 153 | 0.14854589 |
| <i>FYN</i> | Hs00176628_m1 | 3-4 | 99 | 0.27740355 |
| <i>FGR</i> | Hs00178340_m1 | 5-6 | 61 | 0.22993330 |
| <i>HCK</i> | Hs00176654_m1 | 6-7 | 64 | 0.37934458 |
| <i>BLK</i> | Hs00176441_m1 | 1-2 | 85 | 0.23531063 |
| <i>GAPDH</i> | 4310884E | 3 | 118 | 0.26113370 |
| <i>HPRT</i> | 4310890E | 6-7 | 100 | 0.25742040 |

Table 2.1 reveals intron-skipping primers (eight SKF member and two housekeeping genes) used for real-time PCR and their fixed threshold Ct values.

Negative controls (RNAse/DNAse free H₂O and negative RTPCR sample) for each primer were included on every 96 well PCR plate (Applied Biosystems, UK). Quantitative values were obtained from the threshold cycle (Ct value) at which the increase TaqMan® probe fluorescent signal associated with an exponential increase of each individual PCR product reaching a fixed threshold value. Each individual primer had a fixed threshold Ct value. These fixed threshold values were used for every cDNA sample (table 2.1).

To enable comparison of different mRNA expression levels, their relation to the average expression level of two housekeeping genes (*GAPDH*, glyceraldehyde-3-phosphate dehydrogenase and *HPRT*, hypoxanthine-guanine phosphoribosyl-transferase) were

evaluated. The housekeeping gene with the lowest standard deviation (*HPRT*) was used for evaluation of the different mRNA expression levels. Data were analysed using the Sequence Detection Software, which calculates the threshold cycle (Ct) value. The expression of the target assay was normalised by subtracting the Ct value of the housekeeping gene from the Ct value of the relevant target assay. The fold increase, relative to the control, was obtained by using the formula $2^{-\Delta Ct}$, and then expressed as a percentage (x100).

Formula: $2^{-(\text{Mean Ct target gene} - \text{Mean Ct house keeping gene})} \times 100$

All samples were measured in duplicates.

Methods were established by the author. However, supportive technical assistance was given by laboratory technician Fiona Jordan, who processed the last remaining 32 samples. Result analysis of TaqMan® mRNA quantification and statistical analysis were performed again by the author.

2.2.3 Statistical Analysis

Differences in expression levels were analysed using the Mann-Whitney U test or Kruskal-Wallis test, including a Wilcoxon-type test for trends, when appropriate. Associations between continuous variables were assessed with the Spearman Rank test. Disease specific survival rates were generated using the Kaplan-Meier method. The log rank test was used to compare significant differences between subgroups using univariate analysis. Based on the results of the univariate analysis a multivariate analysis was then carried out. The multivariate stepwise Cox-regression analysis was performed to identify factors that were independently associated with disease specific death. A stepwise backward procedure was used to derive a final model of the variables that had a significant independent relationship with survival. To remove a variable from the model the corresponding p-value had to be greater than 0.05.

Inter-relationships between clinical parameters, ER, PgR and HER2 status were calculated using the Chi square test. Nonparametric correlations between Src and other SFK members were determined using 2-tailed Spearman's rho test. Because of the number of statistical comparisons, a p-value of <0.01 was considered to be significant. Data are expressed as median and range. The statistical analyses were performed using a statistical software package (SPSS 15.0 Inc., Chicago, IL, USA).

2.3 Results

2.3.1 Clinico-pathological details of cohort

The PCR cohort consisted of 81 invasive breast cancers (M), 48 non-malignant (NM) and 10 normal (N) breast tissue samples. Clinical and pathological characteristics of those three groups are shown in table 2.2.

Median age of the breast cancer patients was 61 years (IQR 49-74 years). Median size of breast cancer was 30mm (IQR 20-42mm). 40% of the specimens were pathologically graded G2 and 48% G3. 52 breast cancer patients were ER positive compared to 29 ER negative patients. 55% of breast cancer patients were axillary lymph node positive. Median NPI was 4.6 (IQR 4.3-5.4). Patients underwent either breast conserving wide local excision (16%) or a simple mastectomy (67%; the rest 17% unknown). Axillary dissection was performed in 83% of cases. At time of analysis 37 out of 79 patients were deceased. 18 of those 37 patients died of breast cancer related causes. Median follow-up time was 5.6 years (IQR 1.8- 17.6 years).

Median age of breast cancer patients, from whom a non-malignant specimen of breast tissue was obtained, was also 61 years (IQR 52-71 years). 63% of those patients were ER positive, 17% ER negative. ER status was not significantly different between tissue types ($p=0.847$).

Median age of breast reduction patients supplying normal breast tissue was 37 years (IQR 33-48 years).

Table 2.2: Overview of clinico-pathological features of mRNA cohorts

| Variables | | Cohort 1 (M) | | Cohort 2 (NM) | | Cohort 3 (N) | |
|--------------|----------|--------------|----|---------------|----|--------------|-----|
| | | No: 81 | % | No: 48 | % | No: 10 | % |
| Age | <= 50 | 20 | 25 | 11 | 23 | 8 | 80 |
| | > 50 | 61 | 75 | 37 | 77 | 2 | 20 |
| Histology | ductal | 75 | 93 | 44 | 92 | | |
| | lobular | 4 | 5 | 3 | 6 | | |
| | others | 2 | 2 | 1 | 2 | | |
| | unknown | | | | | 10 | 100 |
| Grade | 1 | 5 | 6 | 6 | 12 | | |
| | 2 | 32 | 40 | 21 | 44 | | |
| | 3 | 39 | 48 | 20 | 42 | | |
| | unknown | 5 | 6 | 1 | 2 | 10 | 100 |
| Size | <20mm | 10 | 13 | 10 | 21 | | |
| | 20-50mm | 55 | 68 | 30 | 63 | | |
| | >50mm | 14 | 17 | 5 | 10 | | |
| | unknown | 2 | 2 | 3 | 6 | 10 | 100 |
| Nodal status | positive | 29 | 36 | 26 | 54 | | |
| | negative | 45 | 55 | 19 | 40 | | |
| | unknown | 7 | 9 | 3 | 6 | 10 | 100 |
| ER status | positive | 29 | 36 | 18 | 37 | | |
| | negative | 52 | 64 | 30 | 63 | | |
| | unknown | | | | | 10 | 100 |
| PgR status | positive | 16 | 20 | 14 | 29 | | |
| | negative | 17 | 21 | 8 | 17 | | |
| | unknown | 48 | 59 | 26 | 54 | 10 | 100 |
| HER2 status | positive | 28 | 35 | 17 | 36 | | |
| | negative | 4 | 5 | 4 | 8 | | |
| | unknown | 49 | 60 | 27 | 56 | 10 | 100 |
| NPI | <3.4 | 4 | 5 | 6 | 12 | | |
| | 3.4-5.4 | 49 | 60 | 29 | 60 | | |
| | >5.4 | 15 | 19 | 6 | 12 | | |
| | unknown | 13 | 16 | 7 | 16 | 10 | 100 |

Table 2.2 is giving an overview of clinico-pathological features of the cohorts *M*= invasive breast tissue, *NM*= non-malignant breast tissue and *N*= normal breast tissue. *Histology*= Pathological type: *Ductal*= invasive ductal carcinoma; *Lobular*= invasive lobular carcinoma; *others*: including tubular, medullary, mucinous, and squamous; *Grade* = Bloom and Richardson grade; *Size*= Maximum tumour diameter; *ER*= Oestrogen receptor; *PgR*= Progesterone receptor; *HER2*= Human epidermal growth factor receptor 2; *NPI*= Nottingham Prognostic Index

2.3.2 mRNA expression levels in human breast tissue

2.3.2.1 mRNA expression levels in human breast tissue

Expression levels for SFK member were quantified in all tissue samples (table 2.3). *BLK* was the least expressed SFK member in all breast tissues. No change in the level of *SRC* expression was observed between tissue types ($p=0.976$) (figure 2.3). Whereas *LCK*, *FYN* and *YES* showed significant changes in expression between different breast tissue types (table 2.3).

Table 2.3: Expression levels of SFK members in different breast tissue types

| Gene | Expression levels | Expression levels | Expression levels | p-values |
|------------|-------------------|-------------------|-------------------|------------------|
| | in M | in NM | in N | |
| <i>SRC</i> | 9041 | 9252 | 9493 | 0.976 |
| <i>LCK</i> | 655 | 217 | 255 | <0.001 |
| <i>LYN</i> | 7233 | 8922 | 10521 | 0.076 |
| <i>FYN</i> | 2245 | 5293 | 25484 | <0.001 |
| <i>FGR</i> | 1144 | 1275 | 1072 | 0.043 |
| <i>HCK</i> | 1815 | 2673 | 1712 | 0.070 |
| <i>BLK</i> | 208 | 161 | 234 | 0.114 |
| <i>YES</i> | 2142 | 499 | 3312 | <0.001 |

Table 2.3 shows expression levels of Src kinase family members in different breast tissue types (*M*= invasive breast cancer; *NM*= non-malignant and *N* normal tissue) are stated as medians. *P*-values express alterations of expression in the different breast tissue types (Kruskal-Wallis test). Bold typeface is used to highlight significant *p*-values.

Figure 2.3: *SRC* mRNA expression levels in normal, non-malignant and malignant breast specimens

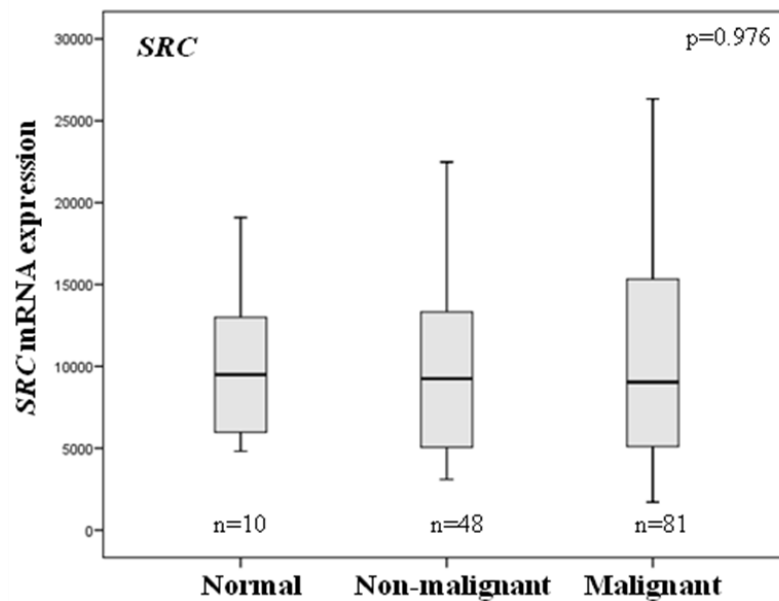


Figure 2.3 demonstrates different SRC mRNA expression levels in normal, non-malignant and malignant breast specimens (p=0.976).

2.3.3 Src kinase family member expression in breast cancer specimen

SRC and *LYN* were the most highly expressed SFK members in malignant breast tissue (figure 2.4).

Higher expression levels of *LCK* were observed in invasive breast cancers compared to non-malignant and normal breast tissue ($p < 0.001$) (figure 2.5). Interestingly, *LCK* was 14 fold less expressed than *SRC*. It also was the only SFK member, which showed a difference in expression levels between ER negative and ER positive patients. *LCK* was higher expressed in ER negative patients, compared to ER positive patients (figure 2.6).

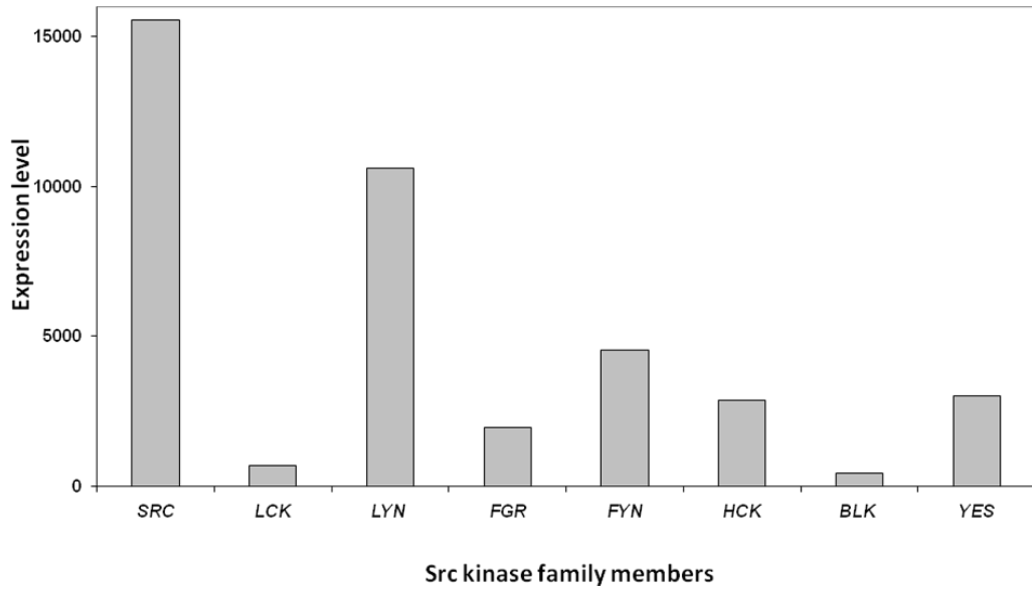
Figure 2.4: Overview of all SFK member expression in malignant breast tissue

Figure 2.4 shows an overview of all SFK member expression in malignant breast tissue. SRC and LYN are the most and BLK the least expressed SFK member.

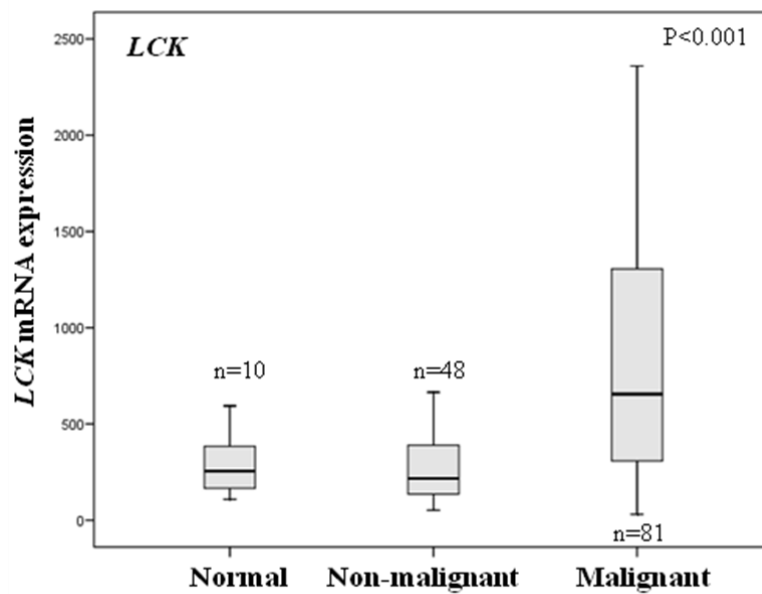
Figure 2.5: LCK mRNA expression in N, NM and M breast tissue

Figure 2.5: LCK is highest expressed in malignant breast tissue ($p < 0.001$).

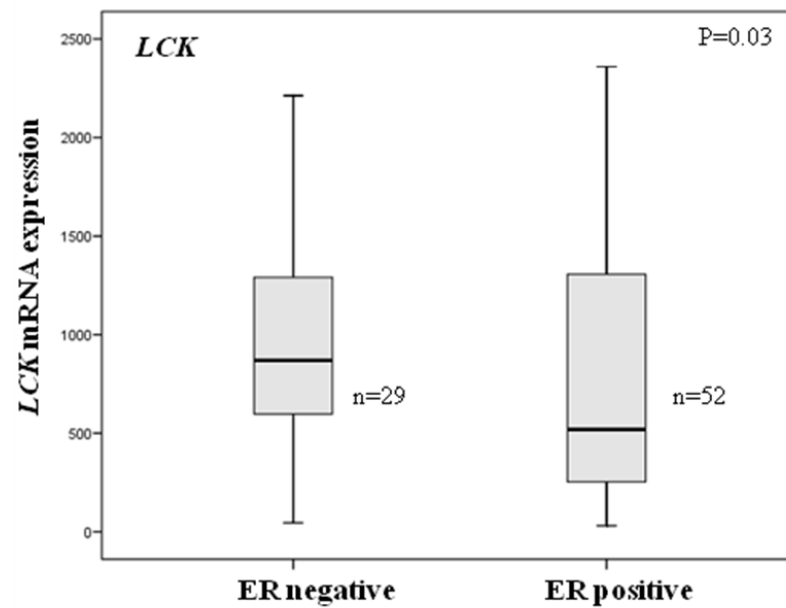
Figure 2.6: *LCK* expression in ER negative compared to ER positive patients

Figure 2.6 highlights the difference between *LCK* mRNA expression in ER negative compared to ER positive breast cancer patients ($p=0.030$).

All SFK members correlated with *SRC* expression. The strongest correlation detected was with *LYN* ($p<0.001$, c.c. 0.570) (figure 2.7), the weakest with *YES* ($p=0.030$, c.c. 0.242) (figure 2.8). An overview of those correlations is provided in table 2.4.

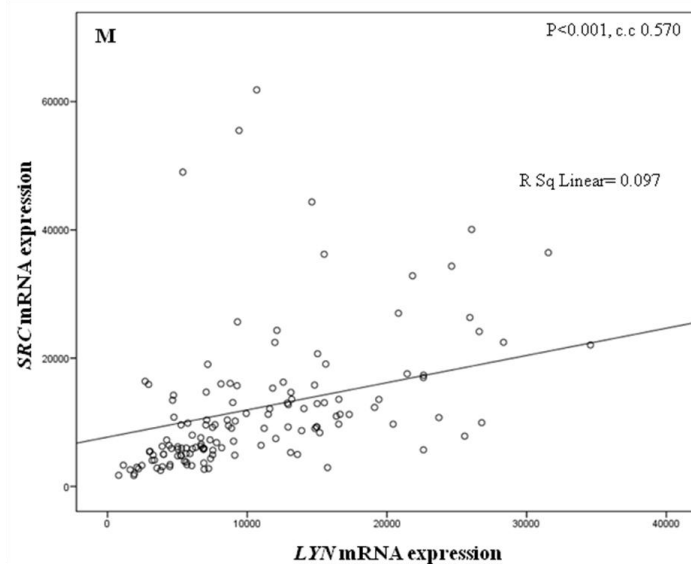
Figure 2.7: Correlation between *SRC* and *LYN* mRNA expression in the M cohort

Figure 2.7 illustrates a high correlation between *SRC* and *LYN* mRNA expression in the malignant PCR cohort ($p < 0.001$, $c.c. 0.570$).

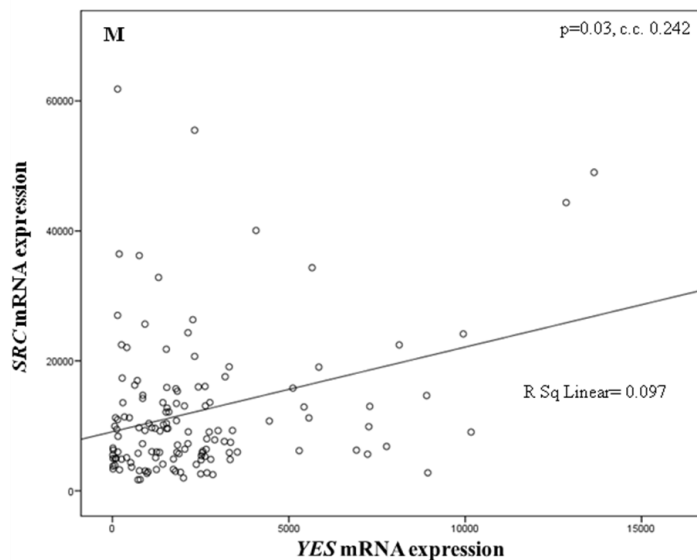
Figure 2.8: Correlation between *SRC* and *YES* mRNA expression in the M cohort

Figure 2.8: *SRC* mRNA expression was least correlating with *YES* mRNA expression in the malignant breast patient cohort ($p = 0.030$, $c.c. 0.242$).

Table 2.4: Non-parametric correlations between each SFK member

| | <i>SRC</i> | <i>LCK</i> | <i>LYN</i> | <i>FGR</i> | <i>FYN</i> | <i>HCK</i> | <i>BLK</i> | <i>YES</i> |
|-------------------|------------|------------|------------|------------|------------|------------|------------|------------|
| <i>SRC</i> | | | | | | | | |
| Cc | 1.00 | 0.410 | 0.570 | 0.521 | 0.448 | 0.473 | 0.316 | 0.242 |
| p-value | | <0.001 | <0.001 | <0.001 | <0.001 | <0.001 | 0.003 | 0.040 |
| <i>LCK</i> | | | | | | | | |
| Cc | 0.410 | 1.00 | 0.680 | 0.648 | 0.575 | 0.613 | 0.640 | 0.394 |
| p-value | <0.001 | | <0.001 | <0.001 | <0.001 | <0.001 | <0.001 | <0.001 |
| <i>LYN</i> | | | | | | | | |
| Cc | 0.570 | 0.680 | 1.00 | 0.683 | 0.742 | 0.756 | 0.527 | 0.274 |
| p-value | <0.001 | <0.001 | | <0.001 | <0.001 | <0.001 | <0.001 | 0.014 |
| <i>FGR</i> | | | | | | | | |
| Cc | 0.521 | 0.648 | 0.683 | 1.00 | 0.759 | 0.810 | 0.543 | 0.315 |
| p-value | <0.001 | <0.001 | <0.001 | | <0.001 | <0.001 | <0.001 | 0.004 |
| <i>FYN</i> | | | | | | | | |
| Cc | 0.448 | 0.575 | 0.742 | 0.759 | 1.00 | 0.858 | 0.649 | 0.323 |
| p-value | <0.001 | <0.001 | <0.001 | <0.001 | | <0.001 | <0.001 | 0.003 |
| <i>HCK</i> | | | | | | | | |
| Cc | 0.473 | 0.613 | 0.756 | 0.810 | 0.858 | 1.00 | 0.622 | 0.382 |
| p-value | <0.001 | <0.001 | <0.001 | <0.001 | <0.001 | | <0.001 | <0.001 |
| <i>BLK</i> | | | | | | | | |
| Cc | 0.316 | 0.640 | 0.527 | 0.543 | 0.649 | 0.622 | 1.00 | 0.349 |
| p-value | 0.004 | <0.001 | <0.001 | <0.001 | <0.001 | <0.001 | | 0.001 |

Table 2.4 demonstrates non-parametric correlations between each SFK member in malignant breast tissue (Spearman's Rank test).

Survival analysis was completed for all SFK members. Only *SRC* was significantly associated with decreased disease specific survival in ER positive breast cancer patients ($p=0.012$; figure 2.9). Patients with high *SRC* mRNA expression had a median survival of 4.5 years (IQR 2.7-6.3) compared to those with low expression with median survival of 11.6 years (IQR 6.9-13.3).

Figure 2.9: Kaplan Meier survival graph for mRNA expression *SRC* in ER positive patients.

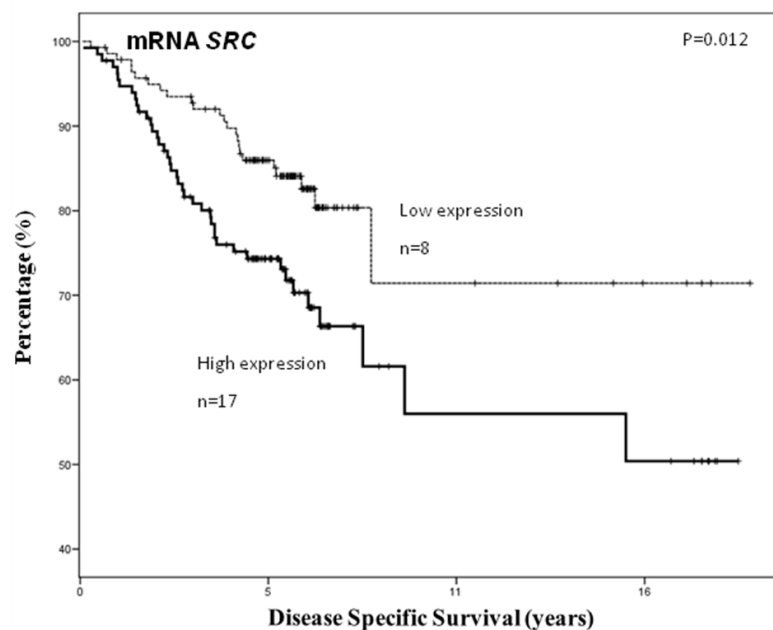


Figure 2.9 shows that high mRNA expression of *SRC* in ER positive patients was significantly associated with poorer clinical outcome ($p=0.012$).

2.3.4 Src kinase family member expression in non-malignant breast tissue

As observed within the invasive breast cancer specimen, *SRC* and *LYN* were the highest expressed Src kinase family members in non-malignant breast tissue and *BLK* the weakest expressed SFK member (figure 2.10).

Figure 2.10: Overview of SFK member expression in non-malignant breast tissue

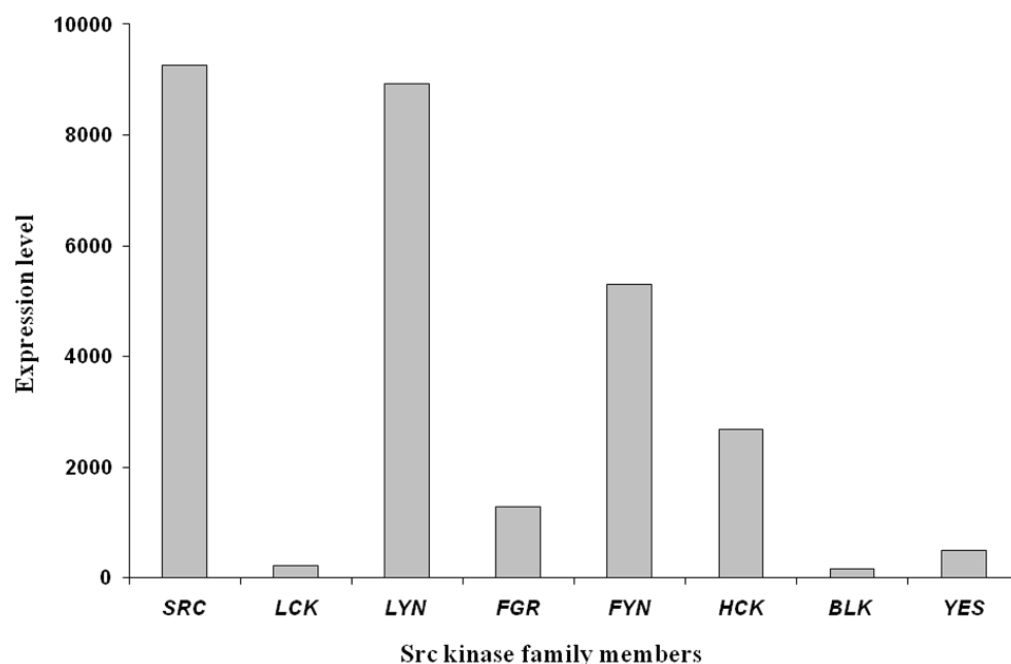


Figure 2.10 gives an overview of SFK member expression in non-malignant breast tissue. Like observed within the malignant breast tissue, *SRC* and *LYN* were the highest and *BLK* the least expressed SFK member in non-malignant breast tissue.

YES was least expressed in non-malignant breast tissue, compared to malignant and normal breast tissue ($p < 0.001$) (figure 2.11). No significant difference in expression between the malignant and non-malignant patient group was observed with *SRC*, *LYN*, *FGR*, *HCK* and *BLK*.

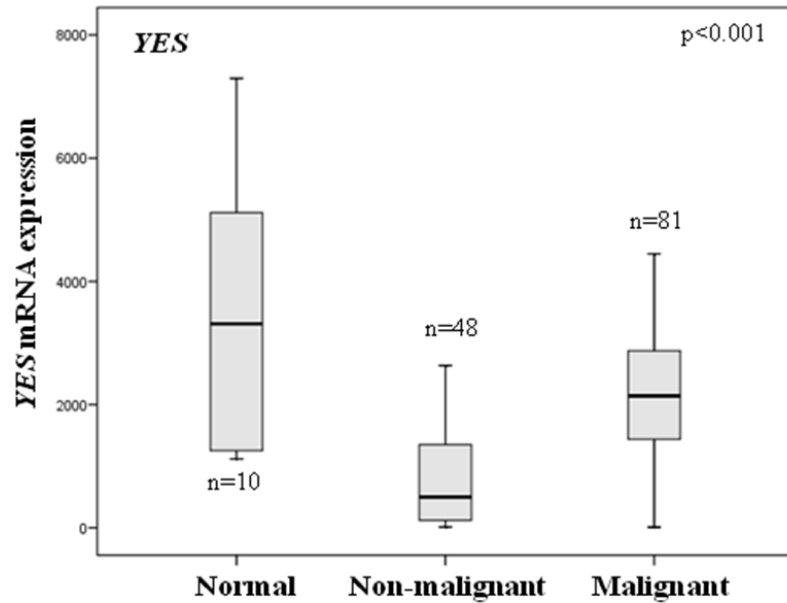
Figure 2.11: YES mRNA expression levels in N, NM and M breast specimens

Figure 2.11: YES is highest expressed in the normal breast specimen cohort compared to the other two cohorts ($p < 0.001$).

As with the invasive breast cancer specimens, all other Src kinase family members correlated with *SRC* expression. Again the strongest correlation was with *LYN* ($p < 0.001$, c.c. 0.799) (figure 2.12) and the weakest with *YES* ($p = 0.027$, c.c. 0.326) (figure 2.13).

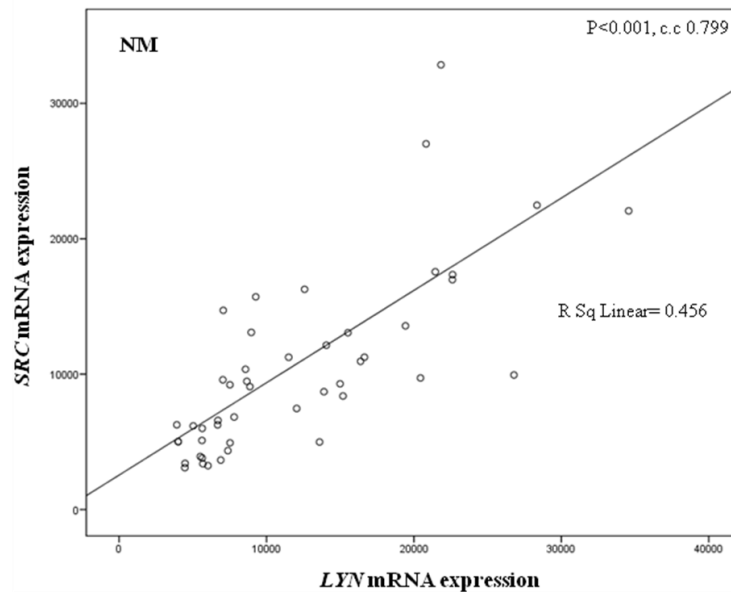
Figure 2.12: Correlations between *SRC* and *LYN* expression in the NM cohort

Figure 2.12 illustrates the correlation of *SRC* mRNA expression with *LYN* in the non-malignant PCR cohort ($p < 0.001$, $c.c. 0.799$).

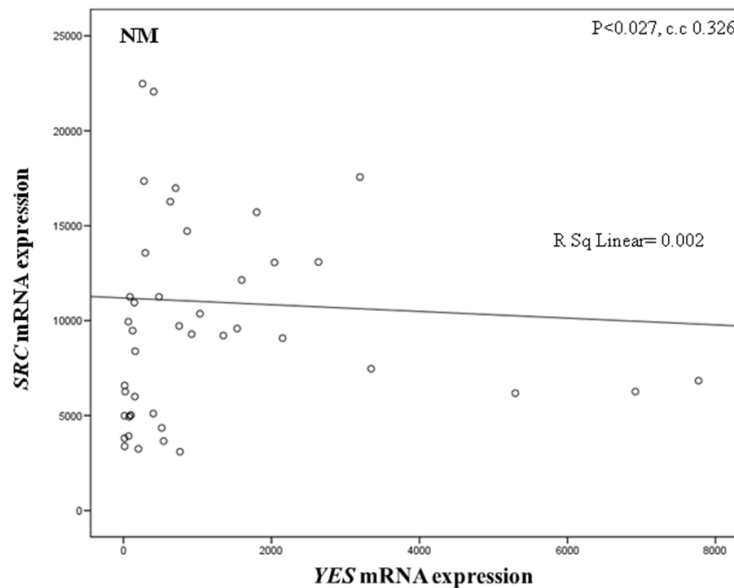
Figure 2.13: Correlations between *SRC* and *YES* expression in the NM cohort

Figure 2.13 demonstrates a low correlation between *SRC* and *YES* mRNA expression in the non-malignant breast patient cohort ($p = 0.027$, $c.c. 0.326$).

2.3.5 SFK member expression in normal/ breast reduction tissue

FYN was the most highly expressed SFK member in normal tissue. It was significantly higher expressed than any other SFK members (figure 2.14); 2.7 fold higher than *Src* and 100 fold higher than *Lck*. Highest expression levels of *Fyn* were observed in normal tissue compared to non-malignant and lowest in invasive breast cancer specimens ($p < 0.001$). No correlations between *Src* and SFK members were observed in normal breast tissue (table 2.5).

Figure 2.14: Overview of SFK member expression in normal breast tissue

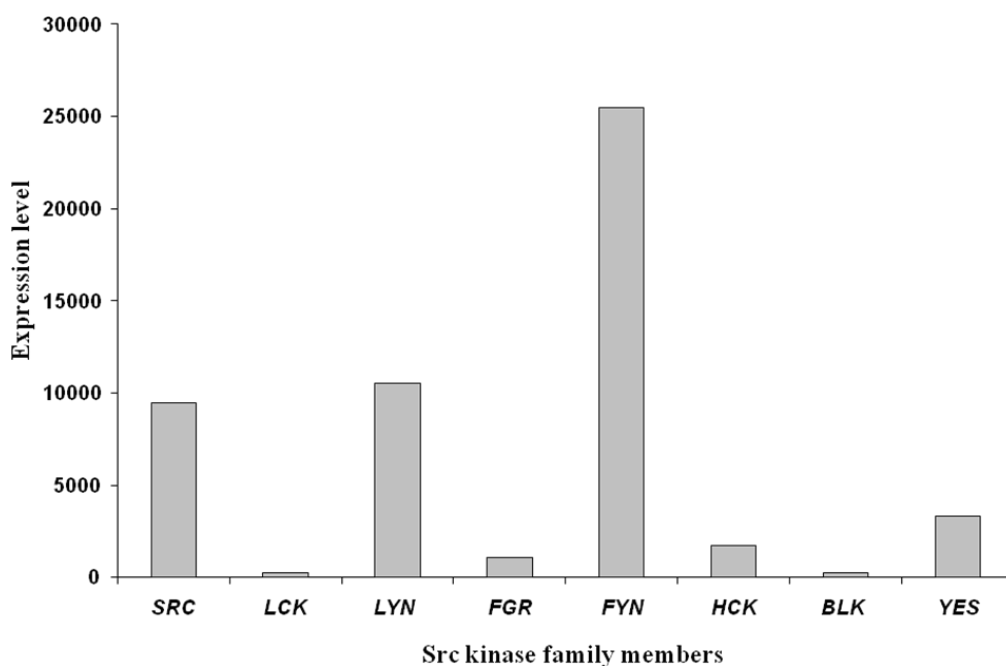


Figure 2.14 gives an overview of SFK member expression in normal breast tissue. *FYN* was highest expressed SFK member, followed by *LYN* and *SRC*.

Only *LCK*, *LYN* and *FYN* expression correlated with *SRC* expression (table 2.5): *LCK* ($p=0.043$, c.c. 0.648 (figure 2.15)), *LYN* ($p= 0.022$, c.c. 0.709) (figure 2.16), *FYN* ($p=0.043$, c.c. 0.648) (figure 2.17).

Table 2.5: Correlations between *SRC* and other SFK members in the N cohort

| | <i>LCK</i> | <i>LYN</i> | <i>FGR</i> | <i>FYN</i> | <i>HCK</i> | <i>BLK</i> | <i>YES</i> |
|------------|------------|------------|------------|------------|------------|------------|------------|
| SRC | | | | | | | |
| Cc | 0.648 | 0.709 | 0.588 | 0.648 | 0.430 | 0.552 | 0.321 |
| p-value | 0.043 | 0.022 | 0.074 | 0.043 | 0.214 | 0.098 | 0.365 |

Table 2.5: Correlations between *SRC*, *LCK*, *LYN* and *FYN* (Spearman's Rank test) were significant.

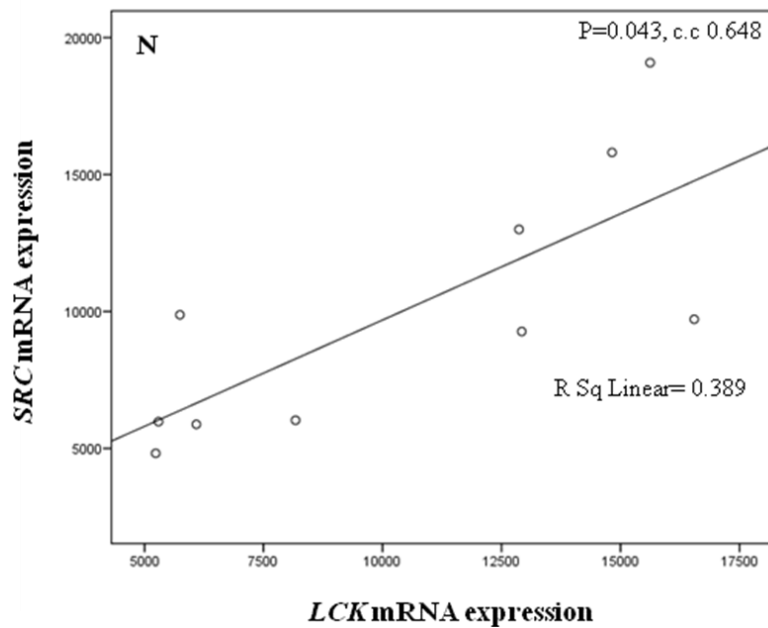
Figure 2.15: Correlation between *SRC* and *LCK* expression in the N cohort

Figure 2.15 displays the correlation of *SRC* mRNA expression with *LCK* mRNA expression in the normal breast tissue specimens ($p=0.043$, *c.c.* 0.648).

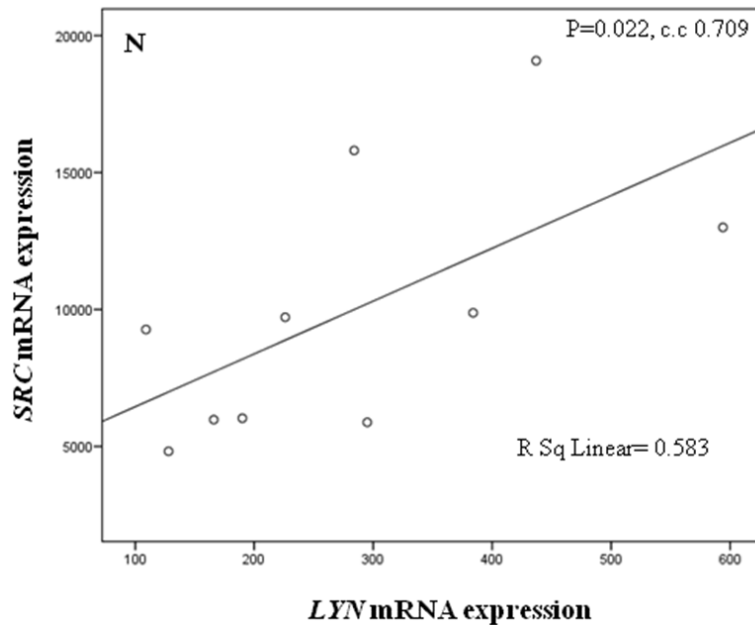
Figure 2.16: Correlation between *SRC* and *LYN* expression in the N cohort

Figure 2.16 illustrates the correlation of *SRC* mRNA expression with *LYN* in the normal PCR cohort ($p=0.022$, *c.c.* 0.709).

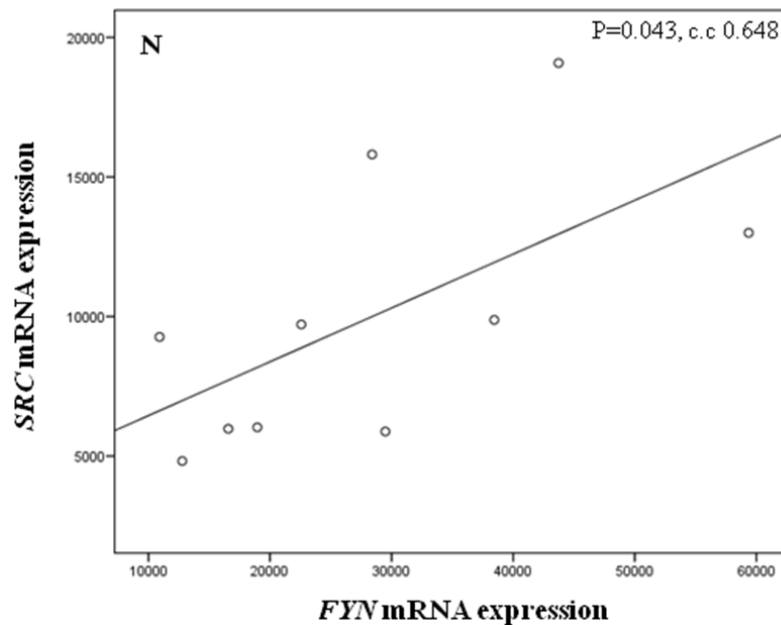
Figure 2.17: Correlation between *SRC* and *FYN* expression in the N cohort

Figure 2.17 elicits the correlation of *SRC* and *FYN* mRNA expression in specimens, collected from breast reduction mammoplasties ($p=0.043$, *c.c.* 0.648).

2.4 Discussion

SFK members are expressed in various cell types and tissues (192) and involved in cancer progression, via transduction of signals for cell growth, differentiation and survival, influencing cellular adhesion, migration and invasion (193). However, there is little translational evidence of SFK member expression in breast tissue.

In this pilot study we used RT-PCR, a molecular quantification method, for investigating mRNA expression of eight SFK members. One disadvantage of this technique is the handling of very labile mRNA. If tissue is not instantly fresh frozen after retrieval, mRNA is able to degrade rapidly and quality suffers leading to faulty results. To extract mRNA from certain tissue, for example bladder cancer, meticulous dissection with a laser is needed in order to achieve purification of tumour tissue that no other tissue type would dampen results. Valuable information about cellular locations is lost due to the necessity for tissue destruction in order to facilitate quantification of specific biomolecules.

Initially we used two housekeeping genes (*HPRT* and *GAPDH*) to establish which one of them was most suitable for evaluation of the different mRNA expression levels. Because of the least standard deviation with *HPRT* in our analysis and to use less reagent and materials (=financial resources) we only continued our study with *HPRT*. During this test period we also encounter difficulties with the *HPRT* gene assay. Its amplification plots suggested inhibition of the PCR reaction, preventing the PCR to amplify. After serial dilutions of the 100% DNA used originally, we found that a 1/10 dilution was providing us with the best amplification plot indicating that the real time PCR reached its full efficiency.

mRNA of all eight SFK members was investigated in normal, non-malignant and malignant breast tissue and confirmed to be present in all those tissue types in different expression levels. Interestingly, *SRC* expression levels were unchanged between the tissue types, despite being the highest expressed SFK member in malignant and non-malignant, but not in normal breast tissue. We only conducted a survival analysis within the malignant breast tissue cohort. *SRC* was the only SFK member, which was significantly associated with patients' survival. However we sensed that the study was slightly underpowered. The patient number in this cohort was only 81. To gain trustworthy results and draw reliable conclusions we saw the necessity to increase the patient number for survival analysis.

As *SRC*, *LYN* was also expressed at high mRNA levels in malignant and non-malignant, but not in normal breast tissue. It's unclear if the dissimilar expression profile of normal breast patients, with *FYN* being the highest expressed SFK member, is caused by the age discrepancy between this cohort and the others or is based on other clinico-pathological parameters. Nevertheless there was a significant correlation present between *FYN* and *SRC* expression.

We are undecided if this finding is of any importance. It's well known that Fyn is expressed in other normal tissue (68) e.g. osteoblasts. A recent study showed that *FYN* was expressed in those cells, but had no influence on proliferation or differentiation. Only Src, activated at high level, was inhibited by Src kinase inhibitor Dasatinib enhancing osteoblast differentiation (194). This patient cohort was originally thought to be only a control group. For this reason we only analysed a small number of samples.

LCK mRNA expression was highest in invasive breast cancer compared to the other groups, but was 14fold less expressed than *SRC*. It was not surprising to find Lck

expression in breast cancer specimen, a previous proto-oncogene screening study (194) had already recorded its presence in cancer. Increased Lck activity was also associated with SCLC (150) and with the development of thymic tumours (154). No data was yet available regarding relationship to other SFK member expression.

LCK is known to be mainly expressed in T-lymphocytes and thymocytes (135). It's uncertain if this reflects a higher immunoreactivity of the breast tumours. Over recent years it has become clear that disease progression in patients with cancer is dependent on complex interactions between the tumour and host inflammatory response (195). There is increasing evidence that both local and systemic inflammatory responses play an important role in the progression of a variety of common solid tumours (196). Several studies have demonstrated the relationship between markers of the systemic inflammatory response and survival in advanced metastatic breast cancer (197). Up till now, there is no evidence if high expression of SFK members (Lck) in breast tumours, an association with inflammatory markers (e.g. CRP) nor even high expression of lymphocytes in the surrounding stroma, expressing Lck, could lead to a poor clinical outcome.

With Src kinase inhibitors being commercially developed and made available for clinical trials, the lack of predictive and prognostic indicators in this area makes it more apparent to find an appropriate biomarker. This study established that all SFK member expression levels were correlating with *SRC* kinase expression. Additionally, *SRC* was the only gene where high mRNA expression was linked with poorer disease specific survival, suggesting that *SRC* could be used as a surrogate marker.

Due to small patient numbers in the malignant breast tissue PCR cohort and the lack of knowledge regards transcription of mRNA into protein level, there was a need to expand

the investigations into the role of Src and other noteworthy SFK members (Lck, Lyn) into a larger cohort of patients with more detailed clinical information and mature long term clinical follow-up.

With the knowledge that mRNA expression does not necessarily correlate with protein synthesis and protein expression, immunohistochemistry was employed to formalin fixed paraffin embedded breast cancer specimens to explore if observations made with mRNA expression regards survival, were still valid. It also would give us the opportunity to assess the importance of Src kinase protein activation investigating different activation sites of this non-receptor tyrosine kinase (next chapter).

CHAPTER 3

PROTEIN EXPRESSION OF SRC KINASE FAMILY MEMBERS AND THEIR ASSOCIATION WITH CLINICAL OUTCOME OF BREAST CANCER PATIENTS

3.1 Introduction

Having established mRNA expression and different expression levels of SFK members in different breast tissue types, this study aimed to prove the hypothesis that protein over-expression of Src, activated Src (phosphorylated and dephosphorylated tyrosine site 530, phosphorylated tyrosine site 419 and 215) and other most noteworthy expressed SFK members (e.g. Lyn, Lck,) would be associated with disease specific survival in breast cancer patients.

Immunohistochemistry was employed to assess the clinical significance of Src kinase protein expression and activation in larger cohort of invasive breast cancer patients, to establish which clinical subgroups (e.g. ER/PgR positive/negative, HER2 positive, triple negative) are more affected by Src mediated expression and to determine if these are linked to clinical outcome measures. Validity/specificity of these antibodies was verified by Western Blotting prior to Immunohistochemistry staining.

In addition, nuclear Ki67 expression was investigated to determine if SFK members are linked to high tumour proliferation.

3.2 Methods

Materials used within this chapter are listed in appendix 2.

3.2.1 Tissue microarray construction

Tissue microarrays were constructed because of the large number of patients in our cohort (n=895). It allows rapid tumour processing under standardised conditions (198). There are several advantages to be listed for using TMAs. Working with tissue arrays instead of whole tissue sections is an extremely useful method in saving limited human tissue, since whole tissue sections only allow a restricted number of experiments to be conducted. It is also a time and money saving technique, having to apply less quantity of primary antibody in one experiment run. Performing all experiments at the same time on all the tumour tissue ensures experimental uniformity.

Construction of the TMAs involved haematoxylin and eosin staining of the tissue sections of the breast cancer specimen, which was taken at time of the primary tumour resection. A consultant breast pathologist identified representative areas prior to coring. Individual tumour cores of those designated areas were then placed into a single recipient paraffin block.

For our cohort six different TMAs (TMA1= 197 cores, TMA2= 80 cores, TMA3= 43 cores, TMA4= 161 cores, TMA5= 187 cores, TMA6= 227cores) were constructed by Sylvia Brown. Each TMA was replicated in triplicates, using 3 * 0.6mm cores from each block to take into account heterogeneity of whole tumour sections. It also raises the possibility to gain results for all patients having three chances of obtaining informative cores.

3.2.2 Patient cohort

The patient cohort consisted of a total of 895 patients. All patients were diagnosed with operable invasive breast carcinoma between 1980 and 1999 in the Greater Glasgow area. These patients received standard adjuvant treatment according to protocols at the time of diagnosis. Patients were excluded from the study if clinical follow up data was incomplete, tissue blocks were not available or had insufficient tumour tissue as determined by the pathologist. Clinical and pathological characteristics, including age, tumour grade, size and histology, lymph node status, ER and HER2 status are summarised in Table 3.3, result section of this chapter.

The result analysis included only patients who had all clinical data, ER, PgR and HER status, full Src kinase, activated Src kinase, other Src kinase family member and Ki67 expression data available. The cohort patient number was therefore reduced to 314 patients.

Ethical approval was granted by the Glasgow Royal Infirmary Local Ethics Committee.

3.2.3 Western blotting

Western Blotting was performed to confirm antibody specificity before their usage in immunohistochemical staining of the TMAs. Proteins were prepared and kindly provided by Dr Liane McGlynn using breast cancer cell line lysates (MCF7 and MDAMB231). Western Blotting, also known as immunoblotting, detects and quantifies the amount of a specific protein in tissue or cells. Preparations for this technique include extracting protein samples from cultivated tissue or cells, separating the denaturated proteins by gel electrophoresis and transferring them to a PVDF membrane. This membrane is then exposed to a primary antibody specific to the protein of interest, followed by a secondary antibody recognising the antibody-antigen complex. To detect the proteins chemi-luminescent and chemi-fluorescent method is used. Those methods verify the specificity of all antibodies and measure the amount of proteins in samples from time course treatments.

3.2.3.1 Preparation

Determination of protein concentration

It is essential to determine the protein concentration of each sample before starting immunoblotting. Using the same amount of protein from all the tested samples ensures experimental consistency. The method used is the Bio-Rad protein assay. It is based on the Bradford dye-binding procedure (Bradford 1976) and involves a colorimetric assay for measuring the total protein concentration.

The protein samples were prepared as a low-concentration assay in disposable cuvettes (Gibo). A standard solution consisting of 200 μ l of Bio-Rad Reagent and 795 μ l dH₂O was pipette into one cuvette, subsequently followed by 5 μ l of protein sample.

To obtain an accurate concentration reading it is important to mix the solution thoroughly for even distribution of the protein. For comparison of the protein concentrations of each sample, protein standards were prepared using Bovine Serum Albumin (BSA). BSA was diluted with dH₂O to 1 mg/ml. Reference samples (only dH₂O and Bio-Rad Dye) and serial dilutions (for protein standards) from 1-50 µg/ml were set up afterwards. Reference sample and protein standard samples were used to calibrate the spectrophotometer (Bio-Rad) applying the Protein 595 Assay program.

The Bio-Rad protein assay is based on a colour change of Coomassie brilliant blue G-250 dye. The Coomassie dye binds to basic and aromatic acids residues of proteins. Protein concentration was determined via the absorbance change of the dye when bound to protein. Bound Coomassie blue dye has an absorption spectrum maximum at 595nm, whereas unbound dye has an absorbance maximum at 470 nm. Consequently an increased absorption at 595 nm is proportional to the amount of protein within the sample.

Optical density for the reference and the seven protein standard samples were measured at 595 nm. Optical density at 595 nm (O.D. 595) was then read for all other protein samples. The spectrophotometer calculated at that time the amount of protein (µg/ml) present in the sample, plotting a graph of absorbance at 595 nm against the protein concentration of the standard samples. This standard curve is used to determine the protein concentration of the measured sample from its O.D. 595 value.

The initial protein concentration (µl/ml) was calculated from a diluted protein sample (1:200). To determine the final protein concentration in mg/ml following formula was used:

$$\text{Protein reading } (\mu\text{l/ml}) \times 0.2 = \text{Final protein concentration (mg/ml)}$$

A standard amount of 20 µg of protein was used for western blotting, the volume of the sample required (µl) calculated from the final concentration.

Preparation of SDS-PAGE Gels

All Western Blots were performed using the Bio-Rad Mini-PROTEAN 3 Electrophoresis System. For the size (kDa) of all the analysed proteins it was appropriate to use a 10% resolving gel.

The formation of the gels is based on polymerisation of the Acrylamide and N-N-methylene-bis-acrylamide (Bis). Bis acts as cross-linking agent for the gel and TEMED and APS are the catalysts for the gel polymerisation. The separation of proteins is dependant on the size of the gel pores, which is determined by the amount of Acrylamide/Bis-Acrylamide present in the resolving gel. Increasing the volume of Acrylamide decreases the pore size. In general a higher percentage of resolving gel is used for smaller proteins. Larger proteins are more effectively separated in a lower percentage gel.

Gels with 1.5 and 0.75 mm thickness, were used throughout the studies in this project. They were produced using either a 1.5 or a 0.75 mm spacer plate (Bio-Rad Laboratories) respectively. Once the 10% resolving gel was prepared, the gel plates and gel casting apparatus (Bio-Rad Laboratories) assembled the gel mix was titrated slowly between the two glass plates using a plastic pastette leaving enough space to the top for adding stacking gel and comb (Bio-Rad Laboratories).

To flatten the top of the gel and to remove air bubbles, a layer of isopropanol is applied before the resolving gel is left for at least 30 minutes for polymerisation.

Once set, the isopropanol is poured off from the top of the resolving gel and the already prepared 4.5% stacking gel is added until it reaches the top of the plates. The appropriate gel comb (10 well comb for 0.75 mm spacer plates and 15 well comb for 1.5 mm spacer plates) is inserted from the top. The polymerising gel is left for about another 30 minutes.

Protein Denaturation

Denaturation of the proteins unfolds the protein. It gives the antibody access to bind onto its epitope and lets the proteins run better through the gel. Protein of interest was 60 kDa (Src and Src kinase family members) and 120 kDa (FAK) in size.

Having measured the concentration of each protein sample a defined amount (25 or 30 μg) of protein was removed from each sample, placed into a new Eppendorf cup and stored on ice. To each sample a Laemmli's sample reducing buffer is added (2x protein + 1x Laemmli's buffer).

After the samples were thoroughly mixed they were boiled at 98 °C for 4 minutes. SDS, Laemmli's buffer, contains a detergent with a high negative charge. It binds with its hydrophobic tail onto the protein, charges the protein negative and disrupts the tertiary structure of the protein resulting into its unfolding. Boiling the samples contributes to its complete unfolding. 2-Mercaptoethanol prevents the reformation of disulphide bonds and helps to maintain the protein in its denaturated state. The Biotinylated Protein Ladder, a molecular weight marker, which is used to determine the size of the detected protein, was also boiled for 4 minutes. All boiled samples were immediately stored back onto ice.

3.2.3.2 Immunoblotting

Gel Electrophoresis

The proteins moved through the polyacrylamide gel, because of electrical charge. SDS transfers a negative charge onto the proteins allowing them to be attracted towards the positive anode. Smaller protein molecules travelling much faster through the acrylamide pores of the gel than larger molecules, therefore those can be found further down the gel. Gel electrophoresis separates protein by their molecular weight.

Gels were placed into the electrode assembly in a mini buffer tank. After removing the combs and rinsing the wells the tank was filled with running buffer (details in appendix 2) to submerge the whole gel complex. The ladder (7 μ l) and denaturated protein samples (x μ l/ samples- depending on protein concentration) were carefully loaded into dedicated wells, as per protocol and Bradford Protein Assay reading, to achieve equal protein loading. Specific long fine tipped pipettes (alpha laboratories) were used to prevent overspill and contamination of other wells. Once all samples were loaded the gel was run at 100V for approximately 60 minutes.

Protein Transfer

The proteins need to be transferred from the polyacrylamide gel to a PVDF (polyvinylidene difluoride) membrane to enable the next step of protein detection via antibody exposure and binding to specific proteins molecules. Transfer was achieved using Mini-Trans Blot Cell tank (Bio-Rad Laboratories) to transfer the proteins onto the membrane over a time period of 60 minutes.

After the gel electrophoresis is completed and the proteins have run sufficiently through the gel, the protein transfer onto PVDF membrane (Bio-Rad Laboratories) can begin. The PVDF membrane, fibre pads and 3M Whatmann paper (VWR) need to be cut slightly bigger than the size of the polyacrylamide gel and soaked in transfer buffer (details in appendix 2). For optimal transfer it's necessary to pre-treat the PVDF membrane in 100% methanol for five minute before immersing it in transfer buffer.

The glass plates were carefully lifted, the stacking gel on the top discarded and the remaining gel was equilibrated in transfer buffer for approximately five minutes before assembling the "transfer sandwich". This step should prevent the gel from shrinking during the transfer process.

The "transfer sandwich" consisted of fibre pads, 3M Whatmann paper, gel and PVDF membrane, compiled in a gel holder cassette (figure 3.1).

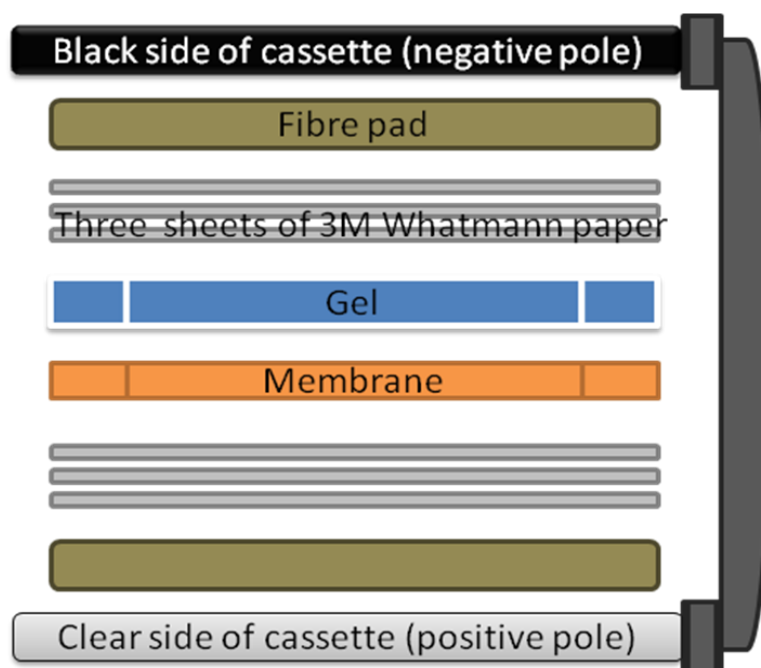
Figure 3.1: Western blot transfer sandwich

Figure 3.1 shows a schematic representation of the Western Blot “Transfer Sandwich”, the order and the different layers of various materials.

Whilst building the “transfer sandwich”, a glass rod was used to ensure no air bubbles were present between the layers, by rolling over the top surface. Air bubbles prevent proficient transfer. The constructed sandwich was then slotted into the electrode assembly and positioned into the mini-tank, which was filled with transfer buffer. Bio-Ice cooling unit (Bio-Rad Laboratories) and a magnetic stirrer were also placed in the tank to reduce temperature of the buffer during the transfer process and to maintain even buffer temperature and ion distribution. The protein transfer process from gel (negative/cathode) to membrane (positive/anode) was completed after approximately 60 minutes at 100 Volts.

Blocking of Membrane

To avoid non-specific binding of the primary antibody to the membrane and consequently reduce background staining it was necessary to block the membrane by

incubating the membrane in 5% Non-Fat Dry Milk (Marvel) blocking solution (details in appendix 2) for one hour at room temperature. This step and all future steps were carried out on a rotatest shaker (R100/TW, Luckham), rotating at 70 rpm.

After transferring the proteins the gel was stained with Coomassie blue solution (details in appendix 2) to determine how efficient the transfer was. The gel was left for 40 minutes in Coomassie blue followed by destaining solution overnight. Any protein that remained on the gel was visible the next morning as blue bands.

Incubation of Membrane with Primary Antibody

During blocking time primary antibody solutions were prepared in 5% Non-Fat Dry Milk/TTBS (solution details in appendix 2) and stored at 4°C- again to reduce non-specific binding. After 60 minutes blocking the membrane then was incubated with the primary antibody overnight (approximately 18 hours) at 4°C. For the size of membrane used (about 10 mm x 7 mm) 10 ml of antibody was adequate to cover the entire membrane.

Incubation of Membrane with Secondary Antibody

Following incubation with primary antibody the membrane was washed in TTBS three times for 10 minutes to remove any excess antibody. To detect the protein of interest a secondary antibody is needed to bind either to biotin or an enzyme conjugate, e.g. horseradish peroxidase (HRP), which was species-specific to the primary antibody. The secondary antibody used, was HRP-linked anti-rabbit (1:5000) or anti-mouse IgG at a dilution of 1:10000. As the primary antibodies all secondary antibody solutions were prepared in 10 mls of 5% Non-Fat Dry Milk/TTBS. Anti-biotin HRP linked antibody was added to detect the biotinylated ladder (details in appendix 2). The membrane was incubated for 60 minutes at room temperature.

Protein Visualisation

A chemiluminescent method was employed to detect the protein of interest. Luminescence is the emission of light due to the dissipation of energy from a substance in an excited state. Horseradish peroxidase catalyzes oxidation of luminol, a chemiluminescent substrate, in alkaline conditions. Oxidation results in luminal being in an excited state, then decaying to ground state via emitting light. For this method ECL Plus pack was used: horse-radish peroxidase, conjugated to the secondary antibody, oxidases the ECL Plus chemiluminescent substrate (Lumigen PS-3 Acridan) producing thousands of acridinium ester intermediates per minute. These intermediates then interact with the peroxidase to produce a sustained high intensity chemiluminescence with a maximum emission at 430nm. This light is detected on autoradiography film (X-ray film).

After 60 minutes of incubation with secondary antibodies the membrane was washed three times in TTBS for 10 minutes. During this process the ECL Plus reagents were warmed to room temperature. ECL reagents are sensitive to light therefore all following steps were performed in semi-darkness. ECL Plus solution A and solution B were mixed in a ratio 40:1. The use of 3 mls of the combined solution was adequate to cover the membrane.

The membrane was then placed protein side up on a sheet of cellophane wrap. ECL solution was pipetted onto the membrane ensuring complete coverage and incubated for 5 minutes. Excess solution was then removed and the membrane passed over onto a fresh sheet of cellophane wrap, in which it was enclosed. Finally the membrane was transferred into a film cassette. In complete darkness autoradiography films (Kodak Medical X-ray films, 18x24 cm) were exposed to the membrane for various times- 1, 5 and 15 minutes. The films were then developed by passing it through X-ray developer

machine XOMAT 1000 (Kodak). Both marker and protein bands visualised and analyzed accordingly.

3.2.3.3 Stripping of Membrane

Restoring the membrane for further use, antibodies were removed from the probed membrane by incubating in 20 ml of Re-Blot Stripping Buffer at 37°C for 15 minutes, followed by being washed three times for 10 minutes in TTBS. Subsequently the membranes were blocked again in 5% Non-Fat Dry Milk/TTBS and stored at 4°C until probed with the next primary and secondary antibody, as described above.

3.2.4 Immunohistochemistry

The IHC method used in this study was indirect immunohistochemistry. This method uses another antibody (secondary antibody), already labelled with the marker, which recognises and binds with the primary antibody.

The method used here for investigating the expression levels of Src kinase family members and their activated forms in breast tumour tissue involved rabbit and mouse monoclonal antibodies and the DAKO Envision System, staining and visualising antigenic sites with peroxidase and DAB (3,3,-diaminobenzidine). This method has built on dextran polymer technology. The primary antibody recognises the expressed protein. Applied Envision attaches itself to the secondary antibody. This is followed by appliance of Vector-DAB solution. Peroxidase then reacts with DAB to produce an insoluble yellow-brown precipitate, representing the target antigen, which can be seen and analysed under the light microscope (figure 3.2).

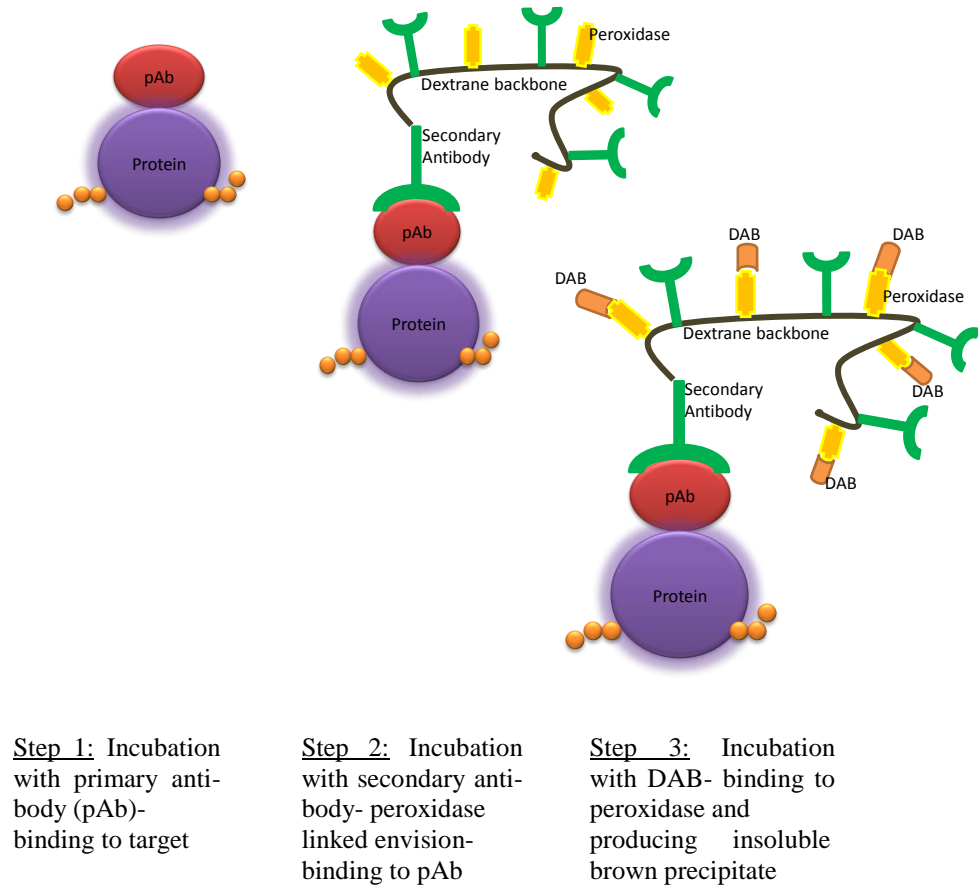
Figure 3.2: Indirect immunohistochemistry method

Figure 3.2: Schematic illustration of the indirect immunohistochemistry method amplifying the signal by the primary antibody.

3.2.4.1 Preparation

TMA's were cut into 3-4 μm thick paraffin wax sections and mounted on 3-aminopropylethoxysilane coated slides. Slides then can be stored for 3-6 months at a temperature of 4°C. Before specific slides were used for IHC, there were incubated at 56°C overnight.

3.2.4.2 Removal of Wax

Prior to IHC staining tissue arrays were dewaxed with Xylene (2x2min) and rehydrated through a series of alcohol washes (100% 2x2min; 90% 2x2min, 70% 2x2min).

3.2.4.3 Antigen Retrieval

It's necessary to include an antigen retrieval step to optimise immunohistochemical staining. Formation of methylene bridges, which may have developed during the formalin fixation, can cross link proteins and mask antigenic sites. Exposure of those antigen binding sites is essential for primary antibodies to bind correctly.

Two different antigen retrieval solutions were used: 10 mM Citrate Buffer (1:10 dilution of pre-made Epitope Retrieval Buffer at pH 6.0 and TE Buffer (1 mM EDTA, 5 mM Tris buffer at pH 8.0). Both solution were preheated in the microwave for 13.5 min to a temperature of 96 °C before tissue array slides were placed into the solution and pressure cooked for 5 min followed by a cool down period of 20 min (table 3.1).

Table 3.1: Immunohistochemistry antibody information

| Protein | Antibody | Antigen Retrieval | H₂O₂ Conc. | Horse Serum Conc. | Antibody Dilutions | Incubation Time and Temp |
|-------------------|------------------------------|-----------------------------|---|--------------------------|---------------------------|---------------------------------|
| Total Src | Rabbit Cell Signalling | Citrate Buffer pH 6.0 | 0.3% | 1.5% | 1:200 | 60 min at room temp |
| Anti- clone 28 | Rabbit Invitrogen | Citrate Buffer pH 6.0 | 3.0% | 5% | 1:1500 | Overnight at 4°C |
| Clone 28 | Mouse Invitrogen | Citrate Buffer pH 6.0 | 3.0% | 5% | 1:500 | Overnight at 4°C |
| Y416Src | Rabbit Cell Signalling | Citrate Buffer pH 6.0 | 0.3% | 5% | 1:2000 | Overnight at 4°C |
| Y216Src | Rabbit Santa Cruz | Citrate Buffer pH 6.0 | 3.0% | 5% | 1:25 | Overnight at 4°C |
| Lyn | Mouse BD Biosciences | TE Buffer pH 8.0 | 1.0% | 5% | 1:5 | Overnight at 4°C |
| Lck | Rabbit Cell Signalling | TE Buffer pH 8.0 | 3.0% | 5% | 1:50 | 60 min at room temp |
| Ki67 | Mouse DAKO | TE Buffer pH 8.0 | 3.0% | 5% | 1:150 | 60 min at room temp |

Table 3.1: Details of the primary antibodies used to detect total Src, its activated forms (Y216, Y416), the SFK protein Lyn and Lck and proliferation marker Ki67. Further information is given regarding antibody source, antigen retrieval method, blocking reagent concentrations (H₂O₂ and Horse Serum), antibody dilutions, incubation time and temperature are all listed above.

Citrate Buffer= 10mM Citrate buffer, TE Buffer= 1 mM EDTA, 5 mM Tris buffer at pH 8.0. Both solutions were preheated in the microwave for 13.5 min to a temperature of 96 °C before slides were pressure cooked for 5 min with a cool down period of 20 min.

3.2.4.4 Blocking of Other Proteins

The presence of endogenous peroxidase activity in tissue is a regular problem in IHC, causing background staining. To block endogenous peroxidase activity the slides were incubated in hydrogen peroxide (0.3% or 3.0% H₂O₂- depending on antibody, table 3.1) for ten minutes followed by a wash in running water.

Formations of hydrophobic bonds between immunoglobulins and tissue proteins can cause non-specific binding of the primary and/or secondary antibody to the tissue sections resulting again in back ground staining. To avoid this non-specific binding tissue arrays were incubated in horse serum (1.5% or 5%- depending on antibody, table 3.1) with antibody diluent for 20 min at room temperature.

3.2.4.5 Staining of TMA Slides

Incubation with Primary Antibody

Antibodies for the following proteins were used: c-Src, Lyn, Lck, phosphorylated and dephosphorylated Y530Src, Y419Src and Y215Src. To establish optimum conditions for highest quality of antigen staining, a series of investigations were performed varying antigen retrieval, antibody dilutions, incubation times and temperature (table 3.1). In each experiment run a positive and negative isotype matched control was included to ensure no false positive staining. The positive control confirmed that the chosen IHC method was working whilst the negative control checked for non-specific binding of the antibody.

Incubation with Secondary Antibody

Following incubation with antibody or no isotype matched control (negative control), the tissue array slides were thoroughly washed twice in TBS buffer (details in appendix 2) for 5 minutes. A secondary antibody is required to bind onto the primary antibody to detect the protein of interest in the breast tissue. The DAKO Envision system was used, which is based on dextran polymer technology. A large number of enzyme molecules, including horseradish peroxidase, attach themselves to the secondary antibody via a dextran backbone (figure 3.2) with the advantage of increased sensitivity and decreased non-specific background staining. A substrate chromagen binds then to the peroxidase molecules producing a yellow-brown coloured product matching the quantity of the protein being investigated. The slides were incubated with Envision solution for thirty minutes at room temperature and then again thoroughly washed twice with TBS Buffer before Vector DAB solution was applied. Slides were left for 10 minutes at room temperature followed by a final wash in running water.

Detection and Visualisation

The chromagen used for staining the TMA slides was DAB (3,3'-diaminobenzidine), a combination of 5mls dH₂O, 2 drops of DAB Buffer solution, 4 drops of DAB Substrate solution, and 2 drops of Hydrogen Peroxidase solution. DAB was applied onto the slides, left for 10 minutes to permit brown staining to develop and then washed with running water.

3.2.4.6 Counterstaining of TMA Slides

TMA slides were counterstained with haematoxylin and Scott's Tap Water Substitute (S.T.W.S.). Slides were submerged in haematoxylin for around thirty seconds until a red colour develop on the tissue arrays; the arrays were cleared by dipping them into acid alcohol to remove excess colouring. Subsequently they were then immersed in

S.T.W.S. for about thirty seconds to produce blue staining as a contrast to the yellow-brown staining of the antigen.

3.2.4.7 Dehydrating and Mounting of TMA slides

The last steps comprise dehydrating the TMAs immersing the slides through a series of alcohol washes with increasing percentage: 70% 1 min, 90% 1 min, 100% 2x1 min and 2x 1 min Xylene. The slides were then mounted with coverslips using DPX mountant and stored away, covered at room temperature.

3.2.5 Immunohistochemistry Scoring

3.2.5.1 Weighted Histoscore (H-Score)

All TMAs were scored independently by Joanne Edwards (JE) and myself (BE) for their nuclear, cytoplasmic and membrane protein staining within each tumour core, using a semi-quantitative weighted histoscore method (199;200). The intensity of staining was assessed and graded as negative (0), weak (1), moderate (2) and strong (3) staining. The percentage of tumour cells within each category was then estimated and a histoscore was calculated using the following formula:

$$\begin{aligned}
 & 0 * X\% && \text{of negative tumour cells} \\
 & + 1 * X\% && \text{of weakly stained tumour cells} \\
 & + 2 * X\% && \text{of moderated stained tumour cells} \\
 & + \underline{3 * X\%} && \text{of strong stained tumour cells} \\
 & = && \mathbf{Y} \text{ total histoscore}
 \end{aligned}$$

The weighted histoscore ranged from zero (minimum) to 300 (maximum). Conformity of the two observers' scoring was assessed by calculating intra- (variation in individual scoring) and inter- (variation between the observers) class coefficients.

A scoring difference of more than 50 was considered as conflicting and resulted in re-evaluation of those particular tumour cores by each observer. ICCC scores greater than 0.8 are regarded as excellent. Comparison of both JE and BE scores generated ICCC scores between 0.84 – 1.00 as shown below in table 3.2.

Table 3.2: ICCC scores for each protein expression analysis

| ICCC | Nuclear | Cytoplasm | Membrane |
|---------------|---------|-----------|----------|
| c-Src | 0.95 | 0.93 | 0.88 |
| anti-Clone 28 | 0.91 | 0.83 | 1.00 |
| Clone 28 | 0.91 | 0.95 | 1.00 |
| Y416Src | 0.98 | 0.95 | 0.96 |
| Y216Src | 0.84 | 0.94 | 0.87 |
| Lyn | 0.90 | 0.95 | 0.98 |
| Lck | 0.99 | 0.95 | 1.00 |

Table 3.2: Breast tumour cores were independently scored by two observers (BE and JE) for nuclear, cytoplasmic and nuclear staining of c-Src, Y419Src, Y215Src and SKF members (Lyn, Lck). A semi-quantitative weighted histoscore method was applied. Ki-67 staining was scored using the Ki-67 labeling index. Agreement between scores was measured using inter-class correlation coefficients. The ICCC scores for all primary antibodies are listed above. ICCC scores above 0.8 are considered as excellent.

ICCCs were performed to verify consistency between scorers. Scattered plots for each antibody are displaying this data below. To confirm no bias between scorers was present Bland-Altman plots were constructed (figure 3.3).

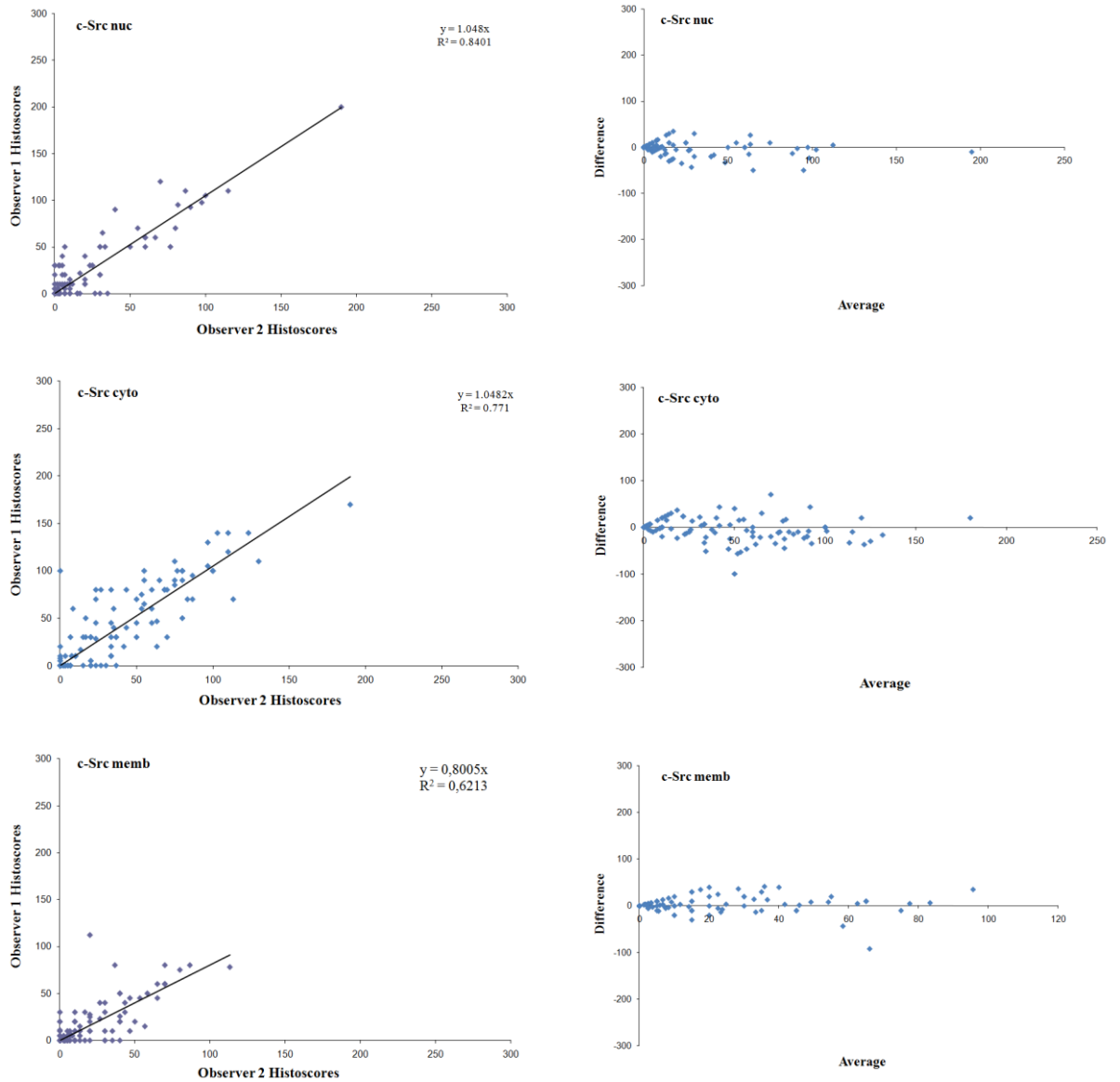
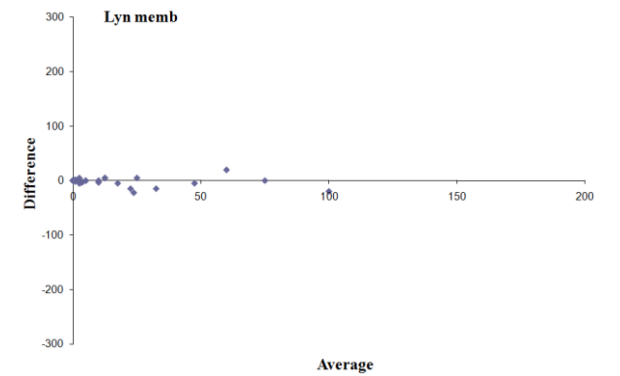
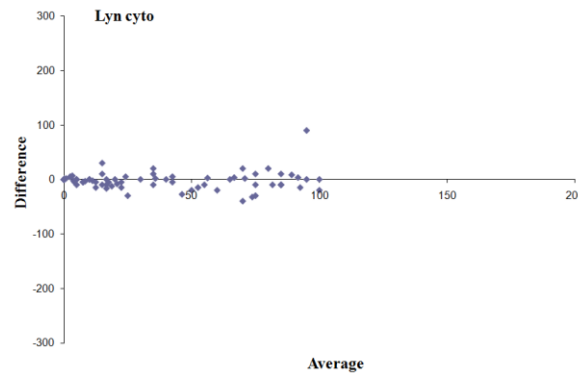
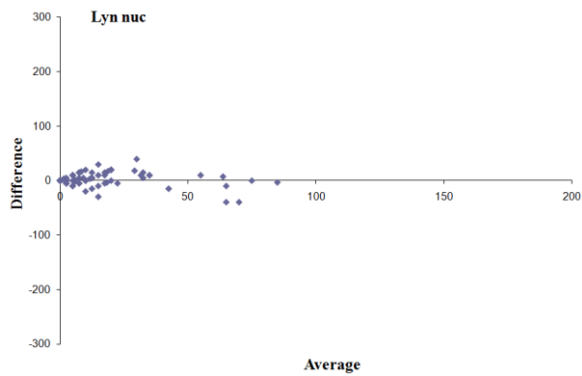
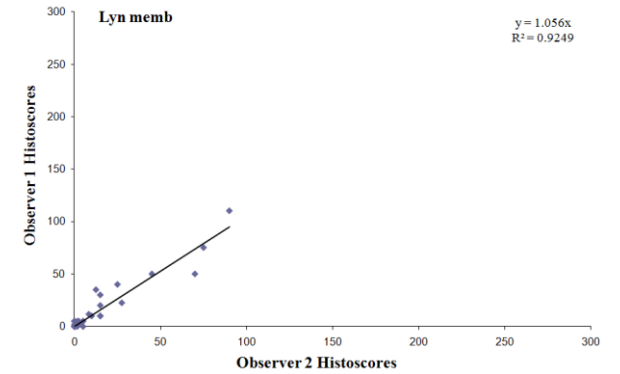
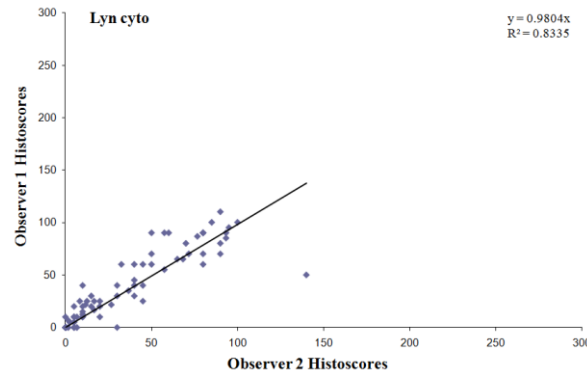
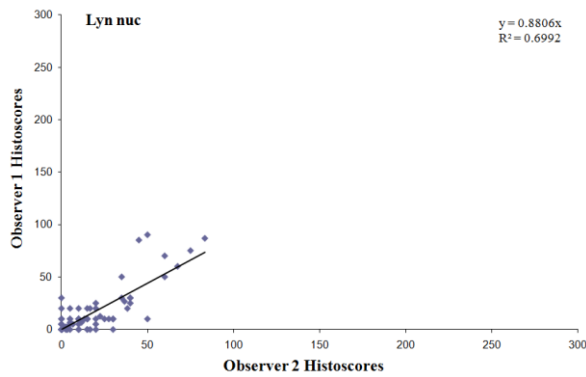
Figure 3.3: Scattered Plots and Bland-Altman Plots for all antibodies**c-Src**

Figure 3.3: Scattered plots and Bland-Altman plots for nuclear, cytoplasmic and membrane c-Src expression based on scorer-observer variation. The range and distribution of scores confirm appropriate scorer-observer correlation.

Lyn

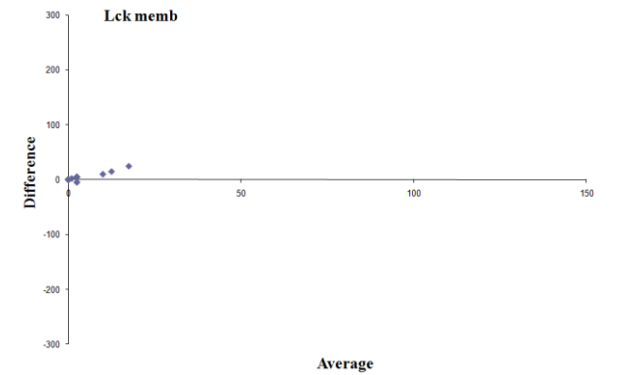
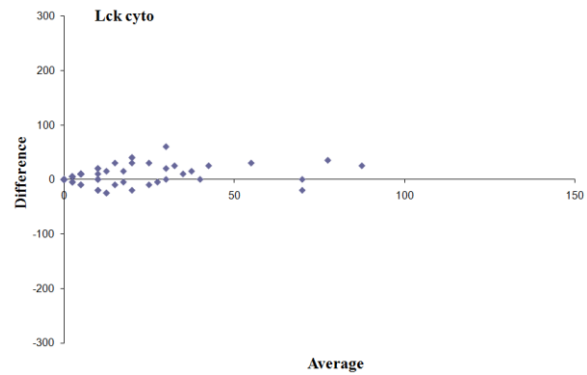
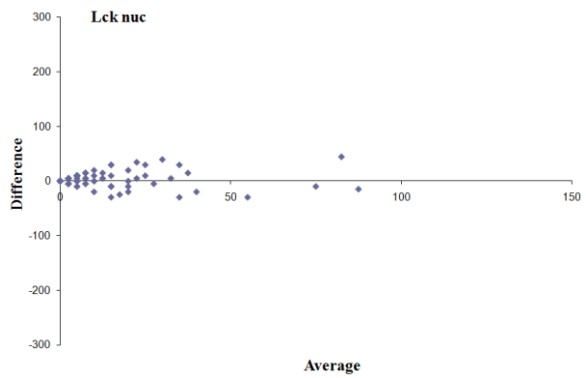
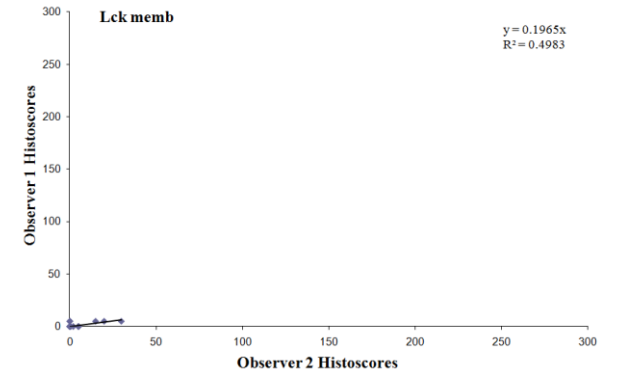
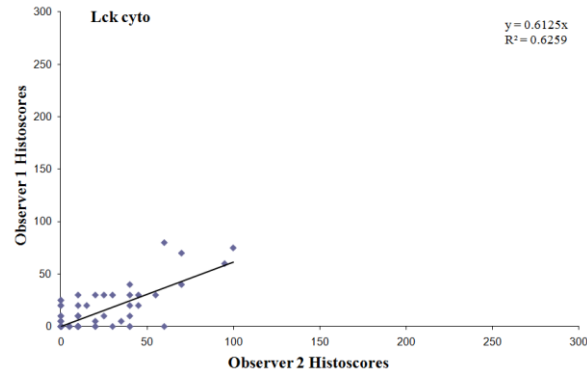
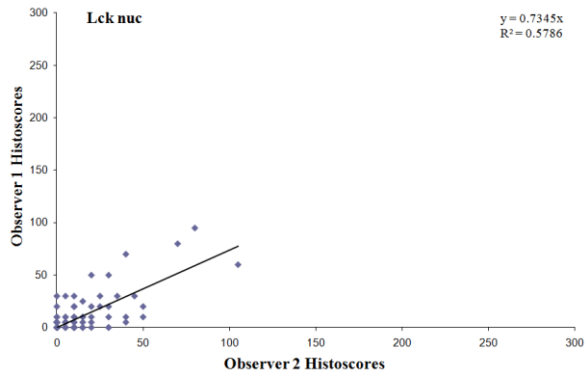


Scattered plot and Bland-Altman plot for nuclear Lyn expression.

Scattered plot and Bland-Altman plot for cytoplasmic Lyn expression.

Scattered plot and Bland-Altman plot for membrane Lyn expression.

Lck

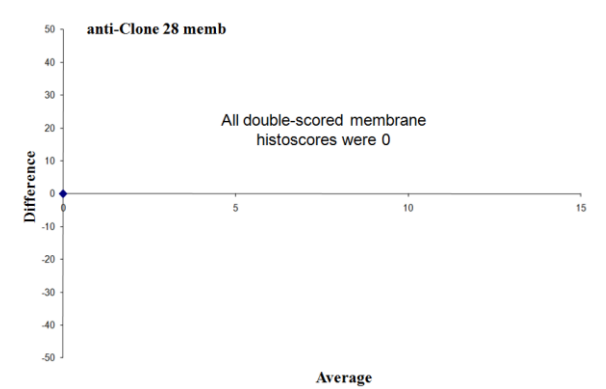
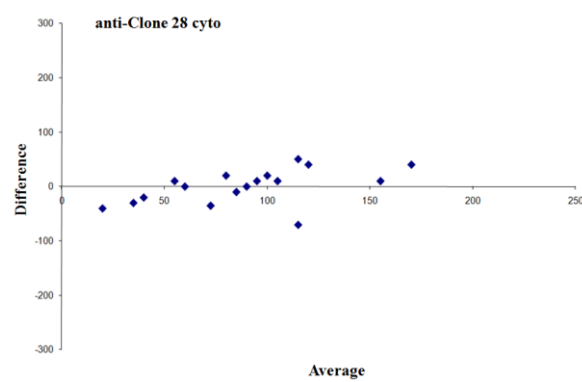
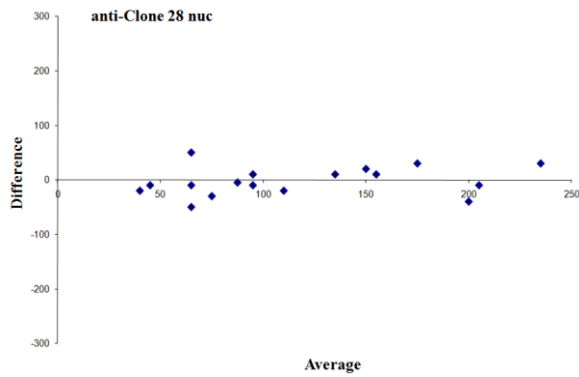
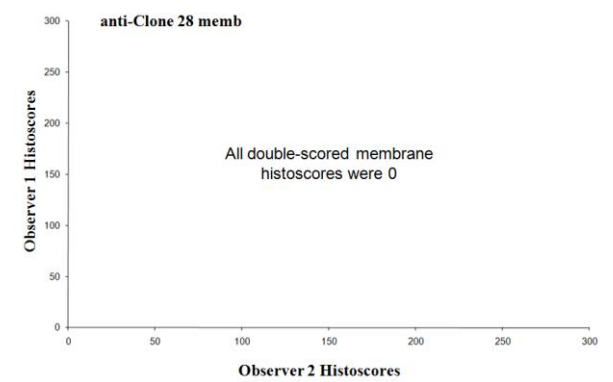
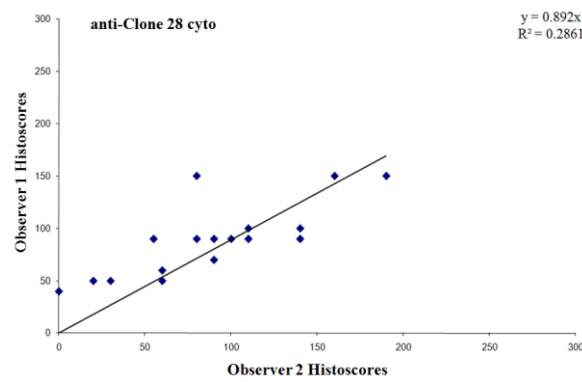
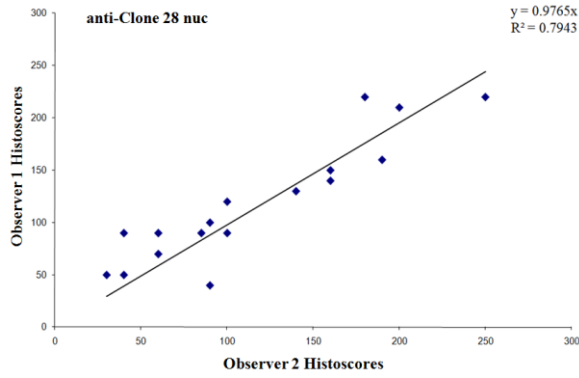


Scattered plot and Bland-Altman plot for nuclear Lck expression.

Scattered plot and Bland-Altman plot for cytoplasmic Lck expression.

Scattered plot and Bland-Altman plot for membrane Lck expression.

AC 28

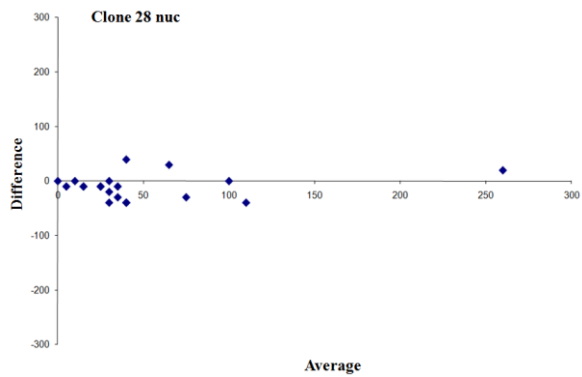
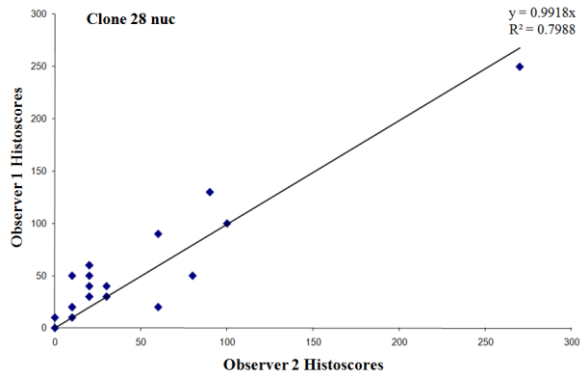


Scattered plot and Bland-Altman plot for nuclear AC 28 expression.

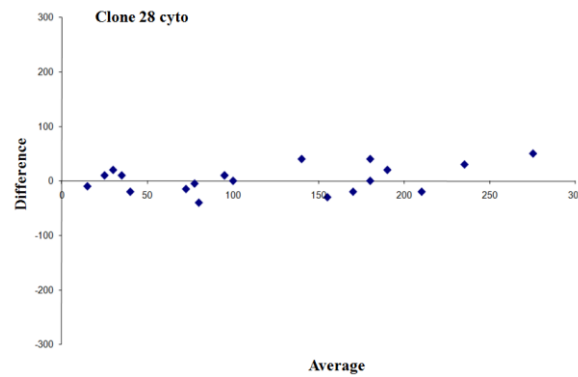
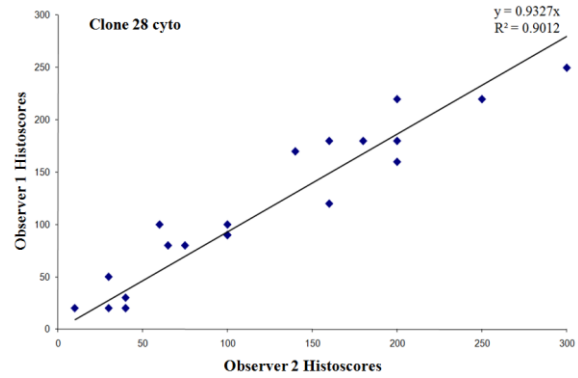
Scattered plot and Bland-Altman plot for cytoplasmic AC 28 expression.

No Scattered plot and Bland-Altman plot for membrane AC 28 expression available (all membrane histoscores 0).

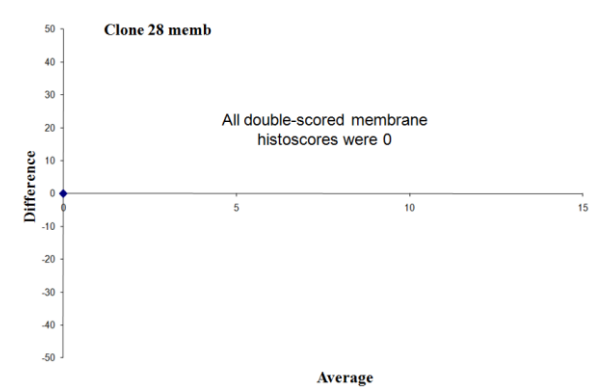
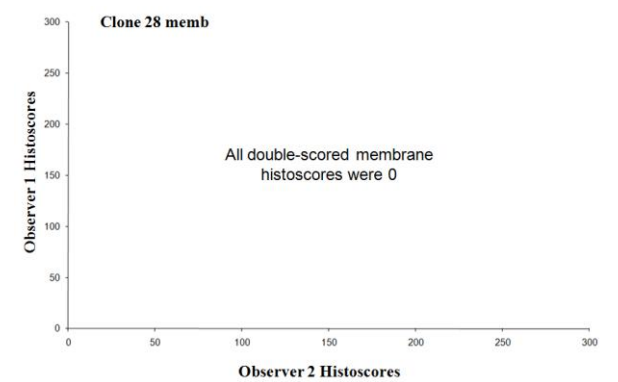
Clone 28



Scattered plot and Bland-Altman plot for nuclear Clone 28 expression.

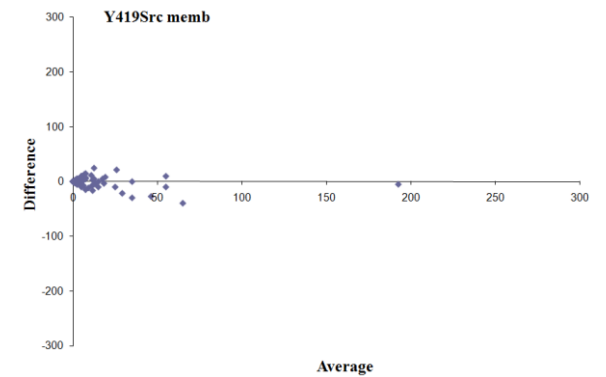
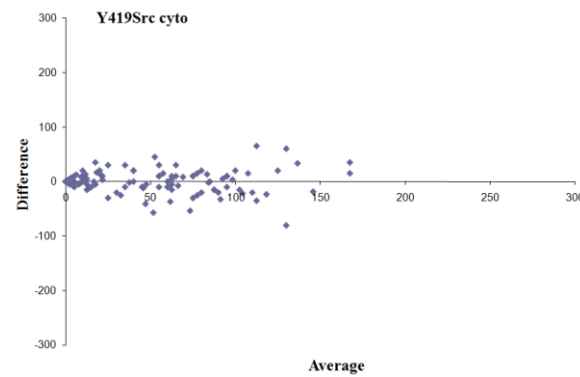
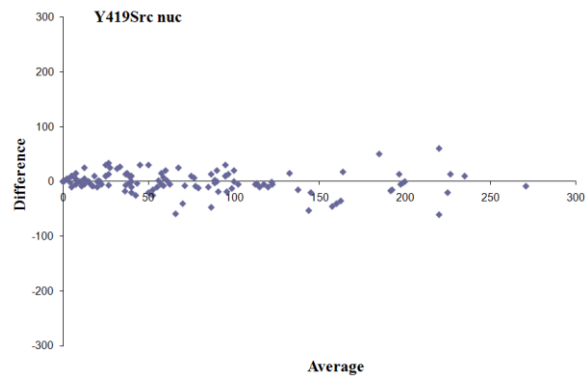
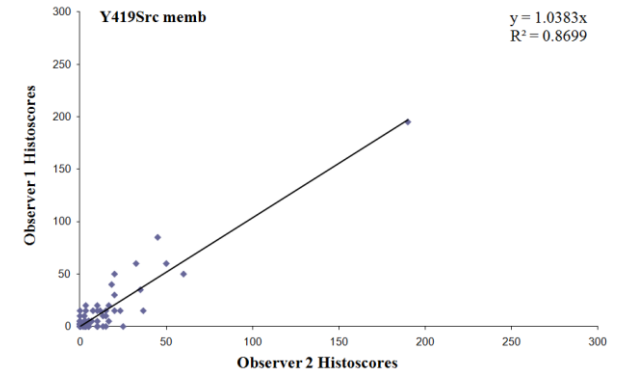
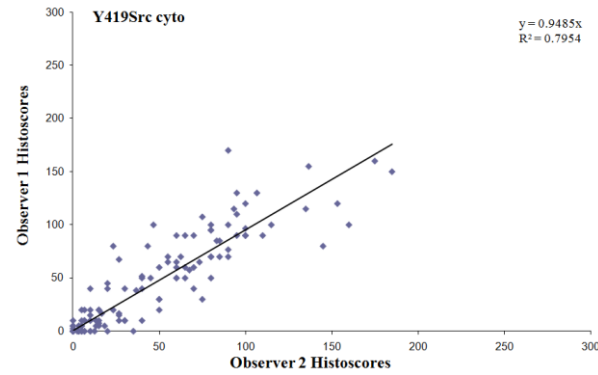
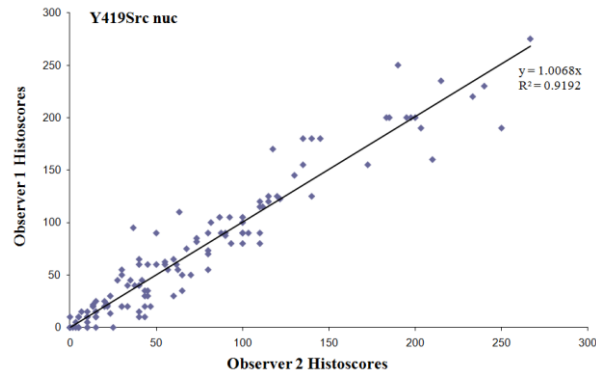


Scattered plot and Bland-Altman plot for cytoplasmic Clone 28 expression.



No Scattered plot and Bland-Altman plot for membrane Clone 28 expression available (all membrane histoscores 0).

Y419Src

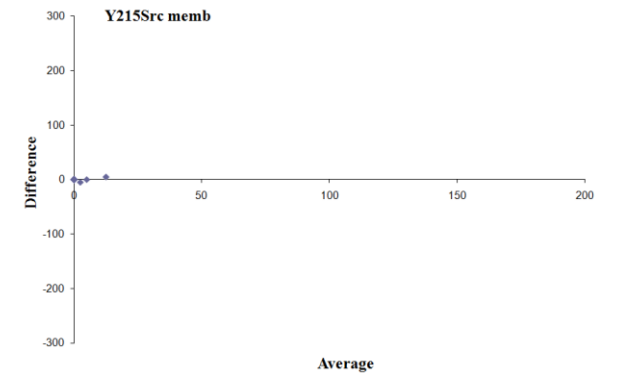
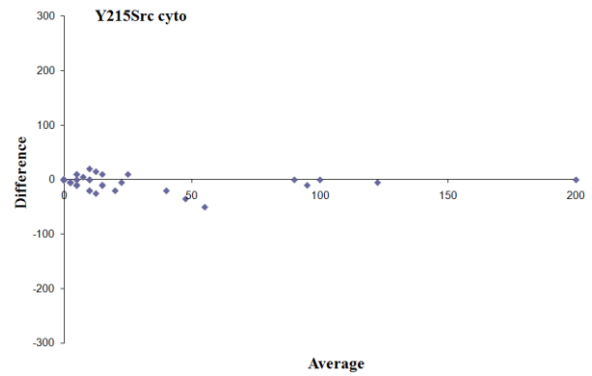
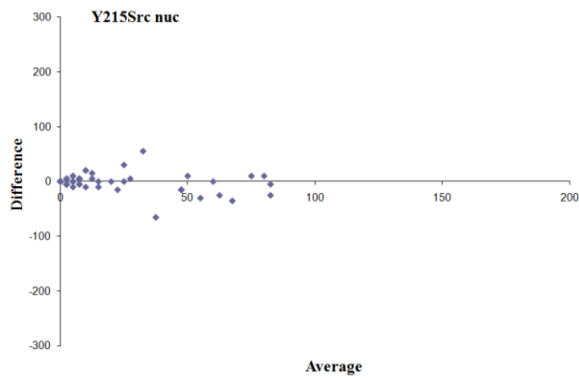
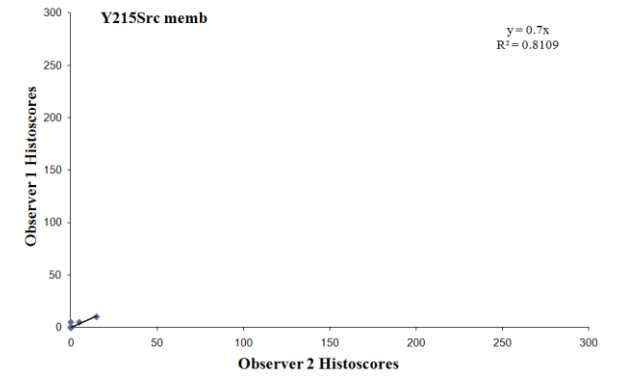
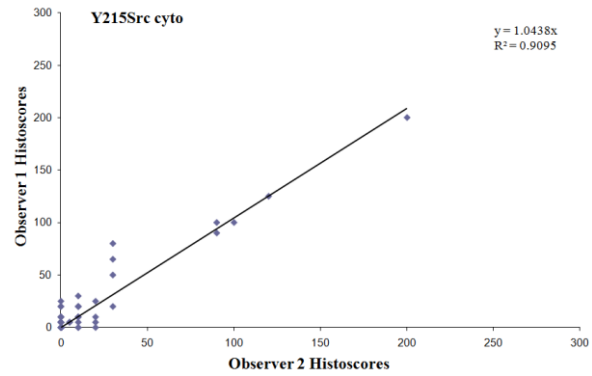
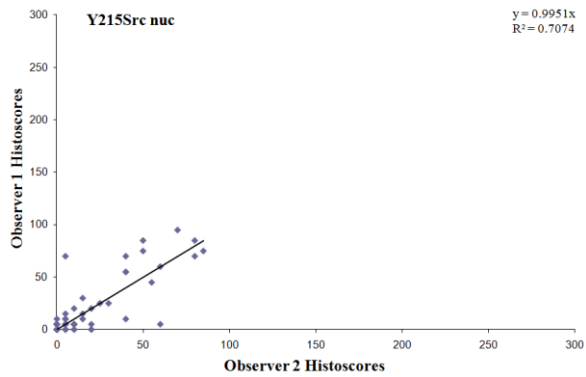


Scattered plot and Bland-Altman plot for nuclear Y419Src expression.

Scattered plot and Bland-Altman plot for cytoplasmic Y419Src expression.

Scattered plot and Bland-Altman plot for membrane Y419Src expression.

Y215Src



Scattered plot and Bland-Altman plot for nuclear Y215Src expression.

Scattered plot and Bland-Altman plot for cytoplasmic Y215Src expression.

Scattered plot and Bland-Altman plot for membrane Y215Src expression.

3.2.5.2 Ki-67 scoring

The Ki-67 antigen is a large nuclear protein (345, 395 kDa) preferentially expressed during all active phases of the cell cycle (G₁, S, G₂ and M-phases), but absent in resting cells (G₀-phase). In diagnostic histopathology and cell biology, antibodies against the Ki-67 antigen have proven valuable by allowing direct monitoring of the growth fraction of normal and neoplastic cells.

The percentage of Ki-67-reactive tumour cells were evaluated at x400 magnification by scoring a minimum of 1000 tumour cells of each core of the tissue microarray (Ki67-labelling index).

(Number of positive cells/ Number of negative cells) x100= Y%

Ki-67 scoring was performed by two independent observers (Ruth Fullerton and Alfred Tan, BmedScience students under my supervision). Again ICC scores were taken to establish unity of scoring (Ki67nuc: 0.78). As before, Scattered plots and Bland-Altman plots were constructed for Ki67 double scores (figure 3.4).

Figure 3.4: Scattered Plot and Bland-Altman Plot for Ki67

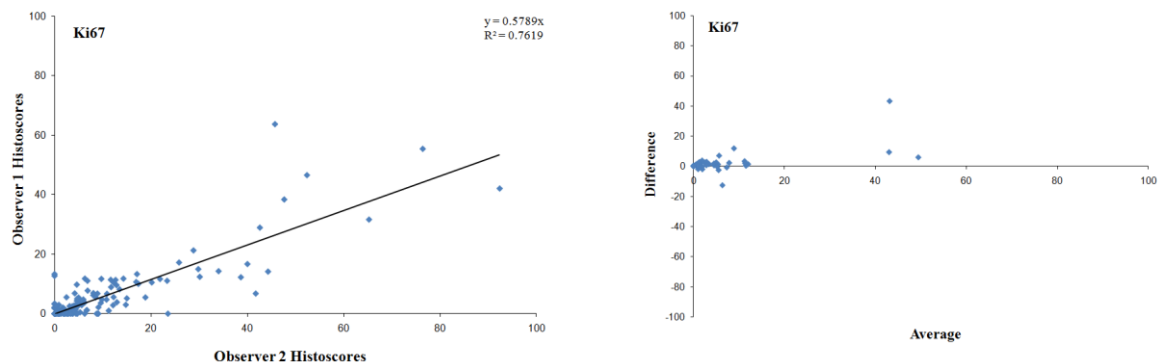


Figure 3.4: Scattered plot and Bland-Altman plot for nuclear Ki67 expression.

3.2.6 Statistical Analysis of all Immunohistochemistry Studies

The statistical analyses were performed using a statistical software package (SPSS 15.0 Inc., Chicago, IL, USA).

Basic descriptive statistics were performed to calculate frequencies, mean, median and inter-quartile ranges for all the histoscores for each antibody. These values were then used to establish appropriate cut-off points to define with either low or expression of the protein. Kaplan-Meier life table analysis (univariate analysis) was carried out to estimate differences in breast cancer related survival (DSS= disease specific survival) due to the increased or decreased protein expression in the patient's tumour. Only when univariate analysis was significant a Cox's multiple regression (multivariate analysis) was added. The log rank test was used to compare significant differences between subgroups using univariate analysis. Kaplan Meier survival analysis was also performed after stratification of the patient cohort by ER, PgR and HER2 status. Based on the results of the univariate analysis a multivariate analysis was then carried out.

The multivariate stepwise Cox-regression analysis was performed to identify factors that were independently associated with disease specific death. A stepwise backward procedure was used to derive a final model of the variables that had a significant independent relationship with survival. To remove a variable from the model the corresponding P-value had to be greater than 0.05.

For survival analysis and chi-square tests, patients were split into groups, those whose tumours expressed high or low levels of the protein of interest. To establish the relative risk of a patients dying as a result of either high or low levels of the expressed protein in their breast cancer, hazard ratio analysis was performed.

Correlations between expression of different proteins and a protein's expression level at a certain cellular compartment were calculated using the Spearman Rank Test. Inter-relationships between clinical parameters, ER and HER2 status were calculated using the

Chi square test. Because of the number of statistical comparisons, only a p value of <0.01 was considered to be significant. Bonferroni phenomenon=1 out of every 10 results is found significant by chance. Data are expressed as median and range.

3.3 Results

3.3.1 Clinico-pathological details of patient cohort

Our cohort consisted of 314 breast cancer patients (209 ER positive/ 105 ER negative and 149 PgR positive/ 163 PgR negative) (table 3.3). Median age was 58 years (IQR 50-65). 46% of the cancer specimens were pathologically graded as grade 2 and 3, median size of the invasive cancer was 20 mm (IQR 15-30 mm). 48% of the patients were axillary lymph node positive. Mean patient follow-up was 7.1 years (minimum follow-up was 2.1 years and the maximum follow-up was 20 years). 16 patients were lost to follow-up. During this period, 78 patients died of their cancer and a further 33 patients died of inter-current disease. Correlations between the clinico-pathological characteristics of this cohort are shown below.

Table 3.3: Overview of IHC patient characteristics

| Cohort characteristics | Numbers | Cohort characteristics | Numbers |
|-------------------------------|----------------|-------------------------------|----------------|
| Age | 78/236 | Lymph node | 152/162 |
| (<50 yr/ >50 yr) | | (positive/negative) | |
| Tumour type | 298/10/3/3 | ER status | 209/105 |
| (duct/lob/tub/others) | | (positive/negative) | |
| Grade | 22/146/146 | PgR status | 149/163 |
| (G1/G2/G3) | | (positive/negative) | |
| Size (mm) | 126/169/19 | HER2 status | 51/263 |
| (<20, 20-50, >50) | | (positive/negative) | |

Table 3.3 gives an overview of the patient cohort used for immunohistochemistry studies. *Histology: duct = ductal carcinoma, lob = lobular carcinoma, tub = tubular carcinoma, others including mucinous, mucoïd and micropapillary carcinoma; Grade: Bloom and Richardson grade; size = maximum tumour diameter.*

3.3.2 c-Src kinase protein expression in invasive breast cancers

The Src (36D10) Rabbit monoclonal antibody was used for this study and detects endogenous levels of Src proteins. Specificity of antibody was tested and confirmed by Western Blotting using breast cancer cell line lysates, which were kindly provided by Dr Liane McGlynn (figure 3.5). Each cellular location was independently assessed for c-Src kinase expression levels. 45% of tumours exhibited nuclear expression, 60% cytoplasmic and 43% membrane (figure 3.6, pictures 3.1).

Figure 3.5: Western Blotting for specificity of c-Src antibody

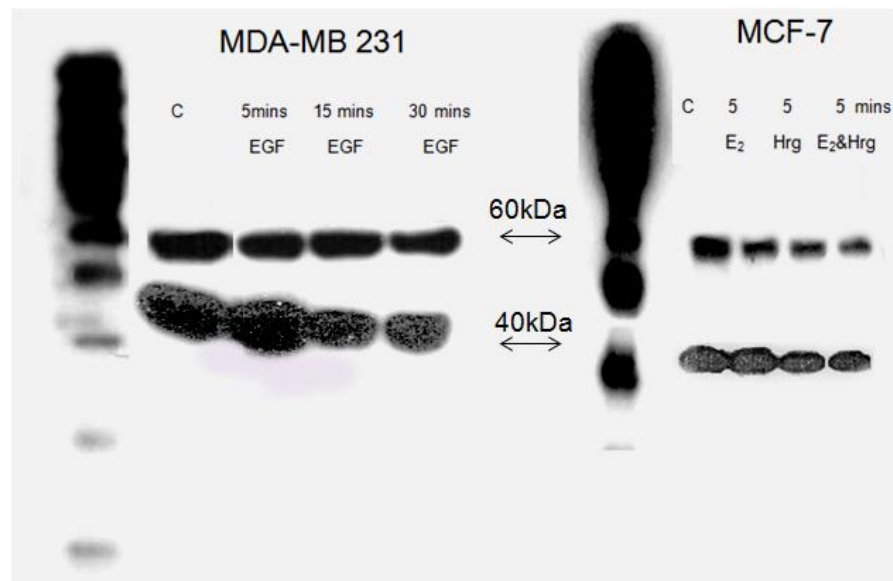


Figure 3.5: Western Blot with c-Src (60kDa) and β-actin (40kDa), as a protein loading control, demonstrating specificity of the c-Src antibody on breast cancer cell line lysates. ER positive (MCF-7) and ER negative (MDAMB231) breast cancer cell line were exposed to stimulant Oestradiol or Epidermal growth factor (E₂/ EGF) and/or inhibitor Heregulin (HRG) at different time points. C= control, untreated cell line lysates.

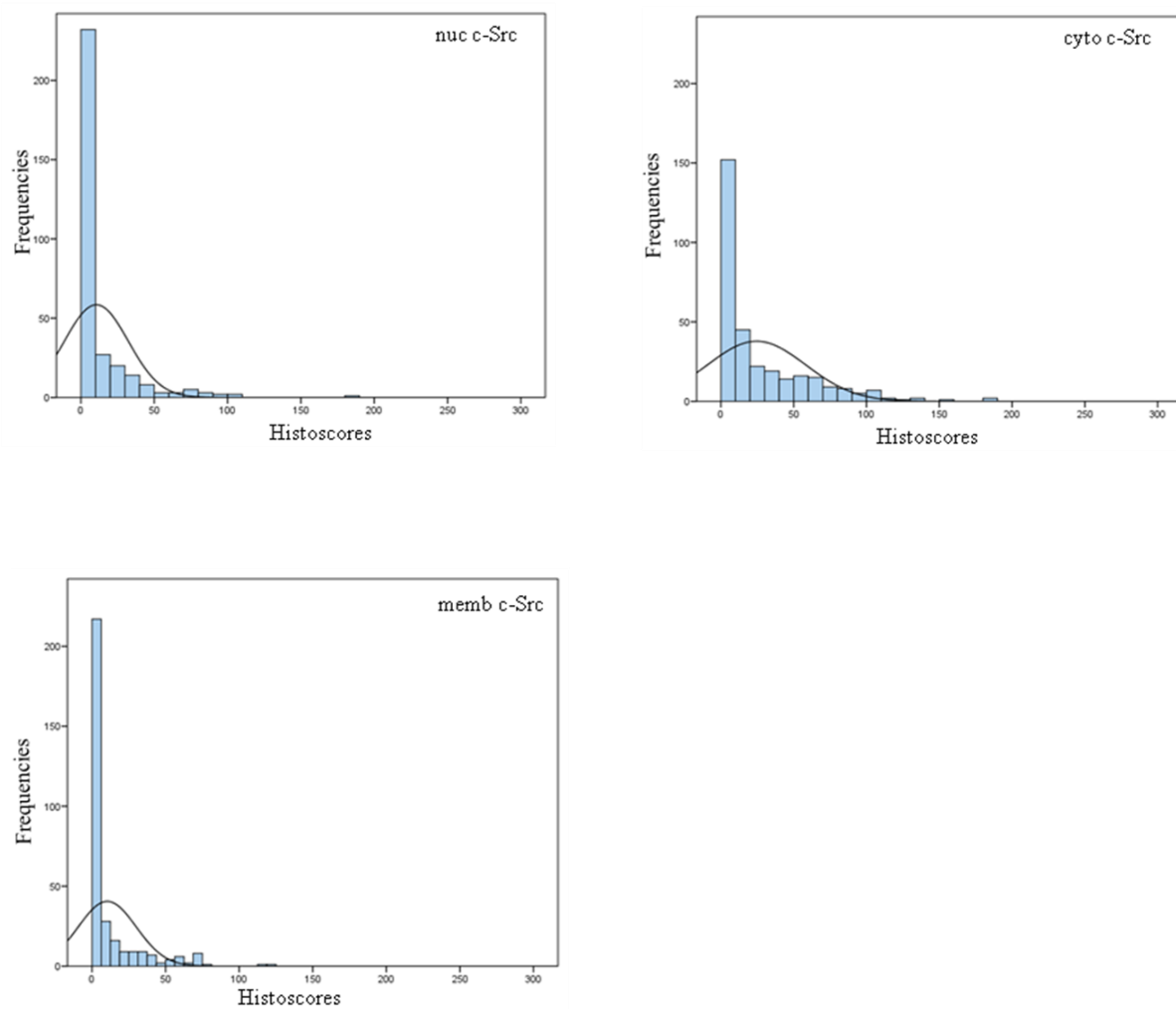
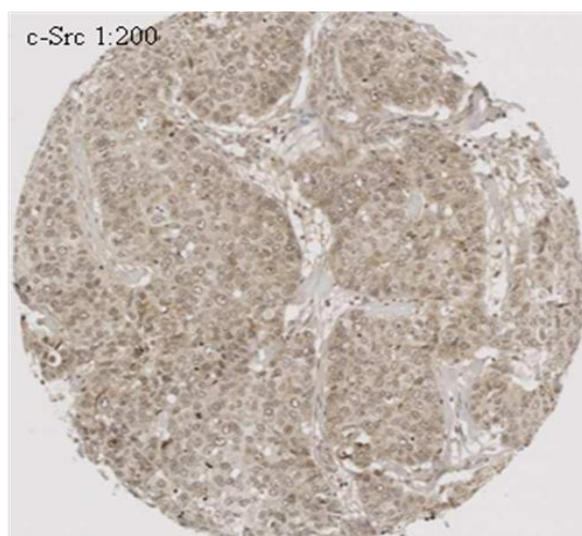
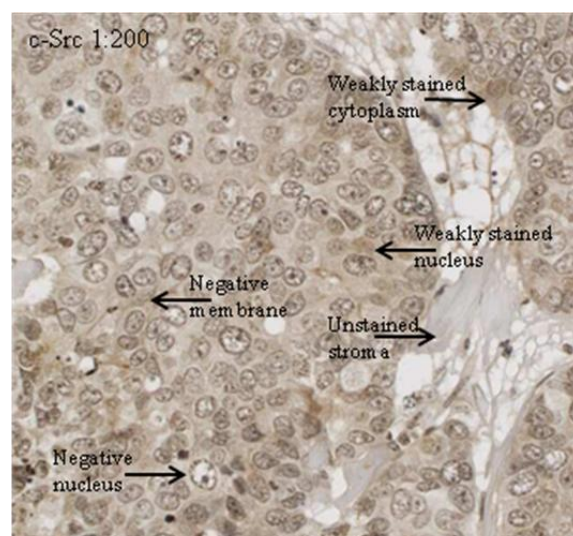
Figure 3.6: Histograms for c-Src

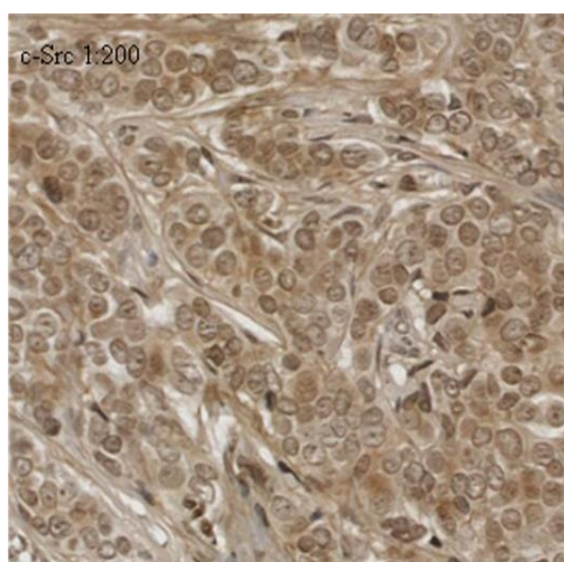
Figure 3.6: Histograms for nuclear, cytoplasmic and membrane c-Src expression displaying the intensity of IHC staining.

Picture 3.1: Immunohistochemistry staining with c-Src antibody

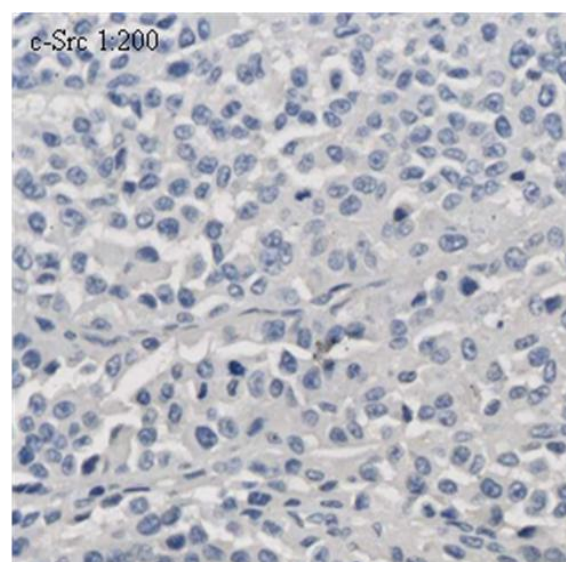
Picture 3.1 A: Overview of a 0.6 mm core of the breast cancer tissue micro array, demonstrating, weak cytoplasmic, none and weak nuclear staining; x10



Picture 3.1 B: demonstrates weak cytoplasmic, none and weak nuclear and negative membrane staining, x100



Picture 3.1 C: Normal Breast tissue, stained with c-Src antibody (Cell Signalling); magnification x100



Picture 3.1 D: Negative staining of stroma and tumour tissue, magnification x100. Negative IHC control.

3.3.2.1 Cellular distribution of nuclear, cytoplasmic and membrane c-Src expression

For statistical analysis tumours were split into those with high (above the median) or low (below or equal to the median) expression (table 3.4). Therefore patients separated into two groups; those with low expression (negative subgroup) and those with higher expression (positive subgroup) (table 3.5).

Table 3.4: Descriptive statistics of c-Src histoscores

| c-Src | Minimum | Maximum | Median | LQ | UQ |
|--------------------|---------|---------|--------|-----|------|
| Histoscores | | | | | |
| nuclear | 0.0 | 190 | 0.0 | 0.0 | 10.0 |
| cytoplasmic | 0.0 | 190 | 0.0 | 0.0 | 40.0 |
| membrane | 0.0 | 123 | 0.0 | 0.0 | 10.0 |

Table 3.4 provides an overview of descriptive statistics of c-Src nuclear, cytoplasmic and membrane histoscores. With the median being 0, patients were grouped into two subgroups: patients with no c-Src expression and with c-Src expression.

Table 3.5: c-Src expression in patient subgroups

| c-Src expression | Nuclear | Cytoplasm | Membrane |
|------------------------|---------|-----------|----------|
| Positive (Patient No) | 139 | 139 | 135 |
| Negative (Patients No) | 175 | 175 | 179 |

Table 3.5 shows the distribution of patients in each subgroup.

3.3.2.2 Correlation of clinic-pathological features of the patient cohort and c-Src expression

Chi square analysis was employed to determine if increasing level of protein expression was linked to histopathological features of the breast tumours, e.g. tumour size, grade, steroid receptor status.

Table 3.6 demonstrates that grade, PgR and HER2 status positively correlate with cytoplasmic c-Src expression; meaning that patients with invasive breast cancers, overexpressing c-Src in the cytoplasm, were more likely to have high grade (G3, χ^2 $p < 0.001$), PgR and HER2 positive (both χ^2 $p < 0.001$) breast tumours. ER status correlated negatively with cytoplasmic (χ^2 $p < 0.001$) and membrane (χ^2 $p = 0.001$) c-Src expression (table 3.6); highlighting that patients with higher c-Src protein expression in the cytoplasm and membrane were most likely patients with ER negative breast cancers.

c-Src expression in the membrane correlates positively with PgR (χ^2 $p < 0.001$) and HER2 status (χ^2 $p = 0.001$, table 3.6).

Nuclear c-Src expression does not significantly correlate patients' age, tumour type, grade, size, axillary lymph node steroid receptor and HER2 status (table 3.6).

Expression levels of c-Src at each cellular location correlate positively with each other (c-Src nuc, cyto and memb χ^2 $p < 0.001$, table 3.6).

Table 3.6: The interrelationships between c-Src expression and the clinico-pathological characteristics of patients

| Total Patient Cohort: 314 | | Chi-squared p-values | | | | | | | | |
|----------------------------------|--------|-----------------------------|--------|--------|--------|--------|---------|--------|-------------------|------------------|
| Variables | Tumour | Grade | Size | LN | ER | PgR | HER | c- Src | c-Src | c-Src |
| | type | | | status | status | status | status | nuc | cyto | memb |
| Age | 0.910 | 0.728 | 0.261 | 0.950 | 0.260 | 0.947 | 0.173 | 0.527 | 0.369 | 0.705 |
| Tumour type | | 0.007 | 0.964 | 0.680 | 0.012 | 0.453 | 0.512 | 0.904 | 0.717 | 0.761 |
| Grade | | | <0.001 | 0.301 | <0.001 | <0.001 | 0.003 | 0.019 | <0.001 | 0.017 |
| Size (mm) | | | | <0.001 | 0.048 | 0.169 | 0.010 | 0.695 | 0.177 | 0.029 |
| Lymph node | | | | | 0.555 | 0.812 | 0.016 | 0.937 | 0.329 | 0.607 |
| ER status | | | | | | <0.001 | <0.001* | 0.037 | <0.001* | 0.001* |
| PgR status | | | | | | | 0.001 | 0.237 | <0.001 | <0.001 |
| HER2 status | | | | | | | | 0.031 | <0.001 | 0.001 |
| c- Src nuc | | | | | | | | | <0.001 | <0.001 |
| c-Src cyto | | | | | | | | | | <0.001 |

Table 3.6 shows the interrelationship between c-*Src* expression at different cellular levels and clinico-pathological characteristics of patients with breast cancer; c-*Src* = total *Src* kinase, Y416*Src* = *Src* kinase phosphorylated at Tyrosine site 416, Y215*Src* = *Src* kinase phosphorylated at Tyrosine site Y215; c-*Src* nuc = c-*Src* nuclear expression, c-*Src* cyto = c-*Src* cytoplasmic expression, c-*Src* memb = c-*Src* membrane expression; *negatively correlated, significant results are highlighted in bold. *p*-values of >0.01 were considered as non-significant due to the large number of statistical comparisons (Bonferroni phenomenon).

3.3.2.3 Effects of c-Src overexpression on patients' clinical outcome

Patient outcome was measured in disease specific survival, where death from breast cancer or breast cancer related illness was used as endpoint respectively. On univariate analysis neither nuclear nor membrane c-Src expression were associated with disease specific survival (c-Src nuc $p=0.328$, c-Src memb $p=0.784$), whereas cytoplasmic c-Src kinase expression (IHC Histoscore > 0) was significantly associated with shorter disease specific survival ($p=0.028$) (figure 3.7, table 3.7). Those patients with cytoplasmic c-Src expression had a median survival of 12.6 years (IQR 10.8-14.5) compared to those with no expression with median survival of 14.6 years (IQR 12.8-16.5).

Figure 3.7: Kaplan Meier survival curve for cytoplasmic c-Src expression

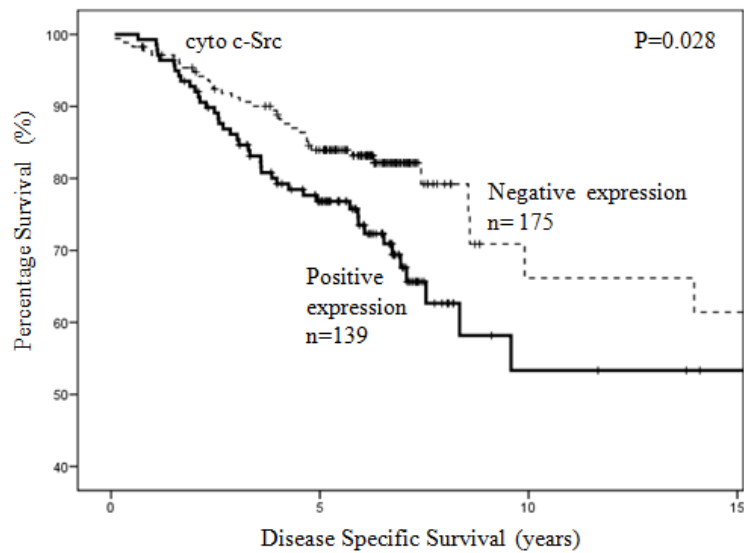


Figure 3.7: Kaplan Meier survival curve demonstrates that cytoplasmic c-Src expression is significantly associated with decreased disease specific survival ($p=0.028$, respectively).

However, there was no statistical evidence on multivariate Cox-regression analysis that cytoplasmic c-Src expression was independent of tumour size, grade and axillary nodal status in influencing disease specific survival. Only tumour size ($p < 0.001$, respectively), lymph node ($p = 0.013$, respectively), ER ($p = 0.027$, respectively) and PgR status ($p = 0.040$, respectively) proved to be independent markers of patients' disease specific survival in this cohort.

Table 3.7: Impact of clinico-pathological factors and c-Src expression on patient survival

| Total Cohort: | Patient | Univariate Analysis | | | Multivariate Analysis | | |
|---------------------------|-----------------------|----------------------------|-----|---------|------------------------------|-----|----------|
| 314 patients | Numbers | P value | HR | IQR | P value | HR | IQR |
| Age | 78/236 | 0.351 | 1.2 | 0.7-2.2 | | | |
| | (<50yr/>50yr) | | | | | | |
| Tumour type | 298/10/3/3 | 0.714 | 0.6 | 0.2-1.4 | | | |
| | (duct/lob/tub/others) | | | | | | |
| Grade | 22/146/146 | 0.014 | 1.8 | 1.2-2.7 | | | |
| | (G1/G2/G3) | | | | | | |
| Size (<20 , 20-50, >50mm) | 126/169/19 | <0.001 | 3.1 | 2.1-4.8 | <0.001 | 6.7 | 3.2-14.2 |
| Lymph node | 152/162 | 0.001 | 2.1 | 1.3-3.3 | 0.013 | 1.9 | 1.1-3.1 |
| | (positive/negative) | | | | | | |
| ER status | 209/105 | <0.001 | 2.3 | 1.5-3.6 | 0.027 | 1.8 | 1.1-3.0 |
| | (positive/negative) | | | | | | |
| PgR status | 149/163 | 0.006 | 1.9 | 1.2-3.0 | 0.040 | 1.7 | 1.0-2.7 |
| | (positive/negative) | | | | | | |
| HER2 status | 51/263 | 0.010 | 1.9 | 1.6-3.2 | | | |
| | (positive/negative) | | | | | | |

| | | | | | | | |
|---------------------|---------|--------------|------|---------|-------|-----|---------|
| c-Src nuc | 139/175 | 0.328 | 1.2 | 0.7-2.0 | | | |
| (positive/negative) | | | | | | | |
| c-Src cyto | 139/175 | 0.028 | 1.6 | 1.1-2.6 | 0.103 | 0.7 | 0.4-1.1 |
| (positive/negative) | | | | | | | |
| c-Src memb | 135/179 | 0.784 | 0.94 | 0.6-1.5 | | | |
| (positive/negative) | | | | | | | |

Table 3.7: Each clinical and pathological parameter was correlated to disease specific survival. Cytoplasmic c-Src expression is associated with disease specific survival ($p=0.028$), but not independent in multivariate analysis ($p=0.103$). HR= Hazard Ratio (95% Confidence Interval (CI)), IQR= interquartile range. Significant results are highlighted in bold.

3.3.3 Src kinase family member expression in invasive breast cancer

We had observed from PCR results that *LYN* was the second highly expressed SFK member in malignant tissue besides *SRC* and that *LCK* was higher expressed in ER negative, compared to ER positive tumours. This guided our interest and we focused on investigating protein expression of those Src kinase family members in a larger cohort to determine if Lyn and Lck had similar expression pattern as Src and if there were any association to clinical outcome of breast cancer patients.

Both antibodies are monoclonal. Lyn is Mouse antibody, which sometimes can be observed on Western Blots as a doublet of about 56 kDa and 53 kDa. The Lck (D88) XP™ Rabbit antibody detects endogenous levels of total Lck protein. These antibodies do not cross-react with other Src family members.

3.3.3.1 Patient Cohort

The patient cohort consisted of 314 patients. Clinico-pathological details are shown in table 3.3. The same patient cohort was used for c-Src analysis.

3.3.3.2 Lyn protein expression in invasive breast cancer specimens

Prior to optimisation of the antibody for immunohistochemistry, its specificity was determined by Western Blotting using the ER positive breast cancer cell line MCF-7. Protein lysates were again provided by Dr Liane McGlynn, as residual time course lysates from previous cell line experiments (figure 3.8).

Figure 3.8: Western Blotting for specificity of Lyn antibody

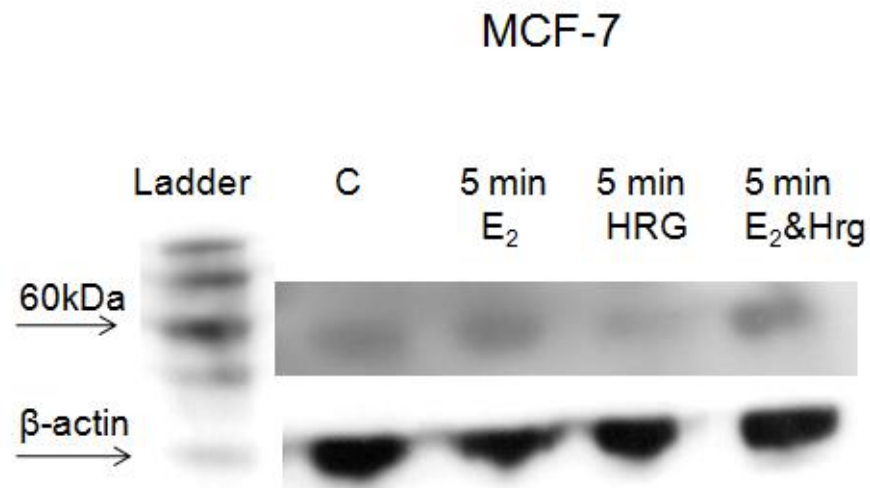


Figure 3.8: Western Blot with Lyn (56 kDa) and β -actin (48kDa), as a protein loading control. Using ER positive (MCF-7) breast cancer cell lines exposed to stimulant oestradiol or epidermal growth factor (E2/ EGF) and/or inhibitor heregulin (HRG), time point 5 min. C= control, untreated cell line lysates.

Due to tissue limitations only 57.3% of the tumours previously available for analysis were able to be stained for Lyn expression (180/314). 37% of Lyn expression was observed in the nucleus, 33% in the cytoplasm and only 4.4% in the membrane.

The cellular distribution of nuclear, cytoplasmic and membrane Lyn expression is demonstrated as histograms (figure 3.9) and displayed in pictures 3.2.

Figure 3.9: Histograms for Lyn expression

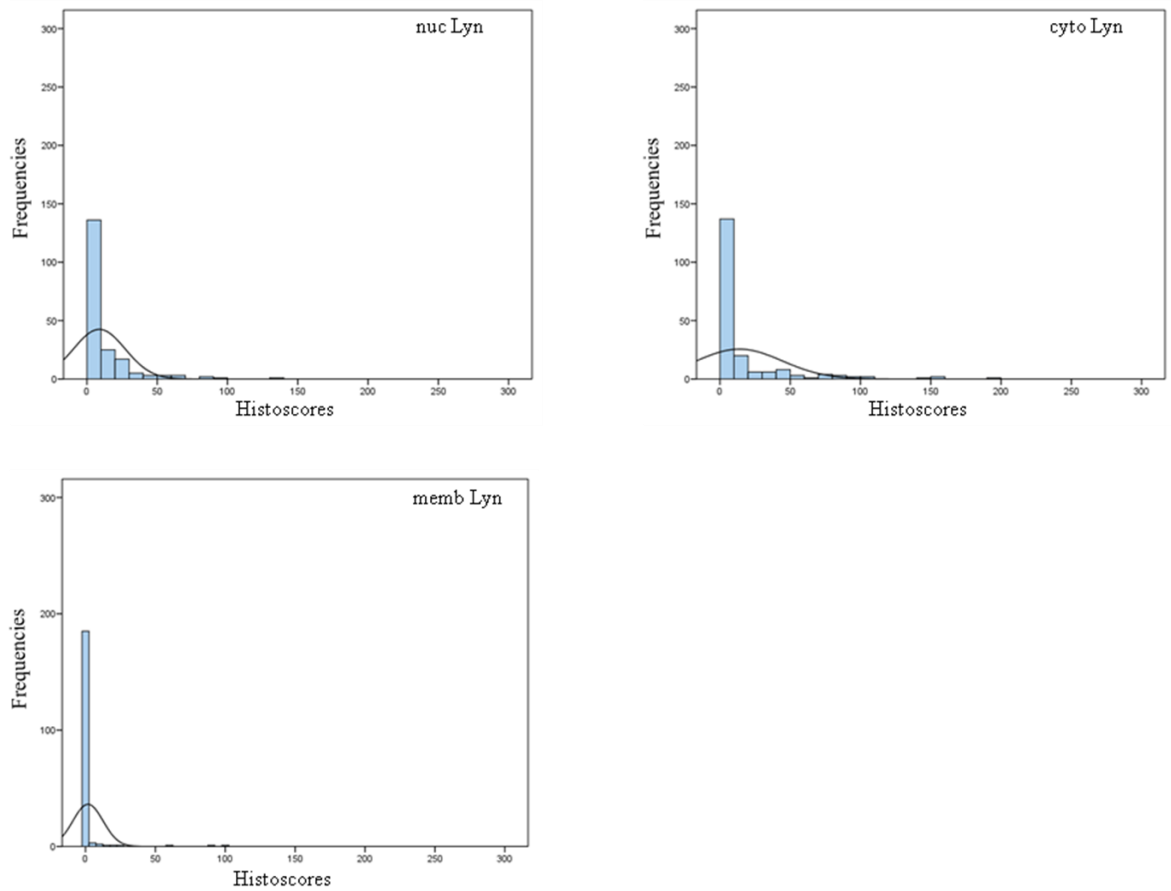
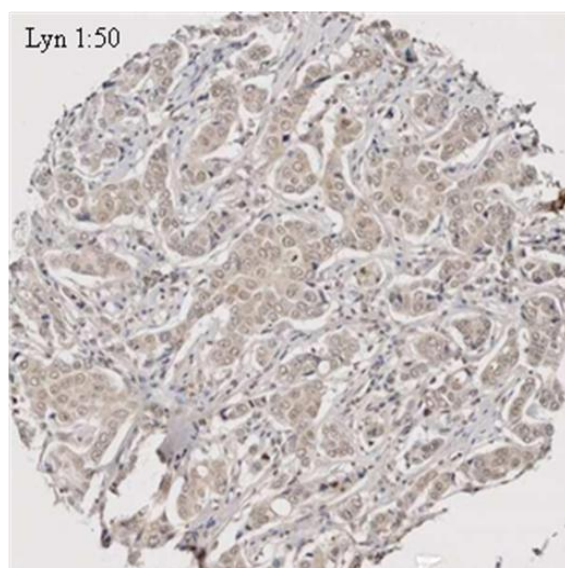
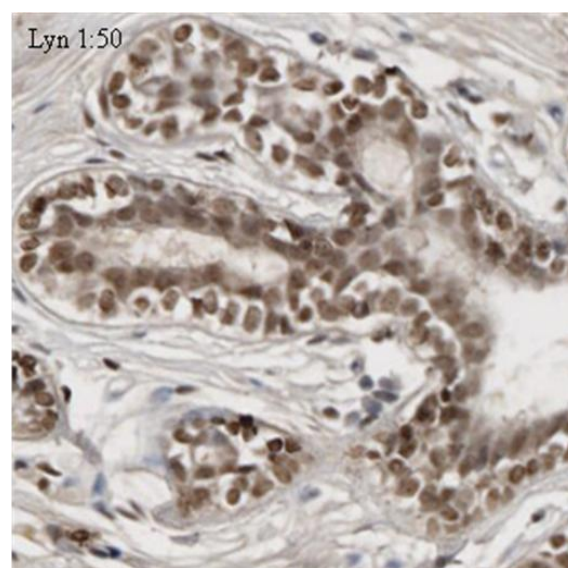


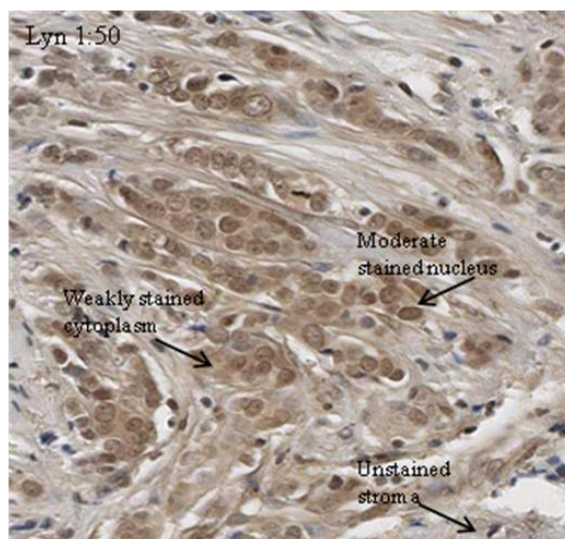
Figure 3.9: Histograms for nuclear, cytoplasmic and membrane Lyn expression displaying the intensity of IHC staining.

Picture 3.2: IHC staining with Lyn antibody

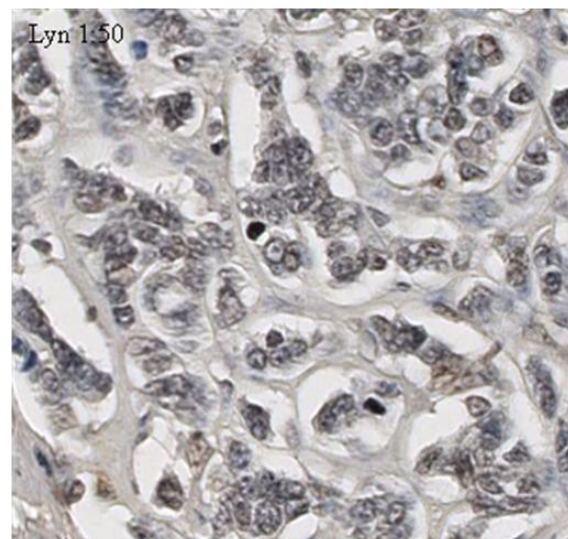
Picture 3.2 A: Overview of a 0.6 mm core of the breast cancer TMA, showing no membrane, weak cytoplasmic, none and weak nuclear staining; $\times 10$



Picture 3.2 B: Normal Breast tissue, stained with Lyn antibody (BD Biosciences); magnification $\times 100$



Picture 3.2 C: demonstrates weak cytoplasmic, weak and moderate nuclear and negative membrane staining, $\times 100$



Picture 3.2 D: Negative staining of stroma and negative to greyish tumour tissue (nuclear histoscore 0), $\times 100$

Again tumours were split into high (above median) and low expression (below or equal to the median) (table 3.8), separating patients into patient group with high (positive subgroup) and low expression (negative subgroup) (table 3.9).

Table 3.8: Descriptive statistics of Lyn histoscores

| Lyn | Minimum | Maximum | Median | LQ | UQ |
|--------------------|---------|---------|--------|-----|------|
| Histoscores | | | | | |
| nuclear | 0.0 | 140 | 0.0 | 0.0 | 10.0 |
| cytoplasmic | 0.0 | 200 | 0.0 | 0.0 | 10.0 |
| membrane | 0.0 | 100 | 0.0 | 0.0 | 0.0 |

Table 3.8 provides an overview of descriptive statistics of Lyn nuclear, cytoplasmic and membrane histoscores. With the median being 0, patients were grouped into two subgroups: patients with no Lyn expression and with Lyn expression.

Table 3.9: Lyn expression in patient subgroups

| Lyn expression | Nuclear | Cytoplasm | Membrane |
|------------------------|---------|-----------|----------|
| Positive (Patient No) | 67 | 59 | 8 |
| Negative (Patients No) | 113 | 121 | 172 |

Table 3.9: shows the distribution of patients in each subgroup.

To determine interrelationships between Lyn, Src and clinic-pathological features of the cohort, chi square analysis was performed. The only significant correlations between Lyn expression and clinico-pathological features of the cohort were observed between Lyn nuclear expression, grade and size of breast cancer specimens ($p=0.019$, $p=0.029$, table 3.10). Higher nuclear Lyn expression occurred in more aggressive and larger breast tumours. No significant correlations between Lyn and Src kinase expression levels and locations were evident.

Lyn nuclear expression correlated with Lyn cytoplasmic expression and Lyn cytoplasmic expression correlated significantly with Lyn membrane expression (table 3.10).

Table 3.10: Interrelationship between clinico-pathological characteristics and Lyn expression of breast cancer patients

| Total Patient Cohort: | | Chi-squared p-values | | |
|------------------------------|------------|-----------------------------|------------------|------------------|
| 314 | Numbers | Lyn | Lyn | Lyn |
| Variables | | nuc | cyto | memb |
| Age | 78/236 | 0.259 | 0.027 | 0.297 |
| Tumour type | 298/10/3/3 | 0.642 | 0.547 | 0.492 |
| Grade | 22/146/146 | 0.019 | 0.632 | 0.991 |
| Size (mm) | 126/169/19 | 0.029 | 0.832 | 0.115 |
| Lymph node | 152/162 | 0.123 | 0.200 | 0.247 |
| ER status | 209/105 | 0.133 | 0.122 | 0.876 |
| PgR status | 149/163 | 0.339 | 0.115 | 0.058 |
| HER2 status | 51/263 | 0.733 | 0.836 | 0.772 |
| c- Src nuc | 139/175 | 0.163 | 0.646 | 0.917 |
| c- Src cyto | 139/175 | 0.621 | 0.579 | 0.780 |
| c- Src memb | 135/179 | 0.691 | 0.497 | 0.410 |
| Lyn nuc | 67/113 | | <0.001 | 0.345 |
| Lyn cyto | 59/121 | | | <0.001 |

Table 3.10 shows the interrelationship between Lyn expression at different cellular levels and clinico-pathological characteristics of patients with breast cancer; Lyn nuc = Lyn nuclear expression, Lyn cyto = Lyn cytoplasmic expression, Lyn memb = Lyn membrane expression; c-Src nuc = c-Src nuclear expression, c-Src cyto = c-Src cytoplasmic expression, c-Src memb = c-Src membrane expression; significant results are highlighted in bold.

On univariate analysis there was no association noticed between Lyn expression and disease specific survival at any cellular location (table 3.11).

Table 3.11: Impact of clinico-pathological factors and Lyn expression on patient survival

| Total | Patient | Univariate | | |
|---------------------|----------------|-------------------|------|---------|
| Cohort: | | Analysis | | |
| 314 patients | Numbers | P value | HR | IQR |
| Lyn nuc | 67/113 | 0.545 | 1.2 | 0.7-2.0 |
| (positive/negative) | | | | |
| Lyn cyto | 59/121 | 0.980 | 1.6 | 1.1-2.6 |
| (positive/negative) | | | | |
| Lyn memb | 8/172 | 0.728 | 0.94 | 0.6-1.5 |
| (positive/negative) | | | | |

Table 3.11: Expression of each cellular location was correlated to disease specific survival. None of the protein expressions were associated with disease specific survival and independent in multivariate analysis. HR= Hazard Ratio (95% Confidence Interval (CI)), IQR= interquartile range. Significant results are highlighted in bold.

3.3.3.3 Lck protein expression in invasive breast cancer specimens

As before with the antibodies of c-Src and Lyn, specificity of the Lck (D88) XP™ Rabbit antibody was determined by Western blotting, using HeLa (cervical cancer) cell line and ER negative breast cancer cell line lysates- MDAMB231 (figure 3.10).

Figure 3.10: Western Blotting for specificity of Lck antibody

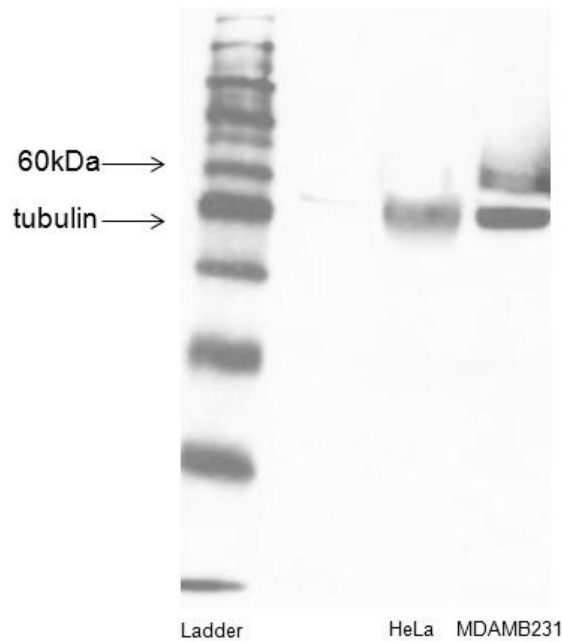


Figure 3.10: Western Blot with Lck and β -tubulin antibody, as a protein loading control. Using cervical cancer (HeLa) and ER negative breast cancer cell lysates (MDA MB231). Positive band expression for Lck antibody is noticed at about 58 kDa. β -tubulin antibody was used as protein loading control.

83.8 % of the tumours previously available for analysis were able to be stained for Lck expression (263/314). Each cellular location was independently assessed. 42 % of Lck expression was observed in the nucleus, 42 % in the cytoplasm and only 5 % in the membrane (table 3.12).

Descriptive statistical analysis revealed a median histoscore of 0. Therefore tumours were divided into expressing Lck or not expressing Lck (table 3.12), separating patients into a positive and negative patient subgroup (table 3.13).

Table 3.12: Descriptive statistics for Lck histoscores

| Lck | Minimum | Maximum | Median | LQ | UQ |
|--------------------|---------|---------|--------|-----|------|
| Histoscores | | | | | |
| nuclear | 0.0 | 93 | 0.0 | 0.0 | 10.0 |
| cytoplasmic | 0.0 | 85 | 0.0 | 0.0 | 10.0 |
| membrane | 0.0 | 15 | 0.0 | 0.0 | 0.0 |

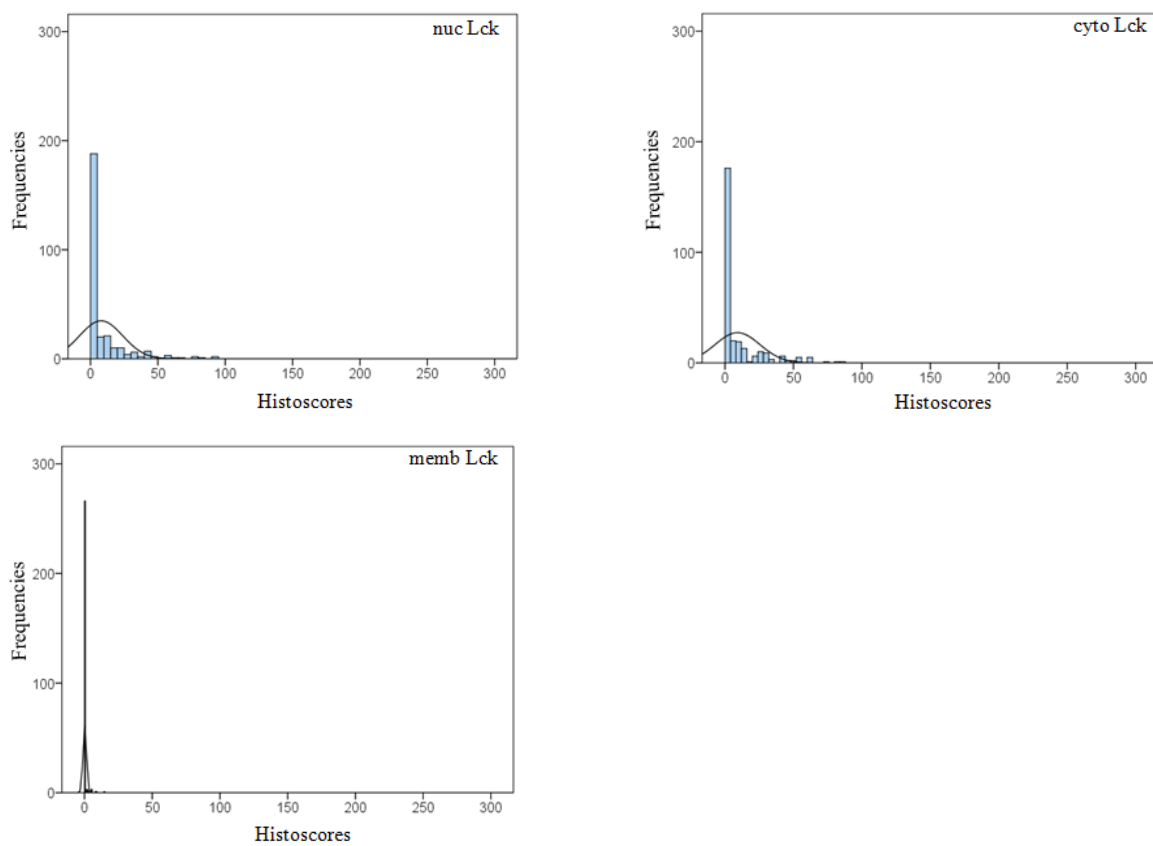
Table 3.12 provides an overview of descriptive statistics of Lck nuclear, cytoplasmic and membrane histoscores. With the median being 0, patients were grouped into two subgroups: patients with no Lck expression and with Lck expression.

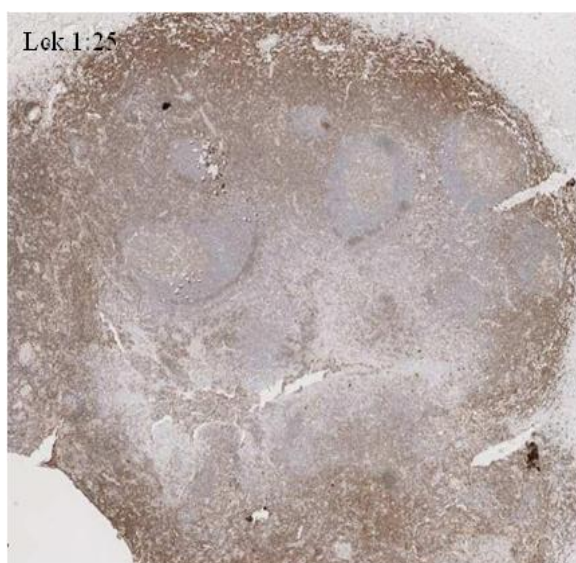
Table 3.13: Lck expression in different patient subgroups

| Lck expression | Nuclear | Cytoplasm | Membrane |
|------------------------|---------|-----------|----------|
| Positive (Patient No) | 111 | 111 | 12 |
| Negative (Patients No) | 152 | 152 | 251 |

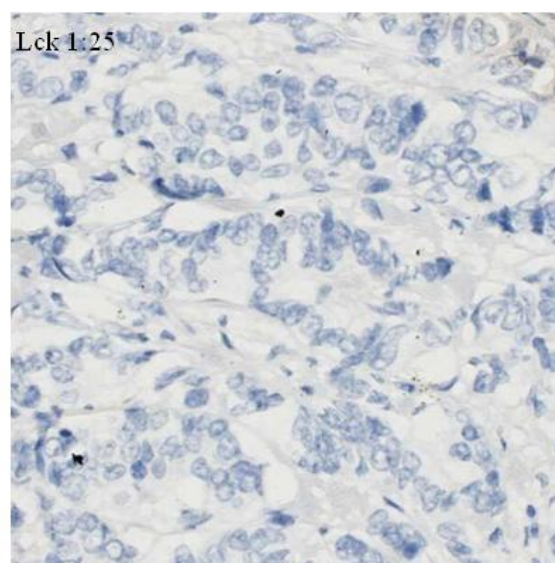
Table 3.13 shows the distribution of patients in each subgroup.

Histograms and IHC pictures below exhibit the cellular distribution and intensity of nuclear, cytoplasmic and membrane Lck expression (figure 3.11, picture 3.3).

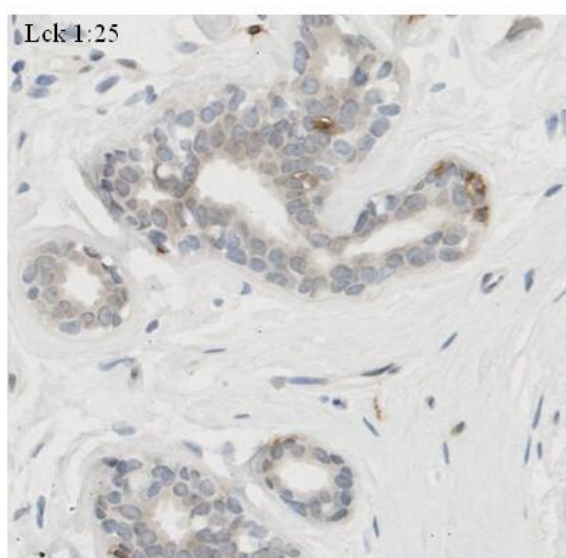
Figure 3.11: Histograms for Lck expression**Figure 3.11:** Histograms for nuclear, cytoplasmic and membrane Lck expression

Picture 3.3: IHC staining with Lck antibody

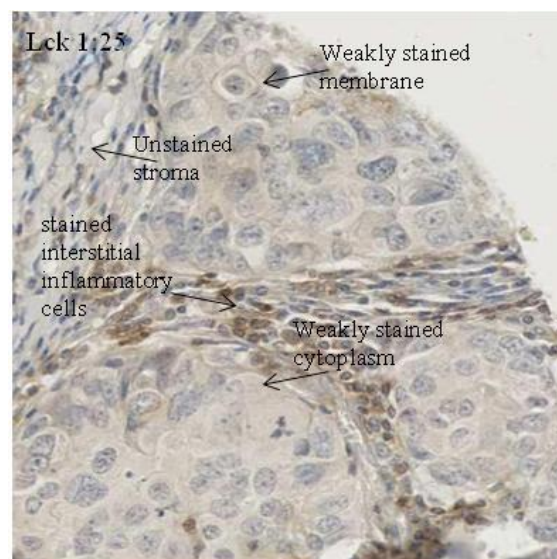
Picture 3.3 A: Overview of a full section of a tonsil, strong staining of inflammatory cells; x10. Positive control.



Picture 3.3 B: Negative staining of stroma and tumour tissue, x100. Negative IHC control.



Picture 3.3 C: Normal Breast tissue, stained with Lck antibody (Cell Signalling); x100.



Picture 3.3 D demonstrates weak cytoplasmic and membrane, weak and negative nuclear staining. Interstitial inflammatory cells stained, x100.

On chi square analysis the only significant positive correlation between protein expression and clinico-pathological characteristics of the cohort was with nuclear Lck expression and ER status (χ^2 p=0.001). Lck expression at all cellular locations correlated strongly with each other (table 3.14).

Table 3.14: Correlations between SFK member and clinico-pathological characteristics of breast cancer patients

| Total Patient Cohort | | Chi-squared p-values | | |
|--------------------------------------|------------|----------------------|-------------|-------------|
| 314 Variables | Numbers | Lck nuc | Lck cyto | Lck memb |
| Age (<50yr/>50yr) | 78/236 | 0.639 | 0.927 | 0.024 |
| Tumour type (duct/lob/tub/others) | 298/10/3/3 | 0.375 | 0.032 | 0.842 |
| Grade (G1/G2/G3) | 22/146/146 | 0.034 | 0.543 | 0.741 |
| Size (<20 , 20-50, >50mm) | 126/169/19 | 0.892 | 0.580 | 0.926 |
| Lymph node (positive/negative) | 152/162 | 0.957 | 0.308 | 0.311 |
| ER status (positive/negative) | 209/105 | 0.001 | 0.600 | 0.118 |
| PgR status (positive/negative) | 149/163 | 0.097 | 0.036 | 0.090 |
| HER2 status (positive/negative) | 51/263 | 0.168 | 0.085 | 1.000 |
| c-Src nuc (positive/negative) | 139/175 | 0.328 | 0.461 | 0.701 |

| | | | | |
|---------------------|---------|-------|------------------|------------------|
| c-Src cyto | 139/175 | 0.299 | 0.508 | 0.934 |
| (positive/negative) | | | | |
| c-Src memb | 135/179 | 0.274 | 0.064 | 0.017 |
| (positive/negative) | | | | |
| Lyn nuc | 67/113 | 0.016 | 0.975 | 0.534 |
| (positive/negative) | | | | |
| Lyn cyto | 59/121 | 0.424 | 0.067 | 0.032 |
| (positive/negative) | | | | |
| Lyn memb | 8/172 | 0.282 | 0.726 | 0.053 |
| (positive/negative) | | | | |
| Lck nuc | 111/152 | | <0.001 | 0.001 |
| (positive/negative) | | | | |
| Lck cyto | 111/152 | | | <0.001 |
| (positive/negative) | | | | |

Table 3.14 shows the interrelationship between *Lck* expression at different cellular levels and clinico-pathological characteristics of patients with breast cancer; *Lck nuc* = *Lck* nuclear expression, *Lck cyto* = *Lck* cytoplasmic expression, *Lck memb* = *Lck* membrane expression; *Lyn nuc* = *Lyn* nuclear expression, *Lyn cyto* = *Lyn* cytoplasmic expression, *Lyn memb* = *Lyn* membrane expression; *c-Src nuc* = *c-Src* nuclear expression, *c-Src cyto* = *c-Src* cytoplasmic expression, *c-Src memb* = *c-Src* membrane expression; significant results are highlighted in bold. *p*-values of >0.01 were considered as non-significant due to the large number of statistical comparisons (Bonferroni phenomenon).

Patient outcome was measured in disease specific survival, where death from breast cancer or breast cancer related illness was used as endpoint respectively. On univariate analysis neither nuclear nor cytoplasmic Lck expression were associated with disease specific survival ($p=0.140$, $p=0.935$). Whereas membrane Lck expression (IHC Histoscore > 0) was associated with longer disease specific survival ($p=0.039$) (figure 3.12, table 3.15).

Figure 3.12: Kaplan Meier survival curve for membrane Lck expression

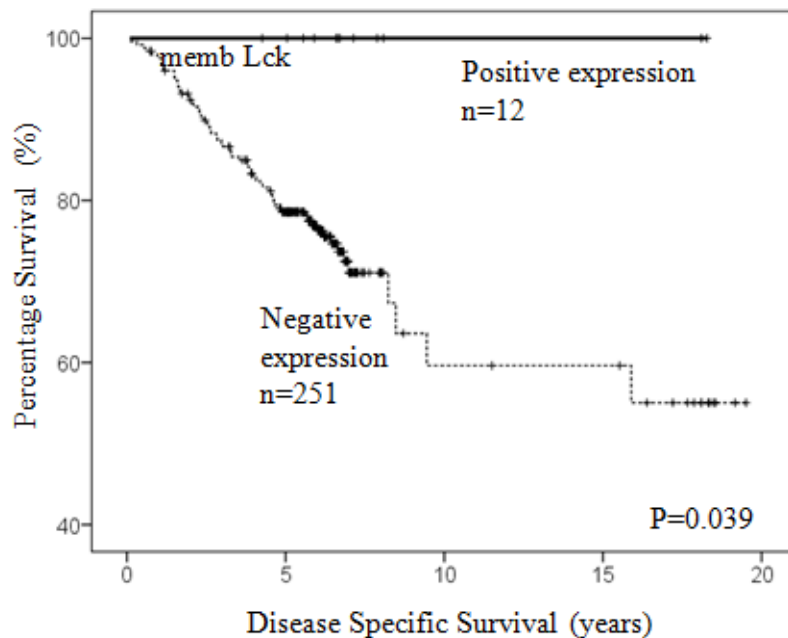


Figure 3.12: Kaplan Meier survival curve demonstrates that membrane Lck expression is associated with improved disease specific survival ($p=0.039$, respectively).

None of patients expressing Lck on the cell membrane died of breast cancer. Median follow-up for patients with positive Lck staining of the membrane was 7.8 years (IQR +/- 4.5), for patients without staining 6.0 years (IQR +/- 3.5).

Table 3.15: Impact of Lck expression on breast cancer patient survival

| Total Patient | | | Univariate | | Multivariate | | |
|---------------------------------|---------|--------------|------------|----------|--------------|-----|-----|
| | Cohort: | | Analysis | | Analysis | | |
| 263 out of 314 patients | Numbers | P value | HR | IQR | P value | HR | IQR |
| Lck nuc (positive/negative) | 111/152 | 0.140 | 1.5 | 0.9-2.5 | | | |
| Lck cyto (positive/negative) | 111/152 | 0.935 | 1.0 | 0.6-1.7 | | | |
| Lck memb (positive/negative) | 12/251 | 0.039 | 0.1 | 0.01-4.0 | 0.972 | 0.0 | |

Table 3.15: Expression of each cellular location was correlated to disease specific survival. None of the protein expressions were associated with disease specific survival and independent in multivariate analysis. HR= Hazard Ratio (95% Confidence Interval (CI)), IQR= interquartile range. Significant results are highlighted in bold.

3.3.4 Protein Expression of various activation sites of Src kinase in breast cancer specimens

As described in more detail in the introductory chapter, c-Src is activated by a number of pathways. Known as the classical activation pathway, dephosphorylation of Y530 is needed to initiate a configuration change of the protein allowing autophosphorylation of tyrosine site 419 at the SH2 protein domain leading to full activation of the protein.

Two antibodies were used to investigate those different stages of Src kinase activation and to link these to patient outcome: Clone 28 antibody is a monoclonal Mouse antibody, which recognises the semi-active form of Src when not phosphorylated at Y530. Whereas, the Y416Src polyclonal Rabbit antibody was applied to determine protein expression of the fully activated Src kinase. It detects endogenous levels of Src only when phosphorylated at tyrosine 419 and does not cross-react with Src phosphorylated at tyrosine 530.

More recently, a different activation pathway has been described (76). Direct phosphorylation of tyrosine site 215 can lead to a more powerful activation of Src. A polyclonal Rabbit antibody was used to assess if there would be significant differences in protein expression and patients' clinical outcome.

Phosphorylation of the tyrosine residual 530 on the c-terminal tail by Csk tyrosine kinase acts as a negative regulatory protein binding site, keeping Src kinase in a closed confirmation. To evaluate protein expression of inactivated Src kinase a polyclonal Rabbit antibody, named by Invitrogen as anti-Src family negative regulatory [pY] site and re-named in our laboratory as anti-Clone28, was utilised for detecting phosphorylated tyrosine site 530.

Investigating the role of the Src kinase in breast cancer at each activated phosphorylation site (Y530, Y419, Y215) and inactivated status (pY530) is thought to be necessary to determine its clinical significance for breast cancer patients.

Immunohistochemistry for the different activation sites of Src (anti-Src family negative regulatory [pY] site/ anti-Clone 28, Clone 28, Y419Src and Y215Src) was performed on the same mixed breast cancer patient cohort (314 patients, table 3.3) used for previous immunohistochemistry staining of SFK members (Src, Lyn and Lck).

3.3.4.1 Inactivated Src kinase (AC 28) protein expression in invasive breast cancer

Before optimising the antibody for immunohistochemistry staining, the specificity of the anti-Src family negative regulatory [pY]/ anti-Clone 28 (AC28) antibody was tested via Western Blotting. Various commercially available cell lysates were used as different protein sample loadings (figure 3.13).

Figure 3.13: Western Blotting for specificity of anti-Clone 28 antibody

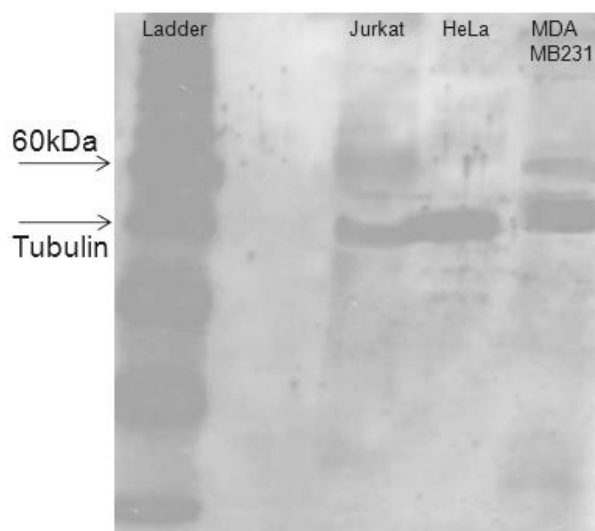


Figure 3.13: Western Blot with anti-Src family negative regulatory site (pAb) antibody (60kDa) and tubulin (48kDa), as a protein loading control, using, Jurkat (human lymphoma cell line), HeLa (cervical cancer cell) and MDAMB231(ER negative breast cancer cell) lysates.

Only 53 % of the tumours, previously available for SFK member analysis, were able to be stained for AC28 expression (165/314). This effect was due to tissue limitation after extensive section cutting of the TMA.

Each cellular location was again independently assessed. 50 % of anti-Clone 28 expression was observed in the nucleus, 44 % in the cytoplasm and only 3.6 % in the membrane (table 3.17). The following histograms and IHC pictures exhibit the cellular distribution and intensity of nuclear, cytoplasmic and membrane anti-Clone 28 expression (figure 3.14, picture 3.4).

Figure 3.14: Histograms for anti-Clone 28 expression in invasive breast carcinoma

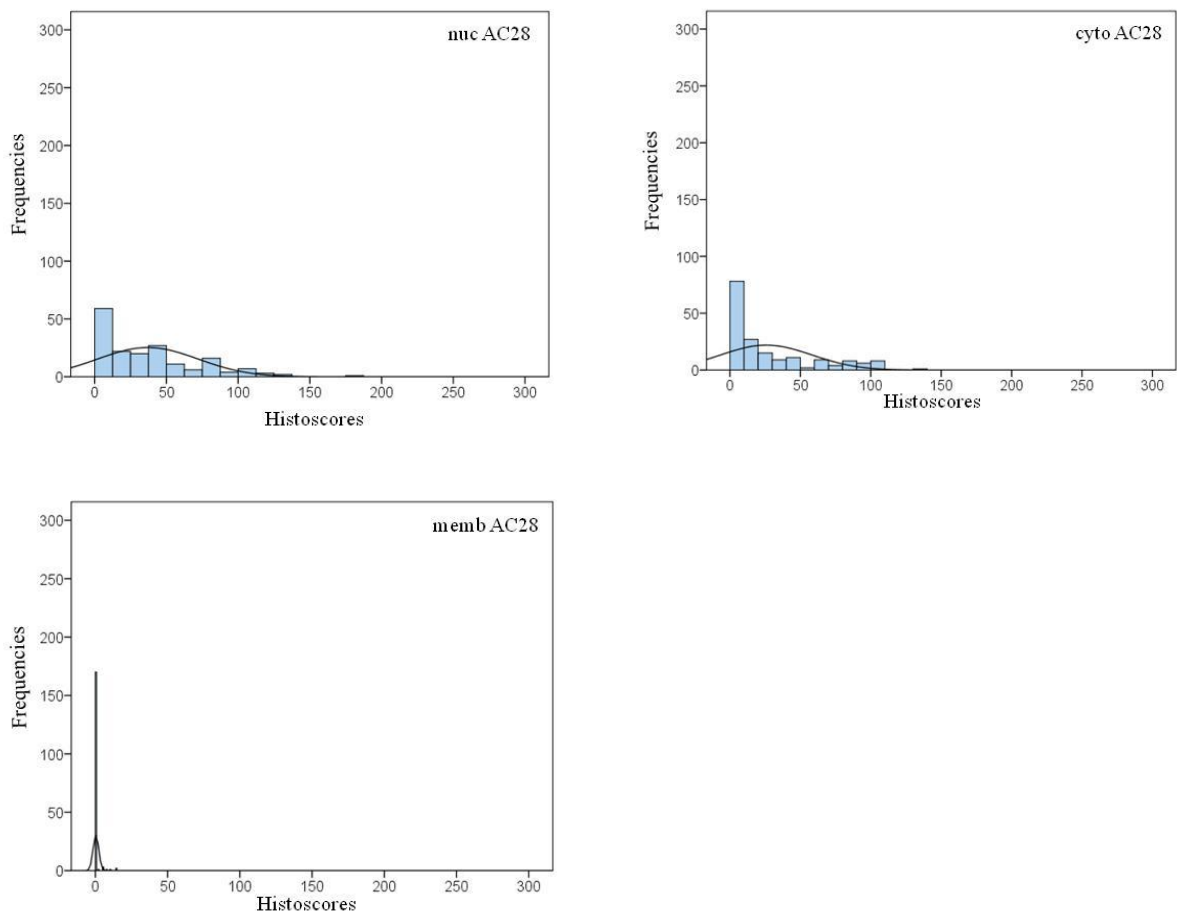
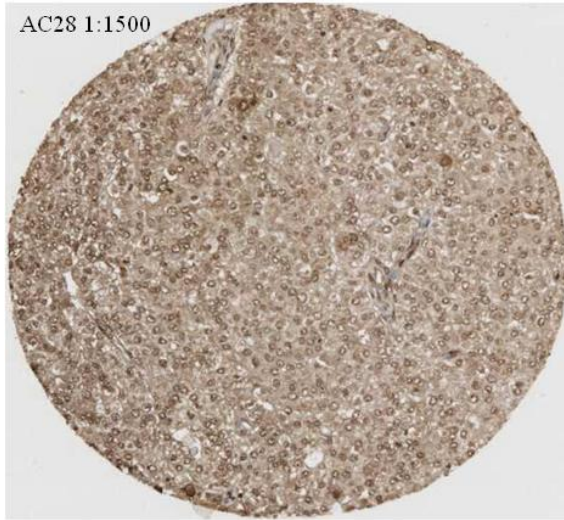
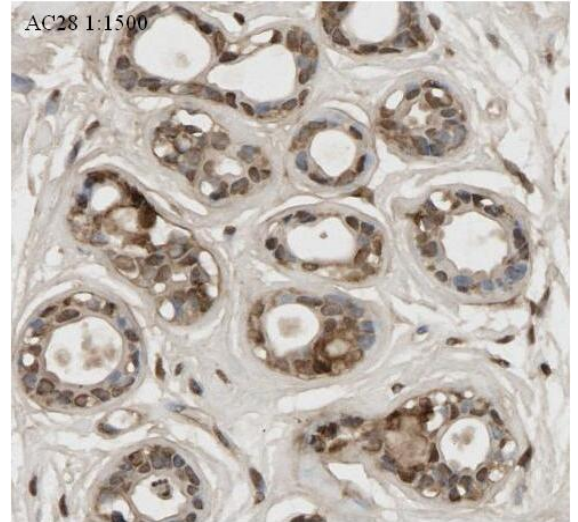


Figure 3.14: Histograms for nuclear, cytoplasmic and membrane AC28 staining revealing the distribution of IHC intensity staining.

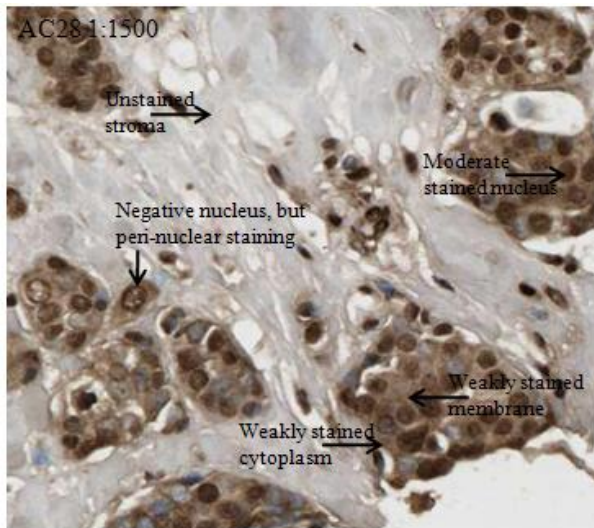
Picture 3.4: IHC staining with AC28 antibody



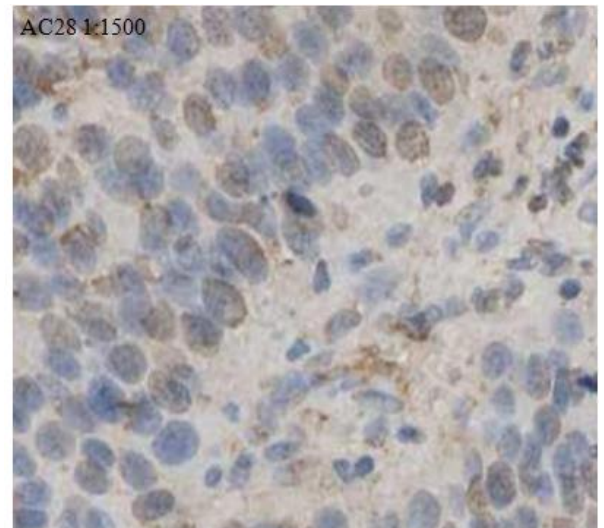
Picture 3.4 A: Overview of a 0.6 mm core of the breast cancer TMA, showing nuclear, cytoplasmic and peri-nuclear staining; magnification x10.



Picture 3.4 B: Normal Breast tissue stained with anti-Clone 28 antibody (Invitrogen); x100.



Picture 3.4 C demonstrates weak cytoplasmic and membrane, negative weak and moderate nuclear staining. x100.



Picture 3.4 D: Negative and weak staining of nuclei, negative cytoplasm, membrane and stroma tissue staining, magnification x100.

Tumours were split into high (above median) and low expression (below or equal to the median) (table 16), separating patients into patient group with high (positive subgroup) and low expression (negative subgroup) (table 3.17). With the membrane anti-Clone 28 median being 0, patients were grouped into two subgroups: patients with no anti-Clone 28 expression and with anti-Clone 28 expression. Median of nuclear, cytoplasmic and membrane anti-Clone 28 was used for statistical analysis.

Table 3.16: Descriptive statistics for anti-Clone 28 histoscores

| AC28 | Minimum | Maximum | Median | LQ | UQ |
|--------------------|---------|---------|--------|------|------|
| Histoscores | | | | | |
| nuclear | 0.0 | 180.0 | 30.0 | 10.0 | 60.0 |
| cytoplasmic | 0.0 | 140.0 | 10.0 | 0.0 | 40.0 |
| membrane | 0.0 | 15.0 | 0.0 | 0.0 | 0.0 |

Table 3.16 provides an overview of descriptive statistics of AC28 nuclear, cytoplasmic and membrane histoscores.

Table 3.17: anti-Clone 28 expression in patient groups

| AC28 expression | Nuclear | Cytoplasm | Membrane |
|------------------------|---------|-----------|----------|
| Positive (Patient No) | 82 | 72 | 6 |
| Negative (Patients No) | 83 | 93 | 159 |

Table 3.17: shows the division into positive and negative expression group.

Associations between anti-Clone 28, Src and clinico-pathological features of the cohort were examined performing Chi square analysis. There was only one significant correlation between clinico-pathological features and AC28 expression. ER status negatively

correlated with nuclear expression of AC28 (χ^2 $p < 0.001$) meaning that patients with ER negative breast cancers were more likely not to express inactive Src in the nucleus.

Interestingly cytoplasmic AC28 correlated negatively with membrane c-Src expression (χ^2 $p = 0.008$), pointing out that breast cancer patients with higher expression of inactive Src in the cytoplasm were more likely not to express c-Src at the membrane.

No significant correlations were noted with AC28 membrane expression.

Interrelationships between the different AC28 cellular locations were insignificant.

However, the negative correlation between AC28 cytoplasmic and AC28 membrane expression was close to reach significance (χ^2 $p = 0.015$, table 3.18).

Table 3.18: Interrelationship between clinico-pathological features of the cohort, c-Src and anti-Clone 28 expression

| Total Patient Cohort | | Chi-squared p-values | | |
|----------------------------|------------|----------------------|--------------|--------------|
| 314 Variables | Numbers | AC28 nuc | AC28 cyto | AC28 memb |
| Age | 78/236 | 0.114 | 0.306 | 0.924 |
| (<50 yr/ >50 yr) | | | | |
| Tumour type | 298/10/3/3 | 0.614 | 0.528 | 0.974 |
| (duct/lob/tub/others) | | | | |
| Grade | 22/146/146 | 0.250 | 0.068 | 0.273 |
| (G1/G2/G3) | | | | |
| Size | 126/169/19 | 0.202 | 0.038* | 0.227 |
| (<20 , 20-50, >50 mm) | | | | |
| Lymph node | 152/162 | 0.870 | 0.923 | 0.114 |
| (positive/negative) | | | | |
| ER status | 209/105 | 0.008* | 0.196* | 0.712 |
| (positive/negative) | | | | |

| | | | | |
|---------------------|---------|--------|-------------------|--------|
| PgR status | 149/163 | 0.020* | 0.552 | 0.883 |
| (positive/negative) | | | | |
| HER2 status | 51/263 | 0.488 | 0.030* | 0.797 |
| (positive/negative) | | | | |
| c-Src nuc | 139/175 | 0.102 | 0.300 | 0.845 |
| (positive/negative) | | | | |
| c-Src cyto | 139/175 | 0.380 | 0.040* | 0.340 |
| (positive/negative) | | | | |
| c-Src memb | 135/179 | 0.075 | <0.001* | 0.080 |
| (positive/negative) | | | | |
| AC28 nuc | 82/83 | | 0.902 | 0.510 |
| (positive/negative) | | | | |
| AC28 cyto | 73/92 | | | 0.015* |
| (positive/negative) | | | | |

Table 3.18 shows the interrelationship between AC28 expression at different cellular levels and clinico-pathological characteristics of patients with breast cancer; Histology: duct = ductal carcinoma, lob = lobular carcinoma, tub = tubular carcinoma, others including mucinous, mucoïd and micropapillary carcinoma; Grade: Bloom and Richardson grade; c-Src = total Src kinase, Y416Src = Src kinase phosphorylated at Tyrosine site 416, Y215Src = Src kinase phosphorylated at Tyrosine site Y215; AC 28= anti-Src family negative regulatory [pY] site, re-named in our laboratory as anti-Clone28, Src kinase phosphorylated at Tyrosine site 530 (inactive); *negatively correlated; significant results are highlighted in bold. p-values of >0.01 were considered as non-significant due to the large number of statistical comparisons (Bonferroni phenomenon).

On univariate and multivariate analysis there was no significant association noticed between anti-Clone 28 expression and disease specific survival at any cellular location (table 3.19).

Table 3.19: Impact of AC28 protein expression on patient survival

| Total | Patient | Univariate | | | |
|---------------------|---------------------|-------------------|----------------|-----------|------------|
| | | Numbers | P value | HR | IQR |
| 314 patients | | | | | |
| AC28 nuc | | 82/83 | 0.192 | 1.5 | 0.8-3.0 |
| | (positive/negative) | | | | |
| AC28 cyto | | 72/93 | 0.294 | 1.4 | 0.7-2.8 |
| | (positive/negative) | | | | |
| AC28 memb | | 6/159 | 0.748 | 1.3 | 0.2-9.6 |
| | (positive/negative) | | | | |

Table 3.19: No impact of AC28 protein expression is detected on patient survival. Expression of each cellular location was correlated to disease specific survival. None of the protein expressions were associated with disease specific survival and independent in multivariate analysis. HR= Hazard Ratio (95% Confidence Interval (CI)), IQR= interquartile range. Significant results are highlighted in bold.

3.3.4.2 Partially activated Src kinase (Clone 28) protein expression in invasive breast cancer

Specificity of the Clone 28 (Cl28) antibody was routinely tested via Western Blotting. Commercially available cell lysates were used as protein samples (figure 3.15).

Figure 3.15: Western Blotting for specificity of Clone 28 antibody

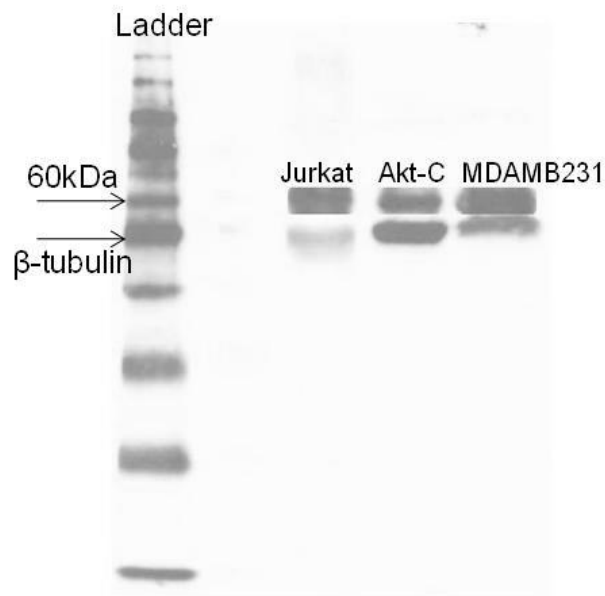


Figure 3.15: Western Blot with Clone 28 antibody (60kDa) and β-tubulin (48kDa), as a protein loading control, using, Jurkat (human lymphoma cell line), Akt control cell lysates (Jurkat cell line) and MDAMB231 (ER negative breast cancer cell) lysates.

Only 48 % of the tumours, previously available for SFK member analysis, were able to be stained for Clone 28 expression (149/314). This effect was due to tissue limitation after extensive section cutting of the TMA.

Nuclear, cytoplasmic and membrane staining was independently assessed. Perinuclear staining was also included in this analysis 50 % of Clone 28 expression was observed in the nucleus, 46 % in the cytoplasm and a remarkable 53 % in the membrane and 55 % perinuclear (table 3.21).

Histograms and IHC pictures below demonstrate the cellular distribution and intensity of nuclear, cytoplasmic and membrane Clone 28 expression (figure 3.16, picture 3.5).

Figure 3.16: Histograms for Clone 28 expression

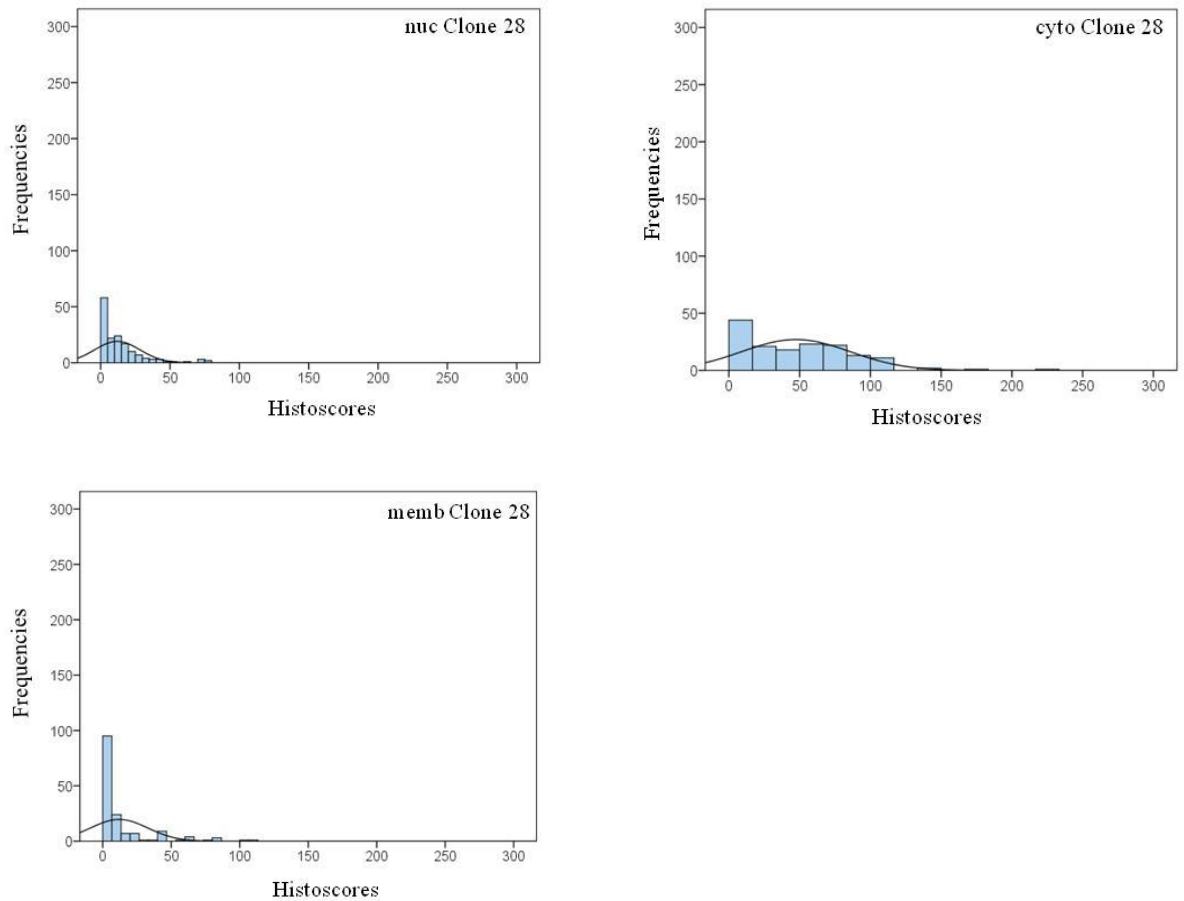
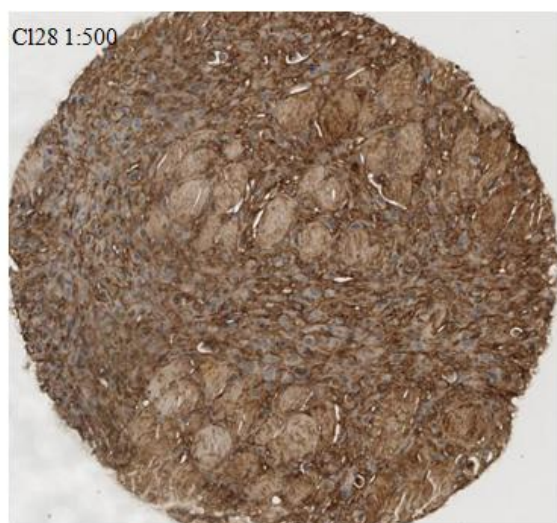
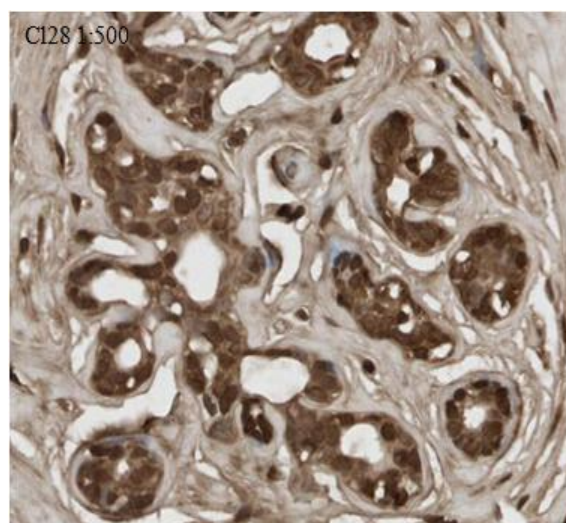


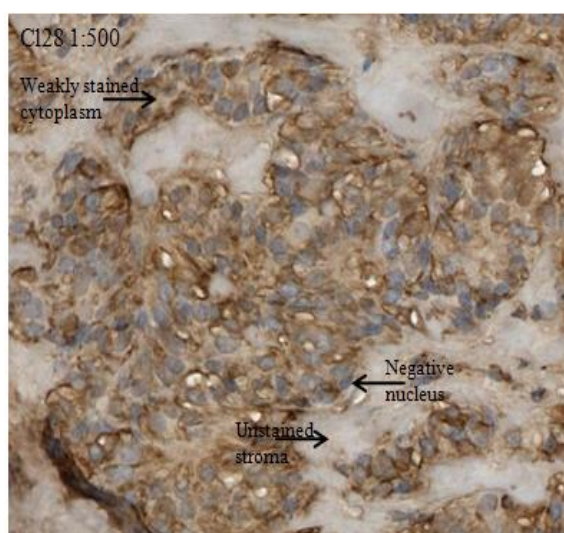
Figure 3.16: Histograms for nuclear, cytoplasmic and membrane Clone 28 staining displaying the distribution of IHC intensity staining.

Picture 3.5: IHC staining with Clone 28 antibody

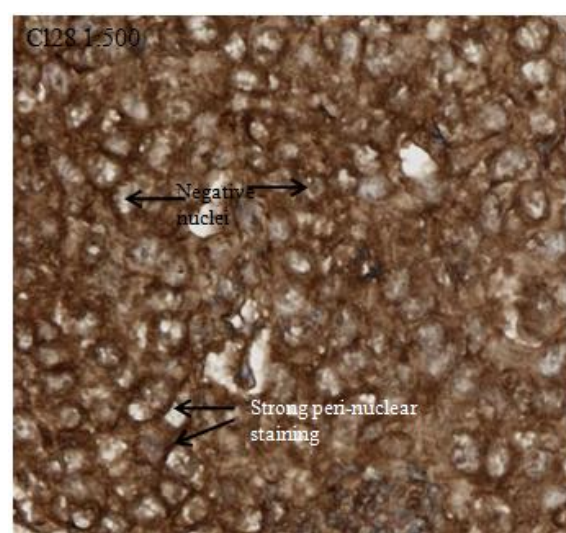
Picture 3.5 A: Overview of a 0.6 mm core of the breast cancer TMA, showing, cytoplasmic, membrane and peri-nuclear staining; magnification x10.



Picture 3.5 B: Normal Breast tissue stained with Clone 28 antibody (Invitrogen); magnification x100.



Picture 3.5 C demonstrates weak cytoplasmic and membrane, negative weak and moderate nuclear staining. x100.



Picture 3.5 D: Negative staining of nuclei, but strong perinuclear staining with Clone 28, x120.

Tumours were split into high (above median) and low expression (below or equal to the median) (table 3.20), separating patients into patient group with high (positive subgroup) and low expression (negative subgroup) (table 3.21). Median of nuclear, cytoplasmic and membrane Clone 28 was used for statistical analysis.

Table 3.20: Descriptive statistics for Clone 28 histoscores

| Clone 28 | Minimum | Maximum | Median | LQ | UQ |
|--------------------|---------|---------|--------|------|------|
| Histoscores | | | | | |
| nuclear | 0.0 | 80.0 | 5.0 | 0.0 | 15.0 |
| cytoplasmic | 0.0 | 227.0 | 40.0 | 10.6 | 74.3 |
| membrane | 0.0 | 110.0 | 2.5 | 0.0 | 10.0 |

Table 3.20 provides an overview of descriptive statistics of Clone 28 nuclear, cytoplasmic and membrane histoscores.

Table 3.21: Clone 28 expression in patient subgroups

| Clone 28 | Nuclear | Cytoplasm | Membrane | Perinuclear |
|------------------------|---------|-----------|----------|-------------|
| expression | | | | |
| Positive (Patient No) | 74 | 69 | 78 | 82 |
| Negative (Patients No) | 85 | 80 | 70 | 67 |

Table 3.21 shows the division into positive and negative expression group.

Chi square analysis was performed to identify associations between Clone 28, anti-Clone 28, Src and clinico-pathological features of the cohort (table 3.22). No significant correlations were noted between clinico-pathological features and any of the Clone 28 expression sites. Nuclear and membrane Clone 28 expression showed no significant correlations with any of the other c-Src and anti-Clone 28 expressions. Interrelationship

analysis of individual cellular locations demonstrated a positive correlation between nuclear and cytoplasmic Clone 28 expression (χ^2 $p < 0.001$) and a negative correlation between nuclear and perinuclear Clone 28 expression (χ^2 $p < 0.001$). Interestingly cytoplasmic Clone28 correlated negatively with membrane c-Src expression (χ^2 $p < 0.001$) and cytoplasmic AC28 (χ^2 $p = 0.001$), highlighting that breast cancer patients with partially activated Src in the cytoplasm were less likely to express c-Src at the membrane (site of activation) or inactivated Src in the cytoplasm. Perinuclear Clone 28 expression correlated negatively with cytoplasmic AC28 (χ^2 $p < 0.001$), nuclear Clone 28 (χ^2 $p < 0.001$) and cytoplasmic Clone 28 (χ^2 $p < 0.001$) (table 3.22).

Table 3.22: Correlations between clinico-pathological features of the cohort, c-Src, AC28 and Clone 28 expression

| Total Cohort | Patient Numbers | Chi-squared p-values | | | |
|-----------------------|-----------------|----------------------|-----------|-----------|--------------|
| | | Cl28 nuc | Cl28 cyto | Cl28 memb | Cl28 perinuc |
| Age | 78/236 | 0.027* | 0.906 | 0.547 | 0.239 |
| (<50yr/>50yr) | | | | | |
| Tumour type | 298/10/3/3 | 0.307 | 0.304 | 0.394 | 0.269 |
| (duct/lob/tub/others) | | | | | |
| Grade | 22/146/146 | 0.312 | 0.010* | 0.655 | 0.204 |
| (G1/G2/G3) | | | | | |
| Size | 126/169/19 | 0.901 | 0.030 | 0.565 | 0.016 |
| (<20 , 20-50, >50mm) | | | | | |
| Lymph node | 152/162 | 1.0 | 0.747 | 0.811 | 0.420 |
| (positive/negative) | | | | | |
| ER status | 209/105 | 0.055 | 0.535 | 0.806 | 0.645 |
| (positive/negative) | | | | | |

| | | | | | |
|---------------------|---------|-------|-------------------|-------|-------------------|
| PgR status | 149/163 | 0.461 | 0.635 | 0.926 | 0.975 |
| (positive/negative) | | | | | |
| HER2 status | 51/263 | 0.628 | 0.038 | 0.306 | 0.181 |
| (positive/negative) | | | | | |
| c-Src nuc | 139/175 | 0.105 | 0.066 | 0.678 | 0.046 |
| (positive/negative) | | | | | |
| c-Src cyto | 139/175 | 0.740 | 1.0 | 0.811 | 0.629 |
| (positive/negative) | | | | | |
| c-Src memb | 135/179 | 0.841 | <0.001* | 0.393 | 0.002* |
| (positive/negative) | | | | | |
| AC28 nuc | 82/83 | 0.187 | 0.428 | 0.848 | 0.406 |
| (positive/negative) | | | | | |
| AC28 cyto | 73/92 | 0.282 | 0.001* | 0.703 | <0.001* |
| (positive/negative) | | | | | |
| AC28 memb | 6/159 | 0.388 | 0.802 | 0.241 | 0.707 |
| (positive/negative) | | | | | |
| Cl28 nuc | 74/85 | | <0.001 | 0.037 | <0.001* |
| (positive/negative) | | | | | |
| Cl28 cyto | 69/90 | | | 0.081 | <0.001* |
| (positive/negative) | | | | | |
| Cl28 memb | 78/70 | | | | 0.770 |
| (positive/negative) | | | | | |

Table 3.22 shows the interrelationship between Clone 28 expression at different cellular levels and clinico-pathological characteristics of patients with breast cancer; Histology: duct = ductal carcinoma, lob = lobular carcinoma, tub = tubular carcinoma, others including mucinous, mucoïd and micropapillary carcinoma; Grade: Bloom and Richardson grade; c-Src = total Src kinase, AC 28= anti-Src family negative regulatory [pY] site, re-named in our laboratory as anti-Clone28, Src kinase phosphorylated at Tyrosine site 530 (inactive); Cl 28= Clone 28, Src kinase

*dephosphorylated at Tyrosine site 530, partially activated. *negatively correlated; significant results are highlighted in bold. p-values of >0.01 were considered as non-significant due to the large number of statistical comparisons (Bonferroni phenomenon).*

On univariate and multivariate analysis there was no significant association noticed between Clone 28 expression and disease specific survival at any cellular location (table 3.23).

Table 3.23: Impact of Clone 28 protein expression on patient survival.

| Total Cohort: | Patient | Univariate Analysis | | | |
|----------------------|---------------------|----------------------------|----------------|-----------|------------|
| | | Numbers | P value | HR | IQR |
| 314 patients | | | | | |
| Cl28 nuc | | 74/85 | 0.313 | 1.4 | 0.7-2.5 |
| | (positive/negative) | | | | |
| Cl28 cyto | | 69/90 | 0.810 | 0.9 | 0.5-1.7 |
| | (positive/negative) | | | | |
| Cl28 memb | | 78/70 | 0.568 | 0.8 | 0.5-1.5 |
| | (positive/negative) | | | | |
| Cl28 perinuclear | | 75/74 | 0.625 | 1.2 | 0.6-2.2 |
| | (positive/negative) | | | | |

Table 3.23: *No impact of Clone 28 protein expression on patient survival was observed. Expression of each cellular location was correlated to disease specific survival. None of the protein expressions were associated with disease specific survival and independent in multivariate analysis. HR= Hazard Ratio (95% Confidence Interval (CI)), IQR= interquartile range. Significant results are highlighted in bold.*

3.3.4.3 Activated Y419Src kinase protein expression in invasive breast cancers

Specificity of the antibody detecting phosphorylation at Tyrosine site 419 was confirmed using a ER negative (MDAMB231) and ER positive (MCF7) cell line (figure 3.17). Time course cell lysates were kindly provided by Dr Liane McGlynn.

Figure 3.17: Western Blotting for specificity of Y416Src antibody

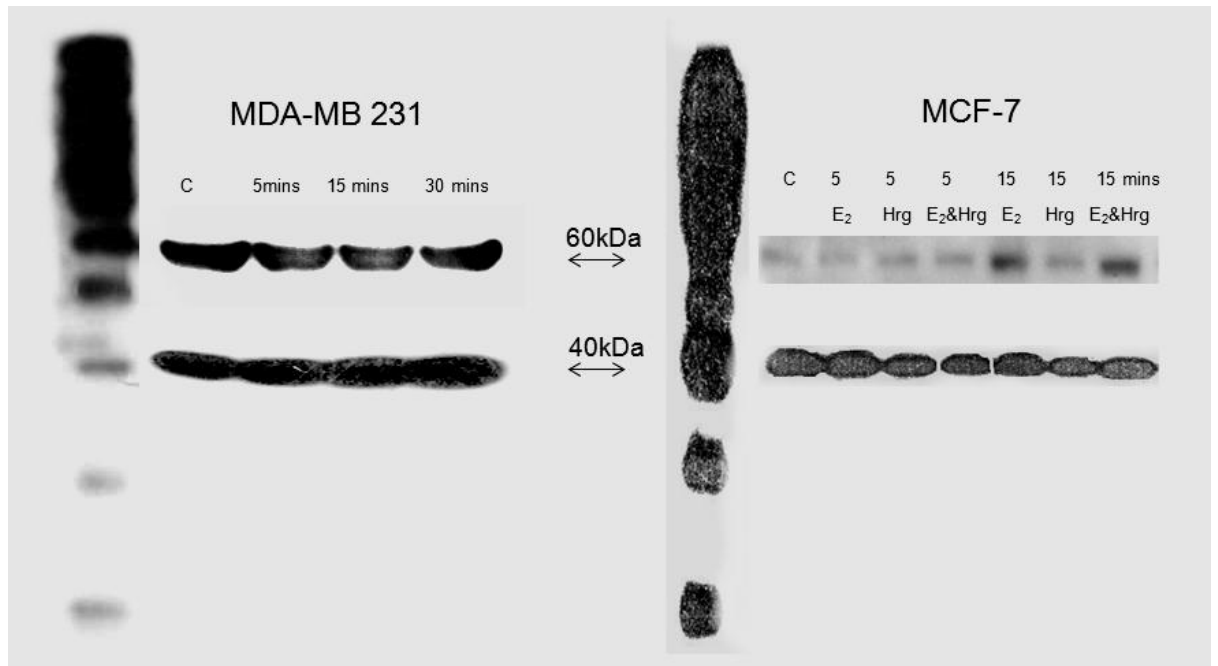


Figure 3.17: Western Blots with Y416Src (60kDa) and β -actin (40kDa), as a protein loading control. Using ER positive (MCF7) and ER negative (MDA MB231) breast cancer cell lines exposed to stimulant oestradiol or epidermal growth factor (E2/ EGF) and/or inhibitor Heregulin (HRG) at different time points. C= control, untreated cell line.

Activated phosphorylated Src kinase expression, at the classical activation site Y419, was predominately observed in the nucleus (39%) and cytoplasm (45%). 51% of tumours expressed Y419Src kinase in the membrane (table 3.24).

Table 3.24: Y419Src expression in patient subgroups

| Y419Src (no. 314) | Nuclear | Cytoplasm | Membrane |
|--------------------------|---------|-----------|----------|
| Positive (Patient No) | 122 | 140 | 161 |
| Negative (Patients No) | 192 | 174 | 153 |

Table 3.24 shows the distribution of patients in each subgroup.

For statistical analysis tumours were split into those with high (above the median) or low (below or equal to the median) expression (table 3.25). Therefore patients separated into two groups; those with low expression (negative subgroup) and those with higher expression (positive subgroup) (table 3.24).

Table 3.25: Descriptive statistics for Y419Src histoscores

| Y419Src | Minimum | Maximum | Median | LQ | UQ |
|--------------------|---------|---------|--------|----|----|
| Histoscores | | | | | |
| nuclear | 0 | 245 | 32 | 10 | 70 |
| cytoplasmic | 0 | 213 | 20 | 3 | 60 |
| membrane | 0 | 135 | 0 | 0 | 5 |

Table 3.25 provides an overview of descriptive statistics of Y419Src nuclear, cytoplasmic and membrane histoscores. With the membrane Y419Src median being 0, patients were grouped into two subgroups: patients with no Y419Src expression and with Y419Src expression.

Histograms and IHC pictures below exhibit the cellular distribution and intensity of nuclear, cytoplasmic and membrane Y419Src expression (figures 3.18, picture 3.6).

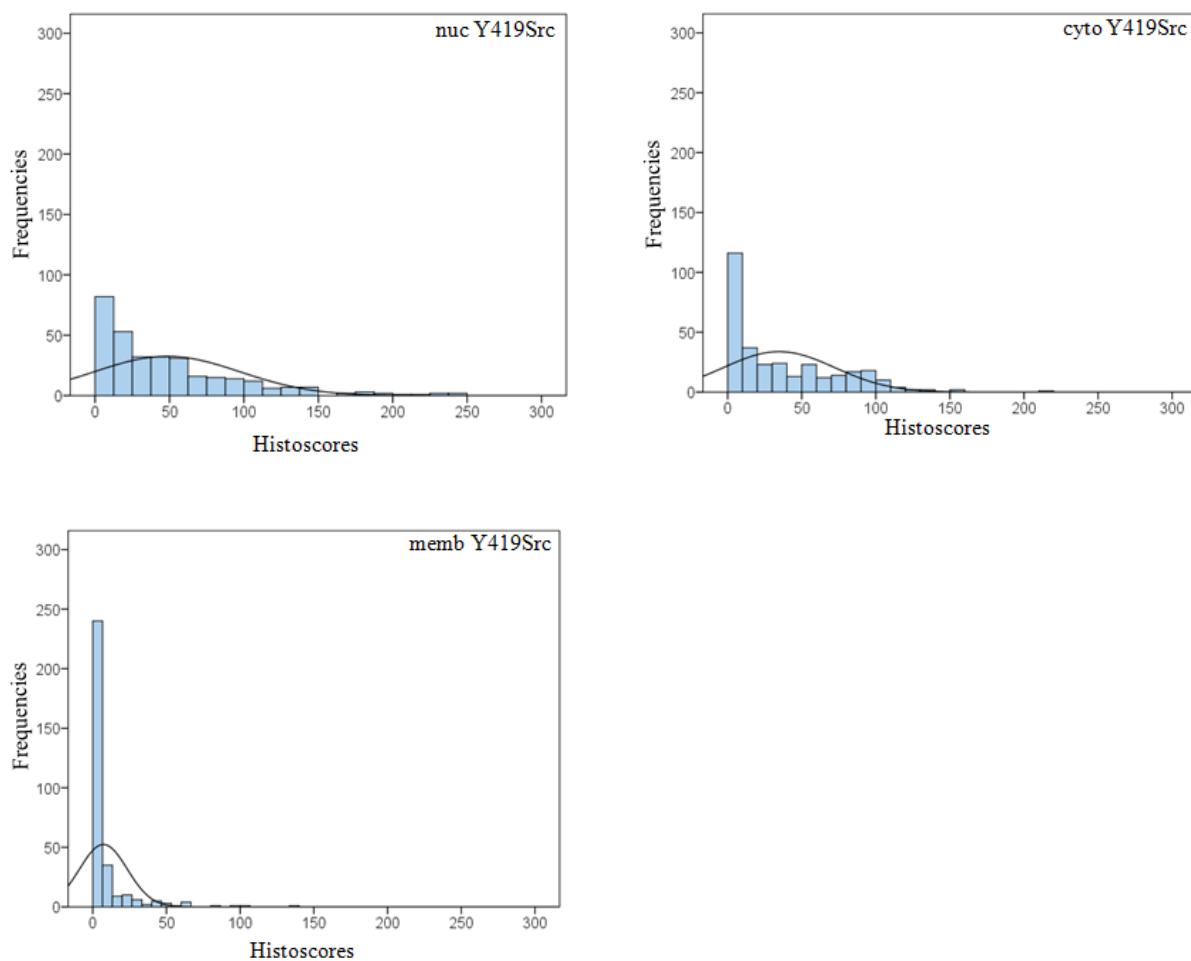
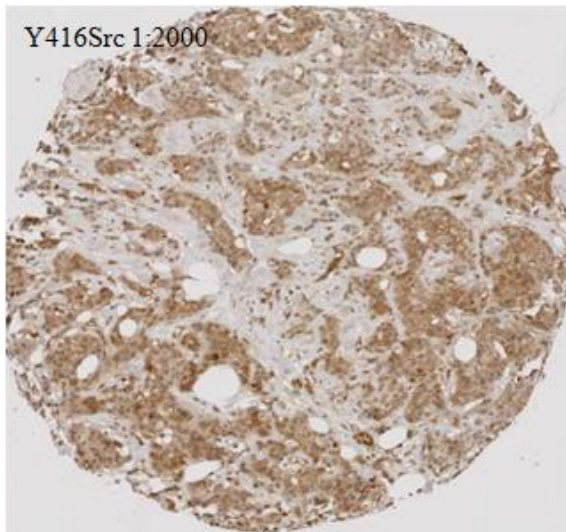
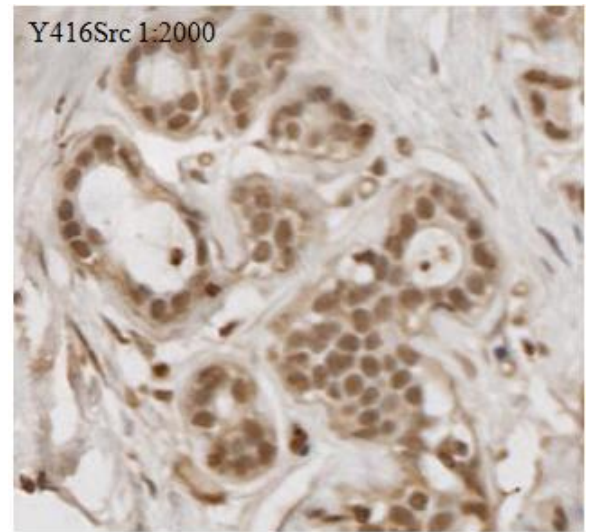
Figure 3.18: Histograms for Y419Src expression

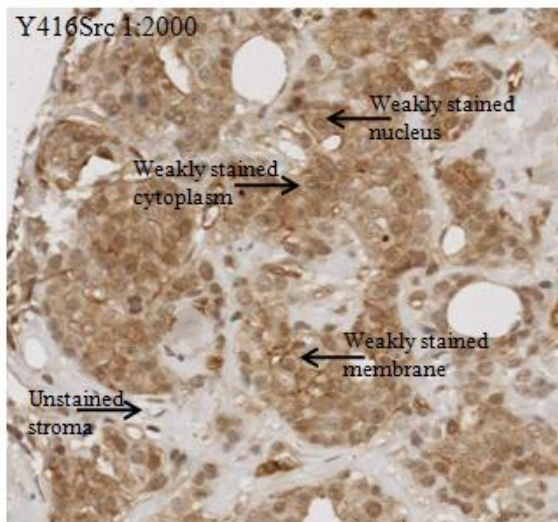
Figure 3.18 demonstrates the intensity of IHC staining for nuclear, cytoplasmic and membrane Y419Src expression

Picture 3.6: IHC staining with Y416Src antibody

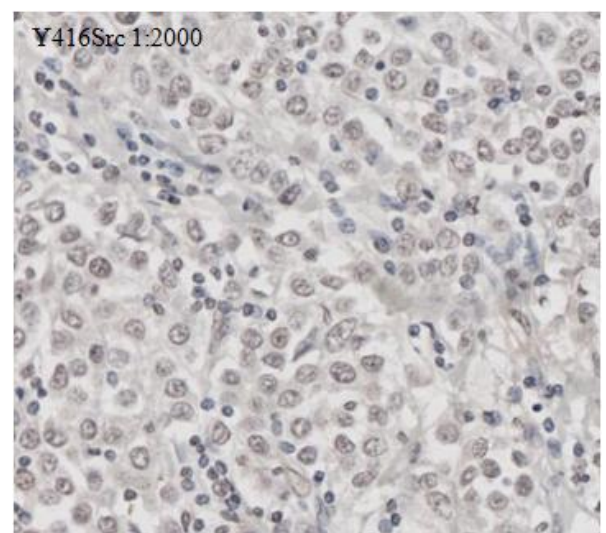
Picture 3.6 A: Overview of a 0.6 mm core of the breast cancer TMA, showing nuclear, cytoplasmic and membrane staining; magnification x10.



Picture 3.6 B: Normal Breast tissue, stained with Y416Src antibody (Cell Signalling); magnification x100.



Picture 3.6 C demonstrates weak cytoplasmic and membrane, weak and negative nuclear staining. magnification x100.



Picture 3.6 D: Negative/greyish staining of stroma and tumour tissue, magnification x100.

With chi square analysis we tried to evaluate if clinico-pathological features of the patient cohort correlated with high Y419Src expression (table 3.26). We found that cytoplasmic Y419Src expression positively correlated with HER2 status; meaning that patients with invasive breast cancer over-expressing Y419Src in the cytoplasm, were more likely to have HER2 positive breast cancers (χ^2 $p < 0.001$). Membrane Y419Src expression positively correlated with grade (χ^2 $p < 0.001$), size (χ^2 $p = 0.002$) and HER2 status (χ^2 $p < 0.001$) and inversely correlated with ER status (χ^2 $p < 0.001$). Nuclear Y419Src expression did not correlate with any known clinico-pathological features or other c-Src location (table 3.26). Cytoplasmic and membrane Y419Src expression correlated significantly with c-Src cyto and membrane expression (χ^2 $p < 0.001$). Expression levels of Y419Src at each cellular location strongly positively correlated with each other (table 3.26).

Table 3.26: Interrelationship between clinico-pathological features of the cohort, c-Src and Y419Src expression

| Total Patient Cohort | | Chi-squared p-values | | |
|--------------------------------------|------------|----------------------|-----------------|------------------|
| 314 Variables | Numbers | Y419Src nuc | Y419Src cyto | Y419Src memb |
| Age (<50yr/>50yr) | 78/236 | 0.622 | 0.391 | 0.287 |
| Tumour type (duct/lob/tub/others) | 298/10/3/3 | 0.753 | 0.293 | 0.416 |
| Grade (G1/G2/G3) | 22/146/146 | 0.627 | 0.069 | <0.001 |
| Size (<20 , 20-50, >50mm) | 126/169/19 | 0.061 | 0.044 | 0.002 |
| Lymph node (positive/negative) | 152/162 | 0.127 | 0.211 | 0.392 |

| | | | | |
|---------------------|---------|-------|------------------|-------------------|
| ER status | 209/105 | 0.143 | 0.108 | <0.001* |
| (positive/negative) | | | | |
| PgR status | 149/163 | 0.412 | 0.042 | <0.001 |
| (positive/negative) | | | | |
| HER2 status | 51/263 | 0.053 | <0.001 | <0.001 |
| (positive/negative) | | | | |
| c-Src nuc | 139/175 | 0.058 | 0.268 | 0.376 |
| (positive/negative) | | | | |
| c-Src cyto | 139/175 | 0.687 | <0.001 | <0.001 |
| (positive/negative) | | | | |
| c-Src memb | 135/179 | 0.370 | <0.001 | <0.001 |
| (positive/negative) | | | | |
| Y419Src nuc | 122/192 | | <0.001 | 0.004 |
| (positive/negative) | | | | |
| Y419Src cyto | 138/174 | | | <0.001 |
| (positive/negative) | | | | |

*Table 3.26 shows the interrelationship between Y419Src expression at different cellular levels and clinico-pathological characteristics of patients with breast cancer; c-Src = total Src kinase, Y419Src = Src kinase phosphorylated at Tyrosine site 419, *negatively correlated, significant results are highlighted in bold. p-values of >0.01 were considered as non-significant due to the large number of statistical comparisons (Bonferroni phenomenon).*

Patients' clinical outcome was analysed using Kaplan Meier survival analysis. Only Y419Src membrane expression was associated with shorter disease specific survival (p=0.023, table 3.27) on univariate analysis (figure 3.19).

However, as with cytoplasmic c-Src expression, it was not independent in multivariate analysis (table 3.27).

Table 3.27: Impact of Y419Src expression on patient survival

| Total Cohort: | Patient | Univariate Analysis | | | Multivariate Analysis | | | |
|---------------------|---------------------|---------------------|---------|---------|-----------------------|---------|---------|-----|
| | | Numbers | P value | HR | IQR | P value | HR | IQR |
| 314 patients | | | | | | | | |
| Y419Src nuc | 135/179 | 0.585 | 0.9 | 0.5-1.4 | | | | |
| | (positive/negative) | | | | | | | |
| Y419Src cyto | 122/192 | 0.625 | 0.9 | 0.6-1.4 | | | | |
| | (positive/negative) | | | | | | | |
| Y419Src memb | 138/174 | 0.023 | 1.7 | 1.1-2.7 | 0.614 | 1.1 | 0.7-1.8 | |
| | (positive/negative) | | | | | | | |

Table 3.27: Expression of each cellular location was correlated to disease specific survival. Membrane Y419Src protein expression was associated with poorer clinical outcome, but was not independent in multivariate analysis. HR= Hazard Ratio (95% Confidence Interval (CI)), IQR= interquartile range. Significant results are highlighted in bold.

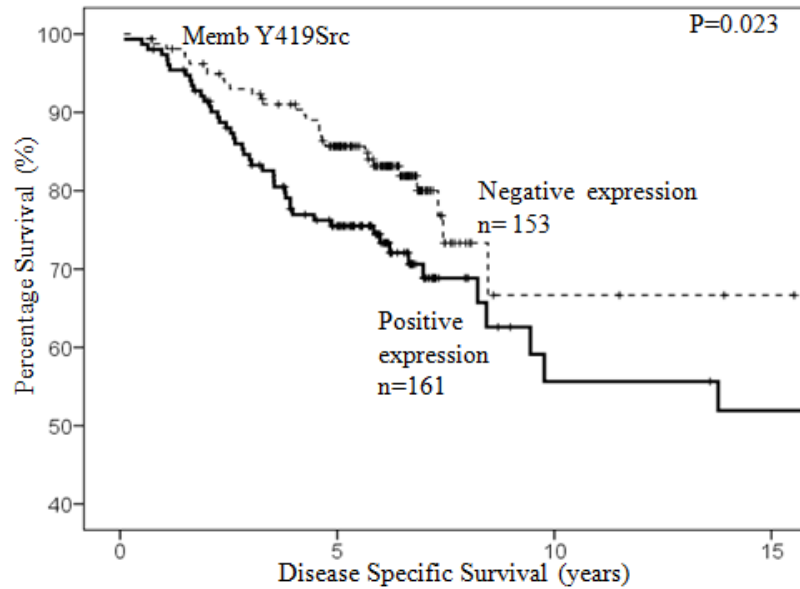
Figure 3.19: Kaplan Meier survival curve for membrane Y419Src expression

Figure 3.19: Kaplan Meier survival curve illustrates that membrane Y419Src expression is significantly associated with decreased disease specific survival ($p=0.023$, respectively).

Patients with high membrane Y419Src expression had a median survival of 12.8 years (IQR 11.1-14.6) compared to those with low expression with median survival of 14.8 years (IQR 12.1-16.8).

3.3.4.4 Activated Y215Src kinase protein expression in invasive breast cancers

Despite the only recent discovery of the activation site Y215, there are already several antibodies commercially available. Specificity of the Y216Src Santa Cruz antibody was confirmed using a ER negative (MDAMB231) and HEK293 (human embryonic kidney) cell line lysates (figure 3.20).

Figure 3.20: Western Blotting for specificity of Y216Src antibody

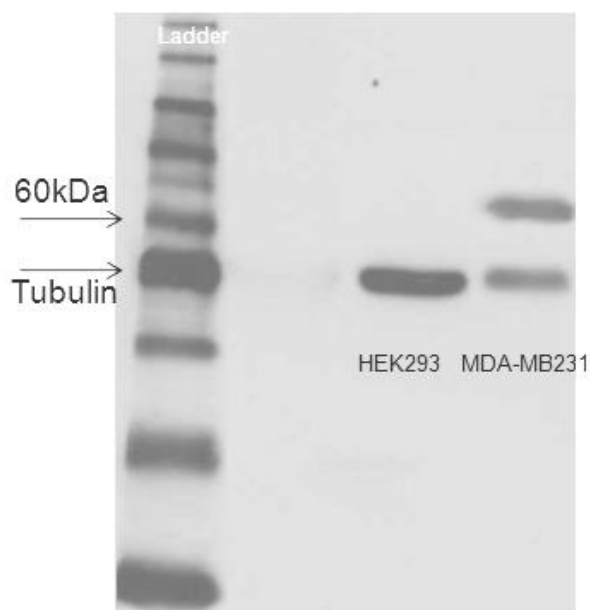


Figure 3.20: Western Blot with Y216Src and β -tubulin (48kDa), as a protein loading control. Using Human Embryonic Kidney cell lysates (HEK293) and ER negative (MDA MB231) breast cancer cell line lysates. No band detected in non-phosphorylated HEK 293 cells with Y216Src antibody (Santa Cruz).

Phosphorylated activated Y215Src kinase expression was predominately observed in the nucleus (49%) and cytoplasm (50%). No more than 4% of tumours expressed Y215Src kinase in the membrane. (table 3.28). Likewise the statistical analysis of Y419Src tumours was split into those with high (above the median) or low (below or equal to the median) expression (table 3.29).

Therefore patients separated into two groups; those with low expression (negative subgroup) and those with higher expression (positive subgroup) (table 3.29).

Table 3.28: Descriptive statistics for Y215Src histoscores

| Y215Src | Minimum | Maximum | Median | LQ | UQ |
|--------------------|---------|---------|--------|----|----|
| Histoscores | | | | | |
| nuclear | 0 | 230 | 5 | 0 | 35 |
| cytoplasmic | 0 | 235 | 8 | 0 | 43 |
| membrane | 0 | 38 | 0 | 0 | 0 |

Table 3.28 provides an overview of descriptive statistics of Y215Src nuclear, cytoplasmic and membrane histoscores. With the membrane Y215Src median being 0, patients were grouped into two subgroups: patients with no Y215Src expression and with Y215Src expression.

Table 3.29: Y215Src expression in patient subgroups

| Y215Src (no. 314) | Nuclear | Cytoplasm | Membrane |
|--------------------------|---------|-----------|----------|
| Positive (Patient No) | 154 | 158 | 14 |
| Negative (Patients No) | 160 | 156 | 299 |

Table 3.29 shows the distribution of patients in each subgroup.

Histograms and IHC pictures below exhibit the cellular distribution and intensity of nuclear, cytoplasmic and membrane Y215Src expression (figure 3.21, picture 3.7).

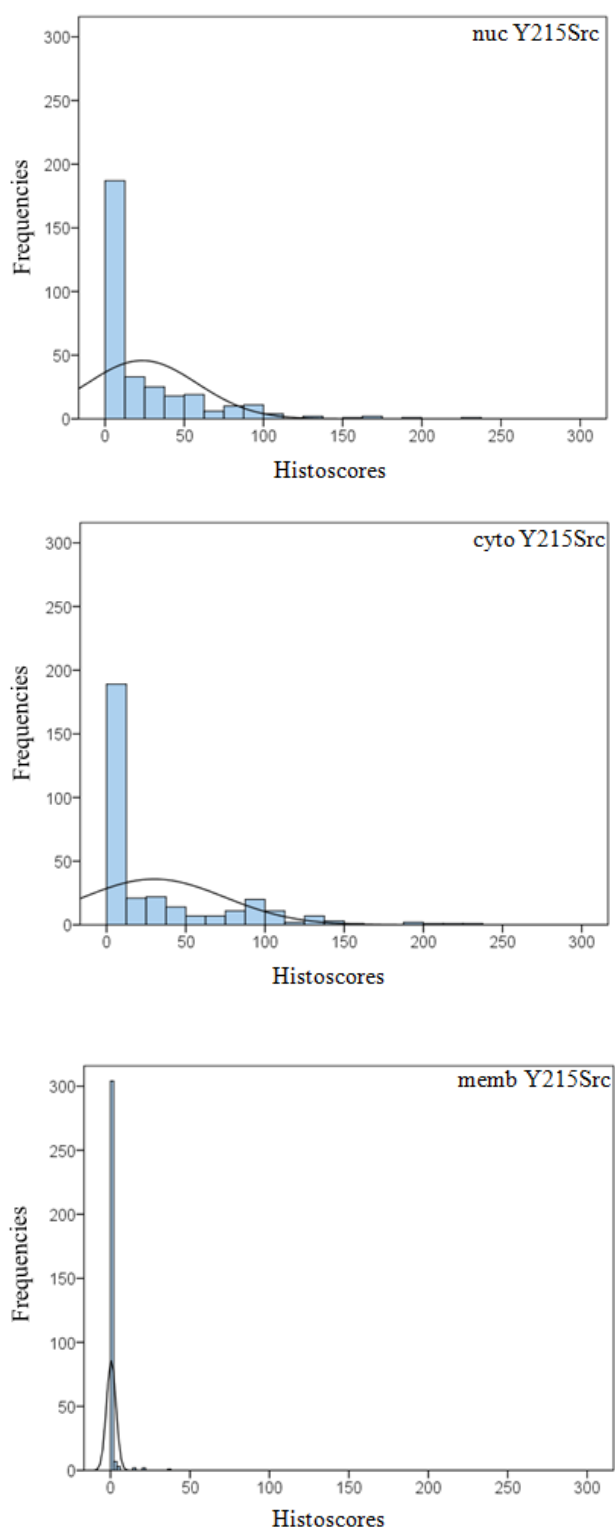
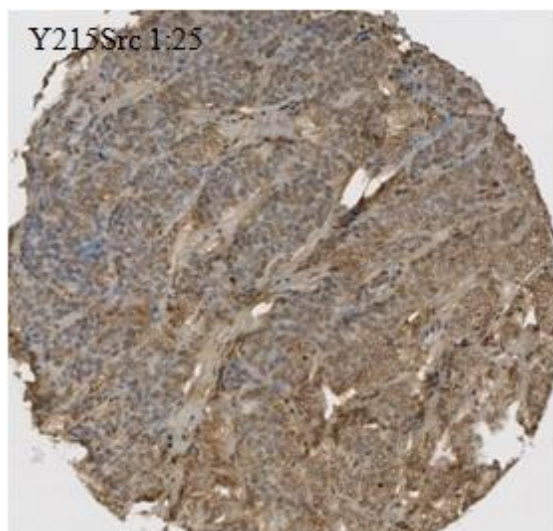
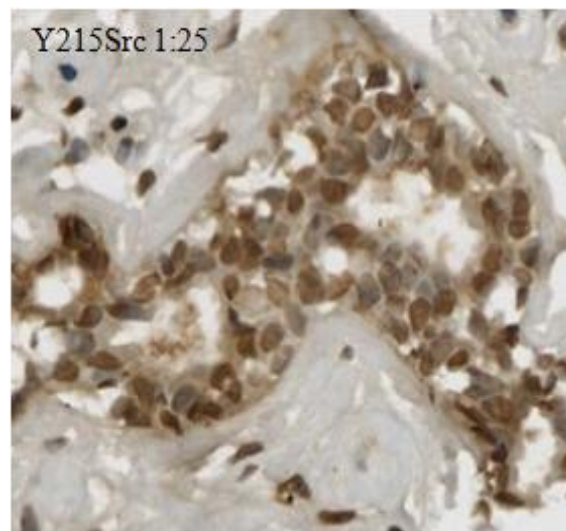
Figure 3.21: Histograms for Y215Src expression in invasive breast carcinoma

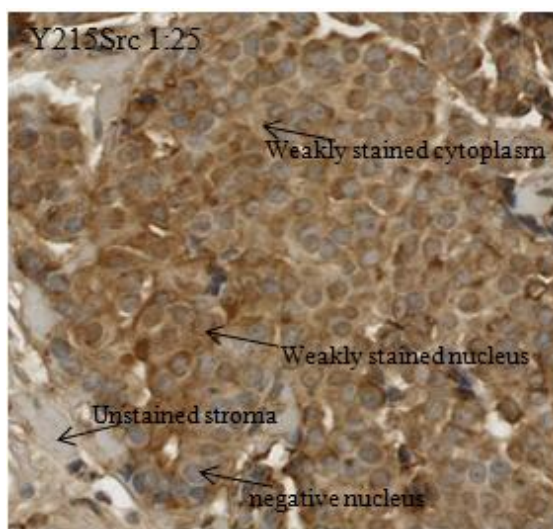
Figure 3.21: Each histogram displays the distribution of nuclear, cytoplasmic and membrane Y215Src expression and its IHC staining intensity.

Picture 3.7: IHC staining with Y215Src

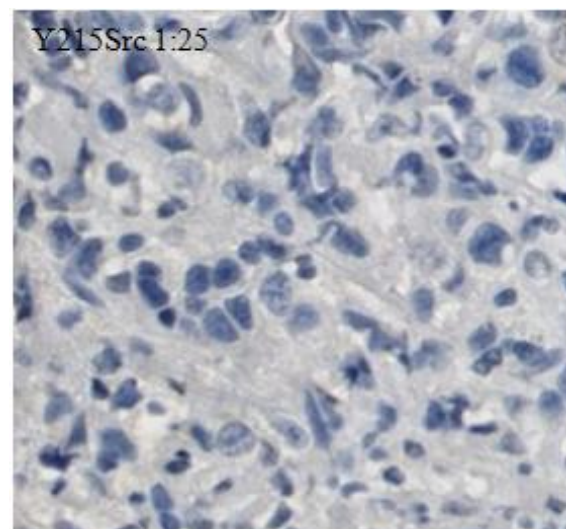
Picture 3.7 A: Overview of a 0.6 mm core of the breast cancer TMA; showing areas of nuclear and cytoplasmic mixed with no nuclear staining, x10.



Picture 3.7 B: Normal Breast tissue, stained with Y216Src antibody (Santa Cruz); magnification x100.



Picture 3.7 C: demonstrates weak and moderate cytoplasmic, weak and negative nuclear and no membrane staining, x100.



Picture 3.7 D: Negative staining of stroma and tumour tissue, magnification x100. Negative control.

Correlations between Y215Src expression and clinico-pathological features of the patient cohort were assessed with Chi square analysis. Nuclear Y215Src expression positively correlated with grade and ER status (table 3.30), meaning that patients with invasive breast cancer over-expressing Y215Src in the nucleus, were more likely to have high grade, ER positive breast cancers (χ^2 p=0.006 and χ^2 p<0.001). The only correlation observed with cytoplasmic Y215Src expression and clinico-pathological features was a positive correlation with HER2 status (table 3.30).

Table 3.30: Correlations between pathological features of cohort and Y215Src expression

| Total Patient Cohort: 314 | | Chi-squared p-values | | |
|----------------------------------|----------------|-----------------------------|---------------------|---------------------|
| Variables | Numbers | Y215Src nuc | Y215Src cyto | Y215Src memb |
| Age | 78/236 | 0.332 | 0.649 | 0.861 |
| (<50yr/>50yr) | | | | |
| Tumour type | 298/10/3/3 | 0.015 | 0.515 | 0.424 |
| (duct/lob/tub/others) | | | | |
| Grade | 22/146/146 | 0.006 | 0.674 | 0.372 |
| (G1/G2/G3) | | | | |
| Size | 126/169/19 | 0.061 | 0.921 | 0.399 |
| (<20 , 20-50, >50mm) | | | | |
| Lymph node | 152/162 | 0.504 | 0.828 | 0.217 |
| (positive/negative) | | | | |
| ER status | 209/105 | <0.001 | 0.902 | 0.972 |
| (positive/negative) | | | | |
| PgR status | 149/163 | 0.014 | 0.266 | 0.087 |
| (positive/negative) | | | | |
| HER2 status | 51/263 | 0.161 | <0.001† | 0.075 |
| (positive/negative) | | | | |

Table 3.30 shows the interrelationship between Y215Src expression at different cellular levels and clinico-pathological characteristics of patients with breast cancer. Histology: duct = ductal carcinoma, lob = lobular carcinoma, tub = tubular carcinoma, others including mucinous, mucoïd and micropapillary carcinoma; Grade: Bloom and Richardson grade; Y215Src nuc = Y215Src nuclear expression, Y215Src cyto = Y215Src cytoplasmic expression, Y215Src memb = Y215Src membrane expression. †cytoplasmic Y215Src kinase expression independent on multivariate analysis ($p=0.005$, table 3) as HER2 being displaced from the Cox-regression model.

Interestingly all significant relationships between Y215Src expression and other Src phosphorylation sites were negatively correlated (table 3.31). Most of the correlations were with cytoplasmic Y215Src expression, apart from one Y215Src nuclear expression, which correlated negatively with AC 28 nuclear expression (χ^2 $p=0.004$). Cytoplasmic Y215Src expression correlated negatively with all Y419Src expression sites (Y419Src nuc χ^2 $p=0.005$, Y419Src cyto χ^2 $p<0.001$, Y419Src memb χ^2 $p<0.001$), cytoplasmic and membrane c-Src (χ^2 $p=0.009$ and $p<0.001$), cytoplasmic AC 28 (χ^2 $p<0.001$) and cytoplasmic Clone 28 expression (χ^2 $p=0.004$), meaning that patients with invasive breast cancer over-expressing cytoplasmic Y215Src, were more likely to have low protein expression of the other Src phosphorylation site. No significant correlations were noted with membrane Y215Src expression. Interrelationship between different Y215Src locations only highlighted a positive correlation between nuclear and cytoplasmic Y215Src expression.

Table 3.31: The interrelationships between c-Src and all activation sites

| Total Patient Cohort:314 | | Pearson Chi-squared p-values | | | | | | | | | | | | | |
|---------------------------|---------|------------------------------|---------------|--------------------|---------------------|---------------------|--------------------|---------------------|---------------------|-----------------|------------------|------------------|--------------------|---------------------|---------------------|
| Variables | Numbers | c-Src cyto | c-Src memb | Y416 Src nuc | Y416 Src cyto | Y416 Src memb | Y215 Src nuc | Y215 Src cyto | Y215 Src memb | AC 28 nuc | AC 28 cyto | AC 28 memb | Clone 28 nuc | Clone 28 cyto | Clone 28 memb |
| c-Src nuc (pos/neg) | 139/175 | <0.001 | <0.001 | 0.058 | 0.268 | 0.376 | 0.902 | 0.297 | 0.048 | 0.102 | 0.330 | 0.845 | 0.038 | 0.027 | 0.678 |
| c-Src cyto (pos/neg) | 139/175 | | <0.001 | 0.687 | <0.001 | <0.001 | 0.745 | 0.009* | 0.682 | 0.380 | 0.044 | 0.340 | 0.200 | 0.873 | 0.811 |
| c-Src memb (pos/neg) | 135/179 | | | 0.370 | 0.001 | <0.001 | 0.147 | <0.001* | 0.054 | 0.075 | <0.001 | 0.080 | 0.650 | <0.001 | 0.393 |
| Y416Src nuc (pos/neg) | 122/192 | | | | <0.001 | 0.004 | 0.042 | 0.005* | 0.120 | 0.001 | 0.074 | 0.054 | 0.154 | 0.787 | 0.308 |
| Y416Src cyto (pos/neg) | 138/174 | | | | | <0.001 | 0.294 | <0.001* | 0.489 | 0.058 | <0.001 | 0.002 | 0.952 | 0.522 | 0.718 |
| Y416Src memb (pos/neg) | 138/174 | | | | | | 0.690 | <0.001* | 0.141 | 0.702 | 0.141 | 0.064 | 0.521 | 0.008 | 0.157 |

| | | | | | | | | | |
|------------------|---------|------------------|-------|---------------|-------------------|--------|--------|-------------------|-------|
| Y215Src nuclear | 154/160 | <0.001 | 0.063 | 0.004* | 0.176 | 0.640 | 0.761 | 0.659 | 0.366 |
| (pos/neg) | | | | | | | | | |
| Y215Src cyto | 158/156 | | 0.022 | 0.515 | <0.001* | 0.077 | 0.485 | 0.004* | 0.502 |
| (pos/neg) | | | | | | | | | |
| Y215Src memb | 14/299 | | | 0.430 | 0.323 | 0.263 | 0.423 | 0.101 | 0.174 |
| (pos/neg) | | | | | | | | | |
| AC 28 nuclear | 82/83 | | | | 0.902 | 0.510 | 0.015* | 0.449 | 0.848 |
| (pos/neg) | | | | | | | | | |
| AC 28 cyto | 72/93 | | | | | 0.015* | 0.192 | <0.001* | 0.703 |
| (pos/neg) | | | | | | | | | |
| AC 28 memb | 6/159 | | | | | | 0.305 | 0.696 | 0.241 |
| (pos/neg) | | | | | | | | | |
| Clone 28 nuclear | 74/85 | | | | | | | 0.007* | 0.144 |
| (pos/neg) | | | | | | | | | |
| Clone 28 cyto | 69/80 | | | | | | | | 0.410 |
| (pos/neg) | | | | | | | | | |

Table 3.31 gives an overview of interrelationships between all Src and Src phosphorylation sites. *c-Src* = total Src kinase, *Y416Src* = Src kinase phosphorylated at Tyrosine site 416, *Y215Src* = Src kinase phosphorylated at Tyrosine site Y215; *AC 28* = anti-Src family negative regulatory [pY] site, re-named in our laboratory as anti-Clone28, Src kinase phosphorylated at Tyrosine site 530 (inactive), *Clone 28* = dephosphorylated at Tyrosine site 530 (partially active); *c-Src nuc* = *c-Src* nuclear expression, *c-Src cyto* = *c-Src* cytoplasmic expression, *c-Src memb* = *c-Src* membrane expression, *Y416Src nuc* = *Y416Src* nuclear expression, *Y416Src cyto* = *Y416Src* cytoplasmic expression, *Y416Src memb* = *Y416Src* membrane expression, *Y215Src nuc* = *Y215Src* nuclear expression, *Y215Src cyto* = *Y215Src* cytoplasmic expression, *Y215Src memb* = *Y215Src* membrane expression; *AC 28 nuc* = anti-Clone 28 nuclear expression, *AC 28 cyto* = anti-Clone 28 cytoplasmic expression, *AC 28 memb* = anti-Clone 28 membrane expression; *Clone 28 nuc* = Clone 28 nuclear expression, *Clone 28 cyto* = Clone 28 cytoplasmic expression, *Clone 28 memb* = Clone 28 membrane expression; *pos* = positive, *neg* = negative; *negatively correlated; significant results are highlighted in bold. *p*-values of >0.01 were considered as non-significant due to the large number of statistical comparisons (Bonferroni phenomenon).

In contrast, to the observations made with total c-Src (associated with poor prognosis), high nuclear and cytoplasmic Y215Src kinase expression was strongly associated with improved disease specific survival (nuc Y215Src $p=0.001$, cyto Y215Src $p=0.001$ (figure 3.22) (table 3.32).

Figure 3.22: Kaplan Meier survival curve for nuclear and cytoplasmic Y215Src expression

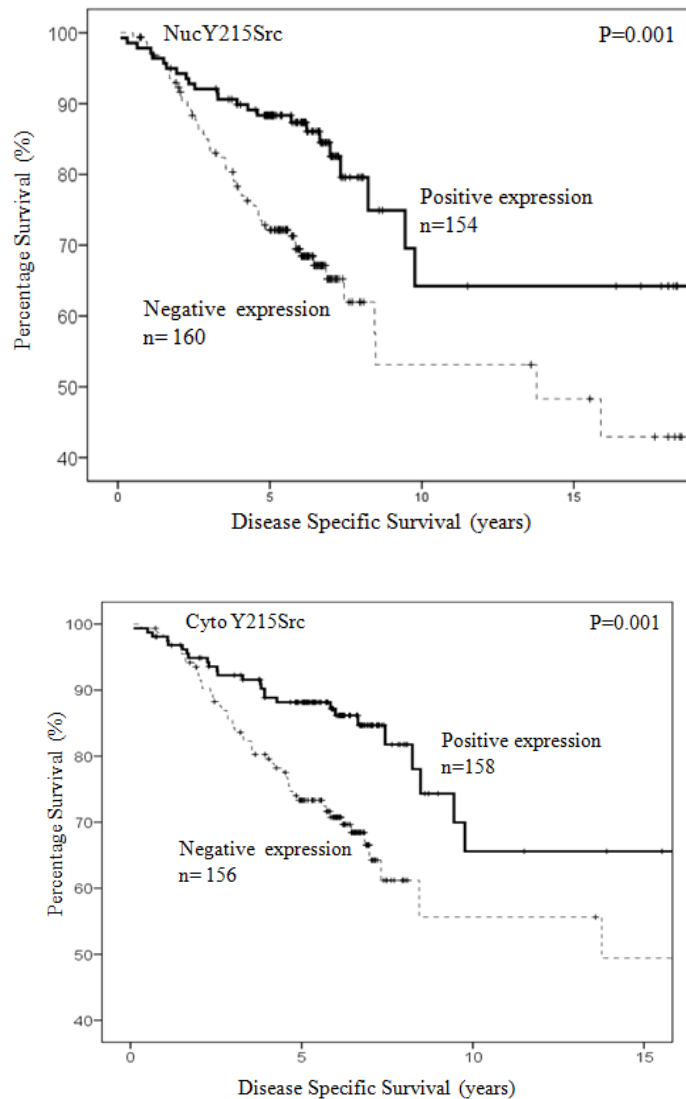


Figure 3.22: Kaplan Meier survival curve shows that nuclear and cytoplasmic Y215Src expression is significantly associated with decreased disease specific survival ($p=0.001$, respectively).

Table 3.32: Impact of Y215Src expression on patient survival

| Total Patient | Numbers | P value | Univariate Analysis | | Multivariate Analysis | | |
|-------------------------------------|---------|--------------|---------------------|---------|-----------------------|-----|---------|
| | | | HR | IQR | P value | HR | IQR |
| 314 patients | | | | | | | |
| Y215Src nuc (positive/negative) | 154/160 | 0.001 | 0.43 | 0.2-0.7 | 0.203 | 0.7 | 0.4-1.2 |
| Y215Src cyto (positive/negative) | 158/156 | 0.001 | 0.45 | 0.3-0.7 | 0.002 | 0.4 | 0.3-0.7 |
| Y215Src memb (positive/negative) | 14/299 | 0.601 | 0.74 | 0.2-2.3 | 0.764 | 1.2 | 0.4-4.0 |

Table 3.32: Expression of each cellular location was correlated to disease specific survival. Nuclear and cytoplasmic Y215Src protein expression was associated with better clinical outcome. Only cytoplasmic Y215Src was independent in multivariate analysis. HR= Hazard Ratio (95% Confidence Interval (CI)), IQR= interquartile range. Significant results are highlighted in bold.

Patients with high nuclear Y215Src kinase expression had a median survival of 15.0 years (IQR 13.1-16.8) compared to those with low expression with a median survival of 12.3 years (IQR 10.5-14.2). Patients with high cytoplasmic Y215Src kinase expression had a median survival of 14.9 years (IQR 13.1-16.7) compared to those with low expression with a median survival of 12.5 years (IQR 10.6-14.4).

Although cytoplasmic Y215Src kinase expression and HER2 status correlated on chi square analysis (table 3.32), only cytoplasmic Y215Src kinase expression was independent on multivariate analysis (p=0.002) with a hazard ratio 0.4 (IQR 0.3-0.7), as HER2 was displaced from the Cox-regression model.

3.3.4.5 Relationship of Src kinase expression to disease specific survival in patients stratified by ER status

Expression of Src kinase, SFK members and all activation sites of Src kinase was stratified by ER status (105 ER negative and 209 ER positive tumours). The only significant results were observed with Y215Src expression.

Patients with ER negative tumours and high cytoplasmic Y215Src kinase expression had significantly improved disease specific survival ($p=0.003$) (figure 3.23). As in the full cohort, this association was also independent on multivariate analysis ($p=0.009$, table 3.33) with a hazard ratio of 0.4 (IQR 0.2-0.8). No association was observed in the ER positive cohort ($p=0.051$).

Figure 3.23: Kaplan Meier Survival Curve for cytoplasmic Y215Src in ER negative patients compared to ER positive patients

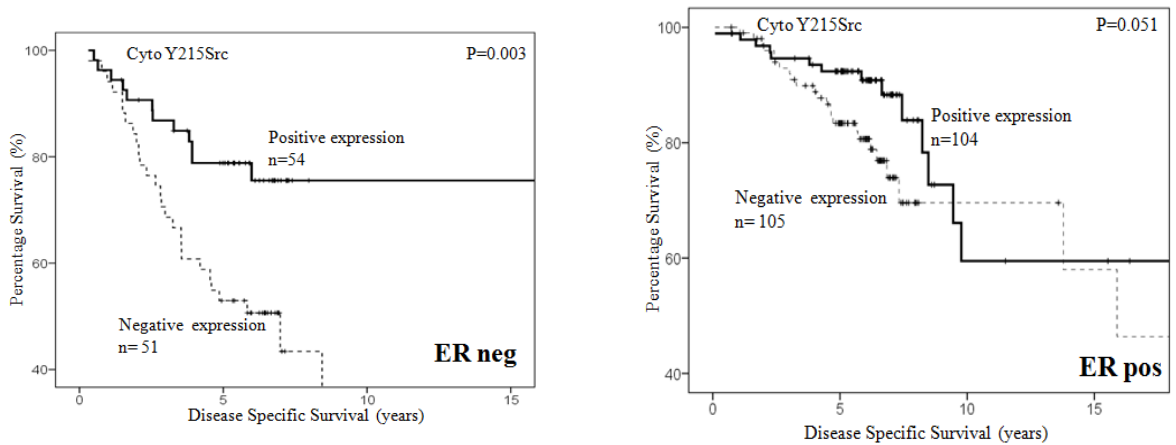


Figure 3.23: Kaplan Meier Survival Curve for cytoplasmic Y215Src in ER negative patients and ER positive patients. Significant survival advantage is present in ER negative patients.

Table 3.33: Survival analysis in ER negative patient cohort with all Src and SFK members

| ER negative patients: | | | Univariate Analysis | | Multivariate analysis | | |
|-------------------------------------|---------|------------------|---------------------|----------|-----------------------|-----|----------|
| | Numbers | P value | HR | IQR | P value | HR | IQR |
| Grade (G1/G2/G3) | 1/23/81 | 0.062 | 1.7 | 0.9-3.1 | | | |
| Size (<20, 20-50, >50mm) | 35/61/9 | <0.001 | 5.4 | 2.1-14.0 | 0.004 | 4.5 | 1.6-12.3 |
| Lymph node (positive/negative) | 54/51 | 0.010 | 2.4 | 1.2-4.6 | 0.001 | 3.2 | 1.6-6.7 |
| HER2 status (positive/negative) | 30/75 | 0.475 | 1.3 | 0.6-2.5 | | | |
| c-Src nuc (positive/negative) | 56/49 | 0.570 | 1.2 | 0.6-2.3 | | | |
| c-Src cyto (positive/negative) | 65/40 | 0.090 | 1.8 | 0.9-3.7 | | | |
| c-Src memb (positive/negative) | 58/47 | 0.982 | 1.0 | 0.5-1.9 | | | |
| Y419Src nuc (positive/negative) | 35/70 | 0.740 | 1.1 | 0.6-2.2 | | | |
| Y419Src cyto (positive/negative) | 53/50 | 0.730 | 1.1 | 0.6-2.1 | | | |
| Y419Src memb (positive/negative) | 67/38 | 0.715 | 1.1 | 0.6-2.2 | | | |
| Y215Src nuc (positive/negative) | 37/68 | 0.345 | 1.1 | 0.7-2.8 | | | |
| Y215Src cyto (positive/negative) | 54/51 | 0.003 | 0.4 | 0.2-0.7 | 0.009 | 0.4 | 0.2-0.8 |
| Y215Src memb (positive/negative) | 5/100 | 0.866 | 1.1 | 0.3-4.8 | | | |
| AC 28 nuc (positive/negative) | 19/33 | 0.665 | 1.2 | 0.5-3.0 | | | |
| AC 28 cyto (positive/negative) | 26/26 | 0.444 | 1.4 | 0.6-3.3 | | | |

| | | | | |
|--------------------------------------|-------|-------|------|---------|
| AC 28 memb (positive/negative) | 2/50 | 0.303 | 0.05 | 0.0-33 |
| Clone 28 nuc (positive/negative) | 21/25 | 0.533 | 1.3 | 0.5-3.2 |
| Clone 28 cyto (positive/negative) | 24/22 | 0.961 | 1.0 | 0.4-2.3 |
| Clone 28 memb (positive/negative) | 24/21 | 0.781 | 0.9 | 0.4-2.1 |
| Lyn nuc (positive/negative) | 15/42 | 0.926 | 1.0 | 0.4-2.6 |
| Lyn cyto (positive/negative) | 23/34 | 0.956 | 1.0 | 0.5-2.3 |
| Lyn memb (positive/negative) | 3/54 | 0.893 | 1.1 | 0.2-8.5 |
| Lck nuc (positive/negative) | 26/65 | 0.577 | 0.8 | 0.4-1.7 |
| Lck cyto (positive/negative) | 40/51 | 0.650 | 0.9 | 0.4-1.7 |
| Lck memb (positive/negative) | 2/89 | 0.316 | 0.05 | 0.0-37 |

Table 3.33 gives an overview of survival analysis in ER negative patient cohort with all Src and SFK antibody used. Only significant association was with Y215Src cytoplasmic expression and was also independent on multivariate analysis. c-Src = total Src kinase, Y416Src = Src kinase phosphorylated at Tyrosine site 416, Y215Src = Src kinase phosphorylated at Tyrosine site Y215; AC 28= anti-Src family negative regulatory [pY] site, re-named in our laboratory as anti-Clone28, Src kinase phosphorylated at Tyrosine site 530 (inactive), Clone 28= dephosphorylated at Tyrosine site 530 (partially active); c-Src nuc = c-Src nuclear expression, c-Src cyto = c-Src cytoplasmic expression, c-Src memb = c-Src membrane expression, Y416Src nuc = Y416Src nuclear expression, Y416Src cyto = Y416Src cytoplasmic expression, Y416Src memb = Y416Src membrane expression, Y215Src nuc = Y215Src nuclear expression, Y215Src cyto = Y215Src cytoplasmic expression, Y215Src memb = Y215Src membrane expression; AC 28 nuc = anti-Clone 28 nuclear expression, AC 28 cyto = anti-Clone 28 cytoplasmic expression, AC 28 memb = anti-Clone 28 membrane expression; Clone 28 nuc = Clone 28 nuclear expression, Clone 28 cyto = Clone 28 cytoplasmic expression, Clone 28

memb = Clone 28 membrane expression; Lyn nuc = Lyn nuclear expression, Lyn cyto = Lyn cytoplasmic expression, Lyn memb = Lyn membrane expression; Lck nuc = Lck nuclear expression, Lck cyto = Lck cytoplasmic expression, Lck memb = Lck membrane expression. Significant results are highlighted in bold.

In contrast, it was nuclear Y215 Src kinase expression that was significantly associated with improved disease specific survival ($p=0.003$) (figure 3.24) in the patients with ER positive tumour and this was also independent on multivariate analysis ($p=0.009$, table 3.34) with a hazard ratio of 0.4 (IQR 0.2-0.8). No association was observed in the ER negative cohort ($p=0.345$) (figure 3.24).

Figure 3.24: Kaplan Meier Survival Curve for cytoplasmic Y215Src in ER negative patients compared to ER positive patients

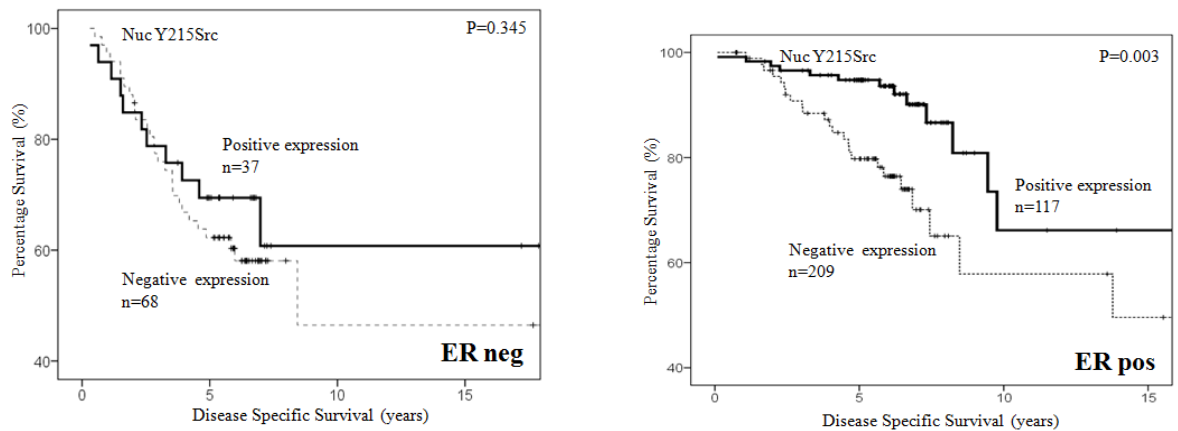


Figure 3.24: Kaplan Meier Survival Curves for nuclear Y215Src in ER negative patients and ER positive patients. ER positive patients with high nuclear Y215Src expression have a significantly better clinical outcome.

Table 3.34: Survival analysis in ER positive patient cohort with all Src and SFK members

| ER positive patients: | | | Univariate Analysis | | Multivariate analysis | | |
|-------------------------------------|-----------|------------------|---------------------|----------|-----------------------|-----|----------|
| | Numbers | P value | HR | IQR | P value | HR | IQR |
| Grade (G1/G2/G3) | 21/123/65 | 0.004 | 6.4 | 1.0-48.3 | | | |
| Size (<20,20-50, >50mm) | 91/108/10 | <0.001 | 22.0 | 7.4-69.6 | <0.001 | 7.0 | 5.3-54.8 |
| Lymph node (positive/negative) | 98/111 | 0.091 | 1.7 | 1.0-3.3 | | | |
| HER2 status (positive/negative) | 21/188 | 0.040 | 2.2 | 1.0-4.9 | | | |
| c-Src nuc (positive/negative) | 83/126 | 0.317 | 1.4 | 0.7-2.7 | | | |
| c-Src cyto (positive/negative) | 74/135 | 0.932 | 1.0 | 0.5-2.0 | | | |
| c-Src memb (positive/negative) | 77/132 | 0.176 | 1.6 | 0.8-3.2 | | | |
| Y419Src nuc (positive/negative) | 87/122 | 0.501 | 1.3 | 0.6-2.5 | | | |
| Y419Src cyto (positive/negative) | 85/124 | 0.288 | 1.4 | 0.7-2.9 | | | |
| Y419Src memb (positive/negative) | 87/122 | 0.099 | 1.7 | 0.9-3.3 | | | |
| Y215Src nuc (positive/negative) | 117/92 | 0.003 | 0.4 | 0.2-0.7 | 0.009 | 0.4 | 0.2-0.8 |
| Y215Src cyto (positive/negative) | 104/105 | 0.051 | 0.5 | 0.3-1.0 | | | |
| Y215Src memb (positive/negative) | 10/199 | 0.693 | 0.7 | 0.1-4.9 | | | |
| AC 28 nuc (positive/negative) | 63/50 | 0.586 | 1.3 | 0.5-3.6 | | | |
| AC 28 cyto (positive/negative) | 67/46 | 0.178 | 2.0 | 0.7-6.3 | | | |
| AC 28 memb | 4/109 | 0.424 | 0.4 | 0.06-3.4 | | | |

| | | | | |
|---------------------|--------|-------|------|---------|
| (positive/negative) | | | | |
| Clone 28 nuc | 53/50 | 0.174 | 1.8 | 0.8-4.5 |
| (positive/negative) | | | | |
| Clone 28 cyto | 45/58 | 0.596 | 1.3 | 0.5-3.0 |
| (positive/negative) | | | | |
| Clone 28 memb | 54/49 | 0.629 | 0.8 | 0.3-1.9 |
| (positive/negative) | | | | |
| Lyn nuc | 52/71 | 0.797 | 0.9 | 0.4-2.2 |
| (positive/negative) | | | | |
| Lyn cyto | 36/87 | 0.420 | 1.6 | 0.5-4.7 |
| (positive/negative) | | | | |
| Lyn memb | 5/118 | 0.556 | 0.6 | 0.1-2.8 |
| (positive/negative) | | | | |
| Lck nuc | 85/87 | 0.570 | 1.2 | 0.6-2.5 |
| (positive/negative) | | | | |
| Lck cyto | 71/101 | 0.536 | 1.3 | 0.6-2.6 |
| (positive/negative) | | | | |
| Lck memb | 10/162 | 0.124 | 0.04 | 0.0-19 |
| (positive/negative) | | | | |

Table 3.34 gives an overview of survival analysis in ER positive patient cohort with all Src and SFK antibody used. Only significant association was with Y215Src cytoplasmic expression and was also independent on multivariate analysis. *c-Src* = total Src kinase, Y416Src = Src kinase phosphorylated at Tyrosine site 416, Y215Src = Src kinase phosphorylated at Tyrosine site Y215; AC 28= anti-Src family negative regulatory [pY] site, re-named in our laboratory as anti-Clone28, Src kinase phosphorylated at Tyrosine site 530 (inactive), Clone 28= dephosphorylated at Tyrosine site 530 (partially active); Significant results are highlighted in bold.

3.3.4.6 Relationship of Src kinase expression to disease specific survival in patients stratified by ER and HER2 status

When patients with ER/HER2 negative tumours were analysed (n=75), cytoplasmic Y215 Src kinase was yet again strongly associated with improved disease free survival (p=0.007) (figure 3.25) and this was again independent on multivariate analysis (p=0.040) with a hazard ratio of 0.3 (IQR 0.2-0.8) (table 3.35). This observation held when ER/PgR/HER2 negative tumours were analysed (n=69) (univariate analysis p=0.015, multivariate analysis p=0.021, table 3.35).

Figure 3.25: Kaplan Meier Survival Curve for cytoplasmic Y215Src in ER/HER2 negative patients.

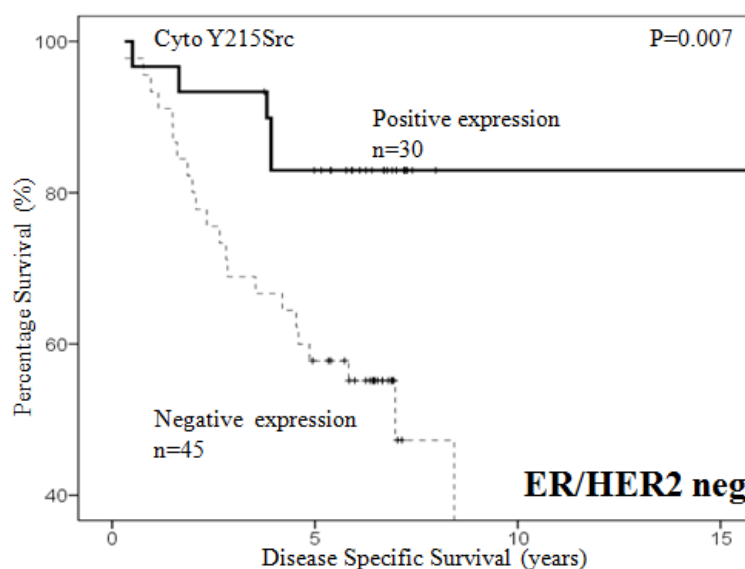


Figure 3.25: High cytoplasmic Y215Src is associated with better disease specific survival in ER/HER2 negative patients.

Table 3.35: Overview of the ER/HER2 negative patient and ER/PgR/HER2 negative patient subgroup and their survival analysis with Y215Src expression

| ER /HER2 negative patients: | | Univariate | | | Multivariate | | |
|---------------------------------------|---------|-------------------|-----|----------|---------------------|-----|----------|
| 75 patients | | Analysis | | | Analysis | | |
| | Numbers | P value | HR | IQR | P value | HR | IQR |
| Grade | 1/13/61 | 0.214 | 2.0 | 0.9-4.5 | | | |
| (G1/G2/G3) | | | | | | | |
| Size | 31/37/7 | <0.001 | 5.2 | 1.9-14.7 | 0.030 | 5.1 | 1.7-15.0 |
| (<20,20-50, >50mm) | | | | | | | |
| Lymph node | 35/40 | 0.021 | 2.4 | 1.1-5.4 | 0.005 | 3.3 | 1.4-7.5 |
| (positive/negative) | | | | | | | |
| Y215Src nuc | 22/53 | 0.590 | 1.3 | 0.5-3.0 | | | |
| (positive/negative) | | | | | | | |
| Y215Src cyto | 30/45 | 0.007 | 0.3 | 0.1-0.8 | 0.040 | 0.3 | 0.1-0.9 |
| (positive/negative) | | | | | | | |
| Y215Src memb | 3/72 | 0.771 | 1.3 | 0.2-10.1 | | | |
| (positive/negative) | | | | | | | |
| ER/PgR/HER2 negative patients: | | Univariate | | | Multivariate | | |
| 69 patients | | Analysis | | | Analysis | | |
| | Numbers | P value | HR | IQR | P value | HR | IQR |
| Y215Src nuc | 18/51 | 0.937 | | | | | |
| (positive/negative) | | | | | | | |
| Y215Src cyto | 25/44 | 0.015 | 0.3 | 0.2-0.7 | 0.021 | 0.2 | 0.1-0.9 |
| (positive/negative) | | | | | | | |
| Y215Src memb | 3/66 | 0.679 | | | | | |
| (positive/negative) | | | | | | | |

Table 3.35 shows an overview of the ER/HER2 negative patients' characteristics. Each clinical and pathological parameter was correlated to disease specific survival (p-values). Grade = Bloom and Richardson grade. Y215Src = Src kinase phosphorylated at Tyrosine site Y215; Y215Src nuc = Y215Src nuclear expression, Y215Src cyto = Y215Src cytoplasmic expression, Y215Src memb = Y215Src membrane expression. In the ER/HER2 negative and triple negative patient cohort Y215Src was significantly associated with improved disease specific survival, and this was also independent in multivariate analysis.

3.3.5 Ki67 expression and its association with Src kinase expression

Ki67 antigen MIB-1 (DAKO, UK) was used to determine proliferation status of the tumours. This antibody has been validated previously in our department and used in different studies (201). As before with other antibodies, nuclear Ki67 immunohistochemistry was obtained from 71% (194/274) of the TMA tumours of the initial patient cohort. This was due to tissue limitation through previous extensive section cutting.

Median Ki67 score was 3.8 (IQR: 0-9.8, table 3.36). Scores were classified into three groups (low-medium-high). 54% of the tumour specimens had a low proliferation rate, with a Ki67 score of <5, 30% had a medium proliferation rate of 5-20 and only 9% of the tumours had a high proliferation >20 (Table 3.37).

Table 3.36: Descriptive statistics for Ki67 expression in patient cohort

| Ki67 scores | Minimum | Maximum | Median | LQ | UQ |
|--------------------|---------|---------|--------|-----|-----|
| nuclear | 0.0 | 111 | 3.8 | 0.0 | 9.8 |

Table 3.36 provides an overview of descriptive statistics of Ki67 nuclear histoscores.

Table 3.37: Distribution of patients in each Ki67 subgroup

| Ki67 expression | Low (<5%) | Moderate (5-20%) | High (>20%) |
|------------------------|-----------|------------------|-------------|
| Patient No | 105 | 58 | 17 |

Table 3.37 Majority of breast cancers of this cohort had a low to moderate shows proliferation index

Histogram and IHC pictures below exhibit the different expression intensity of nuclear Ki67 (figure 3.26, pictures 3.8).

Figure 3.26: Histogram for Ki67 histoscores

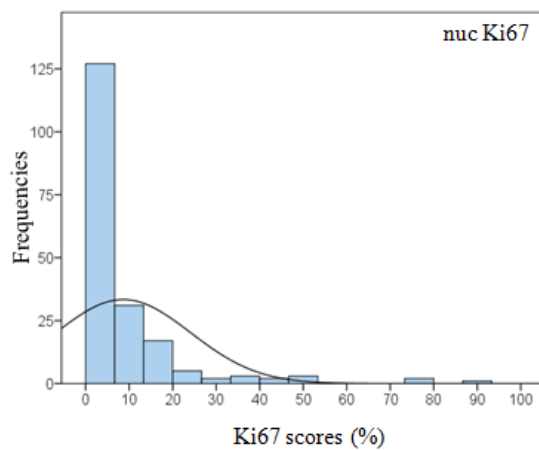
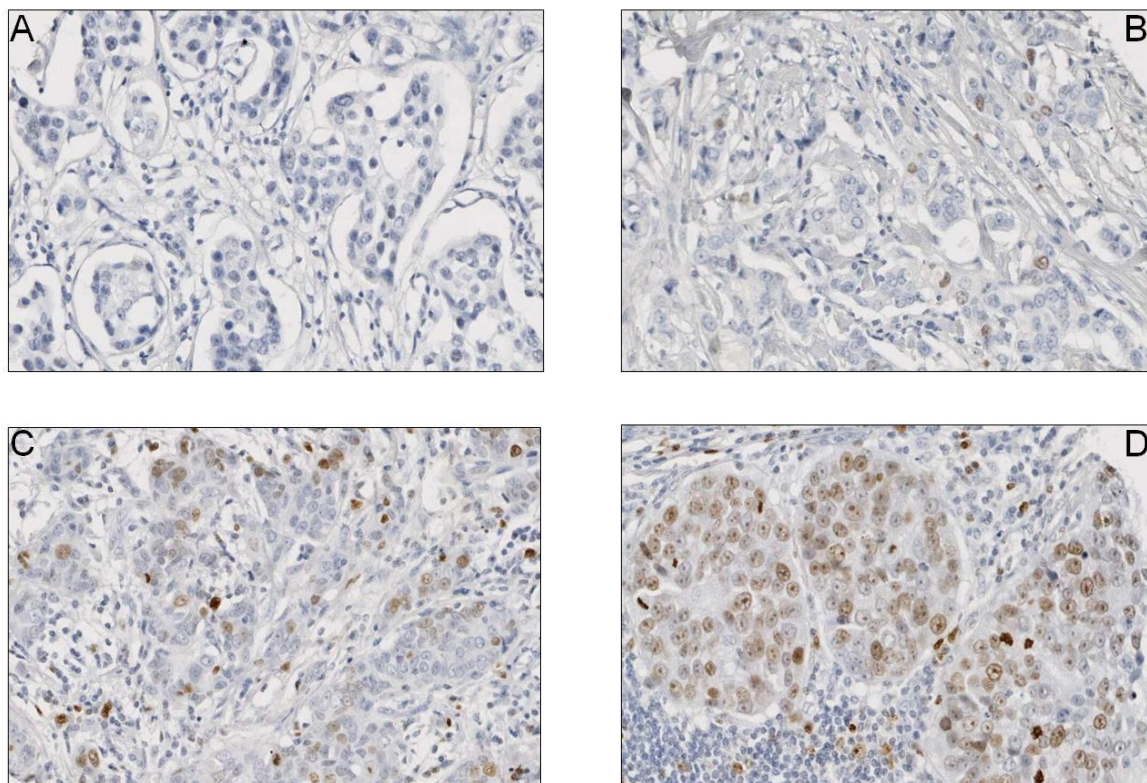


Figure 3.26 displays the staining intensity with Ki67 within the cohort

Picture 3.8: IHC staining with Ki67



Picture 3.8 shows Ki67 staining of invasive breast cancer specimens (1:150), **A**= negative staining of stroma and tumour tissue, **B**= Ki67 staining classed as weak staining, **C**= Ki67 staining classed as moderate staining, **D**= Ki67 staining classed as strong staining, magnification $\times 100$

On chi square analysis the only significant positive correlation between Ki67 scores and clinico-pathological characteristics of the cohort was with tumour grade (χ^2 $p=0.006$), nuclear c-Src (χ^2 $p=0.001$) and nuclear Y419Src (χ^2 $p=0.008$) (table 3.38).

On univariate analysis Ki67 score was not associated with disease specific survival ($p=0.254$, HR1.0 range 0.5-1.9) (figure 3.27).

Figure 3.27: Kaplan Meier survival curves for all three Ki67 subgroups

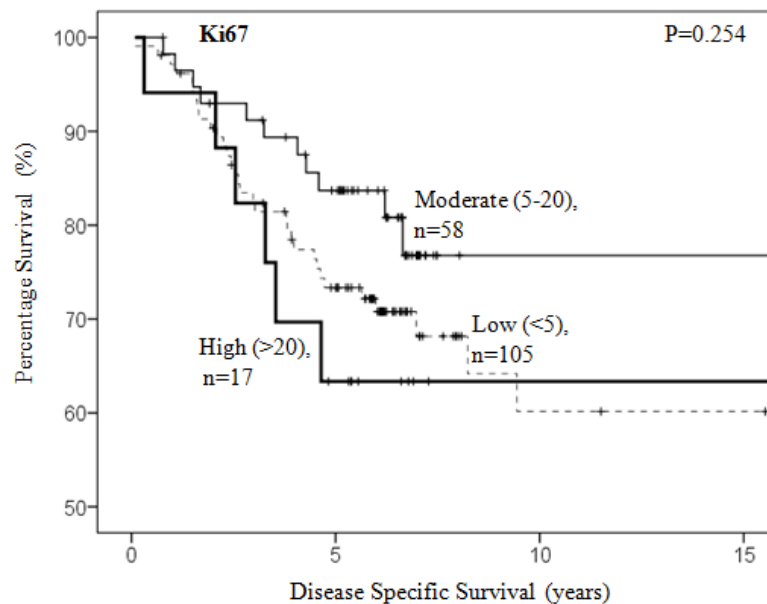


Figure 3.27 demonstrates no association with patients' disease specific survival and Ki67 expression ($p=0.254$).

Table 3.38: Correlations between Ki67, clinico-pathological features of the cohort and all Src and SFK expressions

| Total Patient Cohort:314 | | Pearson Chi-squared p-values | | | | | | | | | | | | | |
|---------------------------------|---------|-------------------------------------|--------------|--------|--------|--------|----------|----------|--------------|-------|-------|--------------|----------|----------|-------|
| Variables | Age | Tumour | Tumour | Tumour | LN | ER | PgR | HER2 | c-Src | c-Src | c-Src | Y416 | Y416 | Y416 | |
| (pos/neg) | | type | grade | size | status | status | status | status | nuc | cyto | memb | Src nuc | Src cyto | Src memb | |
| Ki67 nuc | 0.965 | 0.360 | 0.006 | 0.186 | 0.590 | 0.997 | 0.280 | 0.200 | 0.001 | 0.110 | 0.110 | 0.008 | 0.055 | 0.781 | |
| 180/194 | | | | | | | | | | | | | | | |
| Total Patient Cohort:314 | | Pearson Chi-squared p-values | | | | | | | | | | | | | |
| Variables | Y215 | Y215 | Y215 | AC 28 | AC 28 | AC 28 | Clone 28 | Clone 28 | Clone 28 | Lck | Lck | Lck | Lyn | Lyn | Lyn |
| (pos/neg) | Src nuc | Src cyto | Src memb | nuc | cyto | memb | nuc | cyto | memb | nuc | cyto | memb | nuc | cyto | memb |
| Ki67 nuc | 0.766 | 0.948 | 0.258 | 0.523 | 0.199 | 0.658 | 0.889 | 0.450 | 0.014 | 0.045 | 0.572 | 0.506 | 0.081 | 0.598 | 0.010 |
| 180/194 | | | | | | | | | | | | | | | |

Table 3.38 shows the interrelationship between Ki67scores, Src, phosphorylated Src sites, SFK members and clinico-pathological characteristics of patients with breast cancer.

3.4 Discussion

Histopathology continues to be a very important tool in the world of surgical oncology. Decisions regarding patients' treatments are founded on the appearance of cell and tissue morphology and its interpretation by the observer. A breast cancer patient's prognosis can currently alone be determined by grading and sizing of the tumour and lymphatic involvement (NPI). Immunohistochemistry has enhanced the spectrum and aspects of morphological appearances by providing additional information of the molecular constitution of the specimen. Hormonal adjuvant therapy is now being administrate based on a steroid receptor immunohistochemistry score. Human Epidermal Growth Factor Receptor analysis, in particular HER2 for breast cancer patients, has broadened treatment options by targeting and blocking this membrane-bound receptor, when overexpressed, with now commercially available antibodies; known as trastuzumab/ herceptin for HER2 and lapatinib/ Tykerb for HER1/HER2. To test for HER2 positivity/ overexpression of HER2, a hercept score of 3+ in IHC or 2+ in IHC and positive gene amplification in FISH is at present the standardised method/ recommendation worldwide (202). Breast cancer specimens should now undergo routinely an assessment of their steroid and HER2 receptors done to increase the amount of information available for clinicians to individualise therapies for the best possible outcome of their patients. It's been shown that ER and PgR positive patients have a higher risk of relapsing on tamoxifen therapy and increase benefit from a aromatase inhibitor (203). We also know that HER2 positivity is associated with increased mortality, a higher rate of disease recurrence and could predict resistance to certain systemic therapy (204).

Indirect immunohistochemistry is used widely to examine cell signalling processes in cancer using paraffin embedded tissue sections. Our laboratory has extensive experience in

optimising conditions for usage of primary antibodies in immunohistochemistry (205-207). Different techniques to achieve best antigen retrieval were trialled for each individual SFK antibody. We established that the procedure was best performed when the TMA slides were submerged in preheated buffer (Citrate or TE) at a certain pH (6.0-9.0) in pressure cooker placed in a microwave for 5 minutes (details in material and methods section). Different concentrations of horse serum were tested to avoid non-specific protein binding of individual primary antibodies. Accurate application time and concentration of the primary antibody is essential to accomplish not just true differential IHC staining, but also consistent and replicable immunostaining. Only c-Src, Lck and Ki67 were applied for 60 minutes at room temperature. All other antibodies were left overnight at 4 °C. Secondary antibodies were chosen depending on the species the primary antibody was raised (rabbit or mouse).

Compared to RT-PCR, this method allowed us to retrieve important information about the intensity and cellular location of the expressed protein. Thorough evaluation was performed of each cellular (nuclear, cytoplasmic, membrane and peri-nuclear) expression of every antibody. Significant results were seen when activated Src (pY419) was expressed at the membrane, the site of activation, whereas the majority of inactivated Src expression (anti-Clone 28) was observed in the nucleus and cytoplasm. Interestingly, partially activated Src (Clone 28) was found to a larger extent in the peri-nuclear region. It remains unclear if this hints an intention to be activated/ recruited.

It may seem that IHC scoring is a subjective method and would need a standardised approach for clinical routine medical practice to prevent inaccurate results leading to erroneous treatment decisions. Individual protein expression was assessed using the weighted histoscore technique, also known as H-score. This has been shown to be a robust,

reproducible scoring method to interpret immune-reactivities of signalling molecules. Protein expression is quantified objectively by means of continuous variable (199;200). Each tumour was assessed and scored respectively by two independent, histoscore trained observers. Quality and standard of inter-observer variation can be determined by inter class correlation coefficients (ICCC). It's defined as the variance between subjects relative to the sum of the variance components for subjects, observers and random error (199). ICCCs were calculated to ensure intra and inter-scorer consistency and reproducibility. ICCC scores above 0.8 are considered as excellent and certifying a sufficient data interpretation. Another way of visualising a validated range and distribution of histoscores is through Scattered (X and Y axis: Each axis representing each scorer's histoscores for a core) and Bland-Altman plots (X-axis: average between Histoscores of each scorer, Y: difference between scorer's Histoscore). These were presented in the material and method section for each individual antibody confirming appropriate scorer-observer correlation.

Due to small patient numbers in the PCR cohort (previous chapter), we transferred our interest towards a larger cohort to investigate the role of Src and Src kinase family members in breast cancer in formalin fixed paraffin embedded specimens (IHC cohort).

Clinical details of the IHC cohort were retrospectively collected by Dr Sylvia Brown during her investigations into the association of deprivation and breast cancer incidence between 1980s and 1990s in the area of Greater Glasgow (208). This cohort represents a large heterogenic group of patients from one geographical region with mature clinical follow-up. But because of the long duration of time, tissue specimens were collected by different individuals during these years, pathology laboratory fixation protocols were altered and even more aromatase inhibitors were commenced routinely in clinical practice. These inconsistencies could influence and alter results.

HE sections from each breast cancer specimen were examined by Consultant Pathologist Dr Elizabeth Mallon and marked for tissue microarray construction. Oestrogen-, progesterone- and HER2 receptor status (IHC and FISH) were the first investigations performed for each specimen to achieve a uniform database (209). Kaplan Meier Survival analyses were carried on all clinico-pathological patients' details to ensure the collected data of this cohort were validated (table 3.3). Initially 895 patients were identified and recruited through Dr. Brown's study. However, due to the retrospective collection of data only 314 patients/ tumour specimens were eligible for this project. For a rounder and more detailed interpretation of the protein expression results further data on recurrence of disease or even more particularized adjuvant treatment received by patients would have been of interest and we currently constructing retrospectively an expanded cohort with more detailed patient information.

It is known from the literature that certain fixation methods or/ and duration of fixation could affect quality of the specimen and variability of IHC staining results. Tissue microarray construction allows rapid tumour processing under standardised conditions and has been extensively validated in breast cancer. Up to 100-200 (0.6-2mm diameter) individual tumour cores can be placed into a single recipient block enabling simultaneous multiple tumour analysis and increase cost effectiveness by using less antibody. Three 0.6 mm cores from each block were taken to account for biological tumour heterogeneity. Each immunohistochemistry run included a positive and negative control to ensure no false positive staining. Full sections and normal breast tissue specimens were added to evaluate significant staining differences.

Initially we were able to analyse Src expression data of 314 patients. Over time and extensive section cutting of the tissue microarray, tissue/ cores vanished, resulting to an expression analysis of 48% of the original tumour with the Clone 28 antibody.

Src kinase has been investigated for a long time in a variety of solid tumours. Data from human cancer tissues have further defined the role of Src in tumour development in a more clinically relevant setting. Elevated levels of Src or SFKs have been detected in a range of human solid tumours, including glioblastoma (210), cancers of the prostate (90), breast (114), pancreas (211), and lung (212). Either overexpression or increased activity of Src is responsible for oncogenesis in different tumours. For example, in colon carcinoma lysates, Src activity was elevated compared with normal human colon mucosa cells, which appeared to be as a result of increased kinase signalling by Src, rather than increased protein levels (213;214).

This differs to breast cancer. *In vitro* evidence for a role for c-Src in breast cancer is convincing, but currently not supported by translational clinical studies. Elevated c-Src activity promotes cellular invasion and motility in Tamoxifen resistant breast cancer cells and provides a link between the HER family and steroid receptors (215). Other Src family members have also been linked with breast cancer. Microarray studies have demonstrated that Lyn is induced in models of endocrine resistance (216) and Lck is implicated in hypoxia induced breast cancer progression (159). Again, there is little published evidence on the role of other Src family members in clinical breast cancer specimens. Translational studies, investigating human breast tumour Src kinase expression and correlating expression and Src activation to clinical parameters including survival, are surprisingly limited. Only three *in vivo* studies have been published so far (114-116). Two of those clinical studies used immunohistochemistry (IHC) method to show that Src is associated with aggressive disease studies in breast cancer. Additionally, they noted that Src expression was higher in malignant tissue compared with normal tissue (114;116).

Elevated Src kinase activity has also been witnessed in metastatic disease. Compared with primary tumour tissue, Src activity is increased in metastatic tissue and in cells with a high metastatic potential (217;218). A study in colorectal cancer has demonstrated that

increasing Src expression and activity correlated with the progression of colorectal cancer from colonic polyps to primary lesions and liver metastases. With each step in disease progression, an increase in Src activity was seen. This was confirmed within individual patients by comparing Src activity in metastatic lesions with synchronous primary and metastatic tumour excisions at the same time (217).

Increased Src activity has been associated with poor prognosis in patients with colon carcinoma showed that when Src expression correlated with patient survival, Src activity was an independent indicator of poor prognosis at each stage of colon carcinoma. This suggests that measurement of Src activity may help in selecting patients most suitable for adjuvant therapy (219).

It's well known that advanced breast cancer has the tendency to develop bone metastasis. Araujo *et al.* described the role of Src in normal bone cells and bone remodelling in metastatic disease (108). Abnormal Src signalling may contribute to the increased osteoclastic activity associated with bone metastases. This implies that Src kinase inhibitors could not only be used for early stage high risk breast cancer to prevent metastatic spread, but also in the advanced or even palliative setting to limit growth of established metastasis sites and reduction of patients' symptoms.

This is currently the largest published study investigating the role of Src kinase expression and its different phosphorylation status in a cohort of clinical breast cancer specimens. Our study suggests that Src kinase expression and phosphorylation status may be employed as prognostic markers in breast cancer.

Increased cytoplasmic c-Src kinase expression is significantly associated with decreased disease specific survival. Most of the existing *in vitro* literature provides compelling evidence that c-Src activation is associated with high tumour proliferation, increased invasion and increased migration in breast cancer cells (65;220). This has been supported

by an *in vivo* study, carried out by Nigel Bundred's group, where Src kinase expression in ductal carcinoma in situ (DCIS) breast tumors correlated with HER2 positivity, high tumor grade, comedo necrosis and elevated epithelial proliferation. In addition, high c-Src levels were associated with lower recurrence free survival (115). The results obtained from our study are in keeping with cell line studies, too, demonstrating that c-Src is associated with more aggressive growth and poor clinical outcome. c-Src expression not only correlated with decreased survival, but also with increased tumor grade, ER negativity and HER positivity. In breast cancer, Src activity and distribution might impact on resistance to endocrine therapy in patients with oestrogen receptor/progesterone receptor (ER/PgR)-positive disease. A recent study of our group illustrated in a hundred per cent ER positive cohort that activated Src localised to the nucleus was significantly associated with improved overall survival and a lower recurrence rate during tamoxifen treatment of ER/PgR-positive tumours (221).

Parallel to this finding Src kinase was investigated in a cohort of castrate resistant prostate cancer and an increase in Src activity within tumour tissue with the development of hormone resistance was observed. Patients within this subpopulation had a significantly shorter overall survival than those with tumours that had a decrease or no change in Src activity (90), again, suggesting that increased Src activity may play a role in resistance to endocrine therapies in more than one type of cancer.

Although it is important to assess c-Src protein levels, it is of equal importance to determine the activation status of Src kinase. Ito *et al.* reported that high activated c-Src expression was frequently observed in breast tumors with lower aggressiveness as indicated by low Ki-67, absence of lymph node spread, small size and a low histological grade. This suggests that activation of Src is associated with early stages of breast carcinoma, but there was no correlation made with patient outcome measures (116).

However, Src activation in this study was determined using an antibody (Clone 28) to tyrosine site 530 and was classed as activated if un-phosphorylated at this site. Clone 28 is a marker for partial activation of c-Src, detecting dephosphorylated Y530Src at first protein configuration change before phosphorylation of Y419Src leading to full activation. It has previously been suggested, that a more appropriate biomarker for prediction of clinical response to Src kinase inhibitors would be to measure phosphorylation of the protein at a site associated with activity (213;222). Currently there are two sites within c-Src known to be associated with activation. Tyrosine site 419 (Y419Src) in human, is known as the classical site, which is most commonly utilised in cell line studies investigating the functional relevance of Src kinase activation (169). Src kinase when activated is moved to the membrane (65).

Indeed in our study, when Src kinase is activated at the classical site Y419 and located in the cellular membrane, it is associated with shorter disease specific survival, increasing grade, tumour size, ER negativity and HER2 positivity. Whilst our results with Y419 support the role of Src kinase activation, currently described in the literature.

The other site of activation is at tyrosine 215 (Y215Src). Stover *et al.* reported a 50-fold increase in activation of Src kinase associated with Y215Src phosphorylation (76). We obtained contradictory results with this alternative phosphorylation site.

Interestingly our study observes poor prognosis associated with membrane expression of phosphorylated Y419Src, but good prognosis with cytoplasmic expression of phosphorylated Y215Src. These results suggest that location and not only phosphorylation site influences downstream effectors of Src kinase.

Phosphorylation at Y215Src was strongly associated with improved survival (high nuclear and cytoplasmic Y215Src expression) and was demonstrated to be independent of other known clinical parameters on multivariate analysis (only seen with high cytoplasmic Y215

Src kinase expression). It is of note, that all significant associations between cytoplasmic Y215Src, c-Src and Y419Src were all negatively correlated.

It is unclear why Y416Src and Y215Src are associated with different outcome measures. These contrasting roles may be due to phosphorylation at Y215 and Y419 residing in different SH domains. Phosphorylation in different domains may result in varying protein configurations, which might enable activation of other downstream signalling pathways. An alternative explanation of these results may be that the antibodies detect phosphorylation of other Src kinase family members (e.g. Lyn, Lck, Yes) in addition or in preference to c-Src, as the phosphorylated regions are highly conserved (76).

Activated phosphorylated Y215Src kinase was independent in multivariate analysis (tumour grade, tumour size, axillary lymph node involvement, ER and HER2 status), providing evidence that Y215Src could be utilised as a prognostic marker to determine which subgroup of breast cancer patients should not be targeted with Src kinase inhibitors. Although Y215Src was independent on multivariate analysis, there was a positive association observed between cytoplasmic Y215Src kinase expression and HER2 status. These results support the observation that HER2 may phosphorylate Src kinase at Y215 (125). Vadlamudi *et al.* suggested that the interaction with HER2 would result in a more aggressive phenotype of cancer (125).

This is in direct contrast with results obtained in the current study. Further investigations, to determine the underlying molecular interactions between HER2 and Src kinase, are therefore warranted.

Approximately 10-15% of breast cancers fall into the receptor negative or triple negative group of breast cancers as defined by the absence of ER, PgR and HER2 receptors. This group of breast tumours are currently the focus of much attention because of their poor prognosis and the lack of an effective treatment target (72;223). *In vitro* studies, using gene expression profiling, have identified triple negative breast cancer tumours to be sensitive to

dasatinib, a non-receptor tyrosine kinase inhibitor. A reduction in cell proliferation was demonstrated (169). When we examined the ER, PgR and HER2 negative breast tumours as a representation of the triple negative group of breast tumours, we found that high cytoplasmic Y215 Src kinase expression resulted again in a significant survival advantage. With this in mind further investigations are urgently needed to determine what effect the Src inhibitor Dasatinib has on this phosphorylation site.

To conclude the assessment of the various phosphorylation sites we studied phosphorylated and dephosphorylated tyrosine site 530, using an antibody called anti-Src family negative regulatory antibody (anti-Clone 28) and Clone 28. These antibodies should represent c-Src in its inactive form and partially activated appearance. Clone 28 has been used in previous studies (116;224;225) to determine whether c-Src plays a role in colorectal, hepatocellular or mammary tumorigenesis. Intense staining was frequently observed in colonic adenomas and in well- and moderately differentiated hepatocellular carcinomas and colonic adenocarcinomas at an early stage, suggesting that expression of Clone 28 was linked to an early event in carcinogenesis in situ before invasive and metastatic elements manifest.

Therefore it is not surprising that none of the expression patterns of both antibodies were significantly associated with disease specific survival of mixed breast cancer patient cohort.

Anti-Clone 28 and Clone 28 were more or less equally expressed in the nucleus and cytoplasm. However, there was a noteworthy divergence of their expression at the cell membrane. Anti-Clone 28 was rarely detected in the membrane compared to Clone28. Clone 28 was mainly expressed in the membrane and perinuclear, which corresponds with features seen in Sakai's colonic tissue immunohistochemistry study (224).

Interestingly, cytoplasmic anti-Clone 28 and Clone28 correlated negatively with membrane c-Src expression (χ^2 $p=0.008$, χ^2 $p<0.001$), confirming the validity of the results regarding functional and cellular location e.g. cell membrane being site of Src activation.

Another negative correlation was observed between nuclear expression of anti-Clone 28 and ER status (χ^2 $p<0.001$), suggesting that ER negative breast cancer patients are more likely to express anti-Clone 28 in the nucleus, valued as the site of inactivation. In vitro experiments with c-Src showed that the oestradiol receptor can activate c-Src, proposing that c-Src is an initial and integral part of the signalling events mediated by the oestradiol receptor (120).

No significant associations were noted between Lyn protein expression, clinico-pathological features and survival. Other studies report that Lyn plays a part in developing chemo-resistance of colon cancer (134), progression of prostate tumours (226) and leukaemia (227). The latter is not surprising, since Lyn is associated as with a number of haematopoietic cell surface receptors, cytokine receptors and is a key mediator in several pathways of B cell activation (228). These observations are congruent with a role for Lyn associated with the development of chemo-resistance.

Our study does not utilise any hormone resistant, or chemo-resistant tumours; only operable tumours obtained at primary diagnosis. However, a recently published study elicit that Lyn was associated with shorter overall survival and that RNAi- knockdown of Lyn in breast cancer cell lines inhibited cell migration and invasion, but not proliferation (229). The same observation was made in ovarian cancer cell lines. Cell lines with high expression of Lyn were particularly sensitive to Dasatinib. Dasatinib inhibited invasion significantly, but caused less cell-cycle arrest suggesting Dasatinib should be used in combination with other systemic cytotoxic agents (230).

Surprisingly, Lck protein expression showed similar results like activated Src kinase expressed at tyrosine site 215. Membrane Lck was associated with improved disease specific survival in the IHC cohort and not associated with patient mortality. This was the reverse to the observation made with c-Src and activated Y419Src.

With the knowledge that phosphorylation antibodies are able to detect other Src kinase family members, hypothesis was stated that the Y216Src antibody used, could have identified Lck as the other SFK member associated with good clinical outcome. However, this observation with Lck membrane expression and good prognosis was only observed in a small number of patients and there was no significant correlation detected on chi square analysis between membrane Y215Src and membrane Lck expression. Therefore further analysis in a much larger cohort is required to verify these results.

Nevertheless, the positive findings are consistent with results reported by Rody *et al.* (231). Gene array analysis showed that Lck was associated with improved disease free survival within an ER positive and ER/ HER2 positive breast cancer subgroup. Though, this study proposed that the survival benefit associated with the Lck metagene was at least partly related to predicting response of certain breast cancer subgroups to chemotherapeutic treatment (231).

Since Lck is known to be involved in T-cell proliferation (149), it was hypothesised that expression of this gene was linked with the presence of lymphocyte infiltration within the tumour and interacting with it. Results of the current study demonstrated that Lck is expressed within the tumour, providing evidence that Lck itself may be involved with signal transduction in the tumour. Other studies suggest that Syk, a member of another non-receptor tyrosine family, is involved in hypoxia driven tumour progression via cross-talk to Lck in the nucleus (159).

Lck has been implicated in the mitochondrial apoptosis pathway by controlling the expression of pro-apoptotic factor Bak (151). Cell line experiments have shown that a Lck

deficiency resulted in resistance to anticancer drugs induced apoptosis. T-lymphoma cells lacking Lck have shown marked resistance to apoptosis reduction upon ionizing radiation (232). A more recent study from the same group adjusted their previous findings that not just the lack of Lck caused pronounced apoptosis resistance in response to stimuli of the intrinsic pathway; the additional loss of Bak was responsible for reduced sensitivity (233). Decreased levels of other pro-apoptotic Bcl-2 family members, e.g. Bax, have been shown to correspond to shorter survival in women with metastatic breast cancer. However, as yet no significant correlation between Bak and clinical outcome has been seen within breast cancer (234).

Correlations between Ki67 proliferation index, clinical parameters, c-Src, activated Src kinase and other Src kinase family members, were also analysed. Varied evidence exists for the association of Ki67 score and other prognostic variables. Some studies show no significant association, whereas other report links with patient age, grade, lymph node status, tumour size, ER, PgR and EGFR status (235). Some associations with survival have also been seen (236). To measure cell proliferation objectively is difficult and there are a number of limitations to Ki67 scoring. First of all there is no formal agreement on the scoring method. Secondly it doesn't account for tumour heterogeneity. In order to address these issues, each tumour was stained and scored each in triplicates as well as double scored to ensure reliability of the results.

The Bloom-Richardson method of grading takes into account tumour proliferation in terms of mitotic count. Not surprising that Ki67 score, a marker of proliferation, highly correlated with tumour grade of the breast cancer patients.

It could be argued that Ki67 should have also correlated with HER2 status. HER2 receptor when activated stimulates downstream signalling pathways promoting cellular proliferation. Therefore we would expect an increased proliferation rate in tumours with

HER2 over-expression. This observation wasn't made nor was there a correlation between ER and PgR status seen.

These results demonstrated that Ki67 is a good predictor of clinical prognostic variables within the ER positive patient subgroup, where cells are stimulated for proliferation by the normal expected pathways whereby oestrogen binds to the ER stimulating cell division. Ki67 score was not shown to predict patient outcome even within the ER positive group.

It is well established that Src kinase plays a fundamental part in controlling cell proliferation (237). Ki67 correlated highly with c-Src and activated Y419Src kinase expression in the nucleus. Increased proliferation could possibly confer the poorer survival associated with high expression of c-Src and activated Y419Src. However, no significant association was detected between Ki67 and disease specific survival.

With this all-round IHC study we demonstrated in a large mature cohort that the protein Src kinase and its activated forms are expressed in invasive breast cancer in every cellular compartment. We determined that not only protein activation, but also site of activation and cellular location play an important role in breast cancer survival outcome. Cytoplasmic c-Src and membrane Y419Src expression were associated with poor clinical outcome, whereas nuclear and cytoplasmic Y215Src expression was associated with longer disease specific survival. Only Y215Src kinase was independent on multivariate analysis and seemed promising as a potential biomarker. Inactive or partially active Src kinase expression had no association with survival at any cellular location, nor did SFK member Lyn. However, membrane Lck expression was significantly associated with improved disease specific survival. Ki67 expression revealed that Src kinase was higher expressed in patients with less differentiated, more aggressive tumours.

Evaluation of the consequences Src inhibitor may have on Src expression, its location and activation sites, is of importance to ensure none of these molecular bio-agents is used unsafely in the clinical setting.

CHAPTER 4

EFFECTS OF SRC INHIBITOR DASATINIB ON SRC KINASE FAMILY MEMBER EXPRESSION AND PHOSPHORYLATION STATUS IN BREAST CANCER CELL LINES

4.1 Introduction

The previous chapter elicits that clinical outcome of breast cancer patients was linked to protein expression of Src kinase family members. Elevated cytoplasmic c-Src and membrane Y419Src kinase expression was associated with shorter disease specific survival, whereas high cytoplasmic Y215Src and membrane Lck expression was associated with longer disease specific survival. These results highlight not only that over-expression of different activation sites can be associated with different clinical outcome, but also over-expression on different cellular locations could influence downstream effectors of Src kinase.

Additionally it was noticed that cytoplasmic Y215Src kinase expression had a potentiated effect on good prognosis in triple negative breast cancer subgroup.

With Src inhibitors being trialled clinically, there is a requirement to establish which phosphorylation site they target. If subsequent experimental data demonstrate Src kinase inhibitors target Y215, these drugs could be potentially harmful to the specific subgroup of patients, who express phosphorylation at this site. Caution should therefore be applied before these drugs are administered.

We therefore utilised four different breast cancer cell lines representing the breast cancer patients' subgroups (ER pos/HER2 neg, ER pos/HER2 pos, ER neg/HER2 neg, ER neg/HER2 pos) to investigate the effects of the Src kinase inhibitor Dasatinib on expression levels and cellular location of Src, activated Y419Src, activated Y215Src, Lck and activated Y861 FAK, a downstream effector of c-Src.

4.2 Methods

4.2.1 In-vitro studies

Materials used within this chapter are listed in appendix 3.

4.2.1.1 Culturing of breast cancer cell lines

MCF-7, MDAMB 231 and MDAMB453 (American Tissue Culture Collection (ATCC), European Tissue Culture Collection (ETCC), Sigma) and MCF-7HER2 (Rachel Schiff, USA) were the cell lines utilised in the current study. Compared to MCF-7 cell line, HER2 was transfected and upregulated, which is clearly demonstrated by Western blotting (figure 4.1).

Figure 4.1: Upregulated HER2 receptor in MCF-7 cell line

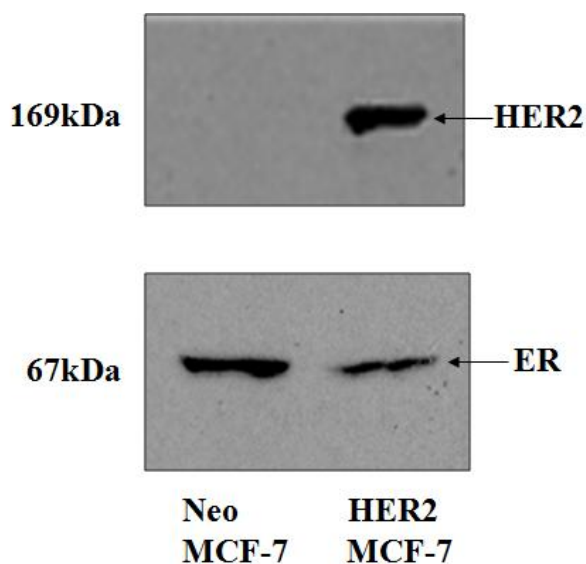


Figure 4.1 clearly demonstrates by Western Blotting an absent/low HER2 expression in MCF-7 cell line (left) compared to upregulated HER2 expression (right). This Western Blot was kindly provided by Jaclyn Long.

These four cell lines were chosen to represent each subgroup of breast cancer patients (ER positive/ HER2 negative, ER positive/ HER2 positive, ER negative/ HER2 negative and ER negative/ HER2 positive). Each cell line varies in different expression levels of the human epidermal growth factor receptor group (HER1-4) as listed in table 4.1.

Table 4.1: Breast cancer cell lines and their ER/HER2 status

| Cell line | ER status | HER1 status (EGFR) | HER2 status | HER3 status | HER4 status |
|-----------|-----------|-----------------------|--------------------------|-------------|-------------|
| MCF-7 | Positive | Negative | Negative (weak positive) | Positive | Negative |
| MCF-7HER2 | Positive | Negative | Positive (up-regulated) | Positive | Negative |
| MDAMB231 | Negative | Positive (weak) | Negative | Negative | Negative |
| MDAMB453 | Negative | Negative | Positive | Positive | Negative |

Table 4.1 displays all breast cancer cell lines used in this study and their oestrogen (ER) and human epidermal growth factor receptor (HER) status.

Cell lines MCF-7, MDAMB231 and MDAMB 453 were cultivated in Dulbecco's Modified Eagle Media (DMEM/FM) with additional heat-inactivated foetal calf serum (10%) (FS), 2mM L-glutamine (G) and penicillin/streptomycin (50units/ ml; 50 µg/ ml) (P/S) (details in appendix 3).

Cell line MCF7HER2 was cultivated in DMEM/HER2 containing 4500mg/L Glucose and additional heat-inactivated foetal calf serum (10%) (FS), penicillin/streptomycin (50units/ ml; 50 µg/ ml) (P/S) and insulin (10mg/ml). Cells were incubated in T-75 flasks (Fisher) at 37°C in 5% CO₂ atmosphere.

Cells were washed twice with warm Hank-Buffered Saline solution (HBBS) and incubated in serum- and phenol free medium (DMEM/SS) overnight before any drug treatment was applied.

4.2.1.2 Counting of Cells

Flasks were all seeded at 2×10^6 cells. Cells were trypsinised and neutralised with the equivalent amount of DMEM. The cell suspension was then transferred into a 50 ml centrifuge tube (Fisher) and centrifuged at 14000 rpm for 5 minutes. The supernatant was removed and the cell pellet resuspended in 1 ml of warm DMEM. 10 μ l were removed, added to 90 μ l of trypan blue (1:10 dilution) in an Eppendorf Cup and thoroughly mixed. A small amount of this mixture was applied onto a haemocytometer. Cells in all four large squares were counted under light microscopy (figure 4.2). The average of the cell count was then multiplied by hundred (1:10 trypan blue dilution).

Figure 4.2: Neubauer haemocytometer

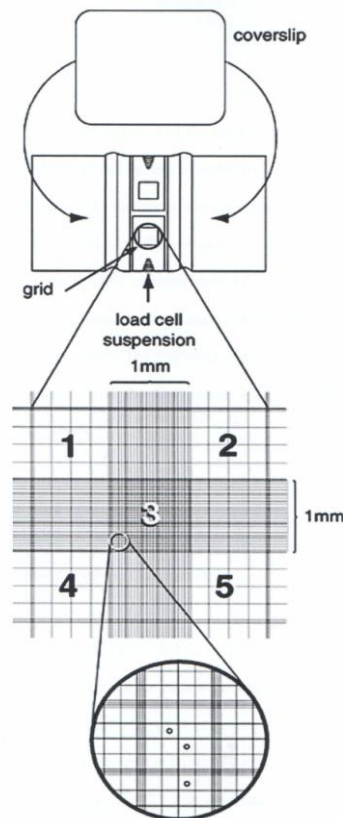


Figure 4.2 shows a Neubauer haemocytometer. Cell suspension is placed on top of the grid. A cover slip is laid above and the haemocytometer is positioned under the light microscope. The cells are then counted in each of the 4 corner squares (marked with 1, 2, 4 and 5).

4.2.2 Effect of steroid exposure and withdrawal on total Src kinase

This experiment was conducted on all four cell lines to determine the effect of exposure and withdrawal of oestrogen on Src kinase activity. To deprive the breast cancer cell lines of hormones, charcoal-stripped foetal calf serum was used, supplying all the necessary growth factors, but holding insignificant amounts of steroid concentrations. Two million cells were seeded into 10 ml of DMEM and grown in T-75 flasks at 37 °C in 5% CO₂ atmosphere. When the cells reached about 70% confluence, they were washed twice with warm HBBS before they were exposed to the different conditions. Each cell line was exposed to three different media in duplicates: DMEM containing 10% fetal calf serum (FM), serum free DMEM (SS) and steroid depleted DMEM containing 10% charcoal-stripped serum (CS) (details in appendix 3). After 48 hours exposure, cell lysates were prepared and Western Blots were performed as described below.

4.2.2.1 Cell lysis for Western Blotting

After incubation with designated drug treatment medium and exposure time, the solution was removed and cells were carefully washed twice with ice-cold HBBS. Immediately before application, the lysis buffer was diluted 1:10 and 1 mM of phenylmethanesulfonyl fluoride (PMSF), a serine protease inhibitor, was added. The prepared buffer was stored on ice at all times. 500 µl of buffer was added to each flask and incubated on ice. After 5 minutes, cells were scraped from the floor of the flask and removed. The cell lysate was transferred into a labelled 1.5 ml Eppendorf Cup. All samples were centrifuged at 14000 rpm for 15 minutes at 4 °C to separate the protein from cell debris. The protein containing supernatant is removed and stored at -70 °C. The experiment for each cell line was performed twice. Therefore, there were four samples of each cell line available for Western Blotting. Western Blots for total Src on all four cell lines was carried out as described in method section in chapter 3.

4.2.3 Quantification of SRC mRNA expression in cell lines

Materials used for cell line RT-PCR are listed in appendix 2

4.2.3.1 RNA isolation

Two flasks of each cell line were grown till they reached 70% confluence. 2 mls of TRIZOL[®] were added to each flask and incubated at room temperature for 5 minutes. 1 ml each was then pipetted into Eppendorf Cups and immediately frozen in -20°C. Total mRNA was extracted using the TRIZOL[®] method according to manufacturer's protocol. RNA quantity and quality was assessed by UV spectrometry (GeneQuant machine) and by examination of rRNA bands after agarose gel electrophoresis. Only samples, which showed both 18S band and a stronger expressed 28S band, were included in this study (figure 2.1).

4.2.3.2 cDNA synthesis

To guarantee no other DNA was present, DNA-free DNase treatment and removal reagent kit was added. Samples were incubated for 30 min at 37°C. To ensure the same amount of cDNA being used for quantification of mRNA, a starting concentration of 2000ng of tRNA was applied for each sample. Oligo (dt) primers (50ng) were used for First Strand cDNA Synthesis using SuperScript[™] II RT according to manufacturer's instructions. Before using cDNA for PCR amplification, 2 units of RNase H were added to samples and incubated for 20 minutes at 37°C. Quality of cDNA was assessed by using a PCR control run with human β -actin. Product bands were assessed by examination of agarose gel electrophoresis. Only samples, which showed equal product bands at 330 bp, were utilised (figure 2.2).

4.2.3.3 Quantification of mRNA

Real-time quantitative PCR was performed using an ABI Prism 7900 Sequence Detection System (Applied Biosystems, UK) and TaqMan® Gene Expression Assays (table 2.11, PCR chapter). For the TaqMan® Gene Expression Assays the manufacturer's protocol with recommended 40 rounds of amplification was applied. Thermal cycler condition were 50°C for 2 min, 95°C for 10 min followed by 40x 95°C for 15 sec and 60°C for 1 min. Product melting curve analysis and gel electrophoresis experiments were used to ensure that only one product of the expected size was amplified.

Negative controls (RNase/DNase free H₂O and negative RTPCR sample) for each primer were included on every 96 well PCR plate (Applied Biosystems, UK). Quantitative values were obtained from the threshold cycle (Ct value) at which the increase TaqMan® probe fluorescent signal associated with an exponential increase of each individual PCR product reaching a fixed threshold value. Each individual primer had a fixed threshold Ct value. These fixed threshold values were used for every cDNA sample (table 2.1).

As housekeeping gene, *HPRT* was used for evaluation of the different mRNA expression levels. Data were analysed as described in previous PCR chapter. All samples were measured in duplicates.

4.2.4 Stimulation and Inhibition of Src kinase, activated Src kinase, SFK members and downstream substrate Y861FAK

Prior to any drug treatment all flasks were washed twice with HBBS and exposed to serum free DMEM (SS) overnight.

4.2.4.1 Drugs

- Epidermal Growth Factor

Epidermal growth Factor (EGF) binds onto the Epidermal Growth Factor Receptor (HER1) causing its phosphorylation and activation of the growth factor receptor pathways. The cell line MDAMB 231, the only EGFR positive cell line, was stimulated with 10 nM EGF. This concentration was verified in previous studies performed in our group to be the most effective concentration. A stock solution of 1.6 μM was prepared and stored at $-20\text{ }^{\circ}\text{C}$ (details in appendix 3). Exposure time to EGF was 30 minutes.

- Heregulin α

Heregulin α (HRG), a ligand for HER3 or HER4, binds to the HER3 or HER4 receptor resulting in its phosphorylation to form homo- or heterodimers with each other or trigger activation downstream signalling pathways. Cell lines MCF7 and MCF7HER2 are HER3 positive and therefore treated with 10 nM HRG. As with EGF, this concentration was determined in previous studies. A stock solution of 1.42 μM was prepared and stored at $-20\text{ }^{\circ}\text{C}$ (details in appendix 3). Exposure time to HRG was 30 minutes.

- Dasatinib

Dasatinib (DASA), a small molecule ATP- competitive multikinase inhibitor, causes cell cycle arrest, blocks cell proliferation, induces apoptosis and inhibits metastasis. Dasatinib binds onto SH1 domain of Src and inhibits its kinase activity. Three cell lines were treated with 100 nM DASA. This concentration, used in previous prostate cancer cell line studies in our group, showed complete inhibition of phosphorylation and activation of Src and

downstream protein FAK (90). A stock solution of 10 mM was prepared and stored at -20 °C (details in appendix 3). Exposure time to DASA was 60 minutes.

4.2.4.2 Drug Treatments

This drug treatment experiment was only performed in duplicates on MCF7, MCF7HER2 and MDAMB 231 breast cancer cell lines due to absence of total Src kinase expression in the cell line MDAMB 453 on Western Blotting. This was repeated twice.

Two million cells were grown in T-75 flasks at 37 °C in 5% CO₂ atmosphere until they reached about 70% confluence.

Table 4.2: Overview of different drug treatments, exposure time and concentration

| Flasks | Flask No | Stimulation | Exposure Time & Drug Concentr. | Inhibition | Exposure Time & Drug Concentr. |
|-----------|----------|-------------|--------------------------------|------------|--------------------------------|
| Cell line | 1 & 2 | - | - | - | - |
| Cell line | 3 & 4 | - | - | DASA | 60 min & 100nM |
| Cell line | 5 & 6 | EGF/ HRG | 30 min & 10nM | - | - |
| Cell line | 7 & 8 | EGF/ HRG | 30 min & 10nM | DASA | 60 min & 100nM |

Table 4.2 displays the different prepared flask. Epidermal growth factor (EGF) or Heregulin (HRG) was used for stimulation depending on the cell line's receptor status. Dasatinib (DASA) was applied for inhibition of Src kinase. Flask 1 & 2 (untreated= UT) were used as control flasks.

After overnight incubation in serum free DMEM, the medium was removed and cells were washed twice with warm HBBS before 10 ml of correctly prepared media (table 4.2) were then applied. Cell lines were exposed to single or consecutive drug treatments: 10nM HRG or 10 nM EGF (Flask 5 & 6), 100 nM DASA (Flask 3 & 4) or a combination of both (Flask 7 & 8). To ensure experimental uniformity, each flask had to contain the same concentration of BSA/PBS (HRG drug preparation), Acetic acid/BSA/PBS (EGF drug

preparation) and DMSO (DASA drug preparation) (table 4.3). Flasks 1 & 2 were incubated in fresh 10 ml of serum free medium for 60 min including 2 ml of DASA and 200 μ l of HRG control.

Table 4.3: Overview of contents of each flask

| Flask No | Drug treatment and exposure time | DASA 1 nM | DASA control | HRG/EGF 1 μ M | HRG/EGF control | Serum free DMEM |
|----------|---|-----------|--------------|-------------------|-----------------|----------------------|
| 1 & 2 | UT (60 min) | - | 2 ml | - | 200 μ l | 17.8 ml |
| 3 & 4 | DASA 100 nM (60 min) | 2 ml | - | - | 200 μ l | 17.8 ml |
| 5 & 6 | EGF/ HRG 10nM (30 min) | | 2 ml | 200 μ l | - | 17.8 ml |
| 7 & 8 | EGF/ HRG 10 nM (30 min) and DASA 100 nM (60 min) | | | 200 μ l | | 19.8 ml 18 ml |

Table 4.3: Overview of the different composition of drug treatments and controls for individual flasks. Dasatinib treatment: 2 μ l of 10 mM stock concentration of dasatinib into 20 ml of serum free DMEM to achieve a concentration of 1 nM DASA. DASA control: 2 μ l of DMSO into 20 ml of serum free DMEM. Heregulin treatment: 422 μ l of HRG stock concentration was added to 176.4 μ l of serum free DMEM to achieve a concentration of 1 μ M HRG. HRG control: 0.1% BSA/PBS solution. EGF treatment: 378 μ l of EGF stock concentration was added to 228 μ l of serum free DMEM to achieve a concentration of 1 μ M of EGF. EGF control: 0.1% BSA/acetic acid plus PBS solution

4.2.4.3 Formation of Cell line Cell Pellets

After incubation with designated drug treatment medium and exposure time, the solution was removed and cells were carefully washed twice with warm HBBS. 3 ml of trypsin was added to the flasks and incubated for 5 minutes at 37 °C in 5% CO₂ atmosphere. To inactivated trypsin was neutralised with the equivalent amount of DMEM. The 6 ml suspension was pipetted gently up and down to dislodge all cells, subsequently transferred into a 15 ml centrifuge tube (Fisher) and centrifuged at 10000 rpm for 10 minutes. This was followed by the supernatant being discarded and the cell pellet re-suspended in 10 ml of DMEM. Each centrifuge tube was placed next on ice and after the experiment was completed transferred to the in-house pathology department for formalin fixation, imbedding in individual paraffin wax-block and cut in sections, placed on salinised glass slides, ready for immunohistochemistry staining. Each cell line experiment was repeated. Therefore 4 samples per cell line and drug treatment were available for analysis.

4.2.4.4 Clot Formation of Cell line Cell Pellets for Immunohistochemistry

10 ml of drug treated solution is transferred from the 15 ml centrifuge tube into 25 ml universal container (McQuilkin and Co) adding 15 ml of normal saline to wash the cells. The containers are placed in the centrifuge for 5 minutes at 1500 rpm. The supernatant is then carefully discarded leaving a cell button at the bottom of the universal container. 2-3 drops of fridge stored human plasma is put on top of the cell button, combined with the cell pellet using a plastic pipette (Alpha laboratories) and subsequently mixed by moderate shaking of the container. Afterwards 1-2 drops of thrombin working solution is applied, gently agitated to allow a clot to form. Then formalin is added slowly to avoid fragmentation of the clot. Fixation of the clot in formalin occurs overnight before being placed into a correctly labelled cell block cassette and taken to histopathology for imbedding in a paraffin wax block.

4.2.4.5 Immunohistochemistry on Cell line Cell Pellets

Indirect immunohistochemistry was performed with the following antibodies: c-Src, Y416Src, Y216Src, Lck and Y861FAK. Reagents, solutions and methods used are described in method section of chapter 3. The protocol for antibody Y416Src had to be slightly modified due to expression variation. This was most likely caused by Lot change of the product. An overview of the primary antibodies used is given in the table below.

Table 4.4: Overview of the primary antibodies used for cell pellet IHC staining

| Protein | Antibody | Antigen Retrieval | H ₂ O ₂ Conc. | Horse Serum Conc. | Antibody Dilutions | Incubation Time and Temp |
|-----------|------------------------|-----------------------|-------------------------------------|-------------------|--------------------|--------------------------|
| Total Src | Rabbit Cell Signalling | Citrate Buffer pH 6.0 | 3% | 1.5% | 1:200 | 60 min at room temp |
| Y416Src | Rabbit Cell Signalling | TE Buffer pH 9.0 | 3% | 5% | 1:50 | Overnight at 4°C |
| Y216Src | Rabbit Santa Cruz | Citrate Buffer pH 6.0 | 3.0% | 5% | 1:25 | Overnight at 4°C |
| Lck | Rabbit Cell Signalling | TE Buffer pH 8.0 | 3.0% | 5% | 1:50 | 60 min at room temp |
| Y861FAK | Rabbit Invitrogen | Citrate Buffer pH 6.0 | 3.0% | 5% | 1:300 | Overnight at 4°C |

Table 4.4 reveals details of the primary antibodies used to detect total Src, its activated forms (Y215, Y419), the SKF member protein Lck and activated downstream protein Y861FAK, a marker for Src activation. Further information is given regarding antibody source, antigen retrieval method, blocking reagent concentrations (H_2O_2 and Horse Serum), antibody dilutions, incubation time and temperature are all listed above. Citrate Buffer= 10mM Citrate buffer, TE Buffer= 1 mM EDTA, 5 mM Tris buffer at pH 8.0 and pH 9.0. Both solutions were preheated in the microwave for 13.5 min to a temperature of 96 °C before slides were pressure cooked for 5 min with a cool down period of 20 min.

Each IHC run had a negative and positive control, full section and tissue microarray control included to ensure no false positive or negative staining of the cell pellets.

4.2.4.6 Immunohistochemistry Cell Pellet Scoring

Each cell line cell pellet was scored according to the Histoscore-method, as already described in chapter 3. Protein expression was assessed at the nuclear, cytoplasmic and membrane location.

Conformity of the two observers' scoring was again assessed by calculating intra- (variation in individual scoring) and inter- (variation between the observers) class coefficients- as described in the previous chapter. Comparison of both JE and BE scores generated ICCC scores between 0.80-0.96, as shown below in table 4.5.

Table 4.5: ICCC scores for nuclear, cytoplasmic and membrane expression

| ICCC | Nuclear | Cytoplasm | Membrane |
|----------------|---------|-----------|----------|
| All antibodies | 0.95 | 0.80 | 0.96 |

Table 4.5: ICCC scores for all double-scores of nuclear, cytoplasmic and membrane protein expression. ICCC scores above 0.8 are considered as excellent

Cell line pellets were independently scored by two observers (BE and JE) for nuclear, cytoplasmic and membrane staining of total Src, Y416Src, Y216Src, SFK member Lck and

Y861FAK. A semi-quantitative weighted histoscore method was applied. Agreement between scores was measured using inter-class correlation coefficients.

ICCCs were performed to verify consistency between scorers. All nuclear, cytoplasmic and membrane double scores were analysed together, because of the small sample number. Scattered plots for these nuclear, cytoplasmic and membrane double-scores are displayed below. To confirm no bias between scorers was present Bland-Altman plots were constructed (figure 4.3).

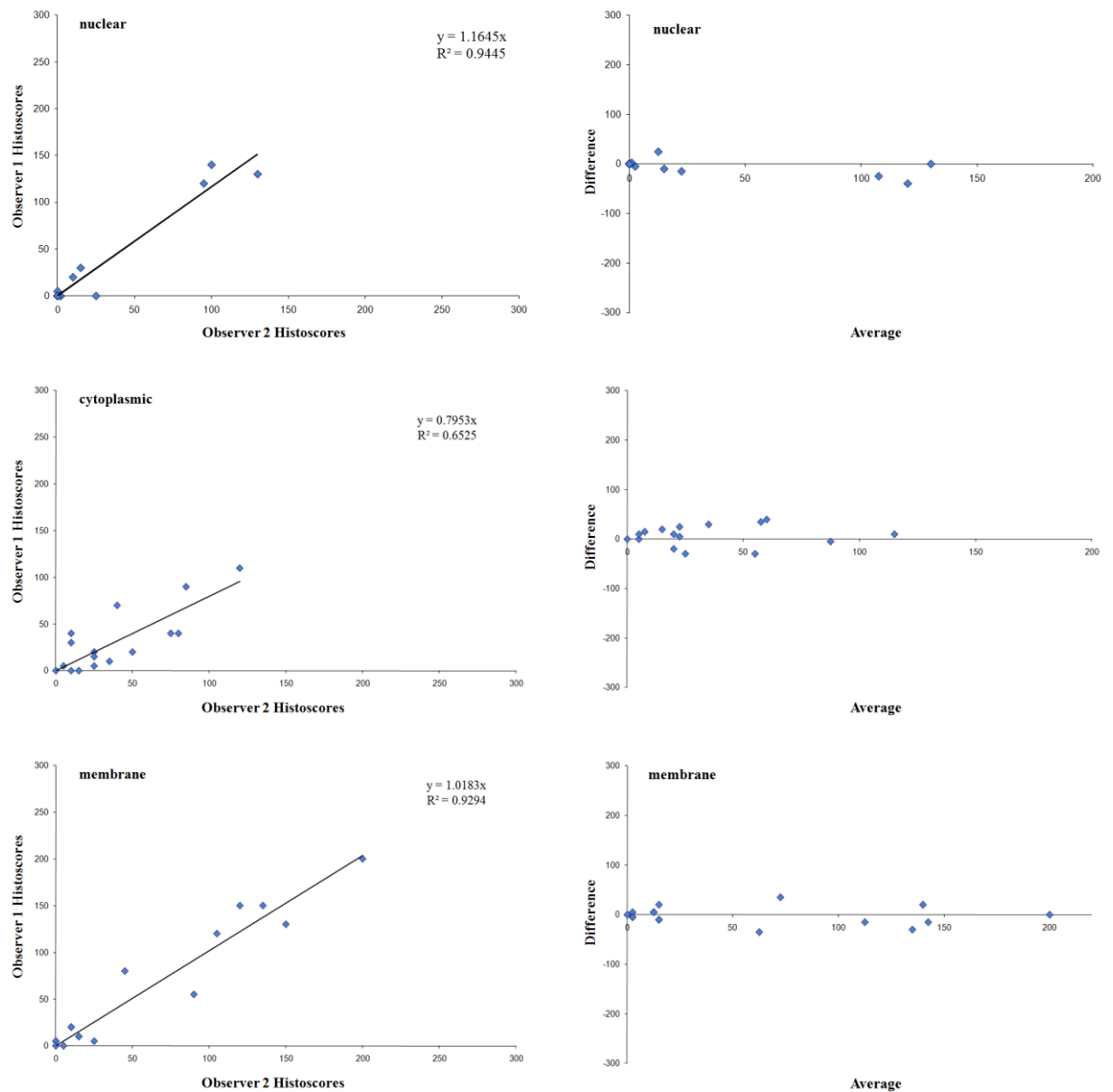
Figure 4.3: Scattered Plots and Bland-Altman Plots for cell pellet double-scores

Figure 4.3: Scattered plots and Bland-Altman plots for nuclear, cytoplasmic and membrane expression based on scorer-observer variation. The range and distribution of scores confirm appropriate scorer-observer correlation.

4.2.4.7 Statistical Analysis of Immunohistochemistry Staining

For statistical analysis the same statistical software package (SPSS 15.0 Inc., Chicago, IL, USA) was used as in chapter 3.

Basic descriptive statistics were performed to calculate frequencies, means, median and inter-quartile ranges for all the histoscores for each antibody. These values were then used to establish appropriate cut-off points to define with either low or expression of the protein. Correlations between expression of different proteins and a protein's expression level at a certain cellular compartment in different cell lines were evaluated with a general linear model via a univariate analysis using Post Hoc multiple comparisons for observed means. Equal variance was calculated with Dunnett's and Fisher's LSD test. Dunnett's test compares group means. Its goal is to identify groups whose means are significantly different from the mean of a reference group. It tests the null hypothesis that no group has its mean significantly different from the mean of the reference group. Fisher's LSD (Least Significant Difference) test was used to compare the mean of one group with the mean of another one. It is different to the Bonferroni and Dunnett methods. Fisher's LSD test does not account for multiple comparisons. It is basically a set of individual t-tests giving a more accurate value for the SD (significant difference).

4.3 Results

4.3.1 Expression of Src kinase after Steroid Exposure and Withdrawal in the breast cancer cell lines

Initially we investigated if Src kinase was expressed in all four breast cancer cell lines in order to conduct further inhibition and stimulation cell line experiments.

The following breast cancer cell lines

MCF7: ER positive/ HER2 negative

MCF7HER2: ER positive/ HER2 positive (upregulated)

MDAMB231: ER negative/ HER2 negative

MDAMB453: ER negative/ HER2 positive

were exposed for 48 hours to three different media with various steroid concentrations. This experiment highlighted that cell line MDAMB 453 did not express Src kinase in measurable concentrations (figure 4.4). The experiment was performed in duplicates. Western Blotting was repeated 4 times to verify this discovery. To strengthen this observation mRNA expression of *SRC* was measured in those cell lines. And again there was a marked difference between the ER negative/ HER2 positive (MDAMB453) cell line compared to the other three ($p= 0.031$, figure 4.5).

Because of these findings, experiments on this cell line were halted at this point.

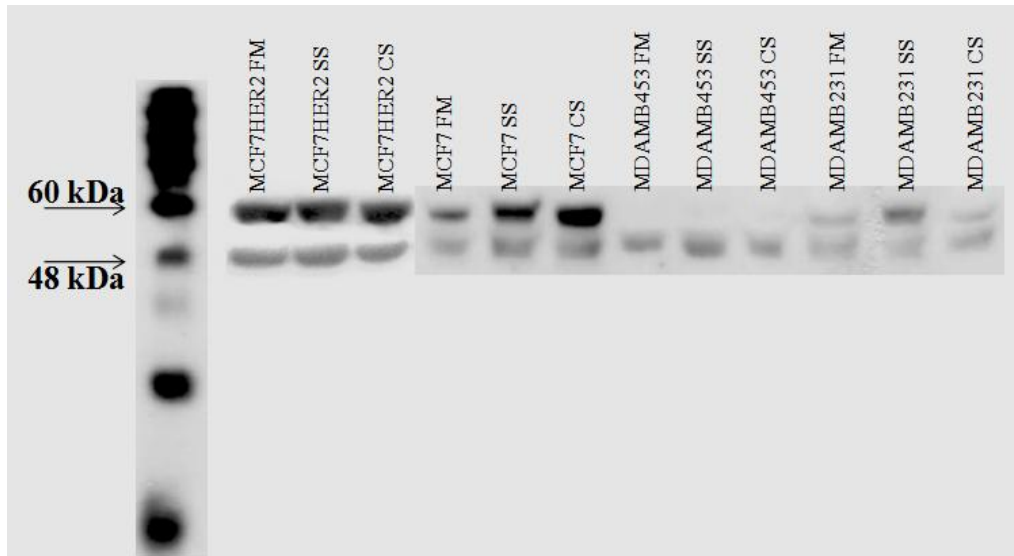
Figure 4.4: Western Blots for c-Src expression after steroid exposure and withdrawal

Figure 4.4: All four cell lines were exposed to various culture media; FM: medium containing full foetal calf serum, SS: serum starved medium, CS: steroid depleted, charcoal-stripped medium. Src kinase expression was examined by Western Blotting. c-Src is expressed at 60 kDa. β-tubulin was used as protein loading control (48 kDa). No expression of c-Src was detected in cell line MDAMB 453.

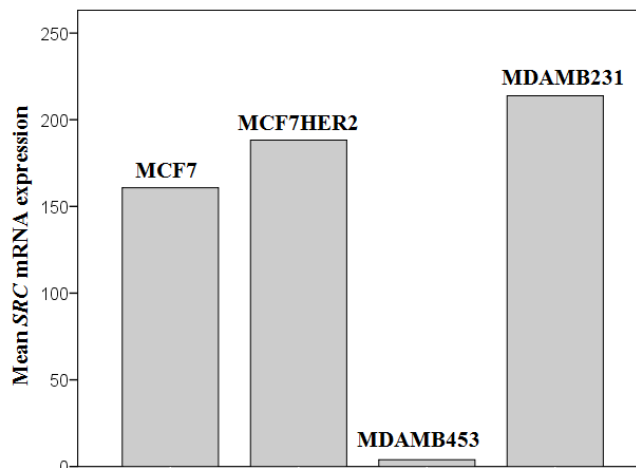
Figure 4.5: SRC mRNA expression in different cell lines

Figure 4.5 displays the mean mRNA expression of SRC in all four breast cancer cell lines (untreated, grown in full medium). There is a significant difference in Src expression between the cell line MDAMB453 and all others.

4.3.2 Drug stimulation and inhibition experiments in breast cancer cell lines

MDAMB231, MCF7 and MCF7HER2 cell line were used to examine the effect of EGF/Heregulin and Src kinase inhibitor Dasatinib on protein expression of c-Src, Y419Src, Y215Src, Y861FAK and Lck and their cellular location in cell pellets. The same antibodies employed in the previous IHC chapter were used in these experiments.

4.3.2.1 Differences in basal protein expression between cell lines in cell pellets

Firstly we wanted to compare expression profiles of each individual cell line when untreated to investigate if there is a basal difference on protein expression present.

c-Src expression

There was no nuclear c-Src expression observed in MDAMB231 and MCF7, but a slight increased expression in the HER2 upregulated MCF7 cell line (difference $p=0.005$, figure 4.6).

The lowest c-Src expression in the cell cytoplasm was seen in MCF7 cell line, followed by the ER neg/HER2 neg cell line (MDAMB231) with no statistical difference regards expression ($p=0.247$). Again MCF7HER2 cell line had the highest cytoplasmic c-Src expression with a statistical difference of $p<0.001$ (MCF7) and $p=0.003$ (MDAMB231) (figure 4.6, picture 4.1).

The highest membrane c-Src expression was noted in the ER negative (MDAMB231) (picture 4.1) compared to the ER positive cell line (MCF7) ($p=0.001$). MCF7HER2 had less c-Src expressed in the membrane compared to MDAMB231, with a significant difference of $p=0.004$. But there was no significant difference in expression between the ER positive cell lines ($p=0.549$) (figure 4.6)

Nuclear and cytoplasmic c-Src expression was highest in HER2 upregulated ER positive cell line, whereas membrane c-Src expression most elevated in the ER negative cell line.

Least c-Src expression at all cellular locations was observed in the ER positive/HER2 negative cell line (picture 4.1).

Figure 4.6: Differences in basal nuclear, cytoplasmic and membrane c-Src expression

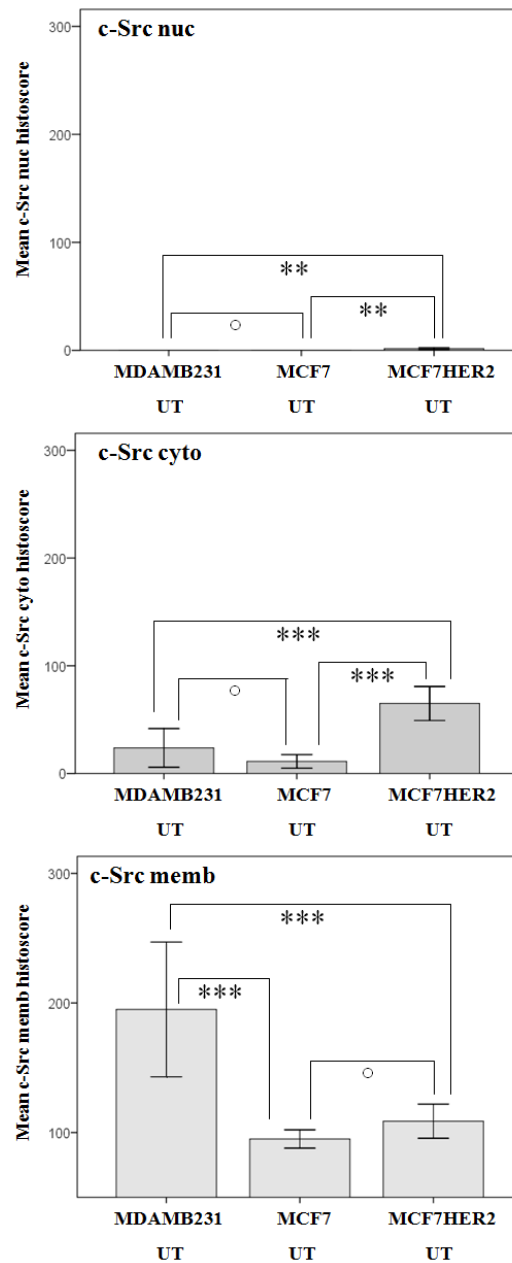
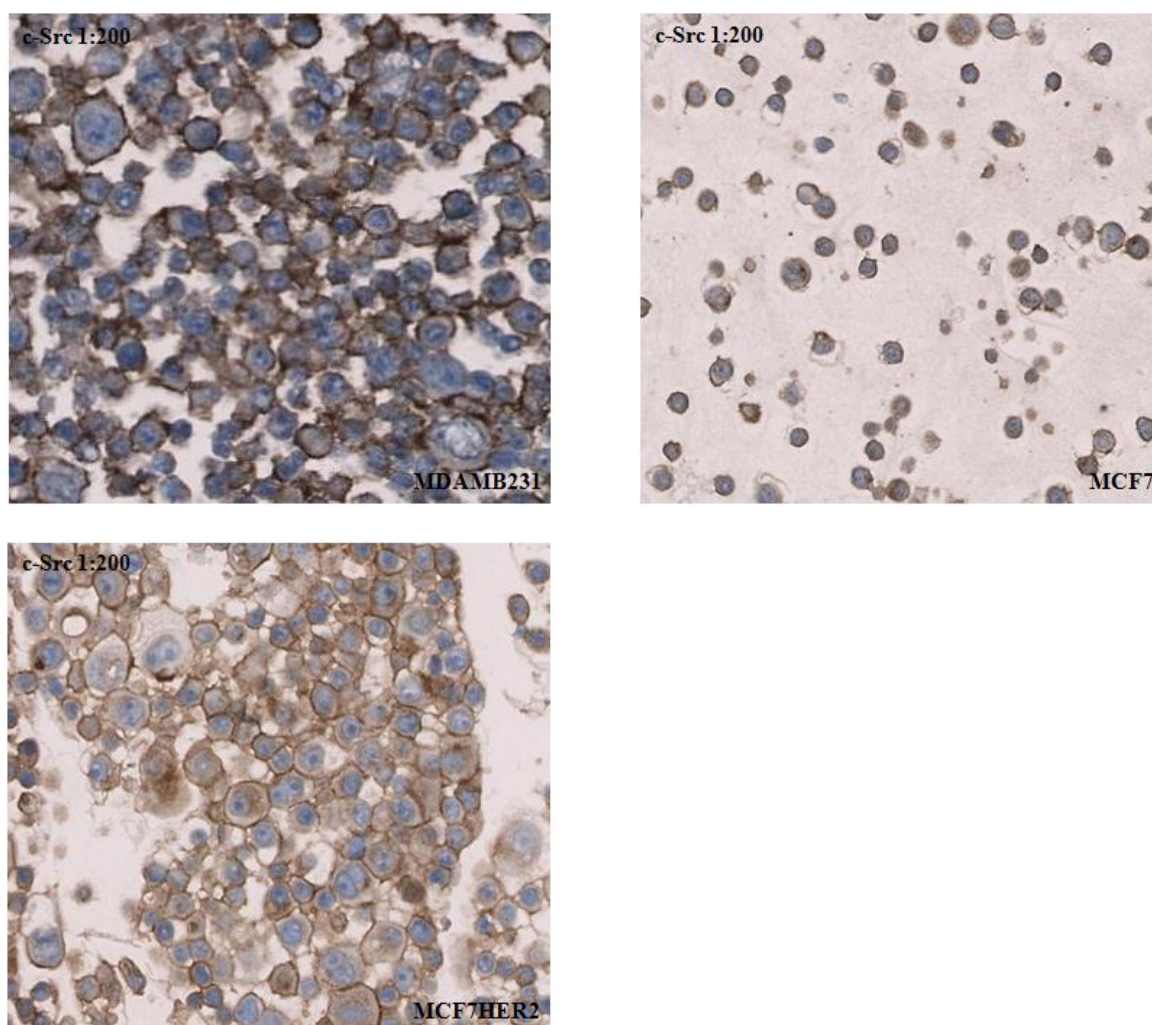


Figure 4.6: Nuclear, cytoplasmic and membrane c-Src expression in the ER negative/HER2 negative cell line MDAMB231, ER positive/HER2 negative cell line MCF7 and ER positive/ HER2 positive (upregulated) MCF7HER2 cell line. Each figure demonstrates protein expression differences between those cell lines when untreated; ° no significant statistical difference p value > 0.05 , * $p < 0.05$, ** $p < 0.01$, *** $p < 0.005$.

Picture 4.1: IHC staining with c-Src on untreated cell line cell pellets

Picture 4.1: IHC pictures from cell pellets of the cell line MDAMB231, MCF7 and MCF7HER2 stained with c-Src antibody (1:200, Cell Signalling); demonstrating the differences in staining intensity and distribution within the cells. Strongest membrane staining was seen in MDAMB231, strongest nuclear and cytoplasmic in MCF7HER2 and weakest IHC staining of all cellular locations in MCF7 cell line.

Y419Src expression

None of the three cell lines expressed Y419Src in the nucleus (Histoscore 0, $p=1.0$, picture 4.2).

Phosphorylated activated Y419Src was highest expressed in the cytoplasm in MDAMB231, followed by MCF7 and least in MCF7HER2 cell line. The only statistical significant expression difference was noticed between ER neg/HER2 neg and ER pos/HER2 pos cell lines ($p=0.007$, figure 4.7).

Activated membrane Y419Src was again highest expressed in the ER neg/HER2 neg cell line. This time MCF7HER2 exhibit a higher protein expression than MCF7, but without any statistical significance ($p=0.214$, figure 4.7). The only noteworthy result between membrane Y419Src expression involved cell line MDAMB231 and MCF7 ($p=0.014$, figure 4.7)

Figure 4.7: Differences in basal cytoplasmic and membrane Y419Src expression

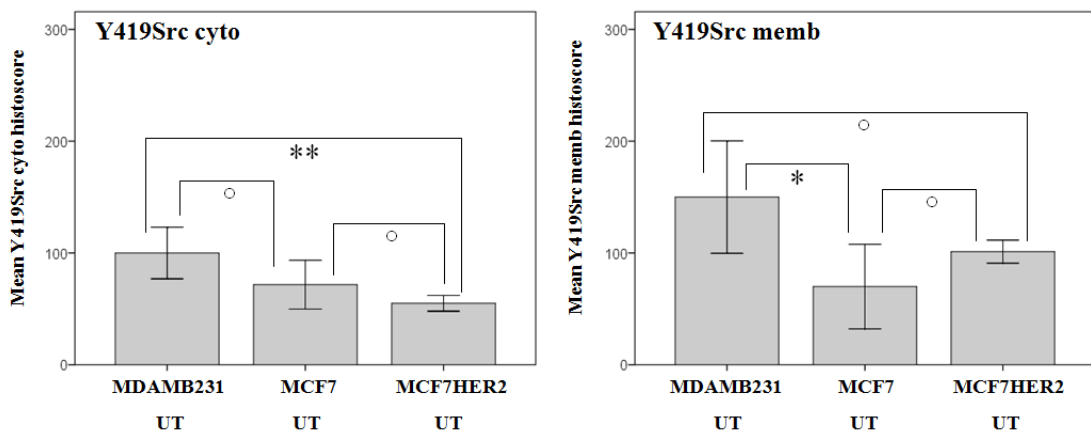
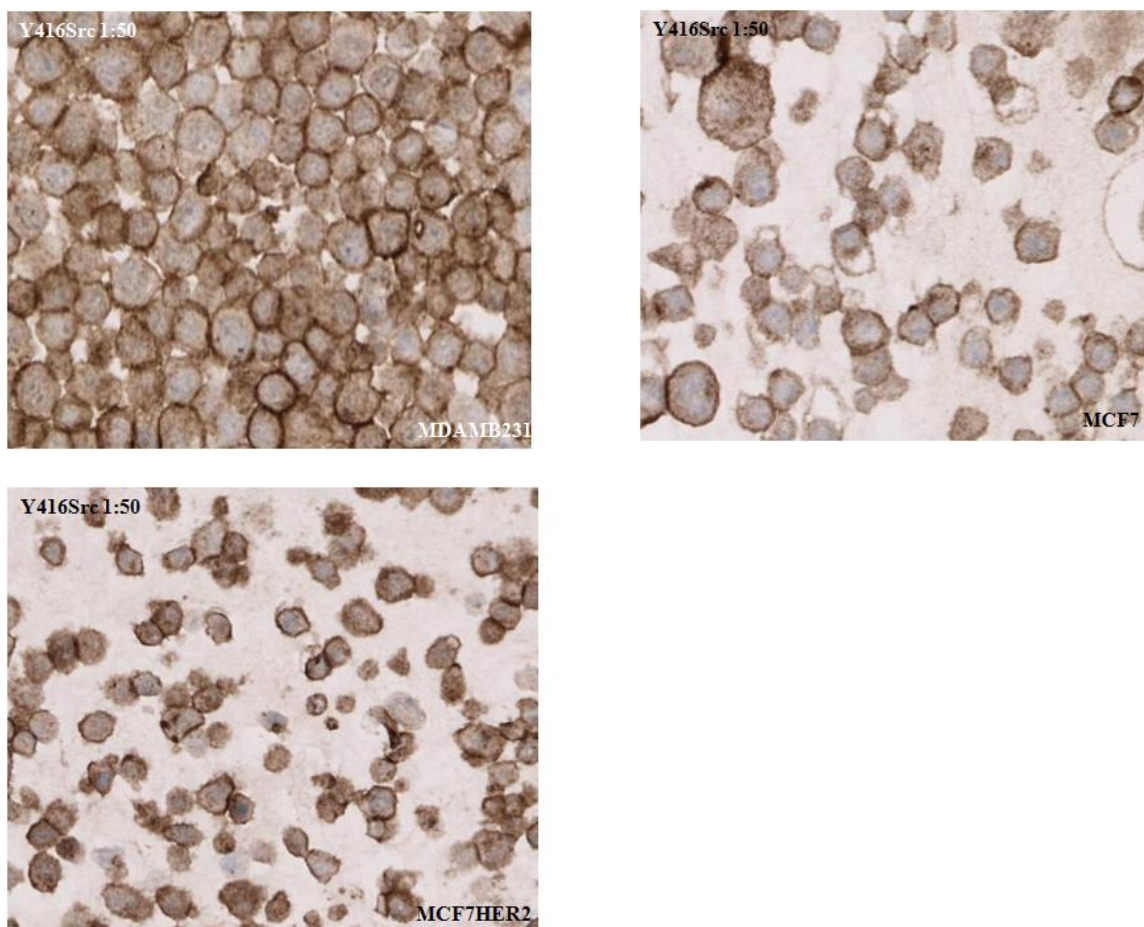


Figure 4.7: Cytoplasmic and membrane Y419Src expression in the ER negative/HER2 negative cell line MDAMB231, ER positive/HER2 negative cell line MCF7 and ER positive/ HER2 positive (upregulated) MCF7HER2 cell line. Each figure demonstrates Y419Src protein expression differences seen in cell pellets obtained of those cell lines at an untreated phase; ° no significant statistical difference p value > 0.05 , * $p < 0.05$, ** $p < 0.01$, *** $p < 0.005$.

Picture 4.2: IHC staining with Y416Src on untreated cell line cell pellets

Picture 4.2: IHC pictures from cell pellets of the cell line MDAMB231, MCF7 and MCF7/HER2 stained with Y416Src antibody (1:50, Cell Signalling); demonstrating the differences in staining intensity and distribution within the cells. Strongest cytoplasmic and membrane staining was seen in the ER neg/HER2 neg cell line (MDAMB231).

Y215Src expression

Phosphorylated activated Y215Src expression showed no statistical difference in basal expression between all three cell lines in the nucleus and cytoplasm (table 4.6). Nuclear and cytoplasmic Y215Src expression pattern was equal in MDAMB231 and MCF7HER2, with least Y215Src protein expression in MCF7 (figure 4.8).

However, membrane Y215Src expression showed a significant difference between ER negative to ER positive cell lines. MDAMB231 showed the least Y215Src membrane expression compared to MCF7HER2, which had the highest expression ($p=0.006$). There was no statistical difference in membrane expression between the two ER positive cell lines ($p=0.495$)

Table 4.6: Statistical overview of expression differences with Y215Src antibody

| Nuc Y215Src (p value) | MCF7 | MCFHER2 |
|-----------------------|-------|---------|
| MDAMB231 | 0.391 | 0.961 |
| MCF7HER2 | 0.298 | |
| Cytoplasmic Y215Src | MCF7 | MCFHER2 |
| MDAMB231 | 0.402 | 0.839 |
| MCF7HER2 | 0.520 | |

Table 4.6 demonstrates that there was no statistically significant difference ($p>0.05$) between nuclear and cytoplasmic Y215Src expression within the three cell lines.

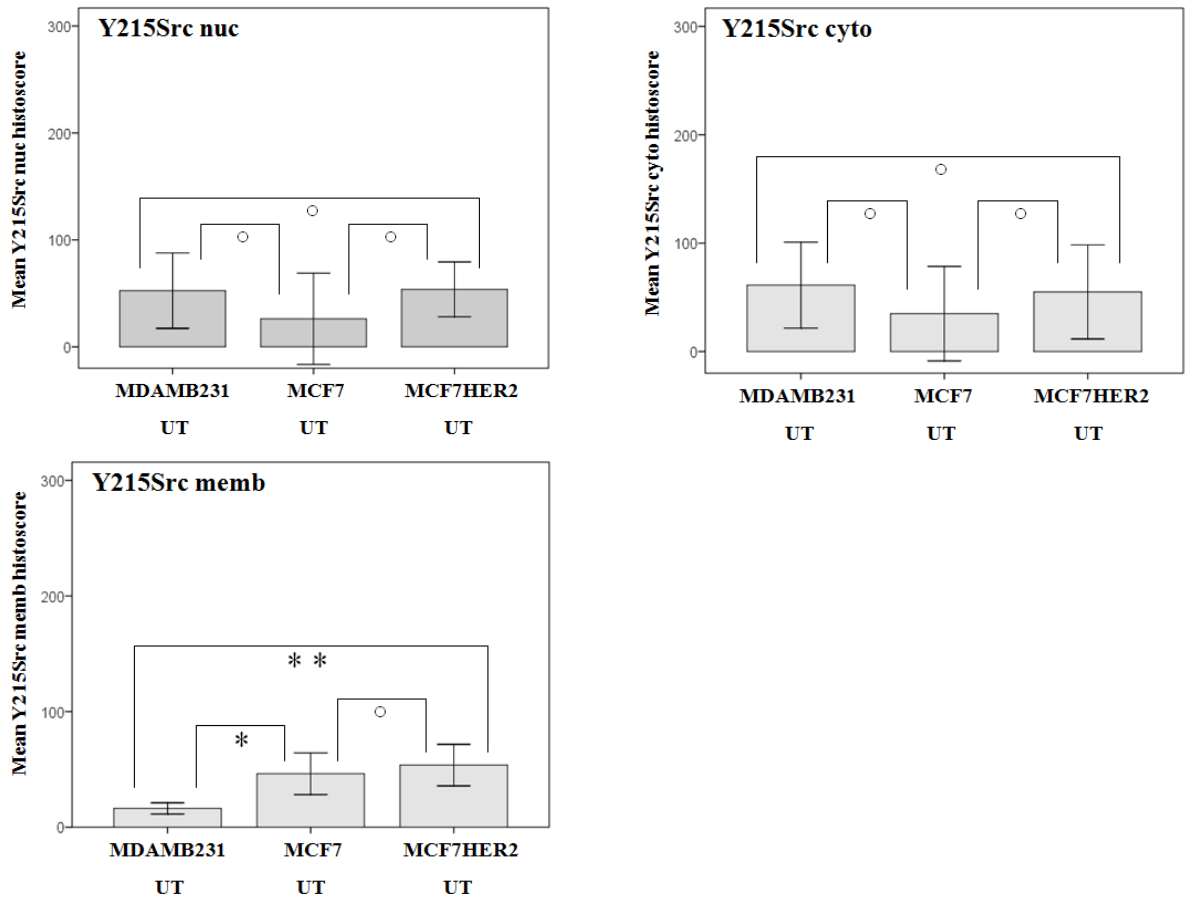
Figure 4.8: Basal Y215Src expression difference in cell line cell pellets

Figure 4.8: Nuclear, cytoplasmic and membrane Y215Src expression in the ER negative/HER2 negative cell line MDAMB231, ER positive/HER2 negative cell line MCF7 and ER positive/ HER2 positive (upregulated) MCF7HER2 cell line. Each figure demonstrates protein expression differences between those cell lines when untreated. Same nuclear and cytoplasmic expression pattern is noted between the cell lines. Whereas membrane Y215Src expression is lowest in the ER neg/HER2 neg cell line compared to ER positive cell lines. ° no significant statistical difference p value > 0.05 , * $p < 0.05$, ** $p < 0.01$, *** $p < 0.005$.

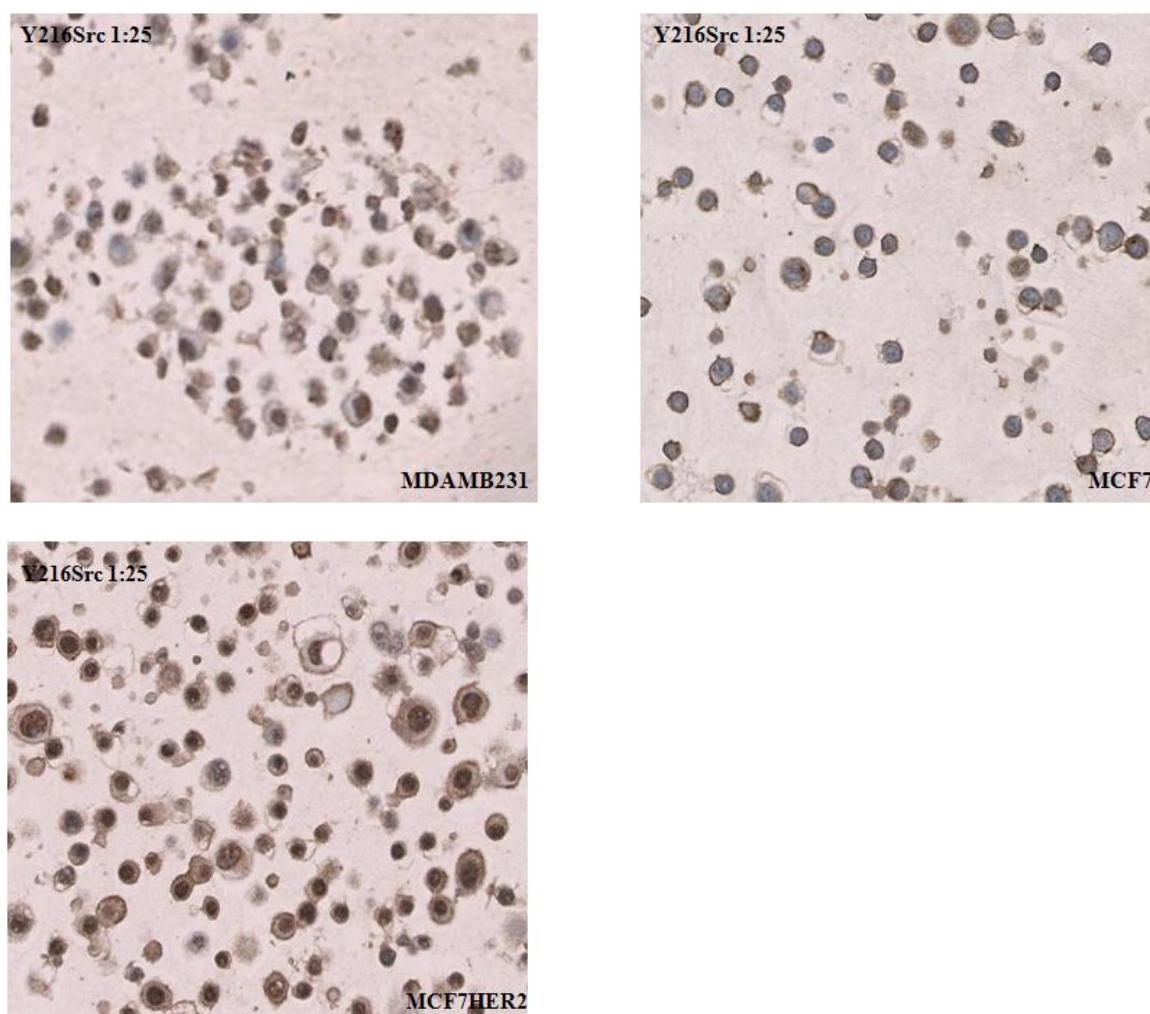
Picture 4.3: IHC staining with Y216Src antibody on untreated cell line cell pellets

Figure 4.3: IHC pictures from cell pellets of the cell line MDAMB231, MCF7 and MCF7HER2 stained with Y216Src antibody (1:25, Santa Cruz); demonstrating the differences in staining intensity and distribution within the cells. Strongest membrane staining was observed in the ER pos/HER2 upregulated cell line (MCF7HER2). There was no difference seen in Y215Src nuclear and cytoplasmic protein expression within those three cell lines.

Y861FAK expression

Nuclear activated Y861FAK protein expression was observed highest in the ER positive/HER2 positive cell line (MCF7HER2), followed by the ER negative/ HER2 negative (MDAMB231) and least detected in the MCF7 cell line. There was a statistically significant difference in expression noticed between MCF7HER2 and MDAMB231 ($p=0.003$) and between MCF7HER2 and MCF7 ($p<0.001$). No significant expression difference was present between MDAMB231 and MCF7 ($p=0.131$, figure 4.9).

Similar expression pattern between the cell lines was seen with cytoplasmic Y861FAK expression, although with lower histoscores. Highest cytoplasmic Y861FAK protein expression was found in MCF7HER2, followed by MDAMB231 and least detected in the MCF7 cell line. Statistically significant p-values were between MCF7HER2 and MDAMB231 ($p=0.001$) and between MCF7HER2 and MCF7 ($p<0.001$). No significant expression difference was again present between MDAMB231 and MCF7 cell line ($p=0.330$, figure 4.9).

IHC picture 4.4 clearly shows a significantly lower membrane Y861FAK expression in the ER neg/HER2 neg cell line compared to ER positive cell lines (MDAMB231/MCF7 $p=0.026$ and MDAMB231/MCF7HER2 $p<0.001$).

MCF7HER2 had the highest nuclear, cytoplasmic and membrane Y861FAK protein expression. ER negative cell line expresses activated membrane Y861FAK in a smaller amount than ER positive cell lines.

Figure 4.9: Differences in basal expression of nuclear, cytoplasmic and membrane Y861FAK on cell pellets

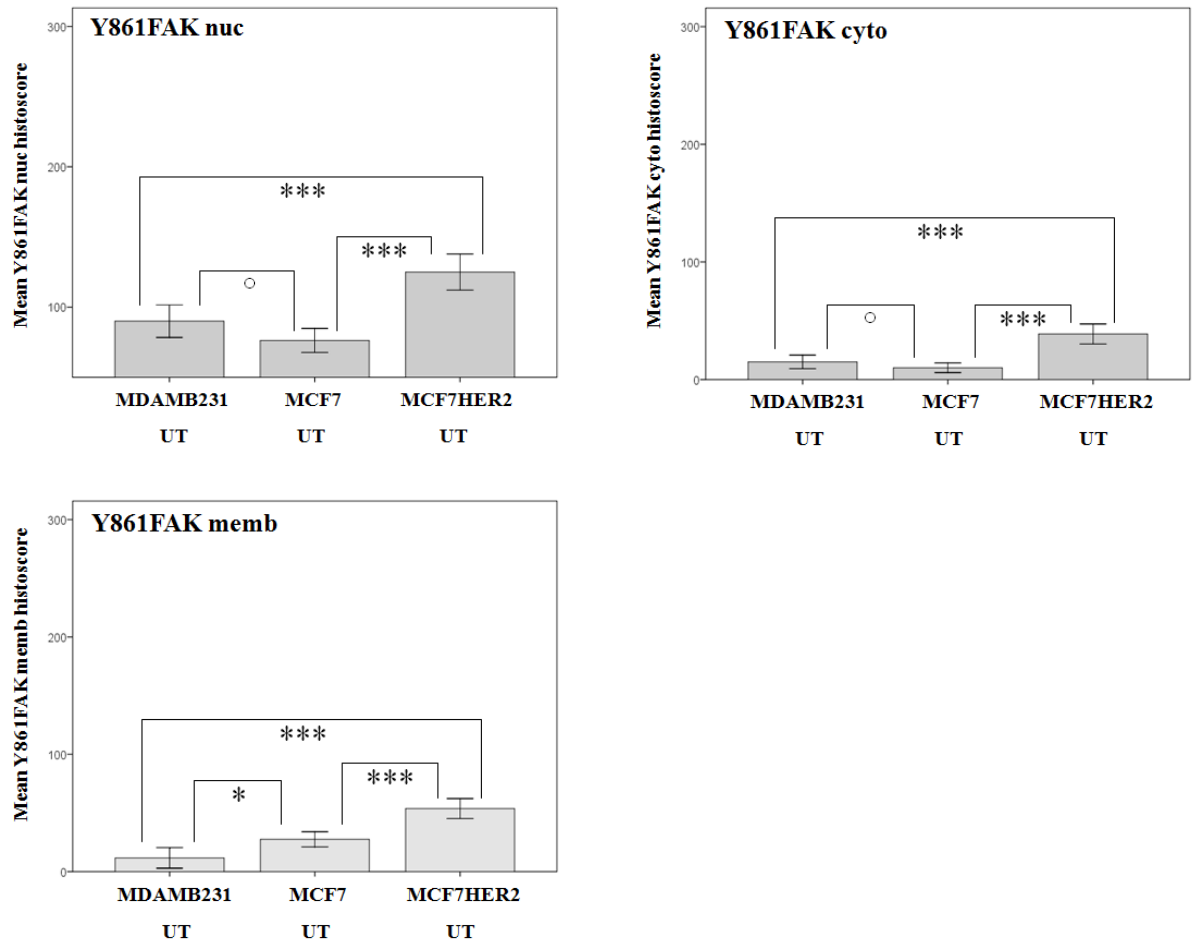
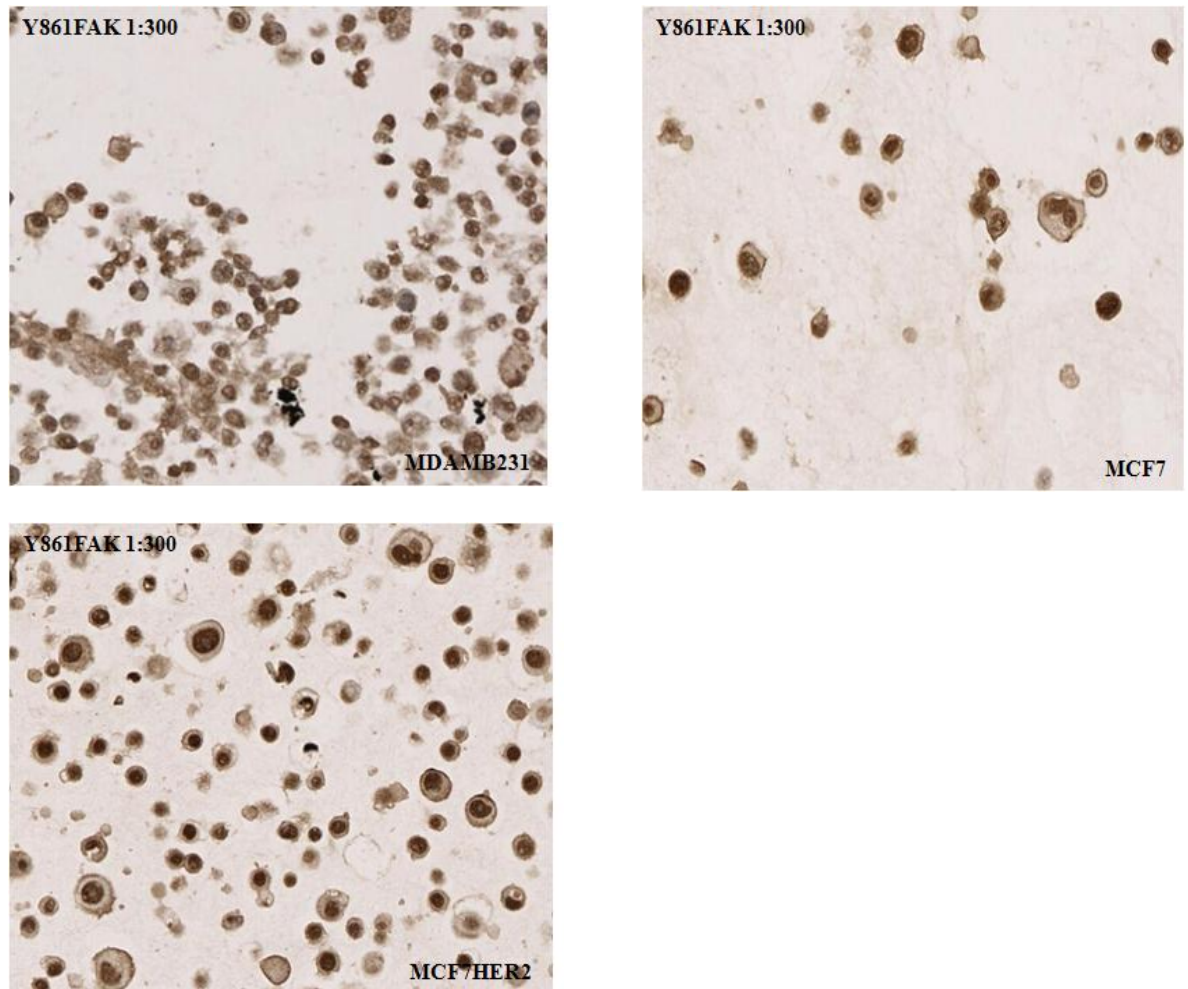


Figure 4.9: Nuclear, cytoplasmic and membrane Y861FAK expression in the ER negative/HER2 negative cell line MDAMB231, ER positive/HER2 negative cell line MCF7 and ER positive/HER2 positive (upregulated) MCF7HER2 cell line. Each figure exhibits protein expression differences between those cell lines. Same nuclear and cytoplasmic expression pattern is noted within the three cell lines. Whereas membrane Y861FAK expression is lowest in the ER neg/HER2 neg cell line compared to ER positive cell lines. ° no significant statistical difference p value > 0.05 , * $p < 0.05$, ** $p < 0.01$, *** $p < 0.005$.

Picture 4.4: IHC staining with Y861FAK on untreated cell line cell pellets

Picture 4.4: IHC pictures from cell pellets of the cell line MDAMB231, MCF7 and MCF7HER2 stained with Y861FAK antibody (1:300, Invitrogen); demonstrating the differences in staining intensity and distribution within the cells. Strongest nuclear, cytoplasmic and membrane staining was observed in the ER pos/HER2 upregulated cell line (MCF7HER2). Least membrane staining was present in the ER neg/HER2 neg cell line.

Lck expression

There was no nuclear, cytoplasmic or membrane Lck protein expression detected in MDAMB231 (ER neg/HER2 neg) and MCF7 (ER pos/HER2 neg) cell line (histoscores 0, figure 4.10).

However, there was a small amount of nuclear Lck expression evident in the HER2 upregulated ER positive cell line (MCF7HER2). A higher Lck protein expression was observed in the cytoplasm and membrane of the MCF7HER2 cells (figure 4.10, picture 4.5).

There was no statistical significant difference in nuclear and membrane protein expression within the three cell lines (table 4.7). The only significant differences were apparent in the cytoplasmic compartment between MCF7HER2 and the other cell lines (both $p=0.012$).

Table 4.7: Statistical overview of basal expression of Lck in untreated cell lines

| Nuclear Lck (p value) | MCF7 | MCFHER2 |
|-----------------------|--------------|--------------|
| MDAMB231 | 1.0 | 0.490 |
| MCF7HER2 | 0.490 | |
| Cytoplasmic Lck | MCF7 | MCFHER2 |
| MDAMB231 | 1.0 | 0.012 |
| MCF7HER2 | 0.012 | |
| Membrane Lck | MCF7 | MCFHER2 |
| MDAMB231 | 1.0 | 0.490 |
| MCF7HER2 | 0.490 | |

Table 4.7 demonstrates that there was no statistically significant difference ($p>0.05$) between nuclear and membrane Lck expression within the three cell lines. Only cytoplasmic Lck expression in MCF7HER2 cell line was significantly different to the other cell lines' protein expression.

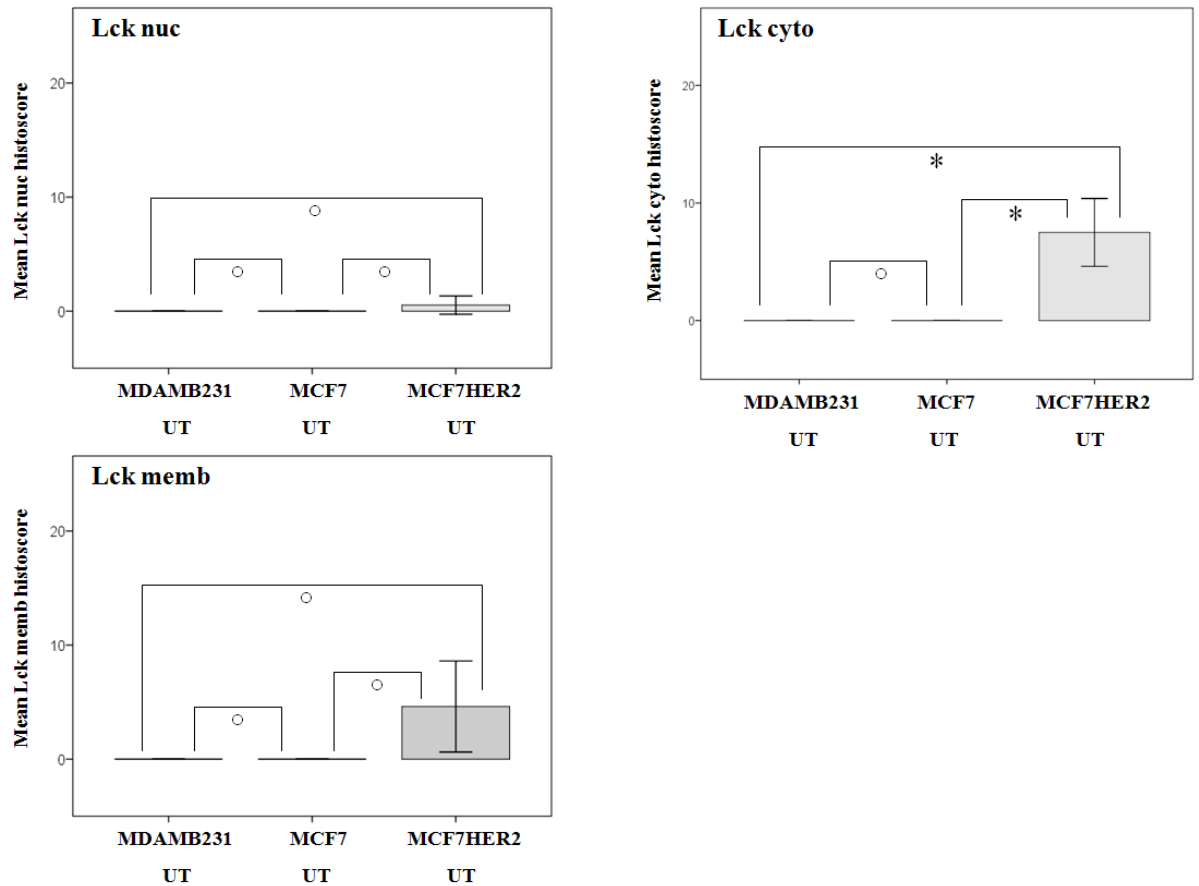
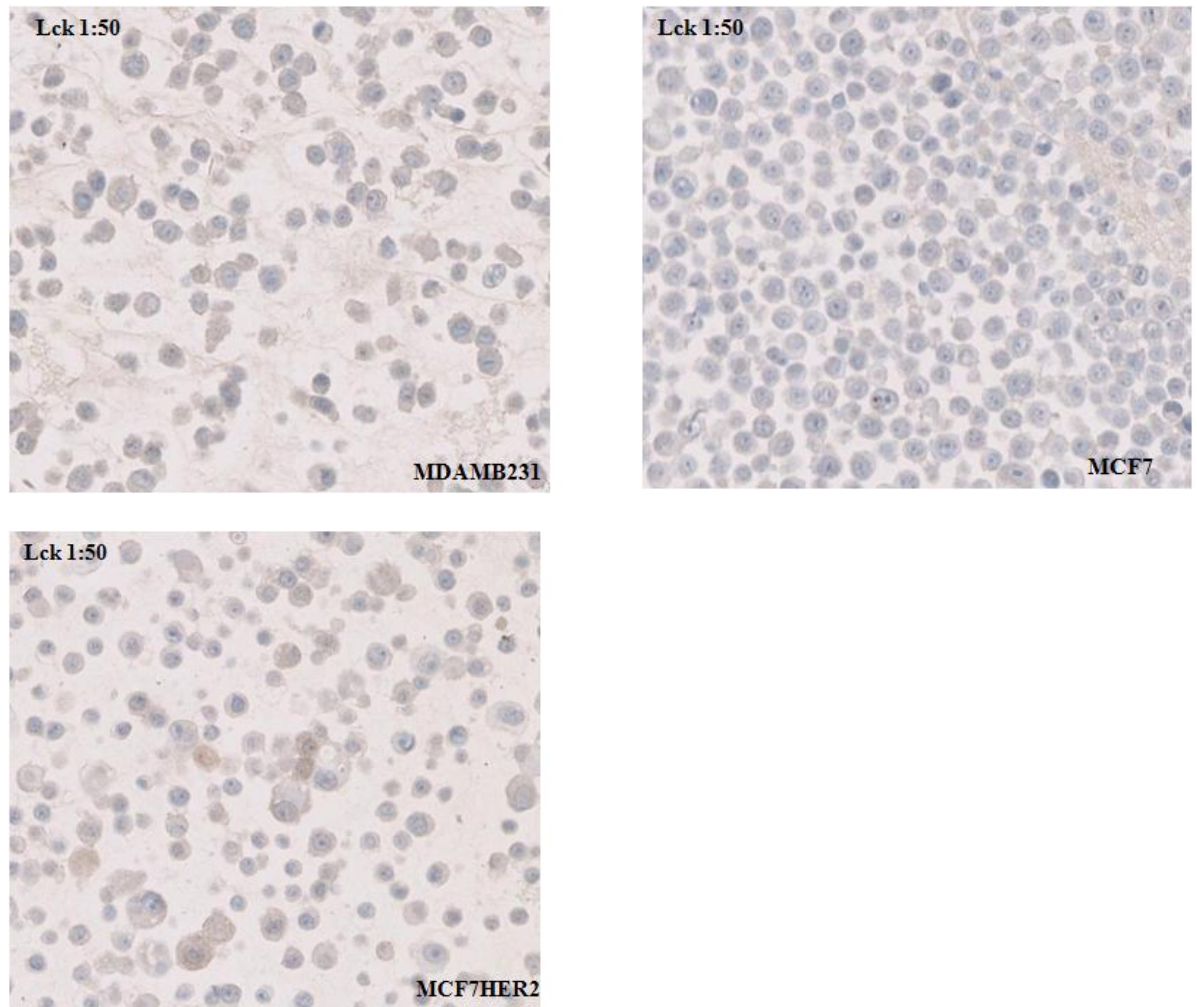
Figure 4.10: Nuclear, cytoplasmic and membrane basal Lck expression in cell lines

Figure 4.10: Nuclear, cytoplasmic and membrane Lck expression in the ER negative/HER2 negative cell line MDAMB231, ER positive/HER2 negative cell line MCF7 and ER positive/ HER2 positive (upregulated) MCF7HER2 cell line. There was no nuclear, cytoplasmic and membrane Lck expression detected in MDAMB231 and MCF7 cell line. The only significant expression difference was seen with MCF7HER2 in the cytoplasm; ° no significant statistical difference p value > 0.05 , * $p < 0.05$, ** $p < 0.01$, *** $p < 0.005$.

Picture 4.5: IHC staining with Lck antibody on untreated cell line cell pellets

Picture 4.5: IHC pictures from cell pellets of the cell line MDAMB231, MCF7 and MCF7HER2 stained with Lck antibody (1:50, Cell Signalling); demonstrating the differences in staining intensity and distribution within the cells. Stromal staining was present in the MDAMB231 and MCF7 cell pellet. Strongest Lck staining was observed in the cytoplasm of MCF7HER2 cells.

4.3.2.2 Protein expression differences in cell lines after Inhibition and Stimulation

Each cell line (depending on their HER status) was exposed for 30 min 10nM EGF or HRG, 60 min 100nM of Src kinase inhibitor Dasatinib and a combination of both (details in appendix 3). After exposure cell pellets were created, imbedded in wax-blocks, cut to sections, placed on slides and baked at 56°C ready for immunohistochemistry staining. Immunohistochemistry on all three cell lines was performed with four antibodies: c-Src, Y416Src, Y216Src- chosen by their significance regards patients' clinical outcome in previous IHC study, and Y861FAK- as a marker of downstream activation of Src. The same antibodies were used on those breast cancer patient tissue microarrays, described in previous chapter.

MDAMB231

Most significant changes in protein expression in this ER/HER2 negative cell line were observed with the Y416Src and Y861FAK antibody.

c-Src was mainly expressed in the membrane, but with no statistically significant change in expression throughout the different drug treatments (all p values above >0.05, figure 4.11). Interestingly, nuclear and cytoplasmic c-Src seemed to have higher expression in the Dasatinib treated cell pellet compared to untreated MDAMB231 cells (c-Src nuc p=0.090 and c-Src cyto p=0.042, figure 4.11).

There was no nuclear **Y419Src** protein expression seen in either cell lines, control cell pellet (UT= untreated) and different treatment exposures (figure 4.12).

However, Y419Src expression in the cytoplasm was significantly higher after EGF stimulation (p=0.008, figure 4.12, picture 4.6 D) and significantly reduced after exposure to

Dasatinib ($p=0.020$, figure 4.12, picture 4.6 E) compared to cytoplasmic Y419Src expression in untreated control cells. Even more substantial was the difference on cytoplasmic Y419Src protein expression caused by the two divergent drug treatments (figure 4.12, $p<0.001$). No statistically significant difference was noted between untreated cells and cells treated with consecutive EGF and Dasatinib treatment ($p=0.311$). On the other hand there was a significant reduction on cytoplasmic Y419Src expression between the cells only stimulated with EGF and cells received the drug combination ($p=0.002$, picture 4.6 F). There was also no statistically significant difference in Y419Src expression in the cytoplasm present between MDAMB231 cells after only Dasatinib exposure and cells treated with the drug combination (EGF followed by Dasatinib) ($p=0.121$).

An even more distinct reduction in Y419Src expression in the membrane (site of activation) was detected between MDAMB231 cells exposed to Dasatinib and untreated cells ($p<0.001$, picture 4.6 C), and cells stimulated with EGF ($p<0.001$) (figure 4.12, picture 4.6 D). There was no significant difference in expression between Dasatinib treatment and the combination of EGF/Dasatinib ($p=0.925$). In both cases the expression was nearly completely abolished (figure 4.12). No difference in protein expression was seen between untreated cells and cells exposed to 30 min of EGF ($p=0.125$).

Y215Src was generally less expressed in the membrane compared to nucleus and cytoplasm (figure 4.13). No statistically significant difference was observed between MDAMB231 cells, which had no treatment and cells which received different drug treatments (table 4.8).

Table 4.8: Statistical analysis of drug treatment Y215Src expression differences

| Y215Src nuc | UT | EGF | DASA |
|---------------------|-------|-------|-------|
| P values | | | |
| EGF | 0.695 | | |
| DASA | 0.695 | 1.0 | |
| ED | 0.488 | 0.760 | 0.760 |
| Y215Src cyto | UT | EGF | DASA |
| EGF | 0.938 | | |
| DASA | 0.757 | 0.816 | |
| ED | 0.757 | 0.816 | 1.0 |
| Y215Src memb | UT | EGF | DASA |
| EGF | 0.451 | | |
| DASA | 0.297 | 0.761 | |
| ED | 0.897 | 0.545 | 0.368 |

Table 4.8 illustrates non-significant associations between Y215Src nuc, Y215Src cyto and Y215Src membrane expression and their different drug treatments.

Activated **Y816FAK** protein was mostly expressed in the nucleus of MDAMB231 cells (figure 4.14). Cells, which were exposed to 60 min Dasatinib, showed a significant reduction in nuclear Y861FAK expression compared to untreated control cells ($p < 0.001$), EGF treated cells ($p < 0.001$) and cells, which were exposed to both treatments ($p < 0.001$) (figure 4.14). There was no significant difference noticed in nuclear Y861FAK protein expression between all other drug treatments (figure 4.14).

A much greater response in cytoplasm Y861FAK expression was observed with EGF exposure ($p = 0.001$) compared to untreated cells. Again MDAMB231, which were exposed to

Dasatinib treatment showed the lowest cytoplasmic Y861FAK expression compared to untreated cells ($p=0.028$), cells stimulated with EGF ($p<0.001$) and cells which received both drug treatments ($p=0.012$). A reduction in cytoplasmic Y861FAK was also detected when cells were exposed to Dasatinib after stimulation with EGF. A significant expression difference was noticed between cells only stimulated with EGF and cells with both drug treatments ($p=0.001$), but not compared to untreated cells ($p=0.805$).

Membrane Y861FAK expression in MDAMB231 cells was elevated after EGF treatment and considerably decreased after Dasatinib exposure ($p=0.010$, figure 4.14). Membrane Y861FAK expression was also reduced in cells when EGF and Dasatinib treatment was combined compared to only EGF exposure ($p=0.032$). No statistically significant difference was achieved between cells with both treatments (ED) and only Dasatinib exposure ($p=0.537$, both membrane expressions were low) and between untreated cells ($p=0.913$).

Figure 4.11: Changes in c-Src expression in MDAMB231 after drug treatments

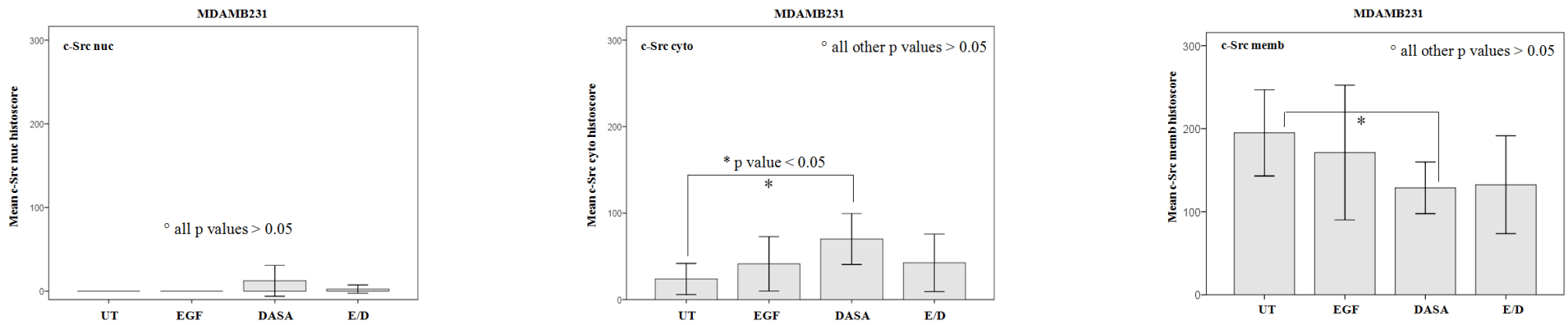


Figure 4.12: Changes Y419Src expression in MDAMB231 after drug treatments

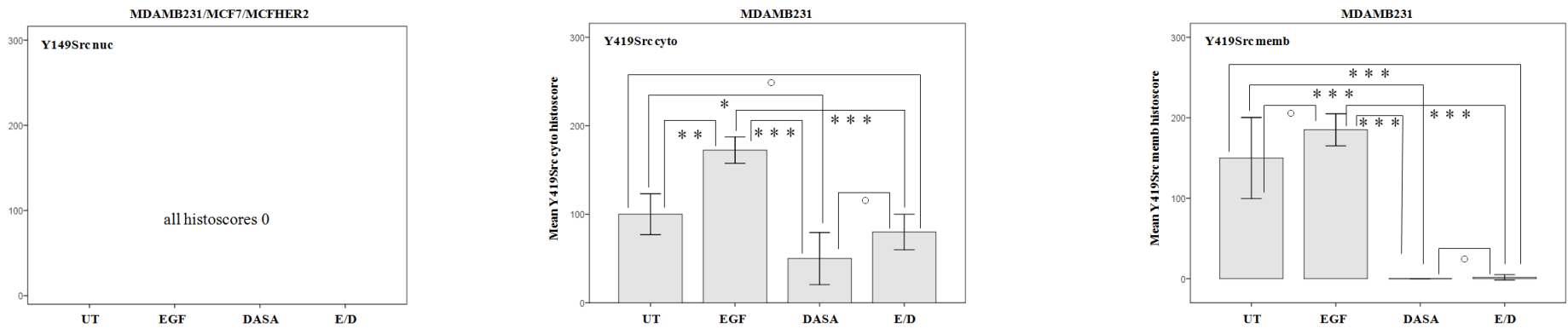


Figure 4.13: Changes Y215Src expression in MDAMB231 after drug treatments

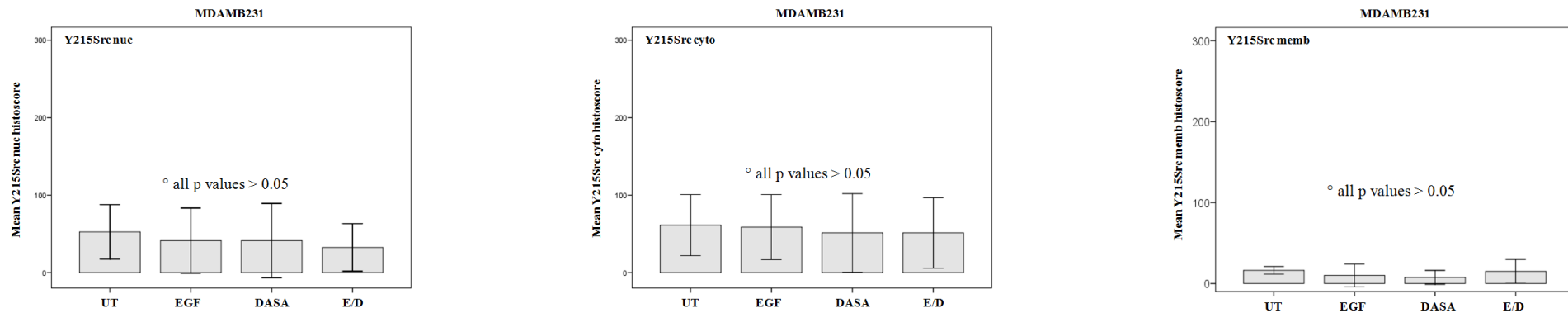


Figure 4.14: Changes Y861FAK expression in MDAMB231 after drug treatments

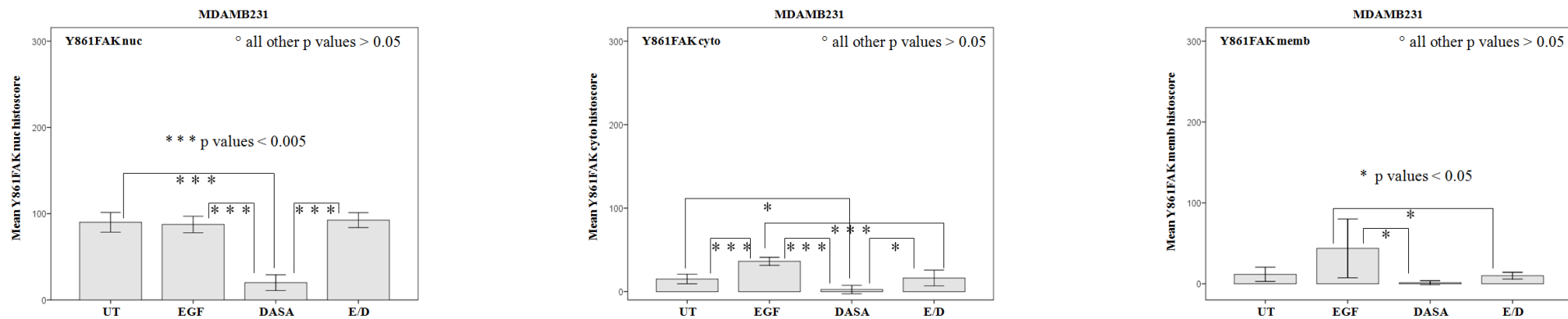
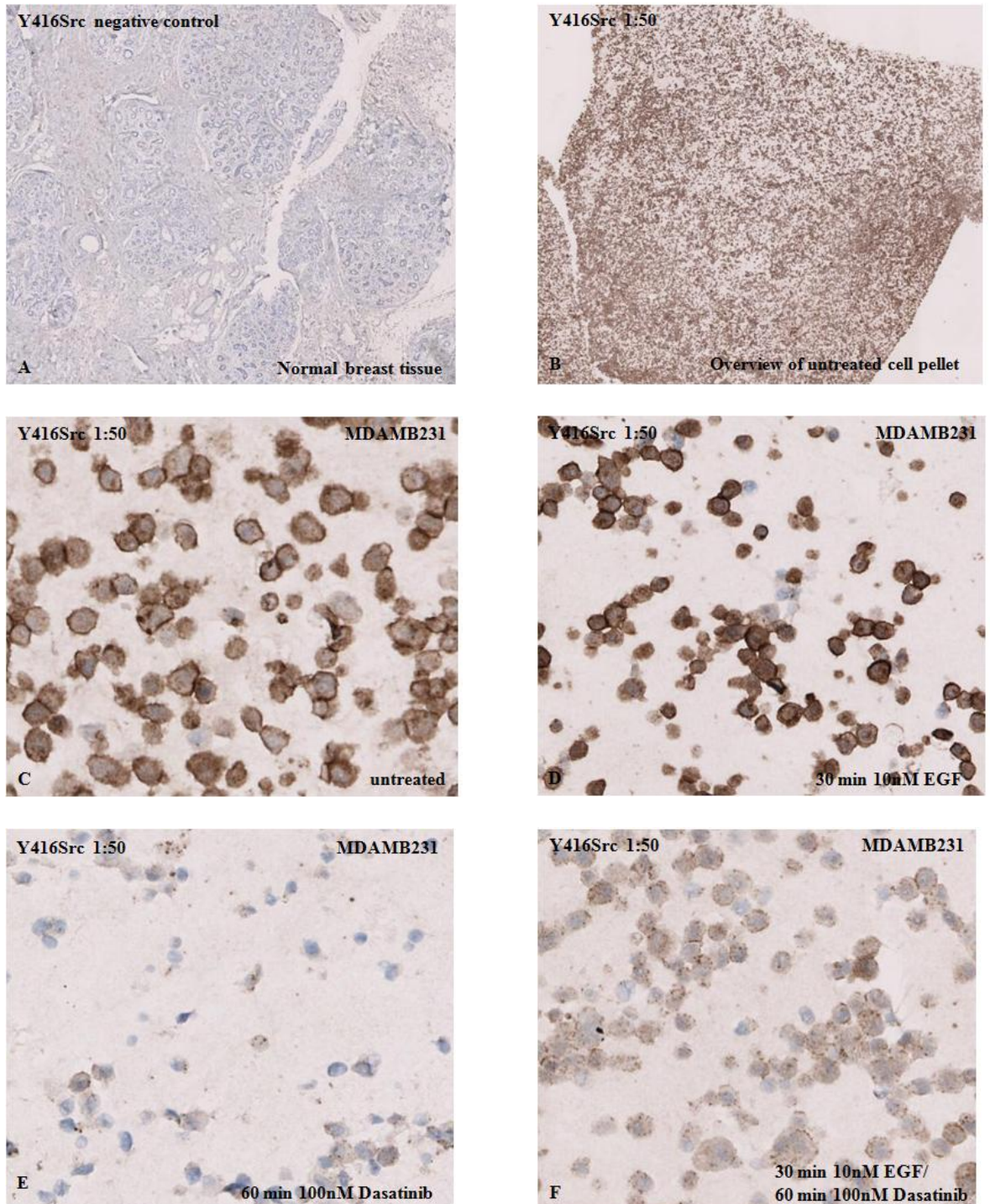


Figure 4.11-4.14: Overview of all protein expression variations for each of the four antibodies within the different cellular compartments after exposure to altered drug treatments. **4.11:** Difference in nuclear, cytoplasmic and membrane c-Src expression after drug treatments; **4.12:** Difference in cytoplasmic and membrane Y419Src expression after drug treatments; **4.13:** Difference in nuclear, cytoplasmic and membrane Y215Src expression after drug treatments; **4.14:** Difference in nuclear, cytoplasmic and membrane Y861FAK expression after drug treatments;

UT= untreated control cells, EGF= epidermal growth factor (for stimulation of HER1), DASA= Dasatinib, Src kinase inhibitor; c-Src = total Src kinase, Y419Src = Src kinase phosphorylated at Tyrosine site 419, Y215Src = Src kinase phosphorylated at Tyrosine site Y215; c-Src nuc = c-Src nuclear expression, c-Src cyto = c-Src cytoplasmic expression, c-Src memb = c-Src membrane expression, Y416Src nuc = Y416Src nuclear expression, Y416Src cyto = Y416Src cytoplasmic expression, Y416Src memb = Y416Src membrane expression, Y215Src nuc = Y215Src nuclear expression, Y215Src cyto = Y215Src cytoplasmic expression, Y215Src memb = Y215Src membrane expression; ° insignificant p values ($p > 0.05$), * p values < 0.05 , ** p values < 0.01 , *** p values < 0.005

There is a significant reduction on Y419Src expression in the cytoplasm and membrane after MDAMB231 cells were treated with 100nM Dasatinib for 60 min. This phenomenon wasn't evident with the Y215Src antibody; no change in expression was seen after Heregulin or Dasatinib or both treatments. However, the activated downstream protein FAK showed a similar effect as activated Y419Src. Its expression was also significantly inhibited after Dasatinib exposure.

Picture 4.6: Change of Y419Src staining after drug treatments

Pictures 4.6: Immunohistochemistry with antibody Y416Src performed on MDAMB231 cell pellets, displaying different protein expression pattern after altered drug treatments.

MCF7

As already observed in the ER negative cell line, nuclear and cytoplasmic **c-Src** had the highest expression in the Dasatinib treated cell pellets compared to all other cell pellets (figure 4.15) (c-Src nuc UT/DASA $p=0.010$, HRG/DASA $p=0.015$, HD/DASA $p=0.015$). A proportionally greater difference in cytoplasmic c-Src expression was noted between untreated and Dasatinib exposed cells (c-Src cyto UT/DASA $p=0.002$, figure 4.15).

c-Src was again mainly expressed in the membrane, though in this ER positive cell line with statistically significant changes in expression right through the different drug treatments (figure 4.15, picture 4.7 C-F).

Cells activated with Heregulin exhibit the highest membrane c-Src expression compared to untreated ($p=0.017$), exposed to Dasatinib treatment ($p=0.021$) and cells treated with Heregulin followed by Dasatinib ($p<0.001$, figure 4.15, picture 4.7). Cells, which were exposed to both treatments, showed the lowest membrane c-Src expression; less than untreated cells ($p=0.017$) and cells with only Dasatinib treatment ($p=0.014$). There was no difference observed in membrane c-Src expression between untreated control cells and cells which received Dasatinib treatment ($p=0.911$).

There was no nuclear **Y419Src** protein expression seen in the control cell pellet (UT) and the different treatment exposures (figure 4.16).

The only statistically significant alteration in cytoplasmic Y419Src expression was detected after exposure to Dasatinib ($p=0.033$) compared to cytoplasmic Y419Src expression in untreated control cells. Dasatinib treated cell pellets had a decreased cytoplasmic expression compared to control cell pellets.

A more considerable reduction in Y419Src expression was witnessed in the membrane. MCF7 cells exposed to Dasatinib retained hardly any detectable expression compared to untreated cells ($p=0.001$), and cells stimulated with HRG ($p<0.001$, figure 4.16). A

comparable effect was noticed with cells after combined drug treatments (HD) and untreated cells ($p=0.001$) as well as with cells only stimulated with HRG ($p<0.001$).

There was no significant difference in membrane Y419Src expression between Dasatinib treatment and the combination of HRG/Dasatinib ($p=0.951$). In both cases the expression was nearly completely abolished (figure 4.16). No difference in protein expression was also seen between untreated cells and cells exposed to 30 min of 10nM HRG ($p=0.134$). A similar assessment was made in the ER negative cell line.

There was no change in **Y215Src** protein expression observed in all three cellular compartments (figure 4.17) nor was there a statistically significant difference in nuclear, cytoplasmic and membrane Y215Src expression between MCF7 cells which had no treatment and cells which received different drug treatments (table 4.9).

Table 4.9: Overview of statistical correlation between Y215Src expression and difference drug treatments

| Y215Src nuc | UT | HRG | DASA |
|---------------------|-------|-------|-------|
| P values | | | |
| HRG | 0.965 | | |
| DASA | 0.202 | 0.220 | |
| HD | 0.630 | 0.623 | 0.460 |
| Y215Src cyto | UT | HRG | DASA |
| HRG | 0.918 | | |
| DASA | 0.589 | 0.548 | |
| HD | 0.677 | 0.961 | 0.515 |
| Y215Src memb | UT | HRG | DASA |
| HRG | 0.949 | | |
| DASA | 0.348 | 0.417 | |
| HD | 0.516 | 0.582 | 0.816 |

Table 4.9 highlights that there were only non-significant associations between Y215Src nuc, Y215Src cyto and Y215Src membrane expression and the different drug treatments.

Activated **Y816FAK** protein was least expressed in the cytoplasm of MCF7 cells (figure 4.18). The only statistically significant variation in cytoplasmic Y861FAK expression was seen between cells, which were exposed to 60 min Dasatinib and cells, which underwent both drug treatments (DASA/HD, $p=0.013$). Nevertheless there was noticeable decline in Y816FAK expression in the cytoplasm in ER positive cell line with Dasatinib treatment compared to the other cell pellets (figure 4.18).

Most of the significant alterations in Y861FAK protein expression were present in the cell nucleus and membrane (figure 4.18).

Dasatinib treated cell pellets showed statistically significant fall in nuclear Y861FAK expression compared to untreated control cells ($p=0.002$), HRG treated cells ($p=0.001$) and cells, which were exposed to both treatments ($p=0.001$). There was no significant difference noticed in nuclear Y861FAK protein expression between all other drug treatments (figure 4.18).

MCF7 cells, which were exposed to Dasatinib treatment, showed the lowest membrane Y861FAK expression compared to untreated cells ($p<0.001$), cells stimulated with HRG ($p<0.001$) and cells which received both drug treatments ($p<0.001$, figure 4.18).

Heregulin stimulated cells had the highest membrane Y861FAK expression evaluated against all other treatment conditions (UT/HRG $p<0.001$, HRG/DASA $p<0.001$, HD/DASA $p<0.001$). There was a slight, but statistically insignificant reduction noticed between membrane Y861FAK expression in untreated cells and cells, exposed to both drug treatments consecutively ($p=0.558$).

Figure 4.15: Changes in c-Src expression in MCF7 cell line after drug treatments

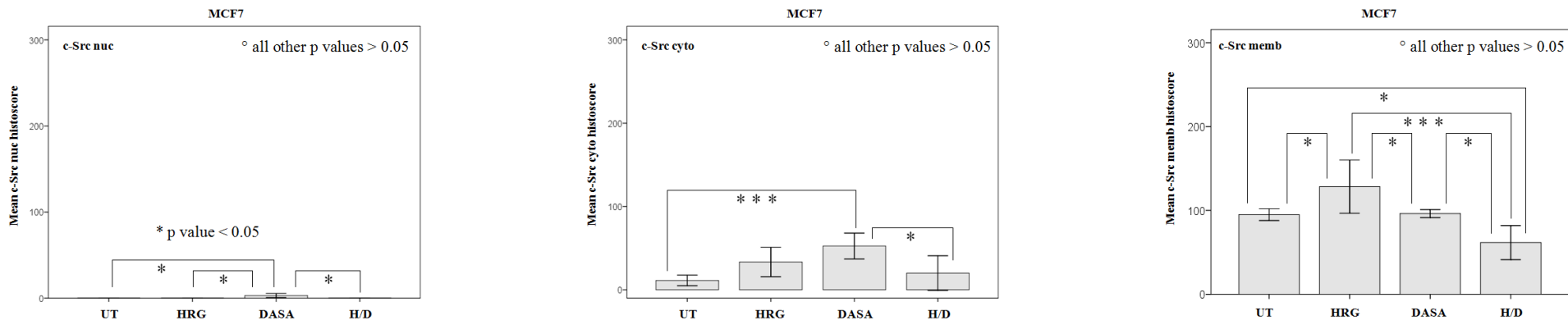


Figure 4.16: Changes in Y419Src expression in MCF7 cell line after drug treatments

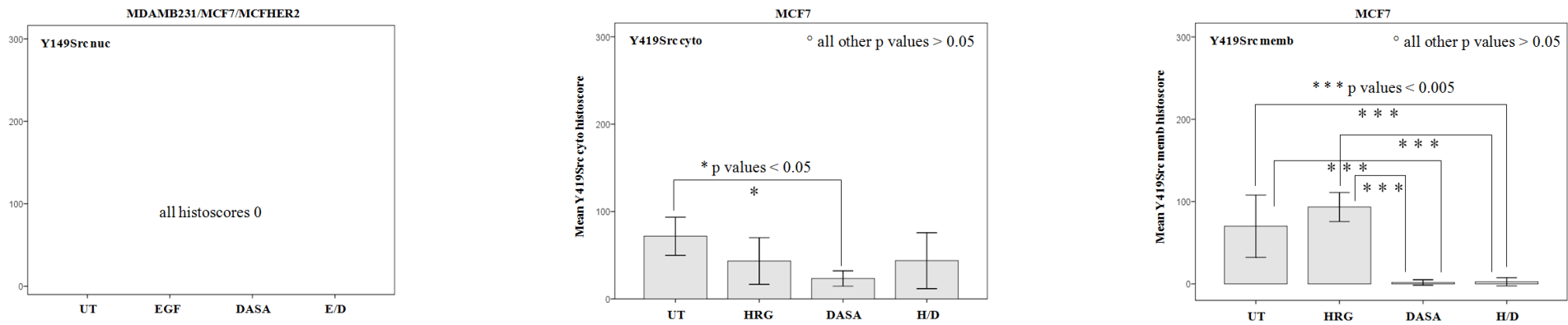


Figure 4.17: Changes in Y215Src expression in MCF7 cell line after drug treatments

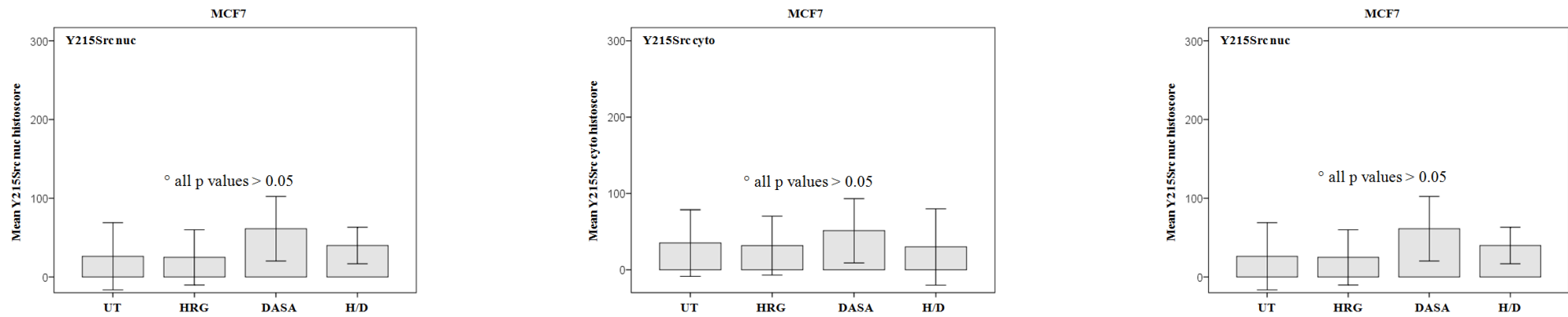


Figure 4.18: Changes in Y861FAK expression in MCF7 cell line after drug treatments

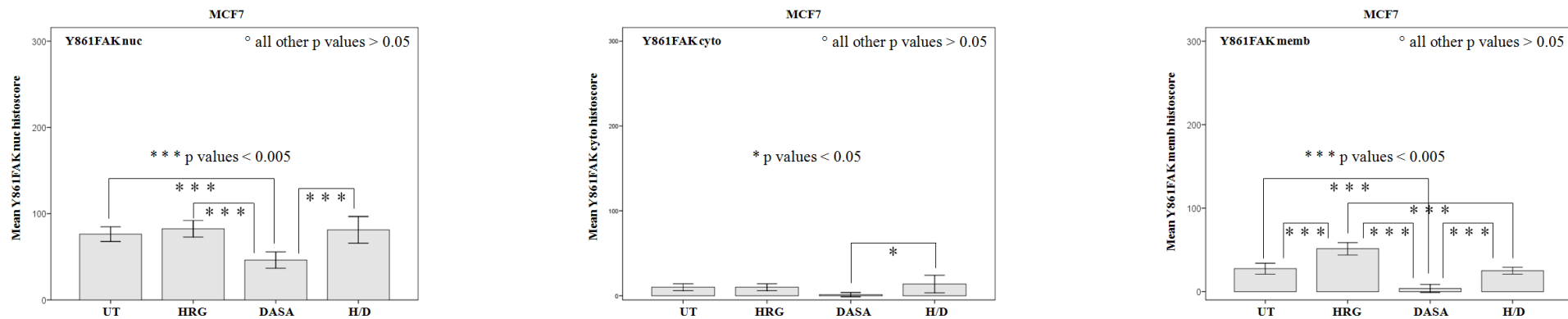
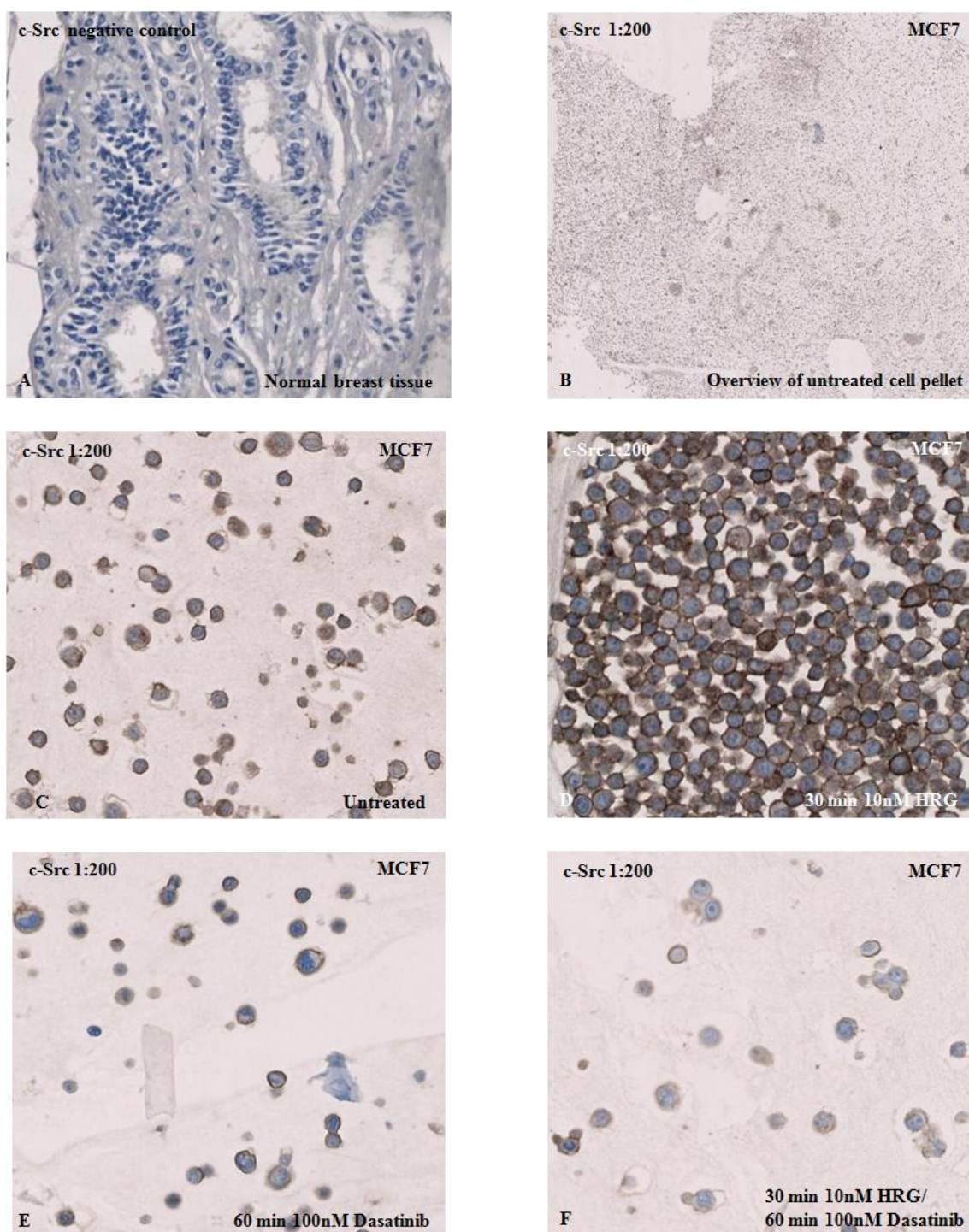


Figure 4.15-4.18: Overview of all protein expression variations for each of the four antibodies within the different cellular compartments after exposure to altered drug treatments in MCF7 cell line. **4.15:** Difference in nuclear, cytoplasmic and membrane c-Src expression after drug treatments; **4.16:** Difference in cytoplasmic and membrane Y419Src expression after drug treatments; **4.17:** Difference in nuclear, cytoplasmic and membrane Y215Src expression after drug treatments; **4.18:** Difference in nuclear, cytoplasmic and membrane Y861FAK expression after drug treatments.

UT= untreated control cells, HRG= Heregulin (for stimulation of HER2/3), DASA= Dasatinib, Src kinase inhibitor; c-Src = total Src kinase, Y419Src = Src kinase phosphorylated at Tyrosine site 419, Y215Src = Src kinase phosphorylated at Tyrosine site Y215; c-Src nuc = c-Src nuclear expression, c-Src cyto = c-Src cytoplasmic expression, c-Src memb = c-Src membrane expression, Y416Src nuc = Y416Src nuclear expression, Y416Src cyto = Y416Src cytoplasmic expression, Y416Src memb = Y416Src membrane expression, Y215Src nuc = Y215Src nuclear expression, Y215Src cyto = Y215Src cytoplasmic expression, Y215Src memb = Y215Src membrane expression; ° insignificant p values ($p > 0.05$), * p values < 0.05 , ** p values < 0.01 , *** p values < 0.005

There is a significant reduction on Y419Src expression in the cytoplasm and membrane after MCF7 cells were treated with 100nM Dasatinib for 60 min. Again no change in nuclear, cytoplasmic and membrane Y215Src expression was apparent. As seen within the ER negative cell line, activated downstream protein FAK showed a similar effect as activated Y419Src. Its expression was also significantly inhibited after Dasatinib exposure.

Picture 4.7: Changes in c-Src expression in MCF7 cell pellets after drug treatments

Pictures 4.7: Immunohistochemistry with c-Src antibody performed on MCF7 cell pellets, demonstrating different protein expression pattern after altered drug treatments.

MCF7HER2

The lowest **c-Src** protein expression was observed in the nucleus (figure 4.19). Again nuclear c-Src expression was highest in the Dasatinib treated cell pellets compared to all other MCF7HER2 cell pellets (figure 4.19), but with no significant p values for expression differences. MCF7HER2 cells treated with 10nM Heregulin followed by 100nM Dasatinib (HD) demonstrated the least cytoplasmic c-Src expression compared to untreated cells ($p=0.004$) and cells exposed to Dasatinib treatment ($p=0.039$). Surprisingly untreated control cells exhibit a higher cytoplasmic c-Src expression than cells exposed to Heregulin ($p=0.012$)

Almost no change in membranous c-Src expression after stimulation with Heregulin and inhibition with Dasatinib or both was an unexpected finding, and differed to what was observed in the other cell lines.

As mentioned before, there was again no nuclear **Y419Src** protein expression seen in the control cell pellet (UT) and the different treatment exposures (figure 4.20) of this cell line.

There was a slight decrease in cytoplasmic Y419Src expression detected in cell pellets treated with Dasatinib, but without any statistically significant p value (figure 4.20).

Assessment of Y419Src expression on the cellular membrane is the site of interest in all three cell lines: Once more there was a critical reduction in Y419Src expression witnessed in cell pellets after 60 min exposure to Dasatinib. MCF7HER2 cells exposed to Dasatinib had the lowest membrane Y419Src expression compared to untreated cells ($p=0.001$) and cells stimulated with HRG ($p<0.001$, figure 4.20). Another significant reduction in Y419Src expression was detected in cell pellets which were treated with both drug treatments (HD) compared to untreated control cell pellets ($p<0.001$) and cell pellets after Heregulin exposure ($p<0.001$).

There was no significant difference in membrane Y419Src expression between Dasatinib treatment and the combination of HRG/Dasatinib ($p=0.058$). Balanced on the observations made in the other two cell lines, MCF7HER2 cell pellets showed a less extreme reduction in membrane Y419Src expression after Dasatinib treatment (figure 4.20).

Yet again there was no change in **Y215Src** protein expression observed in all three cellular compartments (figure 4.21) nor was there a statistically significant difference in nuclear, cytoplasmic and membrane Y215Src expression between MCF7HER2 cells which had no treatment and cells which received different drug treatments (table 4.10).

Table 4.10: Statistical analysis of Y215Src expression changes after drug treatments

| Y215Src nuc | UT | HRG | DASA |
|---------------------|-------|-------|-------|
| P values | | | |
| HRG | 0.570 | | |
| DASA | 0.886 | 0.669 | |
| HD | 0.479 | 0.213 | 0.398 |
| Y215Src cyto | UT | HRG | DASA |
| HRG | 0.214 | | |
| DASA | 0.353 | 0.736 | |
| HD | 0.387 | 0.686 | 0.946 |
| Y215Src memb | UT | HRG | DASA |
| HRG | 0.709 | | |
| DASA | 0.314 | 0.516 | |
| HD | 0.459 | 0.709 | 0.779 |

Table 4.10 highlights that there were only non-significant associations between Y215Src nuc, Y215Src cyto and Y215Src membrane expression and the different drug treatments in the MCF7HER2 cell pellets.

As observed in the other two cell lines, activated **Y816FAK** protein was least expressed in the cytoplasm of MCF7HER2 cell pellets (figure 4.22).

Nuclear Y861FAK expression was significantly reduced in cell pellets, which were exposed to Dasatinib compared to untreated control cell pellets ($p < 0.001$, picture 4.8 C), cell pellets after Heregulin stimulation ($p < 0.001$, picture 4.8 D) and cell pellets after both drug treatments ($p < 0.001$, picture 4.8 F, figure 4.22). Like with cytoplasmic c-Src expression, nuclear Y861FAK expression was found to be reduced in Heregulin stimulated cell pellets compared to untreated cell pellets ($p = 0.002$). The same phenomenon is witness with cytoplasmic Y861FAK expression ($p < 0.001$, figure 4.22).

Dasatinib treated cell pellets showed statistically significant fall in cytoplasmic Y861FAK expression compared to untreated control cells ($p < 0.001$), HRG treated cells ($p = 0.010$) and cells, which were exposed to both treatments ($p = 0.010$). There was a significant difference noticed in cytoplasmic Y861FAK protein expression in cell pellets exposed to both drug treatments and untreated cell pellets ($p < 0.001$, figure 4.22).

Dasatinib treatment again affected membrane Y861FAK expression greatly. Lowest Y861FAK expression was measured in Dasatinib treated MCF7HER2 cells compared to untreated cells ($p < 0.001$, picture 4.8 C and E) and cells stimulated with HRG ($p < 0.001$, picture 4.8 D).

Different to the other cellular compartments, Heregulin had a stimulating effect on membrane Y861FAK expression.

Cell pellets, which received both drug treatments exhibit less membrane Y861FAK expression compared to untreated cell pellet ($p = 0.002$) and cell pellet after Heregulin stimulation ($p < 0.001$).

There was a slight, but statistically insignificant reduction noticed between membrane Y861FAK expression in cells, treated with Dasatinib and cells, exposed to both drug treatments ($p=0.159$, figure 4.22).

Figure 4.19: c-Src expression in MCF7HER2 after drug treatments

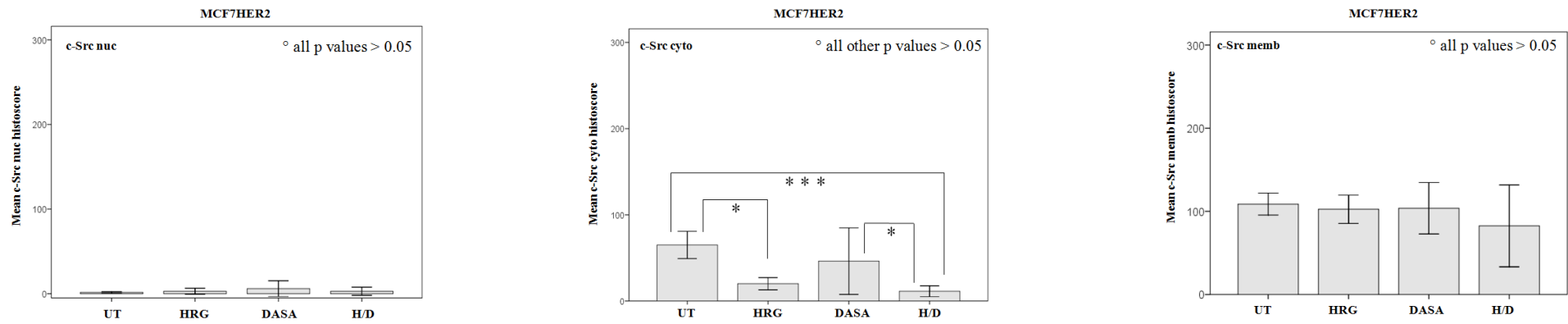


Figure 4.20: Y419Src expression in MCF7HER2 after drug treatments

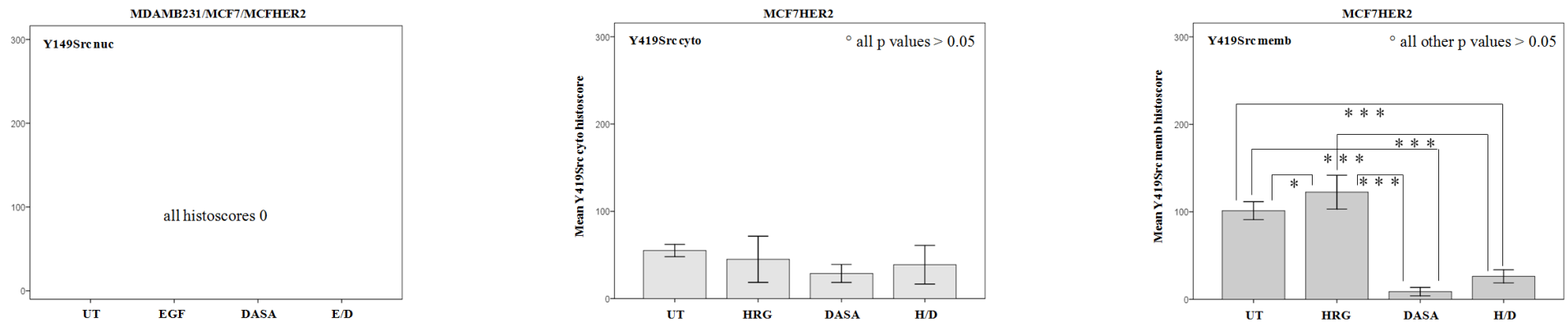


Figure 4.21: Y215Src expression in MCF7HER2 after drug treatments

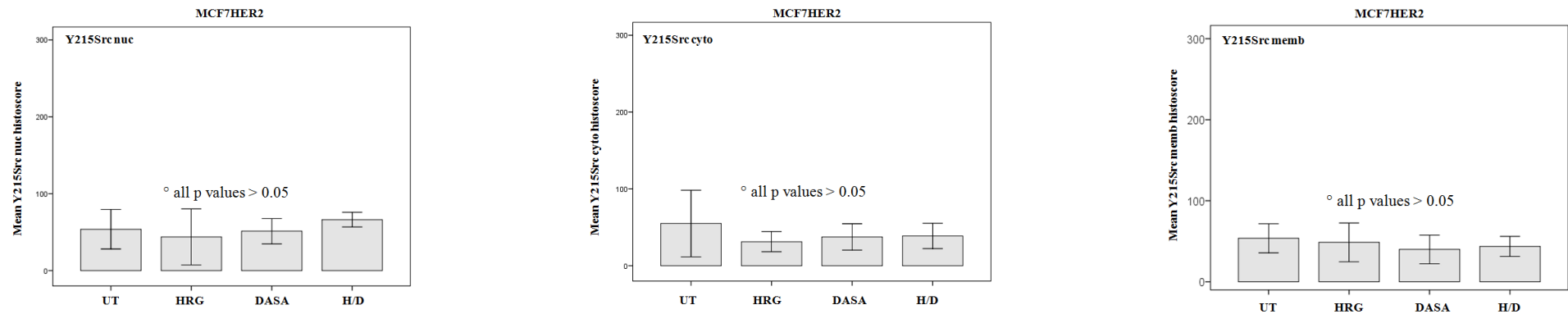


Figure 4.22: Y861FAK in MCF7HER2 after drug treatments

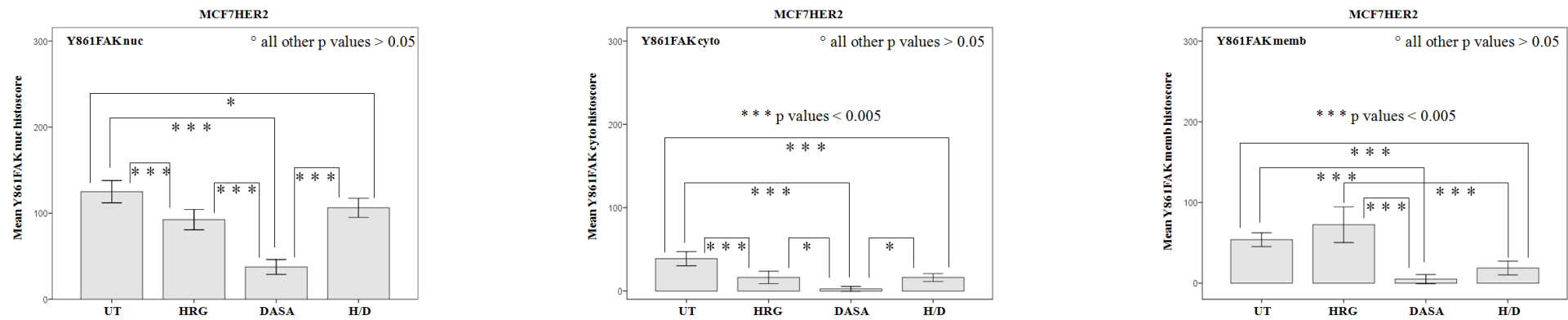
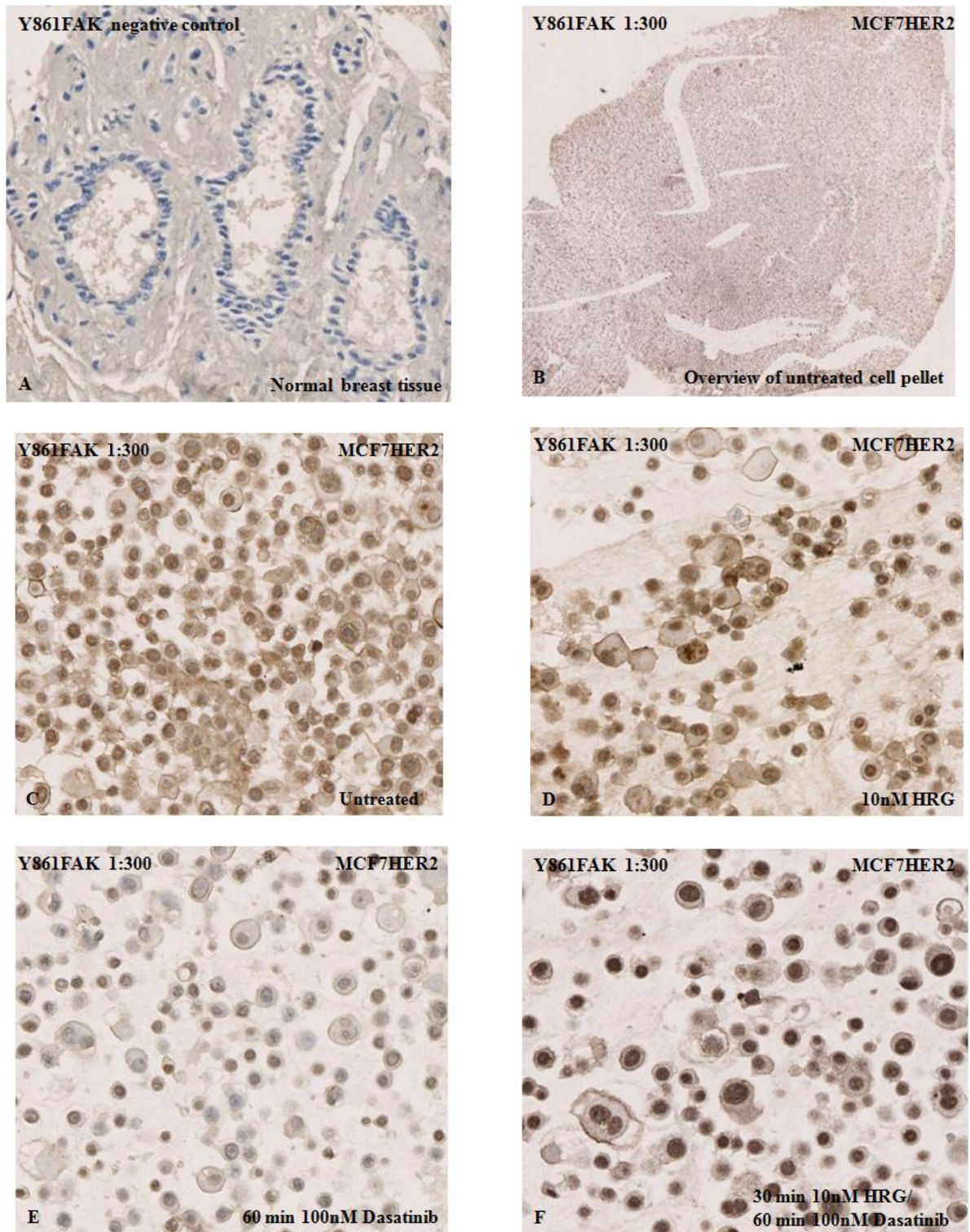


Figure 4.19-4.22: Overview of all protein expression variations for each of the four antibodies within the different cellular compartments after exposure to altered drug treatments in MCF7HER2 cell line. **4.19:** Difference in nuclear, cytoplasmic and membrane c-Src expression after drug treatments; **4.20:** Difference in cytoplasmic and membrane Y419Src expression after drug treatments; **4.21:** Difference in nuclear, cytoplasmic and membrane Y215Src expression after drug treatments; **4.22:** Difference in nuclear, cytoplasmic and membrane Y861FAK expression after drug treatments.

UT= untreated control cells, HRG= Heregulin (for stimulation of HER2/3), DASA= Dasatinib, Src kinase inhibitor; c-Src = total Src kinase, Y419Src = Src kinase phosphorylated at Tyrosine site 419, Y215Src = Src kinase phosphorylated at Tyrosine site Y215; c-Src nuc = c-Src nuclear expression, c-Src cyto = c-Src cytoplasmic expression, c-Src memb = c-Src membrane expression, Y416Src nuc = Y416Src nuclear expression, Y416Src cyto = Y416Src cytoplasmic expression, Y416Src memb = Y416Src membrane expression, Y215Src nuc = Y215Src nuclear expression, Y215Src cyto = Y215Src cytoplasmic expression, Y215Src memb = Y215Src membrane expression; ° insignificant p values ($p > 0.05$), * p values < 0.05 , ** p values < 0.01 , *** p values < 0.005

There is a significant reduction on Y419Src expression in the membrane after MCF7HER2 cells were treated with 100nM Dasatinib for 60 min. No change in nuclear, cytoplasmic and membrane Y215Src expression was observed after Heregulin and Dasatinib or both treatments. However, the activated downstream protein FAK showed a similar effect as activated membrane Y419Src. Its expression was also significantly inhibited after Dasatinib exposure in the nuclear, cytoplasmic and membranous cell compartment.

Picture 4.8: IHC staining with Y861FAK on cell line cell pellets

Pictures 4.8: Immunohistochemistry with Y861FAK antibody performed on MCF7HER2 cell pellets, demonstrating different protein expression pattern after altered drug treatments.

Lck

The drug stimulation and inhibition experiment was only performed in the MCF7HER2 cell line since the basal Lck protein expression was absent in the MDAMB231 and MCF7 cell line (figure 4.10).

Nuclear Lck expression was hardly detected in any of the cell pellets. No significant p value for variation in protein expression was therefore recorded (table 4.11).

Cytoplasmic Lck expression was vaguely more marked (figure 4.23), but again there was no statistically significant difference in expression noticed (table 4.11).

Cell pellets after Heregulin exposure showed a slight increased Lck expression in the membrane compared to untreated cell pellets, but once more without any statistically significant value (table 4.11). There was a faint decrease in membrane Lck expression in Dasatinib exposed cell pellets evident. This observation is based on lower histoscores other than significant p values (table 4.11, figure 4.23).

Table 4.11: Statistical overview of nuclear, cytoplasmic and membrane Lck expression on cell line cell pellets after drug treatments

| Lck nuc | UT | HRG | DASA |
|-----------------|-------|-------|-------|
| P values | | | |
| HRG | 0.374 | | |
| DASA | 0.281 | 1.0 | |
| HD | 0.832 | 0.647 | 0.585 |
| Lck cyto | UT | HRG | DASA |
| HRG | 0.529 | | |
| DASA | 0.443 | 1.0 | |
| HD | 0.477 | 1.0 | 1.0 |

| Lck memb | UT | HRG | DASA |
|-----------------|-------|-------|-------|
| HRG | 0.379 | | |
| DASA | 0.514 | 0.720 | |
| HD | 0.387 | 0.909 | 0.786 |

Table 4.11 highlights that there were only non-significant associations between Lck nuc, Lck cyto and Lck membrane expression and the different drug treatments.

Figure 4.23: Expression differences of Lck in cell pellets after drug treatments

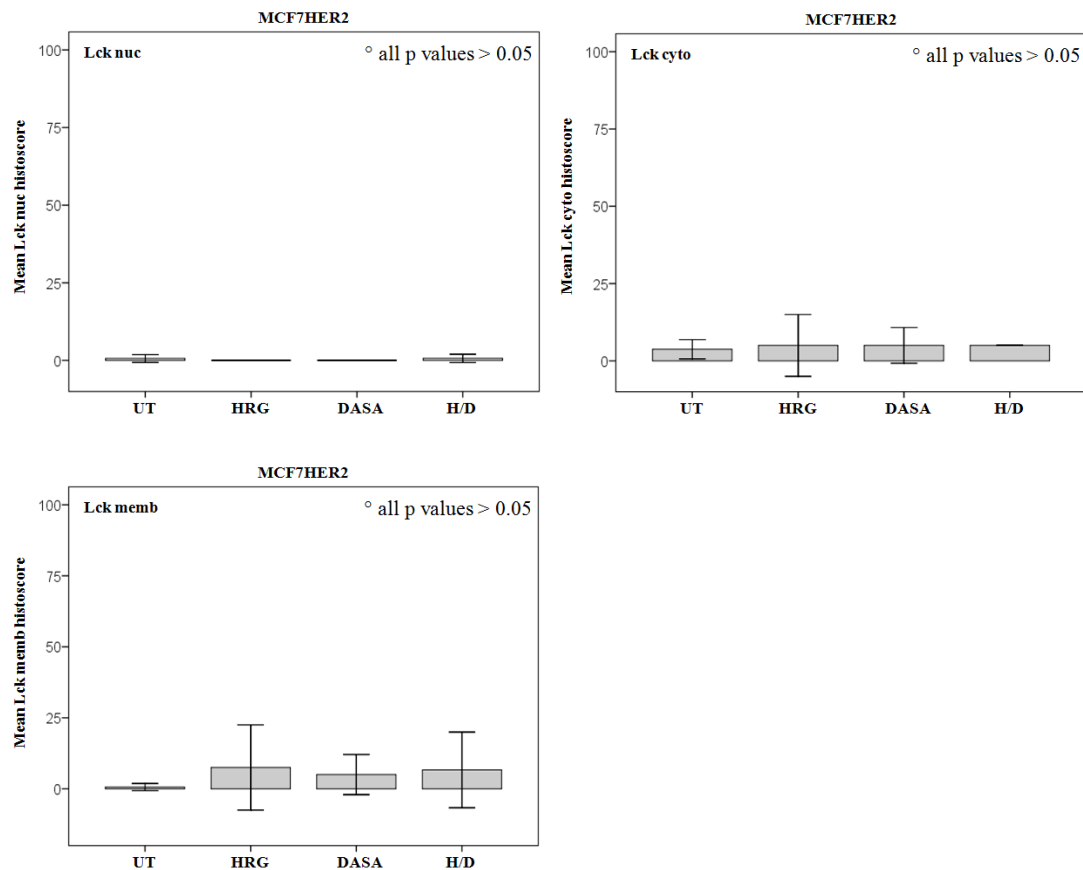
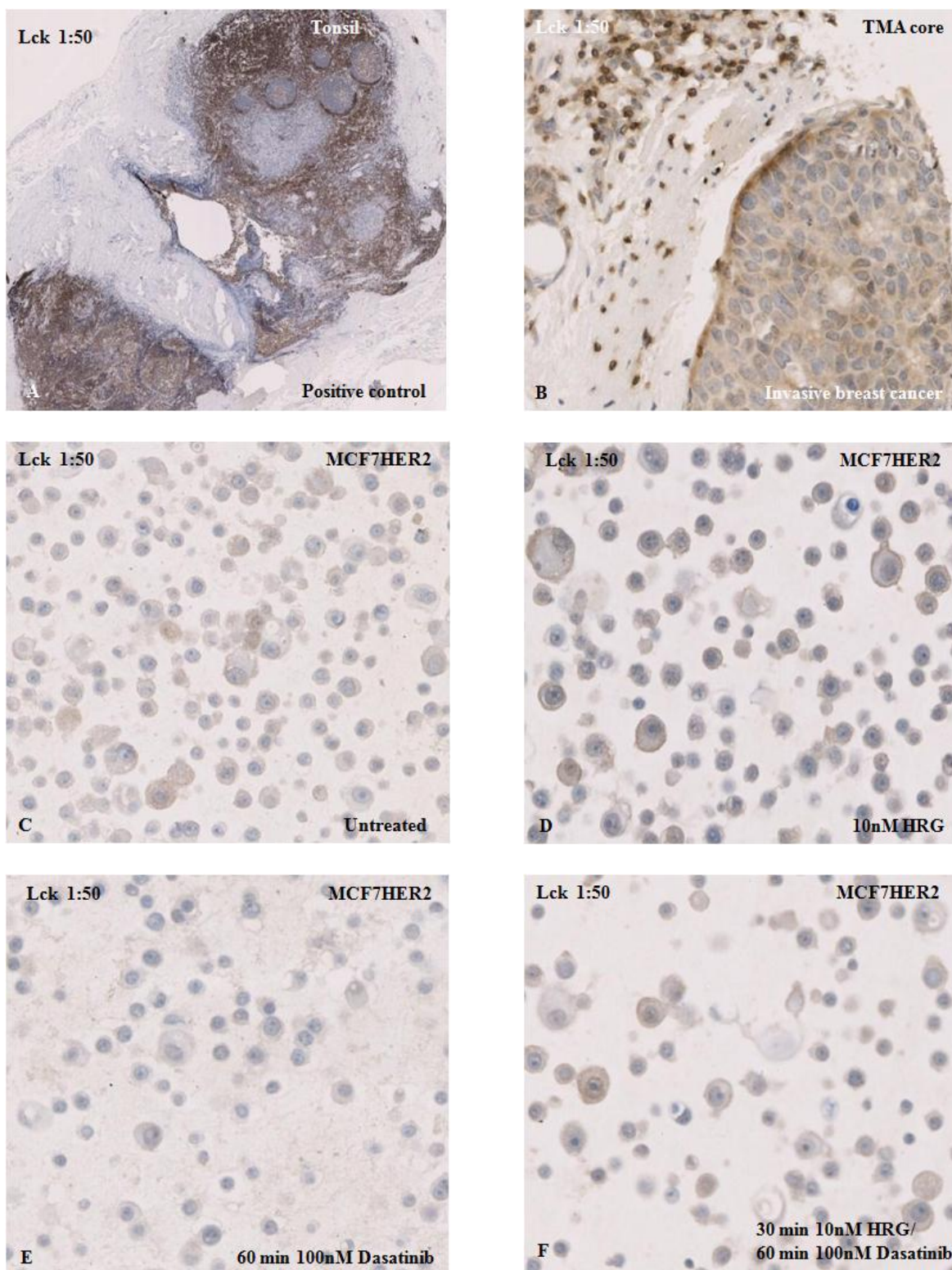


Figure 4.23 displays the differences in nuclear, cytoplasmic and membrane Lck expression after no treatment, exposure to Heregulin and Dasatinib or both treatments. No significant protein expression changes are obvious.

Picture 4.9: IHC staining with Lck antibody on cell pellets

Picture 4.9: Immunohistochemistry performed with Lck antibody on full section of normal breast tissue, invasive breast cancer TMA and cell pellet with various drug treatments in MCF7HER2 cell line.

4.4 Discussion

Several studies in other tumours have consistently demonstrated the role of Src in the development and progression of cancer (114;210;212;214).

A number of Src inhibitory agents are currently under investigations in pre-clinical and clinical studies to establish their efficacy as anti-proliferative and anti-invasive agents.

Having found a negative impact of high Src expression and contrary results from its phosphorylation sites in our IHC cohort, we wanted to establish how exposure to a stimulant drug or/ and Dasatinib, a Src kinase inhibitor would influence Src protein expression, activation and cellular distribution.

Activity of Dasatinib has been studied in various cell lines derived from different solid tumours (prostate, colon, lung, glioblastoma and others). Effects of Dasatinib on cell growth inhibition were also examined in 39 human breast cancer cell lines, categorised into luminal and basal subtypes based on the relative gene expression profiles of cytokeratins, using proliferation assays (169). Dasatinib inhibited cell growth of breast cancer cell lines representing both, luminal and basal breast cancer cell subtypes. It is a potent regulator of MDAMB231 breast cancer cell growth (164). This cell line represents the triple negative breast cancer type with poor prognosis, but with increased sensitivity to growth inhibitory effects of Dasatinib (169).

We chose four cell lines representing the different breast cancer subgroups. Before we embarked on drug stimulation and inhibition experiments we investigated if c-Src kinase protein was expressed in all four cell lines through simple steroid depletion test. To our surprise cell line MDAMB453 did not express c-Src in measurable quantities for Western Blotting. To validate this finding further, we looked into *SRC* mRNA expression in this cell line, discovering that there was no detectable *SRC* mRNA present. Interestingly, Finn

et al. demonstrated that this cell line was resistant to high dose Dasatinib treatment due to unknown mechanism (169). We therefore proceeded with only three cell lines.

Either overexpression or increased activity of Src can be responsible for oncogenesis. In colon carcinoma lysates, Src activity was elevated compared with normal human colon mucosa cells, which appeared to be as a result of increased kinase signalling by Src, rather than increased protein levels (213;214).

To determine effects of inhibitors, reliable biomarkers for kinase activation must be found. Phospho-specific antibodies, targeting activated enzymes, are established tools to investigate molecular signalling pathways. When Src is activated, several downstream proteins are phosphorylated (e.g. paxillin at Tyr118, p130cas at Tyr410 and FAK at Tyr861). These potentially could act as biomarkers (167). The most reliable and applied indicator for Src activity is tyrosine site 419 (168). Activation at FAKY861 and Y419Src were both found to be decreased when hormone sensitive (LNCaP) and refractory (LNCaP-SDM) prostate cancer cell lines were exposed to Dasatinib (90). A complete inhibition of Src activity in LNCaP cells was achieved with a concentration of 50 nM of Dasatinib. A slightly higher concentration (75nM) was needed for LNCaP-SDM. To ensure a definitive result could be achieved in our study, a concentration of 100 nM Dasatinib was selected. This was also based on a colon cancer *in vitro* study (167), demonstrating complete depletion of Src activation with this concentration. However, Dasatinib, used at concentrations of 100 nM and above, can inhibit multiple targets and therefore could be non-specific (164). Our investigations were focused on the effect of Dasatinib on Src kinase and Src activation (Y419Src, Y215Src and downstream protein Y861FAK). To suppress cell proliferation a higher concentration of Dasatinib would have been necessary. It also seems that not all cell lines utilise Src kinase family members in their proliferation signalling pathways (167).

Despite previous optimisation and application of the antibodies in the immunohistochemistry study, it was necessary to re-test antibody dilutions/ conditions on TMA, full section and control cell pellet slides due to the possibility of increased staining intensity on the more delicate cell pellets. A significant adjustment in Y416Src antibody dilution was required. This was most likely due to the article's Lot change by the company. c-Src and its activation sites Tyr419 and Tyr215, and Lck were investigated, because of their significant and contrary associations with clinical outcome of breast cancer patients examined in the previous IHC study. Antibody to Tyr861 of FAK, downstream substrate to Src and indicator for Src activation, was added as a control.

Comparing basal expression of all three cell lines, we found that nuclear and cytoplasmic c-Src was highest expression in ER positive/HER2 upregulated cell line (MCF7HER2), which is in keeping with Src kinase being over-expressed in HER2 over-expressed mammary cancers (124) promoting tumour development and progression in conjunction with the ER receptor. Another study demonstrates that HER2 over-expressing tumours showed increased levels of c-Src phosphorylation at Tyr215 and additionally up-regulating phosphorylation of downstream substrate FAK at Tyr861 (125). Similar we found that baseline Y861FAK expression, but only membrane Y215Src expression was highest in the untreated MCF7HER2 cell line compared to the other two.

It is well established now that Src kinase plays an important role in promoting cancer cell motility (72). Activated Src kinase regulates the motility of cancer cell in building complexes with FAK followed by stimulation of other signalling proteins.

FAK, also a non-receptor tyrosine kinase and downstream substrate to Src kinase, is mainly implicated in the regulation of cell motility, adhesion and anti-apoptotic signalling

(238). Growth factors can induce phosphorylation of FAK on a number of tyrosine sites, triggering distinct cell signals: Tyr397 in recruiting Src to focal adhesions, Tyr576 in up-regulating FAK activity (239), Tyr925 in activating the Ras-mitogen-activated protein kinase pathway (240) and Tyr861 in Ras mediated transformation (241). Cells, which are deficient of FAK, are unresponsive to PDGF and EGF- mediated motility signals (242). Heregulin and activated HER2 can rearrange the cytoskeleton and increase the capability of breast cancer cells to metastasise without phosphorylation of FAK (243). Vadlamudi *et al.* demonstrated that Heregulin (10nM 30 min exposure) and HER2 signalling selectively upregulated phosphorylation of c-Src at Tyr215, increasing Src kinase activity and up-regulating phosphorylation of FAK at Tyr861 (125).

Interestingly we didn't observe a rise or decrease in Y215Src protein expression after 30 min stimulation with 10 nM Heregulin nor when exposed to Dasatinib in all three cell lines. In spite of this, we saw a significant increase and decrease in Y861FAK expression on the membrane after the equivalent drug treatment. Our findings therefore support the hypothesis that Dasatinib selectively inhibits phosphorylation at Tyr419 and not phosphorylation site Y215Src. This needs to be investigated further, validating our results by repeating the experiment with cell lysis and Western Blotting. It would assure that the application of Dasatinib in the clinical setting would not be harmful and detrimental for patients, who express Y215Src in the nucleus or cytoplasm. Even more it would support the usage of Dasatinib in breast cancer patients based on our results. All three cell lines demonstrated a significant diminution of phosphorylated Y419Src and Y861FAK on the cellular membrane reducing Src activation leading to decreased cell proliferation and increased stabilisation of cellular adhesions. Demonstrating no expression difference and response to Dasatinib treatment at any cellular location, Y215Src would not be suitable as a prognostic nor predictive biomarker, despite cytoplasmic Y215Src expression being independent in uni- and multivariate analysis in the previous IHC study.

In our study, Y215Src and Y861FAK had a similar basal protein expression pattern. Nuclear and cytoplasmic expression of those proteins was lowest in the ER positive/HER2 negative (MCF7) cell line, whereas membrane protein expression was lowest in the triple negative (MDAMB231) and highest in the ER positive/HER2 upregulated (MCF7HER2) cell line. This could imply that cellular location of these specific proteins influences cellular function inducing different expression profiles.

Conversely, membrane expression of the classical Src activation site Y419 and c-Src was highest in MDAMB231. This could be the reason why this cell line is highly sensitive to Dasatinib treatment (169). We observed a near complete abolition of membrane Y419Src expression in MDAMB231 and MCF7 cells and a statistically significant reduction in MCF7HER2 cells after Dasatinib exposure. A comparable, but less radical pattern was noticed with membrane c-Src expression; Dasatinib treatment resulted in a significant reduction of membrane c-Src expression in MDAMB231 and MCF7 cells, but statistically non-significant in MCFHER2 cells. It would be of interest to establish if the up-regulated human epidermal growth factor receptor is the reason for the lethargic response to Dasatinib. This could be an indication to trial Dasatinib with Herceptin in HER2/c-Src positive patients.

It also highlights that Y419Src would be a more suitable biomarker in predicting response to Dasatinib treatment, as various studies in other solid tumours have already suggested (90;168). Results from the previous IHC chapter draw attention to membrane Y419Src expression in invasive breast cancer patients and its association with poorer clinical outcome. The striking elimination of activated Y419Src expression on the cell membrane in all cell lines after Dasatinib treatment is supportive in justifying phase III clinical trials with this drug.

Interestingly, in MDAMB231 and MCF7 cells exposure to Dasatinib was followed by a significant increase in nuclear and cytoplasmic c-Src expression. A similar observation was made in LNCaP-SDM cells, where an increase in the dose of Dasatinib resulted in an increase in c-Src (90). With the knowledge that inactive Src is stored in the nucleus and cytoplasm, we hypothesise, that a rise in nuclear and/ or cytoplasmic c-Src expression might be a marker that treatment with Dasatinib could force Src kinase into a state of hibernation or senescence.

Membranous expression of Lck in our IHC study was associated with no breast cancer related deaths. Therefore we were interested to study the effects of Dasatinib on SFK member Lck in our cell lines/ cell pellet experiment. Only cell line MCF7HER2 had quantifiable basal Lck protein expression. Again it raises the question of the role of human epidermal growth factors and their associations with SFK members in breast tumours. However, there was no detectable difference in Lck protein expression after any of the drug treatments. This is similar to results gained with Src activation site Y215. It's doubtful that these observed facts are related with each other. Yet Couture *et al.* reported, that Lck phosphorylated at tyrosine site 192 by Syk was corresponding with phosphorylated Y215Src (244). It would be of interest to perform IHC with an antibody for Tyr192 in our IHC cohort to investigate its correlation to Y215Src and association to clinical outcome.

Our cell line studies revealed that Src kinase expression was not detected in MDAMB453 cell line. Basal expression of activated Y419Src was highest in ER negative cell line. All cell line studies showed a significant decrease in Y419Src activation and phosphorylated downstream substrate Y861FAK after exposure to Src inhibitor Dasatinib.

Upregulated HER2 receptor seems to play a role in basal expression of Src and activated Src, their cellular distribution and response to drug treatments. A discordant effect on nuclear, cytoplasmic and membrane c-Src expression was observed in ER negative and ER positive cell line. No change in protein expression despite stimulation with HRG/EGF and/or inhibition with Dasatinib was witnessed with Y215Src and Lck expression.

Our results support the use of Dasatinib as a reliable Src inhibitor for breast cancer patients. Our results suggest a combination with Herceptin in HER2 over-expressing patients might be of benefit. Membrane expression of Y419Src could be a potential predictive biomarker to monitor response to Dasatinib treatment. These proposals have to be further validated in clinical trials.

CHAPTER 5

DISCUSSION/ CONCLUSION

Src kinase has been extensively investigated in *in-vitro* studies, mainly in colon carcinoma, and haematological malignancies. Src activation can occur via multiple mechanisms, e.g. de-/phosphorylation of different tyrosine sites, downstream activation via over-expressed EGFR receptors and/or interaction with many other cell signalling molecules. This activation of Src contributes significantly to the biological progression of tumours (83). Over the past few years Src inhibitors have been commercially developed and clinically trialled in CML, colon, pancreas and prostate cancer. Recently, without substantive translational research evidence, phase II and III clinical trials have opened and started recruitment of patients with advanced or metastatic breast cancer.

With this project we aimed to enhance the current knowledge regards the role of Src and SFK members in human breast cancer and add significant findings to the current literature. During the course of this translational study we established Src and SFK expression in various human breast tissue samples, evaluated Src expression and activation in invasive breast cancer specimens and examined the impact of a Src inhibitor on those expression and activation sites in breast cancer cell lines to address their relevance in the clinical setting.

Examining SFK mRNA expression in normal, non-malignant and malignant breast tissue we found all SFK members were expressed, but with different expression pattern. *SRC* and *LYN* were most highly expressed in non-malignant and malignant breast tissue samples, whereas *FYN* was highest expressed in the normal breast tissue specimens. *FYN* is known to be expressed in other normal tissue (194), but it's also likely that this finding is ambiguous because of the age difference of this cohort compared to the other two. SFK member *LCK* was higher expressed in ER negative compared to ER positive tumours.

SRC was the only SFK member, which was associated with clinical outcome. Breast cancer patients with high *SRC* mRNA expression had a shorter disease specific survival. Up till now there hasn't been a study which looked into mRNA expression of mammalian expressed SFK members in various breast tissue types, comparing and correlating the diverse expression levels and their significance to clinical parameters (e.g. ER status) and clinical outcome (e.g. disease specific survival).

Due to small patient numbers in the malignant cohort (n=81) and unknown transcription from mRNA to protein synthesis and expression, we want to explore further expression of Src, Lyn and Lck proteins and their association with survival in a larger cohort. Cellular location and activation status of those proteins were able to be evaluated through indirect immunohistochemistry. Only a few studies (114;115;125;221;245) in the breast cancer related literature used this method to investigate if elevated protein expression and cellular distribution in clinical specimens were imperative. Only two other research groups related their findings to important aspects for clinicians like recurrence and/ or survival (115;116). None of these groups linked Src expression and activation to received adjuvant treatment, de-novo or acquired systemic treatment resistance. Parallel to this project, our group examined the role of SFK members in tamoxifen resistance in an unmixed ER positive cohort. No evidence was found to support a role for the Src family in de novo tamoxifen resistance. However, after 5 years of hormonal therapy, patients with high cytoplasmic c-Src expression in their breast tumours had a poorer clinical outcome. This result has raised several questions:

Do patients with high cytoplasmic c-Src need to be selected for aromatase inhibitors?

Do patients need to be selected for continuing endocrine therapy (> 5 years)?

Do patients with advanced breast cancer and acquired endocrine resistance benefit from complementing a Src inhibitor to their systemic hormonal therapy?

Interestingly in our mixed cohort, it was also high expression of c-Src in the cytoplasm, which was associated with poorer clinical outcome.

None of the phosphorylation sites of Src were able to be linked with acquired tamoxifen resistance and disease specific survival in the pure ER positive cohort. This differs significantly to our findings showing a strong association between Src activation and clinical outcome of breast cancer patients.

It is well established in various cell lines derived from colon, lung or prostate tumours (90;212;214) that Dasatinib influences cell growth, proliferation and inhibits Src activation. With Src inhibitors currently being trialled in breast cancer it was necessary to explore what impact Dasatinib could have on the individual phosphorylation sites of Src and other SFK members. Various breast cancer cell lines were chosen to represent the different subgroup of breast cancer patients. To be able to compare results gained from IHC and cell line study and to draw conclusions, we investigated protein expression in cell line cell pellets with the same antibodies used for immunohistochemistry. No *in vitro* study in the currently literature has used this method to establish what influence drug treatments have on protein expression. The method of choice has always been Western Blotting. To strengthen our findings, Western Blotting from cell lysates, exposed to the same drug stimulation and inhibition, should be performed.

Nevertheless it is encouraging that membrane Y419Src expression was significantly decreased in all cell lines after Dasatinib exposure implying that patients with increased activated (p419)Src kinase receiving Dasatinib would improve their clinical outcome and prolong their survival. On the other hand we showed that expression of Y215Src stayed unchanged in all cell lines during exposure to different drug treatments. With the knowledge that patients, expressing nuclear and cytoplasmic Y215Src highly in their breast

cancer, have a better disease specific survival, it is reassuring that exposure/ administration of Dasatinib would not impact negatively on the clinical outcome of those patients.

Due to the lack of Src mutation and gene amplification in the majority of tumours, it is only recently that Src kinase was accepted as a target for drug development. Mainly the increased enzyme activity in primary tumours and further rise in synchronous metastasis (213) has led to advance in molecular targeted therapy.

Four compounds have shown to have sufficient potency and acceptable toxicity for the development as Src kinase inhibitors. Dasatinib has now been approved by NICE for the treatment of chronic myelogenous leukaemia (CML) partially based on a 95% complete haematological response rate for chronic-phase CML (246).

Guided by preclinical studies, clinical trials are being conducted with Src inhibitors as monotherapy or in combination with cytotoxic chemotherapy, hormonal therapy and growth factor inhibitors. More than 50 trials of Src inhibitors are currently ongoing or about to open (189). In the beginning it was thought that Src inhibitors could be potent enough to be used for single agent therapy. However, cell lines studies showed that effects of Src inhibitors on cell proliferation was independent of Src kinase inhibition and more a result of inhibition of other tyrosine kinases (168);(185). Other preclinical studies report a limited affect of Src inhibitors on cell proliferation (83;188;247), questioning the benefit of their administration in the clinical setting. Following on from this, many contemporary trials explore the potential advantage of combining Src inhibitors with chemotherapy agents and other biological targeted molecules.

Several questions still need to be answered:

Is there a subgroup of tumours, which are uniquely susceptible to Src kinase inhibitors?

Would membrane Y419Src expression be suitable as a validated biomarker for predicting response to all Src kinase inhibitors?

Is the role for Src kinase inhibitors more in the anti-invasive and anti-metastatic setting rather than anti-proliferative early stage of tumours?

The ability of Src inhibitors to overcome resistance to standard therapies and tolerable toxicity profile (246) sends out hope that Src inhibitors in combination with cytotoxic anticancer drugs will be available as standard therapy for certain cancer patients.

Within the next few years, ongoing research will provide answers regards Src kinase inhibitors' role in cancer treatment, just in time for the centennial anniversary of Rous's discovery of the sarcoma virus v-Src.

List of References

- (1) www.statistics.gov.uk. Ref Type: Internet Communication
- (2) www.isdscotland.org/isd/1420.html. Ref Type: Internet Communication
- (3) <http://info.cancerresearchuk.org/cancerstats/types/breast>. Ref Type: Internet Communication
- (4) Key TJ, Verkasalo PK, Banks E. Epidemiology of breast cancer. *Lancet Oncol* 2001; 2(3):133-140.
- (5) Banks E. Hormone replacement therapy and the sensitivity and specificity of breast cancer screening: a review. *J Med Screen* 2001; 8(1):29-34.
- (6) Dixon JM. Hormone replacement therapy and the breast. *BMJ* 2001; 323(7326):1381-1382.
- (7) Chlebowski RT, Hendrix SL, Langer RD, Stefanick ML, Gass M, Lane D et al. Influence of estrogen plus progestin on breast cancer and mammography in healthy postmenopausal women: the Women's Health Initiative Randomized Trial. *JAMA* 2003; 289(24):3243-3253.
- (8) Beral V. Breast cancer and hormone-replacement therapy in the Million Women Study. *Lancet* 2003; 362(9382):419-427.
- (9) Bergstrom A, Pisani P, Tenet V, Wolk A, Adami HO. Overweight as an avoidable cause of cancer in Europe. *Int J Cancer* 2001; 91(3):421-430.
- (10) van den Brandt PA, Spiegelman D, Yaun SS, Adami HO, Beeson L, Folsom AR et al. Pooled analysis of prospective cohort studies on height, weight, and breast cancer risk. *Am J Epidemiol* 2000; 152(6):514-527.
- (11) Key TJ, Appleby PN, Reeves GK, Roddam A, Dorgan JF, Longcope C et al. Body mass index, serum sex hormones, and breast cancer risk in postmenopausal women. *J Natl Cancer Inst* 2003; 95(16):1218-1226.

- (12) Vainio H, Kaaks R, Bianchini F. Weight control and physical activity in cancer prevention: international evaluation of the evidence. *Eur J Cancer Prev* 2002; 11 Suppl 2:S94-100.
- (13) Hamajima N, Hirose K, Tajima K, Rohan T, Calle EE, Heath CW, Jr. et al. Alcohol, tobacco and breast cancer--collaborative reanalysis of individual data from 53 epidemiological studies, including 58,515 women with breast cancer and 95,067 women without the disease. *Br J Cancer* 2002; 87(11):1234-1245.
- (14) Berrington dG, Darby S. Risk of cancer from diagnostic X-rays: estimates for the UK and 14 other countries. *Lancet* 2004; 363(9406):345-351.
- (15) www.show.scot.nhs.uk/isd/cancer/cancer.htm(2004). Ref Type: Internet Communication
- (16) Byrne C. Mammographic density: a breast cancer risk factor or diagnostic indicator? *Acad Radiol* 2002; 9(3):253-255.
- (17) Byrne C, Connolly JL, Colditz GA, Schnitt SJ. Biopsy confirmed benign breast disease, postmenopausal use of exogenous female hormones, and breast carcinoma risk. *Cancer* 2000; 89(10):2046-2052.
- (18) Dupont WD, Page DL. Risk factors for breast cancer in women with proliferative breast disease. *N Engl J Med* 1985; 312(3):146-151.
- (19) Chen Y, Thompson W, Semenciw R, Mao Y. Epidemiology of contralateral breast cancer. *Cancer Epidemiol Biomarkers Prev* 1999; 8(10):855-861.
- (20) Clamp A, Danson S, Clemons M. Hormonal risk factors for breast cancer: identification, chemoprevention, and other intervention strategies. *Lancet Oncol* 2002; 3(10):611-619.
- (21) Collaborative Group on Hormonal Factors in Breast Cancer. Familial breast cancer: collaborative reanalysis of individual data from 52 epidemiological studies including 58,209 women with breast cancer and 101,986 women without the disease. *Lancet* 2001; 358(9291):1389-1399.

- (22) Ford D, Easton DF, Stratton M, Narod S, Goldgar D, Devilee P et al. Genetic heterogeneity and penetrance analysis of the BRCA1 and BRCA2 genes in breast cancer families. The Breast Cancer Linkage Consortium. *Am J Hum Genet* 1998; 62(3):676-689.
- (23) Wooster R, Bignell G, Lancaster J, Swift S, Seal S, Mangion J et al. Identification of the breast cancer susceptibility gene BRCA2. *Nature* 1995; 378(6559):789-792.
- (24) Pinder SE, Ellis IO, Elston CW. Prognostic factors in primary breast carcinoma. *J Clin Pathol* 1995; 48(11):981-983.
- (25) Sunil R Lakharu et al. *Basic Pathology- An intro to mechanisms of diseases*. 2006.
- (26) Haybittle JL, Blamey RW, Elston CW, Johnson J, Doyle PJ, Campbell FC et al. A prognostic index in primary breast cancer. *Br J Cancer* 1982; 45(3):361-366.
- (27) Yager JD, Davidson NE. Estrogen carcinogenesis in breast cancer. *N Engl J Med* 2006; 354(3):270-282.
- (28) Levin ER. Cell localization, physiology, and nongenomic actions of estrogen receptors. *J Appl Physiol* 2001; 91(4):1860-1867.
- (29) Govind AP, Thampan RV. Proteins interacting with the mammalian estrogen receptor: proposal for an integrated model for estrogen receptor mediated regulation of transcription. *J Cell Biochem* 2001; 80(4):571-579.
- (30) Pearce ST, Jordan VC. The biological role of estrogen receptors alpha and beta in cancer. *Crit Rev Oncol Hematol* 2004; 50(1):3-22.
- (31) Levin ER. Bidirectional signaling between the estrogen receptor and the epidermal growth factor receptor. *Mol Endocrinol* 2003; 17(3):309-317.
- (32) Early breast cancer trialists' collaborative group. Effects of chemotherapy and hormonal therapy for early breast cancer on recurrence and 15-year survival: an overview of the randomised trials. *Lancet* 2005; 365(9472):1687-1717.

- (33) Rhodes A, Jasani B, Balaton AJ, Barnes DM, Miller KD. Frequency of oestrogen and progesterone receptor positivity by immunohistochemical analysis in 7016 breast carcinomas: correlation with patient age, assay sensitivity, threshold value, and mammographic screening. *J Clin Pathol* 2000; 53(9):688-696.
- (34) Kastner P, Krust A, Turcotte B, Stropp U, Tora L, Gronemeyer H et al. Two distinct estrogen-regulated promoters generate transcripts encoding the two functionally different human progesterone receptor forms A and B. *EMBO J* 1990; 9(5):1603-1614.
- (35) Bardou VJ, Arpino G, Elledge RM, Osborne CK, Clark GM. Progesterone receptor status significantly improves outcome prediction over estrogen receptor status alone for adjuvant endocrine therapy in two large breast cancer databases. *J Clin Oncol* 2003; 21(10):1973-1979.
- (36) Howell A, Cuzick J, Baum M, Buzdar A, Dowsett M, Forbes JF et al. Results of the ATAC (Arimidex, Tamoxifen, Alone or in Combination) trial after completion of 5 years' adjuvant treatment for breast cancer. *Lancet* 2005; 365(9453):60-62.
- (37) Osborne CK, Schiff R. Estrogen-receptor biology: continuing progress and therapeutic implications. *J Clin Oncol* 2005; 23(8):1616-1622.
- (38) Cui X, Zhang P, Deng W, Oesterreich S, Lu Y, Mills GB et al. Insulin-like growth factor-I inhibits progesterone receptor expression in breast cancer cells via the phosphatidylinositol 3-kinase/Akt/mammalian target of rapamycin pathway: progesterone receptor as a potential indicator of growth factor activity in breast cancer. *Mol Endocrinol* 2003; 17(4):575-588.
- (39) King CR, Kraus MH, Aaronson SA. Amplification of a novel v-erbB-related gene in a human mammary carcinoma. *Science* 1985; 229(4717):974-976.
- (40) Coussens L, Yang-Feng TL, Liao YC, Chen E, Gray A, McGrath J et al. Tyrosine kinase receptor with extensive homology to EGF receptor shares chromosomal location with neu oncogene. *Science* 1985; 230(4730):1132-1139.

- (41) Cho HS, Mason K, Ramyar KX, Stanley AM, Gabelli SB, Denney DW, Jr. et al. Structure of the extracellular region of HER2 alone and in complex with the Herceptin Fab. *Nature* 2003; 421(6924):756-760.
- (42) Warnberg F, Casalini P, Nordgren H, Bergkvist L, Holmberg L, Menard S. Ductal carcinoma in situ of the breast: a new phenotype classification system and its relation to prognosis. *Breast Cancer Res Treat* 2002; 73(3):215-221.
- (43) Casalini P, Botta L, Menard S. Role of p53 in HER2-induced proliferation or apoptosis. *J Biol Chem* 2001; 276(15):12449-12453.
- (44) Menard S, Tagliabue E, Campiglio M, Pupa SM. Role of HER2 gene overexpression in breast carcinoma. *J Cell Physiol* 2000; 182(2):150-162.
- (45) Masood S, Bui MM. Prognostic and predictive value of HER2/neu oncogene in breast cancer. *Microsc Res Tech* 2002; 59(2):102-108.
- (46) Grunt TW, Saceda M, Martin MB, Lupu R, Dittrich E, Krupitza G et al. Bidirectional interactions between the estrogen receptor and the *cerbB-2* signaling pathways: heregulin inhibits estrogenic effects in breast cancer cells. *Int J Cancer* 1995; 63(4):560-567.
- (47) Elledge RM, Green S, Ciocca D, Pugh R, Allred DC, Clark GM et al. HER-2 expression and response to tamoxifen in estrogen receptor-positive breast cancer: a Southwest Oncology Group Study. *Clin Cancer Res* 1998; 4(1):7-12.
- (48) Normanno N, Ciardiello F, Brandt R, Salomon DS. Epidermal growth factor-related peptides in the pathogenesis of human breast cancer. *Breast Cancer Res Treat* 1994; 29(1):11-27.
- (49) Mueller H, Kueng W, Schoumacher F, Herzer S, Eppenberger U. Selective regulation of steroid receptor expression in MCF-7 breast cancer cells by a novel member of the heregulin family. *Biochem Biophys Res Commun* 1995; 217(3):1271-1278.

- (50) Tang CK, Perez C, Grunt T, Waibel C, Cho C, Lupu R. Involvement of heregulin-beta2 in the acquisition of the hormone-independent phenotype of breast cancer cells. *Cancer Res* 1996; 56(14):3350-3358.
- (51) Piccart-Gebhart MJ, Procter M, Leyland-Jones B, Goldhirsch A, Untch M, Smith I et al. Trastuzumab after adjuvant chemotherapy in HER2-positive breast cancer. *N Engl J Med* 2005; 353(16):1659-1672.
- (52) Broders AC. Cancer that is not always placed in the cancer category. *Tex Rep Biol Med* 1950; 8(4):468-470.
- (53) Fentiman IS. 8. The dilemma of in situ carcinoma of the breast. *Int J Clin Pract* 2001; 55(10):680-683.
- (54) Houghton J, George WD, Cuzick J, Duggan C, Fentiman IS, Spittle M. Radiotherapy and tamoxifen in women with completely excised ductal carcinoma in situ of the breast in the UK, Australia, and New Zealand: randomised controlled trial. *Lancet* 2003; 362(9378):95-102.
- (55) Early breast cancer trialists' collaborative group. Radiotherapy for early breast cancer. *Cochrane Database Syst Rev* 2002;(2):CD003647.
- (56) Early breast cancer trialists' collaborative group. Multi-agent chemotherapy for early breast cancer. *Cochrane Database Syst Rev* 2002;(1):CD000487.
- (57) Poole CJ, Earl HM, Hiller L, Dunn JA, Bathers S, Grieve RJ et al. Epirubicin and cyclophosphamide, methotrexate, and fluorouracil as adjuvant therapy for early breast cancer. *N Engl J Med* 2006; 355(18):1851-1862.
- (58) Ellis P, Barrett-Lee P, Johnson L, Cameron D, Wardley A, O'Reilly S et al. Sequential docetaxel as adjuvant chemotherapy for early breast cancer (TACT): an open-label, phase III, randomised controlled trial. *Lancet* 2009; 373(9676):1681-1692.

- (59) Wishart GC, Gaston M, Poultsidis AA, Purushotham AD. Hormone receptor status in primary breast cancer--time for a consensus? *Eur J Cancer* 2002; 38(9):1201-1203.
- (60) Early breast cancer trialists' collaborative group. Systemic treatment of early breast cancer by hormonal, cytotoxic, or immune therapy. 133 randomised trials involving 31,000 recurrences and 24,000 deaths among 75,000 women. *Lancet* 1992; 339(8784):1-15.
- (61) Early breast cancer trialists' collaborative group. Tamoxifen for early breast cancer: an overview of the randomised trials. *Lancet* 1998; 351(9114):1451-1467.
- (62) Baum M. The ATAC (Arimidex, Tamoxifen, Alone or in Combination) adjuvant breast cancer trial in postmenopausal patients: factors influencing the success of patient recruitment. *Eur J Cancer* 2002; 38(15):1984-1986.
- (63) Bartlett J, Mallon E, Cooke T. The clinical evaluation of HER-2 status: which test to use? *J Pathol* 2003; 199(4):411-417.
- (64) Eisenhauer EA. From the molecule to the clinic--inhibiting HER2 to treat breast cancer. *N Engl J Med* 2001; 344(11):841-842.
- (65) Frame MC. Src in cancer: deregulation and consequences for cell behaviour. *Biochim Biophys Acta* 2002; 1602(2):114-130.
- (66) Yeatman TJ. A renaissance for SRC. *Nat Rev Cancer* 2004; 4(6):470-480.
- (67) Roskoski R, Jr. Src protein-tyrosine kinase structure and regulation. *Biochem Biophys Res Commun* 2004; 324(4):1155-1164.
- (68) Thomas SM, Brugge JS. Cellular functions regulated by Src family kinases. *Annu Rev Cell Dev Biol* 1997; 13:513-609.
- (69) Rous P. A sarcoma of the fowl transmissible by an agent separable for the tumor cells. *Journal of Experimental Medicine* 13, 397-411. 1911.

- (70) Martin GS. Rous sarcoma virus: a function required for the maintenance of the transformed state. *Nature* 227, 1021-1023. 1970.
- (71) Stehelin D, Guntaka RV, Varmus HE, Bishop JM. Purification of DNA complementary to nucleotide sequences required for neoplastic transformation of fibroblasts by avian sarcoma viruses. *J Mol Biol* 1976; 101(3):349-365.
- (72) Frame MC, Fincham VJ, Carragher NO, Wyke JA. v-Src's hold over actin and cell adhesions. *Nat Rev Mol Cell Biol* 2002; 3(4):233-245.
- (73) Ly QP, Yeatman TJ. Clinical relevance of targeted interference with Src-mediated signal transduction events. *Recent Results Cancer Res* 2007; 172:169-188.
- (74) Cooper JA, Howell B. The when and how of Src regulation. *Cell* 1993; 73(6):1051-1054.
- (75) Roskoski R, Jr. Src kinase regulation by phosphorylation and dephosphorylation. *Biochem Biophys Res Commun* 2005; 331(1):1-14.
- (76) Stover DR, Furet P, Lydon NB. Modulation of the SH2 binding specificity and kinase activity of Src by tyrosine phosphorylation within its SH2 domain. *J Biol Chem* 1996; 271(21):12481-12487.
- (77) Mayer BJ. SH3 domains: complexity in moderation. *J Cell Sci* 2001; 114(Pt 7):1253-1263.
- (78) Elsberger B, Tan BA, Mitchell TJ, Brown SB, Mallon EA, Tovey SM et al. Is expression or activation of Src kinase associated with cancer-specific survival in ER-, PR- and HER2-negative breast cancer patients? *Am J Pathol* 2009; 175(4):1389-1397.
- (79) Bjorge JD, Jakymiw A, Fujita DJ. Selected glimpses into the activation and function of Src kinase. *Oncogene* 2000; 19(49):5620-5635.

- (80) Fincham VJ, Brunton VG, Frame MC. The SH3 domain directs acto-myosin-dependent targeting of v-Src to focal adhesions via phosphatidylinositol 3-kinase. *Mol Cell Biol* 2000; 20(17):6518-6536.
- (81) Lin PH, Shenoy S, Galitski T, Shalloway D. Transformation of mouse cells by wild-type mouse c-Src. *Oncogene* 1995; 10(2):401-405.
- (82) Chambers AF, Groom AC, MacDonald IC. Dissemination and growth of cancer cells in metastatic sites. *Nat Rev Cancer* 2002; 2(8):563-572.
- (83) Boyer B, Bourgeois Y, Poupon MF. Src kinase contributes to the metastatic spread of carcinoma cells. *Oncogene* 2002; 21(15):2347-2356.
- (84) Nakagawa T, Tanaka S, Suzuki H, Takayanagi H, Miyazaki T, Nakamura K et al. Overexpression of the csk gene suppresses tumor metastasis in vivo. *Int J Cancer* 2000; 88(3):384-391.
- (85) Jallal H, Valentino ML, Chen G, Boschelli F, Ali S, Rabbani SA. A Src/Abl kinase inhibitor, SKI-606, blocks breast cancer invasion, growth, and metastasis in vitro and in vivo. *Cancer Res* 2007; 67(4):1580-1588.
- (86) Myoui A, Nishimura R, Williams PJ, Hiraga T, Tamura D, Michigami T et al. C-SRC tyrosine kinase activity is associated with tumor colonization in bone and lung in an animal model of human breast cancer metastasis. *Cancer Res* 2003; 63(16):5028-5033.
- (87) Pichot CS, Hartig SM, Xia L, Arvanitis C, Monisvais D, Lee FY et al. Dasatinib synergizes with doxorubicin to block growth, migration, and invasion of breast cancer cells. *Br J Cancer* 2009; 101(1):38-47.
- (88) Schlaepfer DD, Hauck CR, Sieg DJ. Signaling through focal adhesion kinase. *Prog Biophys Mol Biol* 1999; 71(3-4):435-478.
- (89) Edwards J, Krishna NS, Witton CJ, Bartlett JM. Gene amplifications associated with the development of hormone-resistant prostate cancer. *Clin Cancer Res* 2003; 9(14):5271-5281.

- (90) Tatarov O, Mitchell TJ, Seywright M, Leung HY, Brunton VG, Edwards J. SRC family kinase activity is up-regulated in hormone-refractory prostate cancer. *Clin Cancer Res* 2009; 15(10):3540-3549.
- (91) Fincham VJ, Frame MC. The catalytic activity of Src is dispensable for translocation to focal adhesions but controls the turnover of these structures during cell motility. *EMBO J* 1998; 17(1):81-92.
- (92) Hynes RO. Integrins: versatility, modulation, and signaling in cell adhesion. *Cell* 1992; 69(1):11-25.
- (93) Serrels A, Timpson P, Canel M, Schwarz JP, Carragher NO, Frame MC et al. Real-time study of E-cadherin and membrane dynamics in living animals: implications for disease modeling and drug development. *Cancer Res* 2009; 69(7):2714-2719.
- (94) Guo W, Giancotti FG. Integrin signalling during tumour progression. *Nat Rev Mol Cell Biol* 2004; 5(10):816-826.
- (95) Huang C, Ni Y, Wang T, Gao Y, Haudenschild CC, Zhan X. Down-regulation of the filamentous actin cross-linking activity of cortactin by Src-mediated tyrosine phosphorylation. *J Biol Chem* 1997; 272(21):13911-13915.
- (96) Weaver AM, Karginov AV, Kinley AW, Weed SA, Li Y, Parsons JT et al. Cortactin promotes and stabilizes Arp2/3-induced actin filament network formation. *Curr Biol* 2001; 11(5):370-374.
- (97) Chan KT, Cortesio CL, Huttenlocher A. FAK alters invadopodia and focal adhesion composition and dynamics to regulate breast cancer invasion. *J Cell Biol* 2009; 185(2):357-370.
- (98) Nyalendo C, Michaud M, Beaulieu E, Roghi C, Murphy G, Gingras D et al. Src-dependent phosphorylation of membrane type I matrix metalloproteinase on cytoplasmic tyrosine 573: role in endothelial and tumor cell migration. *J Biol Chem* 2007; 282(21):15690-15699.

- (99) Shih WL, Liao MH, Yu FL, Lin PY, Hsu HY, Chiu SJ. AMF/PGI transactivates the MMP-3 gene through the activation of Src-RhoA-phosphatidylinositol 3-kinase signaling to induce hepatoma cell migration. *Cancer Lett* 2008; 270(2):202-217.
- (100) Leupold JH, Asangani I, Maurer GD, Lengyel E, Post S, Allgayer H. Src induces urokinase receptor gene expression and invasion/intravasation via activator protein-1/p-c-Jun in colorectal cancer. *Mol Cancer Res* 2007; 5(5):485-496.
- (101) Weis S, Cui J, Barnes L, Cheresch D. Endothelial barrier disruption by VEGF-mediated Src activity potentiates tumor cell extravasation and metastasis. *J Cell Biol* 2004; 167(2):223-229.
- (102) Criscuoli ML, Nguyen M, Eliceiri BP. Tumor metastasis but not tumor growth is dependent on Src-mediated vascular permeability. *Blood* 2005; 105(4):1508-1514.
- (103) Frisch SM, Francis H. Disruption of epithelial cell-matrix interactions induces apoptosis. *J Cell Biol* 1994; 124(4):619-626.
- (104) Johnson D, Agochiya M, Samejima K, Earnshaw W, Frame M, Wyke J. Regulation of both apoptosis and cell survival by the v-Src oncoprotein. *Cell Death Differ* 2000; 7(8):685-696.
- (105) Giannoni E, Fiaschi T, Ramponi G, Chiarugi P. Redox regulation of anoikis resistance of metastatic prostate cancer cells: key role for Src and EGFR-mediated pro-survival signals. *Oncogene* 2009; 28(20):2074-2086.
- (106) Mukhopadhyay D, Tsiokas L, Zhou XM, Foster D, Brugge JS, Sukhatme VP. Hypoxic induction of human vascular endothelial growth factor expression through c-Src activation. *Nature* 1995; 375(6532):577-581.
- (107) Summy JM, Trevino JG, Lesslie DP, Baker CH, Shakespeare WC, Wang Y et al. AP23846, a novel and highly potent Src family kinase inhibitor, reduces vascular endothelial growth factor and interleukin-8 expression in human solid tumor cell lines and abrogates downstream angiogenic processes. *Mol Cancer Ther* 2005; 4(12):1900-1911.

- (108) Araujo J, Logothetis C. Targeting Src signaling in metastatic bone disease. *Int J Cancer* 2009; 124(1):1-6.
- (109) Duong LT, Lakkakorpi PT, Nakamura I, Machwate M, Nagy RM, Rodan GA. PYK2 in osteoclasts is an adhesion kinase, localized in the sealing zone, activated by ligation of alpha(v)beta3 integrin, and phosphorylated by src kinase. *J Clin Invest* 1998; 102(5):881-892.
- (110) Soriano P, Montgomery C, Geske R, Bradley A. Targeted disruption of the c-src proto-oncogene leads to osteopetrosis in mice. *Cell* 1991; 64(4):693-702.
- (111) Roodman GD. Mechanisms of bone metastasis. *N Engl J Med* 2004; 350(16):1655-1664.
- (112) Zhang XH, Wang Q, Gerald W, Hudis CA, Norton L, Smid M et al. Latent bone metastasis in breast cancer tied to Src-dependent survival signals. *Cancer Cell* 2009; 16(1):67-78.
- (113) Ottenhoff-Kalff AE, Rijksen G, van Beurden EA, Hennipman A, Michels AA, Staal GE. Characterization of protein tyrosine kinases from human breast cancer: involvement of the c-src oncogene product. *Cancer Res* 1992; 52(17):4773-4778.
- (114) Verbeek BS, Vroom TM, Adriaansen-Slot SS, Ottenhoff-Kalff AE, Geertzema JG, Hennipman A et al. c-Src protein expression is increased in human breast cancer. An immunohistochemical and biochemical analysis. *J Pathol* 1996; 180(4):383-388.
- (115) Wilson GR, Cramer A, Welman A, Knox F, Swindell R, Kawakatsu H et al. Activated c-SRC in ductal carcinoma in situ correlates with high tumour grade, high proliferation and HER2 positivity. *Br J Cancer* 2006; 95(10):1410-1414.
- (116) Ito Y, Kawakatsu H, Takeda T, Tani N, Kawaguchi N, Noguchi S et al. Activation of c-Src is inversely correlated with biological aggressiveness of breast carcinoma. *Breast Cancer Res Treat* 2002; 76(3):261-267.

- (117) Feng W, Webb P, Nguyen P, Liu X, Li J, Karin M et al. Potentiation of estrogen receptor activation function 1 (AF-1) by Src/JNK through a serine 118-independent pathway. *Mol Endocrinol* 2001; 15(1):32-45.
- (118) Shah YM, Rowan BG. The Src kinase pathway promotes tamoxifen agonist action in Ishikawa endometrial cells through phosphorylation-dependent stabilization of estrogen receptor (alpha) promoter interaction and elevated steroid receptor coactivator 1 activity. *Mol Endocrinol* 2005; 19(3):732-748.
- (119) Acconcia F, Kumar R. Signaling regulation of genomic and nongenomic functions of estrogen receptors. *Cancer Lett* 2006; 238(1):1-14.
- (120) Migliaccio A, Di Domenico M, Castoria G, de Falco A, Bontempo P, Nola E et al. Tyrosine kinase/p21ras/MAP-kinase pathway activation by estradiol-receptor complex in MCF-7 cells. *EMBO J* 1996; 15(6):1292-1300.
- (121) Castoria G, Migliaccio A, Bilancio A, Di Domenico M, de Falco A, Lombardi M et al. PI3-kinase in concert with Src promotes the S-phase entry of oestradiol-stimulated MCF-7 cells. *EMBO J* 2001; 20(21):6050-6059.
- (122) Barletta F, Wong CW, McNally C, Komm BS, Katzenellenbogen B, Cheskis BJ. Characterization of the interactions of estrogen receptor and MNAR in the activation of cSrc. *Mol Endocrinol* 2004; 18(5):1096-1108.
- (123) Summy JM, Gallick GE. Src family kinases in tumor progression and metastasis. *Cancer Metastasis Rev* 2003; 22(4):337-358.
- (124) Biscardi JS, Ishizawar RC, Silva CM, Parsons SJ. Tyrosine kinase signalling in breast cancer: epidermal growth factor receptor and c-Src interactions in breast cancer. *Breast Cancer Res* 2000; 2(3):203-210.
- (125) Vadlamudi RK, Sahin AA, Adam L, Wang RA, Kumar R. Heregulin and HER2 signaling selectively activates c-Src phosphorylation at tyrosine 215. *FEBS Lett* 2003; 543(1-3):76-80.

- (126) Mitra SK, Schlaepfer DD. Integrin-regulated FAK-Src signaling in normal and cancer cells. *Curr Opin Cell Biol* 2006; 18(5):516-523.
- (127) Tan M, Li P, Klos KS, Lu J, Lan KH, Nagata Y et al. ErbB2 promotes Src synthesis and stability: novel mechanisms of Src activation that confer breast cancer metastasis. *Cancer Res* 2005; 65(5):1858-1867.
- (128) Ishizawar RC, Miyake T, Parsons SJ. c-Src modulates ErbB2 and ErbB3 heterocomplex formation and function. *Oncogene* 2007; 26(24):3503-3510.
- (129) Silva CM, Shupnik MA. Integration of steroid and growth factor pathways in breast cancer: focus on signal transducers and activators of transcription and their potential role in resistance. *Mol Endocrinol* 2007; 21(7):1499-1512.
- (130) Arpino G, Wiechmann L, Osborne CK, Schiff R. Crosstalk between the estrogen receptor and the HER tyrosine kinase receptor family: molecular mechanism and clinical implications for endocrine therapy resistance. *Endocr Rev* 2008; 29(2):217-233.
- (131) Varricchio L, Migliaccio A, Castoria G, Yamaguchi H, de Falco A, Di Domenico M et al. Inhibition of estradiol receptor/Src association and cell growth by an estradiol receptor alpha tyrosine-phosphorylated peptide. *Mol Cancer Res* 2007; 5(11):1213-1221.
- (132) Bolen JB, Brugge JS. Leukocyte protein tyrosine kinases: potential targets for drug discovery. *Annu Rev Immunol* 1997; 15:371-404.
- (133) Goldenberg-Furmanov M, Stein I, Pikarsky E, Rubin H, Kasem S, Wygoda M et al. Lyn is a target gene for prostate cancer: sequence-based inhibition induces regression of human tumor xenografts. *Cancer Res* 2004; 64(3):1058-1066.
- (134) Bates RC, Edwards NS, Burns GF, Fisher DE. A CD44 survival pathway triggers chemoresistance via lyn kinase and phosphoinositide 3-kinase/Akt in colon carcinoma cells. *Cancer Res* 2001; 61(13):5275-5283.

- (135) Corey SJ, Anderson SM. Src-related protein tyrosine kinases in hematopoiesis. *Blood* 1999; 93(1):1-14.
- (136) Ingley E. Csk-binding protein can regulate Lyn signals controlling cell morphology. *Int J Biochem Cell Biol* 2009; 41(6):1332-1343.
- (137) Cichowski K, McCormick F, Brugge JS. p21rasGAP association with Fyn, Lyn, and Yes in thrombin-activated platelets. *J Biol Chem* 1992; 267(8):5025-5028.
- (138) Ingley E, Klinken SP. Cross-regulation of JAK and Src kinases. *Growth Factors* 2006; 24(1):89-95.
- (139) Ingley E. Src family kinases: regulation of their activities, levels and identification of new pathways. *Biochim Biophys Acta* 2008; 1784(1):56-65.
- (140) Roginskaya V, Zuo S, Caudell E, Nambudiri G, Kraker AJ, Corey SJ. Therapeutic targeting of Src-kinase Lyn in myeloid leukemic cell growth. *Leukemia* 1999; 13(6):855-861.
- (141) Wilson MB, Schreiner SJ, Choi HJ, Kamens J, Smithgall TE. Selective pyrrolo-pyrimidine inhibitors reveal a necessary role for Src family kinases in Bcr-Abl signal transduction and oncogenesis. *Oncogene* 2002; 21(53):8075-8088.
- (142) Warmuth M, Simon N, Mitina O, Mathes R, Fabbro D, Manley PW et al. Dual-specific Src and Abl kinase inhibitors, PP1 and CGP76030, inhibit growth and survival of cells expressing imatinib mesylate-resistant Bcr-Abl kinases. *Blood* 2003; 101(2):664-672.
- (143) Sumitomo M, Shen R, Walburg M, Dai J, Geng Y, Navarro D et al. Neutral endopeptidase inhibits prostate cancer cell migration by blocking focal adhesion kinase signaling. *J Clin Invest* 2000; 106(11):1399-1407.
- (144) Straus DB, Weiss A. Genetic evidence for the involvement of the lck tyrosine kinase in signal transduction through the T cell antigen receptor. *Cell* 1992; 70(4):585-593.

- (145) Ley SC, Marsh M, Bebbington CR, Proudfoot K, Jordan P. Distinct intracellular localization of Lck and Fyn protein tyrosine kinases in human T lymphocytes. *J Cell Biol* 1994; 125(3):639-649.
- (146) Hatakeyama M, Kono T, Kobayashi N, Kawahara A, Levin SD, Perlmutter RM et al. Interaction of the IL-2 receptor with the src-family kinase p56lck: identification of novel intermolecular association. *Science* 1991; 252(5012):1523-1528.
- (147) Marie-Cardine A, Maridonneau-Parini I, Ferrer M, Danielian S, Rothhut B, Fagard R et al. The lymphocyte-specific tyrosine protein kinase p56lck is endocytosed in Jurkat cells stimulated via CD2. *J Immunol* 1992; 148(12):3879-3884.
- (148) Shenoy-Scaria AM, Gauen LK, Kwong J, Shaw AS, Lublin DM. Palmitoylation of an amino-terminal cysteine motif of protein tyrosine kinases p56lck and p59fyn mediates interaction with glycosyl-phosphatidylinositol-anchored proteins. *Mol Cell Biol* 1993; 13(10):6385-6392.
- (149) Palacios EH, Weiss A. Function of the Src-family kinases, Lck and Fyn, in T-cell development and activation. *Oncogene* 2004; 23(48):7990-8000.
- (150) Krystal GW, DeBerry CS, Linnekin D, Litz J. Lck associates with and is activated by Kit in a small cell lung cancer cell line: inhibition of SCF-mediated growth by the Src family kinase inhibitor PP1. *Cancer Res* 1998; 58(20):4660-4666.
- (151) Samraj AK, Stroh C, Fischer U, Schulze-Osthoff K. The tyrosine kinase Lck is a positive regulator of the mitochondrial apoptosis pathway by controlling Bak expression. *Oncogene* 2006; 25(2):186-197.
- (152) Abts H, Jucker M, Diehl V, Tesch H. Human chronic lymphocytic leukemia cells regularly express mRNAs of the protooncogenes lck and c-fgr. *Leuk Res* 1991; 15(11):987-997.
- (153) Majolini MB, Boncristiano M, Baldari CT. Dysregulation of the protein tyrosine kinase LCK in lymphoproliferative disorders and in other neoplasias. *Leuk Lymphoma* 1999; 35(3-4):245-254.

- (154) Abraham KM, Levin SD, Marth JD, Forbush KA, Perlmutter RM. Thymic tumorigenesis induced by overexpression of p56lck. *Proc Natl Acad Sci U S A* 1991; 88(9):3977-3981.
- (155) Kurt RA, Urba WJ, Smith JW, Schoof DD. Peripheral T lymphocytes from women with breast cancer exhibit abnormal protein expression of several signaling molecules. *Int J Cancer* 1998; 78(1):16-20.
- (156) Finke JH, Zea AH, Stanley J, Longo DL, Mizoguchi H, Tubbs RR et al. Loss of T-cell receptor zeta chain and p56lck in T-cells infiltrating human renal cell carcinoma. *Cancer Res* 1993; 53(23):5613-5616.
- (157) Rabinowich H, Banks M, Reichert TE, Logan TF, Kirkwood JM, Whiteside TL. Expression and activity of signaling molecules in T lymphocytes obtained from patients with metastatic melanoma before and after interleukin 2 therapy. *Clin Cancer Res* 1996; 2(8):1263-1274.
- (158) Koster A, Landgraf S, Leipold A, Sachse R, Gebhart E, Tulusan AH et al. Expression of oncogenes in human breast cancer specimens. *Anticancer Res* 1991; 11(1):193-201.
- (159) Chakraborty G, Rangaswami H, Jain S, Kundu GC. Hypoxia regulates cross-talk between Syk and Lck leading to breast cancer progression and angiogenesis. *J Biol Chem* 2006; 281(16):11322-11331.
- (160) Oneyama C, Nakano H, Sharma SV. UCS15A, a novel small molecule, SH3 domain-mediated protein-protein interaction blocking drug. *Oncogene* 2002; 21(13):2037-2050.
- (161) Sharma SV, Oneyama C, Yamashita Y, Nakano H, Sugawara K, Hamada M et al. UCS15A, a non-kinase inhibitor of Src signal transduction. *Oncogene* 2001; 20(17):2068-2079.

- (162) Lau GM, Lau GM, Yu GL, Gelman IH, Gutowski A, Hangauer D et al. Expression of Src and FAK in hepatocellular carcinoma and the effect of Src inhibitors on hepatocellular carcinoma in vitro. *Dig Dis Sci* 2009; 54(7):1465-1474.
- (163) Shakespeare W, Yang M, Bohacek R, Cerasoli F, Stebbins K, Sundaramoorthi R et al. Structure-based design of an osteoclast-selective, nonpeptide src homology 2 inhibitor with in vivo antiresorptive activity. *Proc Natl Acad Sci U S A* 2000; 97(17):9373-9378.
- (164) Lombardo LJ, Lee FY, Chen P, Norris D, Barrish JC, Behnia K et al. Discovery of N-(2-chloro-6-methyl-phenyl)-2-(6-(4-(2-hydroxyethyl)-piperazin-1-yl)-2-methylpyrimidin-4-ylamino)thiazole-5-carboxamide (BMS-354825), a dual Src/Abl kinase inhibitor with potent antitumor activity in preclinical assays. *J Med Chem* 2004; 47(27):6658-6661.
- (165) Chang Q, Jorgensen C, Pawson T, Hedley DW. Effects of dasatinib on EphA2 receptor tyrosine kinase activity and downstream signalling in pancreatic cancer. *Br J Cancer* 2008; 99(7):1074-1082.
- (166) Brave M, Goodman V, Kaminskas E, Farrell A, Timmer W, Pope S et al. Sprycel for chronic myeloid leukemia and Philadelphia chromosome-positive acute lymphoblastic leukemia resistant to or intolerant of imatinib mesylate. *Clin Cancer Res* 2008; 14(2):352-359.
- (167) Nam S, Kim D, Cheng JQ, Zhang S, Lee JH, Buettner R et al. Action of the Src family kinase inhibitor, dasatinib (BMS-354825), on human prostate cancer cells. *Cancer Res* 2005; 65(20):9185-9189.
- (168) Serrels A, Macpherson IR, Evans TR, Lee FY, Clark EA, Sansom OJ et al. Identification of potential biomarkers for measuring inhibition of Src kinase activity in colon cancer cells following treatment with dasatinib. *Mol Cancer Ther* 2006; 5(12):3014-3022.
- (169) Finn RS, Dering J, Ginther C, Wilson CA, Glaspy P, Tchekmedyian N et al. Dasatinib, an orally active small molecule inhibitor of both the src and abl kinases,

selectively inhibits growth of basal-type/"triple-negative" breast cancer cell lines growing in vitro. *Breast Cancer Res Treat* 2007; 105(3):319-326.

- (170) Huang F, Reeves K, Han X, Fairchild C, Platero S, Wong TW et al. Identification of candidate molecular markers predicting sensitivity in solid tumors to dasatinib: rationale for patient selection. *Cancer Res* 2007; 67(5):2226-2238.
- (171) Nautiyal J, Majumder P, Patel BB, Lee FY, Majumdar AP. Src inhibitor dasatinib inhibits growth of breast cancer cells by modulating EGFR signaling. *Cancer Lett* 2009; 283(2):143-151.
- (172) Shor AC, Keschman EA, Lee FY, Muro-Cacho C, Letson GD, Trent JC et al. Dasatinib inhibits migration and invasion in diverse human sarcoma cell lines and induces apoptosis in bone sarcoma cells dependent on SRC kinase for survival. *Cancer Res* 2007; 67(6):2800-2808.
- (173) Song L, Morris M, Bagui T, Lee FY, Jove R, Haura EB. Dasatinib (BMS-354825) selectively induces apoptosis in lung cancer cells dependent on epidermal growth factor receptor signaling for survival. *Cancer Res* 2006; 66(11):5542-5548.
- (174) Yano A, Tsutsumi S, Soga S, Lee MJ, Trepel J, Osada H et al. Inhibition of Hsp90 activates osteoclast c-Src signaling and promotes growth of prostate carcinoma cells in bone. *Proc Natl Acad Sci U S A* 2008; 105(40):15541-15546.
- (175) Koreckij T, Nguyen H, Brown LG, Yu EY, Vessella RL, Corey E. Dasatinib inhibits the growth of prostate cancer in bone and provides additional protection from osteolysis. *Br J Cancer* 2009; 101(2):263-268.
- (176) Green TP, Fennell M, Whittaker R, Curwen J, Jacobs V, Allen J et al. Preclinical anticancer activity of the potent, oral Src inhibitor AZD0530. *Mol Oncol* 2009.
- (177) Chang YM, Bai L, Liu S, Yang JC, Kung HJ, Evans CP. Src family kinase oncogenic potential and pathways in prostate cancer as revealed by AZD0530. *Oncogene* 2008; 27(49):6365-6375.

- (178) Hiscox S, Jordan NJ, Morgan L, Green TP, Nicholson RI. Src kinase promotes adhesion-independent activation of FAK and enhances cellular migration in tamoxifen-resistant breast cancer cells. *Clin Exp Metastasis* 2007; 24(3):157-167.
- (179) Yang JC, Ok JH, Busby JE, Borowsky AD, Kung HJ, Evans CP. Aberrant activation of androgen receptor in a new neuropeptide-autocrine model of androgen-insensitive prostate cancer. *Cancer Res* 2009; 69(1):151-160.
- (180) Messersmith WA, Rajeshkumar NV, Tan AC, Wang XF, Diesl V, Choe SE et al. Efficacy and pharmacodynamic effects of bosutinib (SKI-606), a Src/Abl inhibitor, in freshly generated human pancreas cancer xenografts. *Mol Cancer Ther* 2009; 8(6):1484-1493.
- (181) de Vries TJ, Mullender MG, van Duin MA, Semeins CM, James N, Green TP et al. The Src inhibitor AZD0530 reversibly inhibits the formation and activity of human osteoclasts. *Mol Cancer Res* 2009; 7(4):476-488.
- (182) Puttini M, Coluccia AM, Boschelli F, Cleris L, Marchesi E, Donella-Deana A et al. In vitro and in vivo activity of SKI-606, a novel Src-Abl inhibitor, against imatinib-resistant Bcr-Abl+ neoplastic cells. *Cancer Res* 2006; 66(23):11314-11322.
- (183) Coluccia AM, Benati D, Dekhil H, De Filippo A, Lan C, Gambacorti-Passerini C. SKI-606 decreases growth and motility of colorectal cancer cells by preventing pp60(c-Src)-dependent tyrosine phosphorylation of beta-catenin and its nuclear signaling. *Cancer Res* 2006; 66(4):2279-2286.
- (184) Zhang J, Kalyankrishna S, Wislez M, Thilaganathan N, Saigal B, Wei W et al. SRC-family kinases are activated in non-small cell lung cancer and promote the survival of epidermal growth factor receptor-dependent cell lines. *Am J Pathol* 2007; 170(1):366-376.
- (185) Golas JM, Lucas J, Etienne C, Golas J, Discafani C, Sridharan L et al. SKI-606, a Src/Abl inhibitor with in vivo activity in colon tumor xenograft models. *Cancer Res* 2005; 65(12):5358-5364.

- (186) Mendiratta P, Mostaghel E, Guinney J, Tewari AK, Porrello A, Barry WT et al. Genomic strategy for targeting therapy in castration-resistant prostate cancer. *J Clin Oncol* 2009; 27(12):2022-2029.
- (187) Jones RJ, Young O, Renshaw L, Jacobs V, Fennell M, Marshall A et al. Src inhibitors in early breast cancer: a methodology, feasibility and variability study. *Breast Cancer Res Treat* 2009; 114(2):211-221.
- (188) Johnson FM, Saigal B, Talpaz M, Donato NJ. Dasatinib (BMS-354825) tyrosine kinase inhibitor suppresses invasion and induces cell cycle arrest and apoptosis of head and neck squamous cell carcinoma and non-small cell lung cancer cells. *Clin Cancer Res* 2005; 11(19 Pt 1):6924-6932.
- (189) Araujo J, Logothetis C. Dasatinib: A potent SRC inhibitor in clinical development for the treatment of solid tumors. *Cancer Treat Rev* 2010.
- (190) Ishizawar R, Parsons SJ. c-Src and cooperating partners in human cancer. *Cancer Cell* 2004; 6(3):209-214.
- (191) Duxbury MS, Ito H, Zinner MJ, Ashley SW, Whang EE. Inhibition of SRC tyrosine kinase impairs inherent and acquired gemcitabine resistance in human pancreatic adenocarcinoma cells. *Clin Cancer Res* 2004; 10(7):2307-2318.
- (192) Irby RB, Yeatman TJ. Role of Src expression and activation in human cancer. *Oncogene* 2000; 19(49):5636-5642.
- (193) Brown MT, Cooper JA. Regulation, substrates and functions of src. *Biochim Biophys Acta* 1996; 1287(2-3):121-149.
- (194) Lee YC, Huang CF, Murshed M, Chu K, Araujo JC, Ye X et al. Src family kinase/abl inhibitor dasatinib suppresses proliferation and enhances differentiation of osteoblasts. *Oncogene* 2010.
- (195) Coussens LM, Werb Z. Inflammation and cancer. *Nature* 2002; 420(6917):860-867.

- (196) Mantovani A, Allavena P, Sica A, Balkwill F. Cancer-related inflammation. *Nature* 2008; 454(7203):436-444.
- (197) Roxburgh CS, McMillan DC. Role of systemic inflammatory response in predicting survival in patients with primary operable cancer. *Future Oncol* 2010; 6(1):149-163.
- (198) Schaller MD, Hildebrand JD, Shannon JD, Fox JW, Vines RR, Parsons JT. Autophosphorylation of the focal adhesion kinase, pp125FAK, directs SH2-dependent binding of pp60src. *Mol Cell Biol* 1994; 14(3):1680-1688.
- (199) Kirkegaard T, Edwards J, Tovey S, McGlynn LM, Krishna SN, Mukherjee R et al. Observer variation in immunohistochemical analysis of protein expression, time for a change? *Histopathology* 2006; 48(7):787-794.
- (200) McCarty KS, Jr., Miller LS, Cox EB, Konrath J, McCarty KS, Sr. Estrogen receptor analyses. Correlation of biochemical and immunohistochemical methods using monoclonal antireceptor antibodies. *Arch Pathol Lab Med* 1985; 109(8):716-721.
- (201) Canna K, Hilmy M, McMillan DC, Smith GW, McKee RF, McArdle CS et al. The relationship between tumour proliferative activity, the systemic inflammatory response and survival in patients undergoing curative resection for colorectal cancer. *Colorectal Dis* 2008; 10(7):663-667.
- (202) Wolff AC, Hammond ME, Schwartz JN, Hagerty KL, Allred DC, Cote RJ et al. American Society of Clinical Oncology/College of American Pathologists guideline recommendations for human epidermal growth factor receptor 2 testing in breast cancer. *J Clin Oncol* 2007; 25(1):118-145.
- (203) Tovey S, Dunne B, Witton CJ, Forsyth A, Cooke TG, Bartlett JM. Can molecular markers predict when to implement treatment with aromatase inhibitors in invasive breast cancer? *Clin Cancer Res* 2005; 11(13):4835-4842.

- (204) Yamauchi H, Stearns V, Hayes DF. When is a tumor marker ready for prime time? A case study of c-erbB-2 as a predictive factor in breast cancer. *J Clin Oncol* 2001; 19(8):2334-2356.
- (205) Mukherjee R, Bartlett JM, Krishna NS, Underwood MA, Edwards J. Raf-1 expression may influence progression to androgen insensitive prostate cancer. *Prostate* 2005; 64(1):101-107.
- (206) McCall P, Witton CJ, Grimsley S, Nielsen KV, Edwards J. Is PTEN loss associated with clinical outcome measures in human prostate cancer? *Br J Cancer* 2008; 99(8):1296-1301.
- (207) McGlynn LM, Kirkegaard T, Edwards J, Tovey S, Cameron D, Twelves C et al. Ras/Raf-1/MAPK pathway mediates response to tamoxifen but not chemotherapy in breast cancer patients. *Clin Cancer Res* 2009; 15(4):1487-1495.
- (208) Brown SB, Hole DJ, Cooke TG. Breast cancer incidence trends in deprived and affluent Scottish women. *Breast Cancer Res Treat* 2007; 103(2):233-238.
- (209) Brown SB, Mallon EA, Edwards J, Campbell FM, McGlynn LM, Elsberger B et al. Is the biology of breast cancer changing? A study of hormone receptor status 1984-1986 and 1996-1997. *Br J Cancer* 2009; 100(5):807-810.
- (210) Kleber S, Sancho-Martinez I, Wiestler B, Beisel A, Gieffers C, Hill O et al. Yes and PI3K bind CD95 to signal invasion of glioblastoma. *Cancer Cell* 2008; 13(3):235-248.
- (211) Fu Y, Zagozdzon R, Avraham R, Avraham HK. CHK negatively regulates Lyn kinase and suppresses pancreatic cancer cell invasion. *Int J Oncol* 2006; 29(6):1453-1458.
- (212) Masaki T, Igarashi K, Tokuda M, Yukimasa S, Han F, Jin YJ et al. pp60c-src activation in lung adenocarcinoma. *Eur J Cancer* 2003; 39(10):1447-1455.

- (213) Bolen JB, Veillette A, Schwartz AM, DeSeau V, Rosen N. Activation of pp60c-src protein kinase activity in human colon carcinoma. *Proc Natl Acad Sci U S A* 1987; 84(8):2251-2255.
- (214) Cartwright CA, Kamps MP, Meisler AI, Pipas JM, Eckhart W. pp60c-src activation in human colon carcinoma. *J Clin Invest* 1989; 83(6):2025-2033.
- (215) Hiscox S, Morgan L, Green TP, Barrow D, Gee J, Nicholson RI. Elevated Src activity promotes cellular invasion and motility in tamoxifen resistant breast cancer cells. *Breast Cancer Res Treat* 2006; 97(3):263-274.
- (216) Gee JM, Shaw VE, Hiscox SE, McClelland RA, Rushmere NK, Nicholson RI. Deciphering antihormone-induced compensatory mechanisms in breast cancer and their therapeutic implications. *Endocr Relat Cancer* 2006; 13 Suppl 1:S77-S88.
- (217) Talamonti MS, Roh MS, Curley SA, Gallick GE. Increase in activity and level of pp60c-src in progressive stages of human colorectal cancer. *J Clin Invest* 1993; 91(1):53-60.
- (218) Termuhlen PM, Curley SA, Talamonti MS, Saboorian MH, Gallick GE. Site-specific differences in pp60c-src activity in human colorectal metastases. *J Surg Res* 1993; 54(4):293-298.
- (219) Aligayer H, Boyd DD, Heiss MM, Abdalla EK, Curley SA, Gallick GE. Activation of Src kinase in primary colorectal carcinoma: an indicator of poor clinical prognosis. *Cancer* 2002; 94(2):344-351.
- (220) Hynes NE. Tyrosine kinase signalling in breast cancer. *Breast Cancer Res* 2000; 2(3):154-157.
- (221) Campbell EJ, McDuff E, Tatarov O, Tovey S, Brunton V, Cooke TG et al. Phosphorylated c-Src in the nucleus is associated with improved patient outcome in ER-positive breast cancer. *Br J Cancer* 2008; 99(11):1769-1774.

- (222) Masaki T, Okada M, Shiratori Y, Rengifo W, Matsumoto K, Maeda S et al. pp60c-src activation in hepatocellular carcinoma of humans and LEC rats. *Hepatology* 1998; 27(5):1257-1264.
- (223) Cleator S, Heller W, Coombes RC. Triple-negative breast cancer: therapeutic options. *Lancet Oncol* 2007; 8(3):235-244.
- (224) Sakai T, Kawakatsu H, Fujita M, Yano J, Owada MK. An epitope localized in c-Src negative regulatory domain is a potential marker in early stage of colonic neoplasms. *Lab Invest* 1998; 78(2):219-225.
- (225) Ito Y, Kawakatsu H, Takeda T, Sakon M, Nagano H, Sakai T et al. Activation of c-Src gene product in hepatocellular carcinoma is highly correlated with the indices of early stage phenotype. *J Hepatol* 2001; 35(1):68-73.
- (226) Park SI, Zhang J, Phillips KA, Araujo JC, Najjar AM, Volgin AY et al. Targeting SRC family kinases inhibits growth and lymph node metastases of prostate cancer in an orthotopic nude mouse model. *Cancer Res* 2008; 68(9):3323-3333.
- (227) Lee F, Fandi A, Voi M. Overcoming kinase resistance in chronic myeloid leukemia. *Int J Biochem Cell Biol* 2008; 40(3):334-343.
- (228) Hibbs ML, Dunn AR. Lyn, a src-like tyrosine kinase. *Int J Biochem Cell Biol* 1997; 29(3):397-400.
- (229) Choi YL, Bocanegra M, Kwon MJ, Shin YK, Nam SJ, Yang JH et al. LYN is a mediator of epithelial-mesenchymal transition and a target of dasatinib in breast cancer. *Cancer Res* 2010; 70(6):2296-2306.
- (230) Konecny GE, Glas R, Dering J, Manivong K, Qi J, Finn RS et al. Activity of the multikinase inhibitor dasatinib against ovarian cancer cells. *Br J Cancer* 2009; 101(10):1699-1708.
- (231) Rody A, Holtrich U, Pusztai L, Liedtke C, Gaetje R, Ruckhaeberle E et al. T-cell metagene predicts a favorable prognosis in estrogen receptor-negative and HER2-positive breast cancers. *Breast Cancer Res* 2009; 11(2):R15.

- (232) Belka C, Marini P, Lepple-Wienhues A, Budach W, Jekle A, Los M et al. The tyrosine kinase lck is required for CD95-independent caspase-8 activation and apoptosis in response to ionizing radiation. *Oncogene* 1999; 18(35):4983-4992.
- (233) Rudner J, Mueller AC, Matzner N, Huber SM, Handrick R, Belka C et al. The additional loss of Bak and not the lack of the protein tyrosine kinase p56/Lck in one JCaM1.6 subclone caused pronounced apoptosis resistance in response to stimuli of the intrinsic pathway. *Apoptosis* 2009; 14(5):711-720.
- (234) Reed JC. Dysregulation of apoptosis in cancer. *J Clin Oncol* 1999; 17(9):2941-2953.
- (235) Murri AM, Hilmy M, Bell J, Wilson C, McNicol AM, Lannigan A et al. The relationship between the systemic inflammatory response, tumour proliferative activity, T-lymphocytic and macrophage infiltration, microvessel density and survival in patients with primary operable breast cancer. *Br J Cancer* 2008; 99(7):1013-1019.
- (236) Trihia H, Murray S, Price K, Gelber RD, Golouh R, Goldhirsch A et al. Ki-67 expression in breast carcinoma: its association with grading systems, clinical parameters, and other prognostic factors--a surrogate marker? *Cancer* 2003; 97(5):1321-1331.
- (237) Martin GS. The hunting of the Src. *Nat Rev Mol Cell Biol* 2001; 2(6):467-475.
- (238) Sieg DJ, Hauck CR, Schlaepfer DD. Required role of focal adhesion kinase (FAK) for integrin-stimulated cell migration. *J Cell Sci* 1999; 112 (Pt 16):2677-2691.
- (239) Ruest PJ, Roy S, Shi E, Mernaugh RL, Hanks SK. Phosphospecific antibodies reveal focal adhesion kinase activation loop phosphorylation in nascent and mature focal adhesions and requirement for the autophosphorylation site. *Cell Growth Differ* 2000; 11(1):41-48.

- (240) Schlaepfer DD, Hanks SK, Hunter T, van der GP. Integrin-mediated signal transduction linked to Ras pathway by GRB2 binding to focal adhesion kinase. *Nature* 1994; 372(6508):786-791.
- (241) Lim Y, Han I, Kwon HJ, Oh ES. Trichostatin A-induced detransformation correlates with decreased focal adhesion kinase phosphorylation at tyrosine 861 in ras-transformed fibroblasts. *J Biol Chem* 2002; 277(15):12735-12740.
- (242) Sieg DJ, Hauck CR, Ilic D, Klingbeil CK, Schaefer E, Damsky CH et al. FAK integrates growth-factor and integrin signals to promote cell migration. *Nat Cell Biol* 2000; 2(5):249-256.
- (243) Vadlamudi RK, Adam L, Nguyen D, Santos M, Kumar R. Differential regulation of components of the focal adhesion complex by heregulin: role of phosphatase SHP-2. *J Cell Physiol* 2002; 190(2):189-199.
- (244) Couture C, Baier G, Oetken C, Williams S, Telford D, Marie-Cardine A et al. Activation of p56lck by p72syk through physical association and N-terminal tyrosine phosphorylation. *Mol Cell Biol* 1994; 14(8):5249-5258.
- (245) Muthuswamy SK, Muller WJ. Activation of Src family kinases in Neu-induced mammary tumors correlates with their association with distinct sets of tyrosine phosphorylated proteins in vivo. *Oncogene* 1995; 11(9):1801-1810.
- (246) Talpaz M, Shah NP, Kantarjian H, Donato N, Nicoll J, Paquette R et al. Dasatinib in imatinib-resistant Philadelphia chromosome-positive leukemias. *N Engl J Med* 2006; 354(24):2531-2541.
- (247) Jones RJ, Avizienyte E, Wyke AW, Owens DW, Brunton VG, Frame MC. Elevated c-Src is linked to altered cell-matrix adhesion rather than proliferation in KM12C human colorectal cancer cells. *Br J Cancer* 2002; 87(10):1128-1135.

Appendices

Appendix 1: Materials for mRNA expression of SKF members

RNA extraction

Reagents

| | |
|-----------------------------------|---------------------|
| TRIZOL® | (Invitrogen) |
| Chloroform | (Sigma) |
| Isopropyl alcohol | (Sigma) |
| 75% Ethanol | (Fisher Scientific) |
| RNase/DNase free Water | (Promega) |
| TBE (Tris-borate-EDTA) | (Invitrogen) |
| Agarose | (Invitrogen) |
| 1Kb Plus DNA Ladder | (Invitrogen) |
| Bromophenol Blue loading solution | (Promega) |

RT-PCR

Reagents

| | |
|--------------------------------------|----------------|
| DNA Buffer*** | (Applera) |
| DNase*** | (Applera) |
| DNA Inactivator Reagent | (Applera) |
| Oliga (dt) Primers (1:50) | (Invitrogen) |
| Random Primers (Hexamer) (1:60) | (Invitrogen) |
| 5x First Strand Buffer | (Invitrogen)** |
| DTT | (Invitrogen)** |
| RNase OUT | (Invitrogen) |
| SuperScript II Reverse Transcriptase | (Invitrogen)** |
| RNase H | (Applera) |

Real time PCR

Reagents

| | |
|--|--------------|
| PCR Buffer-Mg | (VH Bio)* |
| Enhancer Solution | (VH Bio)* |
| MolTaq enzyme | (VH Bio)* |
| 10mM dNTP | (VH Bio) |
| Forward Primer (human β -actin, 546-566, TM 68) GGTCACCCACACTGTGCCCAT | (Invitrogen) |
| Reverse Primer (human β -actin, 896-875, TM 68) GGATGCCACAGGACTCCATGC | (Invitrogen) |

TaqMan® PCR

Reagents

| | |
|--|----------------------|
| TaqMan® Universal Master Mix | (Applied Biosystems) |
| Human HPRT1 endogenous control (VIC/TAMRA probe) | (Applied Biosystems) |
| Human GAPDH endogenous control (VIC/TAMRA probe) | (Applied Biosystems) |
| Src (Gene Expression Assay ID: Hs00178494_m1) | (Applied Biosystems) |
| Lck (Gene Expression Assay ID: Hs00176719_m1) | (Applied Biosystems) |
| Lyn (Gene Expression Assay ID: Hs00178427_m1) | (Applied Biosystems) |
| Yes (Gene Expression Assay ID: Hs00736972_m1) | (Applied Biosystems) |
| Fyn (Gene Expression Assay ID: Hs00176628_m1) | (Applied Biosystems) |
| Fgr (Gene Expression Assay ID: Hs00178340_m1) | (Applied Biosystems) |
| Hck (Gene Expression Assay ID: Hs00176654_m1) | (Applied Biosystems) |
| Blk (Gene Expression Assay ID: Hs00176441_m1) | (Applied Biosystems) |

Solutions

MasterMix for RTPCR (per PCR tube)

5x first strand buffer (4 μ l)

DTT (2 μ l)

RNase **OUT** (1 μ l)

Master Mix for Real time PCR (per PCR tube)

10x PCR buffer-Mg (2.5 μ l)

10 mM dNTP (0.5 μ l)

Enhancer solution (0.75 μ l)

Forward primer β -actin (0.5 μ l)

Reverse primer β -actin (0.5 μ l)

Mol Taq (0.25 μ l)

RNA/DNA free H₂O (18 μ l)

Appendix 2: Materials for protein expression of SKF members

Western Blotting

Reagents

- Bio-Rad Reagent (Bio-Rad Laboratories)
- Bovine Serum Albumin (BSA) (Sigma)
- Isopropanolol (Sigma-Aldrich)
- APS (Sigma)
- TEMED (Sigma)
- 40% Acrylamide/Bis-Acrylamide (Sigma)
- Glycine (Sigma)
- Tris-HCL (VWR)
- Glycerol (Sigma)
- 2-Mercaptoethanol (Sigma)
- Bromophenol Blue (0.05% w/v) (Promega)
- PVDF membrane (BioRad)
- 100% Methanol (Fisher Scientific)
- Coomassie blue R250 (Sigma)
- Acetic Acid Glacial (BDH Laboratory Supplies)
- TWEEN 20 (Sigma)
- Marvel-dried skimmed milk (Premier International Foods)
- ECL+Plus: Solution A and B (Amersham Biosciences)
- HeLa cell lysates (Cell Signalling Technology)
- NFkappaB cell lysates (Cell Signalling Technology)
- Jurkat cell lysates (Cell Signalling Technology)

- Biotinylated Protein Ladder (Cell Signalling Technology)
- β -actin antibody (abcam)
- β -tubulin antibody (abcam)
- Total Src (60kDa) (mAb) (Cell Signalling Technology)
- Anti-Src family negative regulatory site (pAb) (Invitrogen)
- Clone 28 (mAb) (Invitrogen)
- Y416 Src antibody (pAb) (Cell Signalling Technology)
- Y216 Src antibody (pAb) (Santa Cruz)
- Lyn (mAb) (BD Biosciences)
- Lck (mAb) (Cell Signalling Technology)
- Y861FAK (pAb) (Invitrogen)
- Ki67 antigen MIB-1 (DAKO)
- Anti-biotin HRP linked antibody (Cell Signalling Technology)
- HRP-linked anti-rabbit IgG (Cell Signalling Technology)
- Re-Blot Plus Strong Antibody Stripping Buffer (Millipore)

Solutions and Buffers**Resolving Gel (10%) (per 50 ml)**

| Reagents | |
|-------------------------------|-------------|
| 40% Acrylamide/Bis-Acrylamide | 6.25 ml |
| 0.5M EDTA | 165 μ l |
| 2M Tris, pH 8.9 | 4.18 ml |
| 10% SDS | 250 μ l |
| dH ₂ O | 14.25 ml |
| 10% APS | 150 μ l |
| TEMED | 15 μ l |

Stacking Gel (4.5 %) (per 50 ml)

Excluding APS and TEDMED Stacking Gel can be made up and stored at 4 °C

| Reagents | |
|-------------------------------|-------------|
| 40% Acrylamide/Bis-Acrylamide | 5.63 ml |
| 0.5M EDTA | 400 μ l |
| 1M Tris, pH 6.8 | 6.25 ml |
| 10% SDS | 500 μ l |
| dH ₂ O | 37.22 ml |
| 10% APS | 30 μ l |
| TEMED | 10 μ l |

1M Tris pH 6.8

Dissolve 60.57 g Tris Base in ~400 ml distilled water

pH to 6.8 with concentrated HCl

Make up volume to 500 ml with distilled water

2M Tris pH 8.9

Dissolve 121.1 g Tris Base in ~400 ml distilled water

pH to 8.9 with concentrated HCl

Make up volume to 500 ml with distilled water

0.5M EDTA

Dissolve 18.6 g EDTA (mw 372.2 g/mol) in ~90 ml distilled water

Add NaOH pellets or concentrated NaOH (alkaline conditions) until EDTA dissolves

Make volume up to 100 ml with distilled water

SDS Running Buffer (10x stronger)

200mM Tris: 24.2 g

2M Glycine: 144.1 g

1% SDS: 10 g (100 ml of 10% SDS) (check pH is ~8.3- but don't adjust)

Make up to 1litre with distilled water

SDS-PAGE Blotting Buffer

Tris: 30 g

Glycine: 95 g

Make up to 1litre with distilled water (for small proteins add 10-20% Methanol to buffer)

Transfer Buffer (10x stronger)

248mM Tris: g

1.3M Glycine: g

20% Methanol

Make up to 1litre with distilled water

Stripping Buffer

0.2M Glycine (pH 2.5): 7.51g

1% SDS: 10 ml of 10% SDS

Laemmli's sample reducing buffer

| Reagents | |
|------------------------------|---------|
| 0.5M Tris-HCL pH6.8 | 1.00 ml |
| Glycerol | 0.8 ml |
| 10% sodioum dodecyl sulphate | 1.6 ml |
| 2-Mercaptoethanol | 0.4 ml |
| Bromophenol Blue (0.05 w/v) | 0.2 ml |
| dH ₂ O | 4.0 ml |

Coomasie Blue Stain

1.25 g Coomassie Blue R250

454 ml 50% Methanol

46 ml Acetic acid

Destain

25 ml Methanol

37.5 ml Acetic Acid

437.5 ml distilled water

TBS (1 litre) (10x stronger)

0.1M Tris/HCl pH 7.4 12.2 g

1.5M NaCl 87.7 g

TTBS (0.001% TBS)

0.1M Tris/HCl pH 7.4 12.2 g

1.5M NaCl 87.7 g

1000 µl TWEEN 20 per litre of TBS (1x)

BLOTTO

5g Marvel (5% Non-Fat Dry Milk)

100ml TTBS

Blocking Solution

5g Marvel (5% Non-Fat Dry Milk)

100ml TTBS

Antibody Dilutions and Concentrations***Primary Antibodies***

| Antibody | Dilution | Concentration |
|-----------------|-----------------|----------------------|
| Total Src | 1:1000 | 0.86 µg/ml |
| anti-Clone 28 | 1:1000 | 0.5 µg/ml |
| Clone28 | 1:1000 | * |
| Y416Src | 1:1000 | 0.04 µg/ml |
| Y216Src | 1:1000 | 0.2 µg/ml |
| Lyn | 1:200 | 1.25 µg/ml |
| Lck | 1:1000 | 0.038 µg/ml |
| Y861FAK | 1:500 | * |

*No information provided by company

Secondary Antibodies

| Secondary Antibody | Primary Antibody | Dilution | Concentration |
|---------------------------|-------------------------|-----------------|----------------------|
| Anti-biotin | Biotin Ladder | 1:1000 | 0.1 µg/ml |
| Rabbit | total Src | 1:5000 | 0.02 µg/ml |
| Rabbit | anti-Clone28 | 1:5000 | 0.02 µg/ml |
| Mouse | Clone28 | 1:10000 | 0.01 µg/ml |
| Rabbit | Y416Src | 1:5000 | 0.02 µg/ml |
| Goat | Y216Src | 1:10000 | 0.01 µg/ml |
| Mouse | Lyn | 1:10000 | 0.01 µg/ml |
| Rabbit | Lck | 1:5000 | 0.02 µg/ml |
| Rabbit | Y861FAK | 1:10000 | 0.01 µg/ml |

Immunohistochemistry

Reagents

| | |
|--|------------------------------|
| Antigen retrieval solution: Epitope Retrieval Buffer | (DAKO) |
| Xylene | (Fisher Scientific) |
| Alcohol solutions (100%, 90%, 70%) | (Fisher Scientific) |
| H ₂ O ₂ | (VWR) |
| Horse Serum | (Vector Laboratories) |
| Antibody diluent | (DAKO) |
| DAKO kit (pen, AB solution, Envision) | (DAKO) |
| Chromagen 3,3'-diaminobenzidine (DAB) | (Vector Laboratories) |
| Haematoxylin | (VWR) |
| DPX glue | (VWR) |
| Total Src (60kDa) (mAb) | (Cell Signalling Technology) |
| Anti-Src family negative regulatory site (pAb)- inactive YSrc530 | (Invitrogen) |
| Clone28 (mAb)- active YSrc530 | (Invitrogen) |
| Y416 Src antibody (pAb) | (Cell Signalling Technology) |
| Y216 Src antibody (pAb) | (Santa Cruz) |
| Lyn (mAb) | (BD Biosciences) |
| Lck (mAb) | (Cell Signalling Technology) |
| Ki67 antigen MIB-1 (mAb) | (DAKO) |

Solutions and Buffers**Antigen retrieval buffer: 10 mM Citrate Buffer (pH 6.0):**

| Reagents | |
|--------------------------|--------|
| dH ₂ O | 990 ml |
| Epitope Retrieval Buffer | 10 ml |

H₂O₂ (4%)13.3 ml H₂O₂ + 386.7 ml dH₂O**Horse Serum (1.5 %)**

15 µl of HS/ ml TBS

Horse Serum (5%)

50 µl of HS/ ml TBS

TBS Buffer diluted**TBS (1 litre) (10x stronger)**

0.1M Tris/HCl pH 7.4 12.2 g

1.5M NaCl 87.7 g

Scotts Tap Water Substitute

| Reagents | |
|---|----------|
| | 2 litres |
| Magnesium sulphate ($\text{MgSO}_4, 7\text{H}_2\text{O}$) | 40g |
| Sodium bicarbonate (NaHCO_3) | 7g |

DABO solution(chromagen 3,3'-diaminobenzidine)

| Reagents | |
|-----------------------|---------|
| DAB buffer | 2 drops |
| DAB substrate | 4 drops |
| DAB hydrogen peroxide | 2 drops |
| dH ₂ O | 5.0 ml |

Antibody Dilutions and Concentrations***Primary Antibodies***

| Antibody | Dilution | Concentration |
|-----------------|-----------------|----------------------|
| Total Src | 1:200 | 4.32 µg/ml |
| antiClone28 | 1:1500 | 0.33 µg/ml |
| Clone28 | 1:500 | * |
| Y416Src | 1:2000 | 0.02 µg/ml |
| Y216Src | 1:25 | 8 µg/ml |
| Lyn | 1:5 | 50 µg/ml |
| Lck | 1:50 | 0.76 µg/ml |
| Ki67 | 1:150 | 533.33 µg/ml |

*No information provided by company

Appendix 3: Materials for Dasatinib and cell line experiments

Reagents

| | |
|---|------------------------------|
| Dulbecco's Modified Eagle Media (DMEM) ¹ | (Invitrogen- 21969) |
| Dulbecco's Modified Eagle Media (DMEM) ² | (Invitrogen- 41966) |
| Hank-Buffered Saline solution (HBBS) | (Lonza) |
| Phosphate Buffered Saline solution (PBS) | (Invitrogen) |
| DMSO-Freeze Medium | (Sigma) |
| Heat-inactivated fetal calf serum | (Invitrogen) |
| Heat-inactivated fetal calf serum (Charcoal stripped) | (Invitrogen) |
| L-glutamine | (Invitrogen) |
| Penicillin/Streptomycin (50 units/ml, 50 µl/ml) | (Invitrogen) |
| Sodium Pyruvate | (Invitrogen) |
| Trypsin/EDTA solution | (Lonza) |
| Tryptan Blue | (Lonza) |
| Dasatinib (Src kinase inhibitor) | (Bristol-Myers-Squib) |
| Heregulin- α | (Sigma H-5529) |
| Epidermal Growth Factor | (Sigma E-9644) |
| Insulin | (Sigma I-6634) |
| Fresh Frozen Human Plasma | (Local Blood bank) |
| Bovine Alpha Thrombin | (Cambridge Bioscience) |
| 10% buffered formal saline ('formalin') | (Genta Medical Formaldehyde) |
| Normal physiological saline (0.9%) | (Baxter, UKF7124) |

Cell line Media and Buffer

| | | | | |
|----------------------------------|--|--|------------------------------------|--|
| Full medium (FM) | DMEM ¹ (500ml) | Foetal calf serum (10%) (50ml) | L-glutamine (2mM) (5ml) | Penicillin/Streptomycin (50units/ ml; 50 µg/ ml) (5ml) |
| Serum free medium (SS) | DMEM ¹ (500ml) | - | L-glutamine (2mM) (5ml) | Penicillin/Streptomycin (50units/ ml; 50 µg/ ml) (5ml) |
| Charcoal strip medium (CS) | DMEM ¹ (500ml) | Foetal calf serum (10%) been charcoal stripped (50ml) | L-glutamine (2mM) (5ml) | Penicillin/Streptomycin (50units/ ml; 50 µg/ ml) (5ml) |
| HER2- medium (HER2) | DMEM ² (500ml)+ 4 mM L-glutamine | Foetal calf serum (10%) (50ml) | + Insulin (10mg/ml) (750 µl) | Penicillin/Streptomycin (50units/ ml; 50 µg/ ml) (5ml) |
| Freeze medium | DMEM ¹ | DMSO (10%) | - | - |

Stock Solutions for Drug Treatment

All stock solutions were filtered through 0.2 μm filters before being aliquoted for longterm storage at $-20\text{ }^{\circ}\text{C}$.

Insulin:

100 μl of glacial acetic acid was added to 10 ml dH_2O , dissolving 100 mg of insulin powder in this solution. Final concentration: 10 mg/ml

EGF:

200 μl of glacial acetic acid containing 0.1% BSA was added to vial (0.2 mg of epidermal growth factor powder) to reach a concentration of 1 mg/ml. A final stock concentration of 10 $\mu\text{g}/\text{ml}$ ($= 1.61\text{ }\mu\text{M}$) was achieved in diluting this solution further with 20 ml of sterile PBS.

HRG:

10 mg of BSA was dissolved in 10 ml of sterile PBS. 5 ml of this solution was then added to the vial (50 μg Heregulin- α) to accomplish a stock solution of 10 $\mu\text{g}/\text{ml}$ ($= 1.42\text{ }\mu\text{M}$).

Dasatinib:

24.8 mg of Dasatinib powder was dissolved in 124 μl of DMSO (Dasatinib soluble at 200 mg/ml). To prepare a 10 mM stock solution, this suspension was further diluted in 4.96 ml of DMSO.

Drug treatment Dilution and Concentrations

| Drug | Molecular weight (Dalton) | Suspended in | Stock Concentration | Final Concentration |
|-------------------------------|---------------------------|----------------------------------|---------------------|---------------------|
| Epidermal Growth Factor (EGF) | 6200 | HBBS and BSA/glacial acetic acid | 1.61 μ M | 10 nM |
| Heregulin (HRG) | 7000 | HBBS and BSA | 1.42 μ M | 10 nM |
| Dasatinib (DASA) | 488.01 | DMSO | 10 mM | 100 nM |

Solutions for cell pellet formation

Thrombin Stock Solution:

1ml of saline (0.9%) is added to 1 mg of thrombin and stored at 4-6 °C.

Thrombin Working Solution for Formation of Cell pellet clots:

1-2 drops of Thrombin stock solution is mixed with a further 1 ml of Saline (0.9%)